

**RBF-BASED MESHLESS METHOD FOR LARGE  
DEFLECTION OF PLATES ON NONLINEAR FOUNDATIONS**

BY

**MOHAMMED MOHAMMED HUSSEIN AL-THOLAIA**

A Dissertation Presented to the  
FACULTY OF THE COLLEGE OF GRADUATE STUDIES

**KING FAHD UNIVERSITY OF PETROLEUM & MINERALS**

DHAHRAN, SAUDI ARABIA

In Partial Fulfillment of the  
Requirements for the Degree of

**DOCTOR OF PHILOSOPHY**

In


**CIVIL ENGINEERING**

**JANUARY, 2015**

KING FAHD UNIVERSITY OF PETROLEUM & MINERALS  
DHAHRAN- 31261, SAUDI ARABIA  
DEANSHIP OF GRADUATE STUDIES

This dissertation, written by *Mohammed Mohammed Hussein Al-Tholaia* under the direction of his dissertation advisor and approved by his dissertation committee, has been presented to and accepted by the Dean of Graduate Studies, in partial fulfillment of the requirements for the degree of **DOCTOR OF PHILOSOPHY IN CIVIL ENGINEERING**.

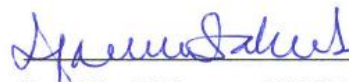
Dissertation Committee

 24/12/14

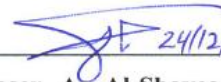
**Prof. Dr. Husain J. Al-Gahtani**  
(Advisor)

Dec. 24, 2014 


**Dr. Ali H. Al-Gadhib**  
(Co-Advisor)

 24.12.14

**Prof. Dr. Muhammed H. Baluch**  
(Member)

 24/12/2014

**Prof. Dr. Naser A. Al-Shayea**  
(Member)

 29/12/2014

**Dr. Faisal A. Fairag**  
(Member)

37/14/c 

**Prof. Dr. Nedal T. Ratrouf**  
(Department Chairman) 24 DEC 2014



**Prof. Dr. Salam A. Zummo**  
(Dean of Graduate Studies)

29/12/14

Date



**©Mohammed Mohammed Hussein Al-Tholaia**

2015

وقل رب زدني علما

**THIS WORK IS DEDICATED  
TO MY FATHER, MOTHER, WIFE,  
CHILDREN, BROTHER AND SISTERS**

## ACKNOWLEDGMENT

Praise and thanks a lot God Almighty, for giving me the health, knowledge and patience to complete this work. I acknowledge the financial support given by King Fahd University for Petroleum and Minerals (KFUPM) and by Thamar University during my Ph.D. study.

My sincerest gratitude and appreciation go to my advisor Prof. Husain Jubran Al-Gahtani for his continuous guidance throughout the research. I am also grateful to my co-advisor Dr. Ali Algadhib and Committee Members, *Prof. Muhammed Hussein Baluch, Prof. Naser A. Al-Shayea, and Dr. Faisal Fairag*, for their constructive guidance and support.

Thanks are also to the Chairman of Civil & Environmental Engineering Department, Prof. Nedal T. Ratrouf and to his secretary and the other staff members for their invaluable academic support.

My heartfelt gratitude is given to my beloved father, mother, wife and my children, who always support me with their love, patience, encouragement and constant prayers. I would like to thank my brother, sisters, and all members of my family in Yemen.

# TABLE OF CONTENTS

<b>ACKNOWLEDGMENT .....</b>	<b>III</b>
<b>TABLE OF CONTENTS .....</b>	<b>IV</b>
<b>LIST OF TABLES .....</b>	<b>IX</b>
<b>LIST OF FIGURES .....</b>	<b>XII</b>
<b>LIST OF SYMBOLS .....</b>	<b>XIX</b>
<b>DISSERTATION ABSTRACT.....</b>	<b>XXI</b>
<b>ملخص الأطروحه .....</b>	<b>XXIII</b>
<b>CHAPTER ONE .....</b>	<b>1</b>
<b>INTRODUCTION.....</b>	<b>1</b>
1.1 General .....	1
1.2 Problem Statement .....	5
1.3 Motivation and Objectives .....	8
1.4 Outline of the Dissertation .....	9
<b>CHAPTER TWO .....</b>	<b>11</b>
<b>LITERATURE REVIEW .....</b>	<b>11</b>
2.1 General .....	11
2.2 Analysis of Plates with Large Deflection.....	17
2.2.1 Analytical Solutions.....	17
2.2.2 Numerical Solutions.....	20

2.3	Analysis of Plates on Foundations .....	23
2.3.1	Analytical Solutions.....	23
2.3.2	Numerical Solutions.....	24
2.4	RBF Methods .....	26
2.5	Models of Soil–Foundation Interaction .....	30
2.5.1	Winkler Model.....	31
2.5.2	Two-Parameter Model (Pasternak Model).....	31
2.5.3	Three-Parameter Model (Nonlinear Winkler-Pasternak Model) .....	31
2.5.4	Elastic Continuous Models .....	32
<b>CHAPTER THREE .....</b>		<b>36</b>
<b>GOVERNING EQUATIONS .....</b>		<b>36</b>
3.1	Large Deflection of a Thin Plate.....	36
3.1.1	w-F Formulations.....	40
3.1.2	w-u-v Formulations.....	44
3.1.3	Non-Dimensional W-F Formulations .....	53
3.1.4	Non-Dimensional W-U-V Formulations .....	55
3.2	Large Deflection of Thin Plates on Foundations .....	62
3.2.1	Governing Equations for Plates on Discrete Foundations .....	62
3.2.2	Elastic Continuous Model.....	63
<b>CHAPTER FOUR.....</b>		<b>66</b>
<b>RBF FORMULATIONS AND COMPUTER IMPLEMENTATION .....</b>		<b>66</b>
4.1	RBF Formulation .....	66



4.2	Computer Implementation .....	73
4.2.1	Mathematica Code for W-F Formulation .....	73
4.2.2	Mathematica Code for W-U-V Formulations .....	78
<b>CHAPTER FIVE .....</b>		<b>84</b>
<b>OPTIMIZATION OF RBF SHAPE VARIABLE C.....</b>		<b>84</b>
<b>CHAPTER SIX .....</b>		<b>94</b>
<b>VERIFICATION OF THE COMPUTER CODE FOR LARGE DEFLECTION OF THIN PLATE WITHOUT FOUNDATION (WOF) .....</b>		<b>94</b>
6.1	General .....	94
6.2	WOF Numerical Examples .....	97
6.2.1	WOF Immovable Square Plates.....	97
6.2.2	WOF Movable Square Plates.....	100
6.2.3	WOF Immovable Circular Plates.....	103
6.2.4	WOF Movable Circular Plates.....	106
6.3	Discussion of Results .....	109
<b>CHAPTER SEVEN.....</b>		<b>112</b>
<b>VERIFICATION OF THE COMPUTER CODES FOR LARGE DEFLECTION OF THIN PLATES ON DISCRETE FOUNDATION (WPF) .....</b>		<b>112</b>
7.1	General .....	112
7.2	WPF Numerical Examples .....	113
7.2.1	WPF Immovable Rectangular Plates .....	113

7.2.2	WPF Movable Square Plates .....	131
7.2.3	WPF Immovable Circular Plates .....	148
7.2.4	WPF Movable Circular Plates .....	157
7.2.5	WPF Small Deflection and Large Deflection Analyses .....	171
7.2.6	WPF Comparing Results with Available Case .....	174
<b>CHAPTER EIGHT.....</b>		<b>176</b>
<b>VERIFICATION OF THE COMPUTER CODE FOR LARGE DEFLECTION OF THIN PLATE ON ELASTIC CONTINUOUS FOUNDATION.....</b>		<b>176</b>
8.1	General .....	176
8.2	Numerical Examples for Plates on Continuous Foundations.....	178
<b>CHAPTER NINE.....</b>		<b>191</b>
<b>CORRELATIONS BETWEEN DISCRETE AND CONTINUOUS FOUNDATION MODELS .....</b>		<b>191</b>
9.1	General .....	191
9.2	Study Details .....	192
9.2.1	Linear Winkler (L-W).....	194
9.2.2	Non-Linear Winkler (NL-W).....	196
9.2.3	Pasternak Model (P).....	198
9.2.4	Winkler-Pasternak Model (W-P) .....	200
9.3	Verification of the Selected Best Statistical Models.....	201
<b>CHAPTER TEN.....</b>		<b>207</b>

<b>PRACTICAL APPLICATION: LARGE DEFLECTION OF THE BASE PLATE OF LARGE STORAGE TANK.....</b>	<b>207</b>
10.1 General .....	207
10.2 Details of the Large Storage Tank .....	210
<b>CHAPTER ELEVEN.....</b>	<b>217</b>
<b>CONCLUSIONS AND RECOMMENDATIONS.....</b>	<b>217</b>
11.1 Summary .....	217
11.2 Conclusions .....	219
11.3 Recommendations .....	222
<b>REFERENCES.....</b>	<b>223</b>
<b>APPENDICES.....</b>	<b>240</b>
Appendix A MATHEMATICA CODES (W-U-V).....	240
Appendix B Optimization of Shape Variable C .....	249
Appendix C Correlations of Foundation Parameters .....	257
<b>VITA.....</b>	<b>261</b>

## LIST OF TABLES

Table 5.1 Designated and Description of Plates Cases of Studies.....	86
Table 5.2 Range of Optimum $c$ for all Cases.....	93
Table 6.1 Designated and Description of Plates Cases of Studies.....	96
Table 6.2 Summary of the Results of SQ-CC-IM without Foundation .....	97
Table 6.3 Summary of the Results of SQ-SS-IM without Foundation.....	98
Table 6.4 Summary of the Results of SQ-CF1-IM without Foundation.....	99
Table 6.5 Summary of the Results of SQ-SF1-IM without Foundation.....	99
Table 6.6 Summary of the Results of SQ-CC-MO without Foundation.....	100
Table 6.7 Summary of the Results of SQ-SS-MO without Foundation .....	101
Table 6.8 Summary of the Results of SQ-CF1-MO without Foundation.....	102
Table 6.9 Summary of the Results of SQ-SF1-MO without Foundation .....	102
Table 6.10 Summary of the Results of CI-CC-IM without Foundation .....	103
Table 6.11 Summary of the Results of CI-SS-IM without Foundation .....	104
Table 6.12 Summary of the Results of CI-CF1-IM without Foundation.....	105
Table 6.13 Summary of the Results of CI-SF1-IM without Foundation .....	105
Table 6.14 Summary of the Results of CI-CC-MO without Foundation.....	106
Table 6.15 Summary of the Results of CI-SS-MO without Foundation.....	107
Table 6.16 Summary of the Results of CI-CF1-MO without Foundation .....	108
Table 6.17 Summary of the Results of CI-SF1-MO without Foundation.....	108
Table 7.1 SQCCIM Results of $\bar{w}, \bar{\sigma}_b, \bar{\sigma}_m$ at Load $\bar{q} = 180$ .....	113
Table 7.2 SQSSIM Results of $\bar{w}, \bar{\sigma}_b, \bar{\sigma}_m$ at Load $\bar{q} = 36$ .....	116
Table 7.3 SQCF1IM Results of $\bar{w}, \bar{\sigma}_b, \bar{\sigma}_m$ at Load $\bar{q} = 80$ .....	119

Table 7.4 SQSF1IM Results of $\bar{w}, \bar{\sigma}_b, \bar{\sigma}_m$ at Load $\bar{q} = 18$ .....	122
Table 7.5 SQCFIM Results of $\bar{w}, \bar{\sigma}_b, \bar{\sigma}_m$ at Load $\bar{q} = 80$ .....	125
Table 7.6 SQSFIM Results of $\bar{w}, \bar{\sigma}_b, \bar{\sigma}_m$ at Load $\bar{q} = 18$ .....	128
Table 7.7 SQSSMO Results of $\bar{w}, \bar{\sigma}_b, \bar{\sigma}_m$ at Load $\bar{q} = 40$ .....	131
Table 7.8 SQCCMO Results of $\bar{w}, \bar{\sigma}_b, \bar{\sigma}_m$ at Load $\bar{q} = 160$ .....	134
Table 7.9 SQSF1MO Results of $\bar{w}, \bar{\sigma}_b, \bar{\sigma}_m$ at Load $\bar{q} = 12$ .....	137
Table 7.10 SQCF1MO Results of $\bar{w}, \bar{\sigma}_b, \bar{\sigma}_m$ at Load $\bar{q} = 40$ .....	140
Table 7.11 SQSFMO Results of $\bar{w}, \bar{\sigma}_b, \bar{\sigma}_m$ at Load $\bar{q} = 12$ .....	143
Table 7.12 SQCFMO Results of $\bar{w}, \bar{\sigma}_b, \bar{\sigma}_m$ at Load $\bar{q} = 40$ .....	145
Table 7.13 CICCIM Results of $\bar{w}, \bar{\sigma}_b, \bar{\sigma}_m$ at Load $\bar{q} = 12$ .....	148
Table 7.14 CICFIM Results of $\bar{w}, \bar{\sigma}_b, \bar{\sigma}_m$ at Load $\bar{q} = 7.2$ .....	151
Table 7.15 CISF1IM Results of $\bar{w}, \bar{\sigma}_b, \bar{\sigma}_m$ at Load $\bar{q} = 3$ .....	154
Table 7.16 CICCMO Results of $\bar{w}, \bar{\sigma}_b, \bar{\sigma}_m$ at Load $\bar{q} = 8$ .....	157
Table 7.17 CISSMO Results of $\bar{w}, \bar{\sigma}_b, \bar{\sigma}_m$ at Load $\bar{q} = 3$ .....	160
Table 7.18 CICFMO Results of $\bar{w}$ , and $\bar{\sigma}_b$ at Load $\bar{q} = 4.8$ .....	163
Table 7.19 CISFMO Results of $\bar{w}, \bar{\sigma}_b, \bar{\sigma}_m$ at Load $\bar{q} = 1.5$ .....	166
Table 7.20 CISF1MO Results of $\bar{w}, \bar{\sigma}_b, \bar{\sigma}_m$ at Load $\bar{q} = 2$ .....	169
Table 7.21 Comparison Between RBF and BEM for CICCMO ( $\bar{q} = 15, G_1=K_1=0;$ $K=100$ ).....	175
Table 8.1 $\bar{w}, \bar{\sigma}_b$ , and $\bar{\sigma}_m$ at the Center of SQCCIM Plate on Continuous Foundation ..	178
Table 8.2 $\bar{w}, \bar{\sigma}_b$ , and $\bar{\sigma}_m$ at the Free Edge of SQCF1IM Plate on Continuous Foundation .....	179

Table 8.3 $\bar{w}$ , $\bar{\sigma}_b$ , and $\bar{\sigma}_m$ at the Free Edge of SQCFIM Plate on Continuous Foundation .....	182
Table 8.4 $\bar{w}$ , $\bar{\sigma}_b$ , and $\bar{\sigma}_m$ at the Center of CICCIM Plate on Continuous Foundation ....	184
Table 8.5 $\bar{w}$ , and $\bar{\sigma}_b$ at the Free Edge of CICF1IM Plate on Continuous Foundation....	186
Table 8.6 $\bar{w}$ , and $\bar{\sigma}_b$ at the Free Edge of CICFIM Plate on Continuous Foundation.....	188
Table 9.1 Young's Modulus of Different Types of Soils .....	192
Table 9.2 Results of K's at Different Values of $\nu_s$ and $E_s$ for L-W .....	194
Table 9.3 Poisson's Ratios and Corresponding Values of Equation Constants for L-W	196
Table 9.4 Comparison of L-W Model and Biot (1937) and Vesic (1961).....	206
Table 10.1 Discrete Foundation Parameters .....	210
Table 10.2 $\bar{w}$ , $\bar{\sigma}_b$ , and $\bar{\sigma}_m$ at the Plate Center For fixed Connection Case ( $\bar{q} = 220000$ ) .....	211
Table 10.3 $\bar{w}$ , $\bar{\sigma}_b$ , and $\bar{\sigma}_m$ at the Plate Center for Pinned Connection Case ( $\bar{q} = 220000$ ) .....	214

## LIST OF FIGURES

Figure 3.1 Definition of in-Plane Internal Forces of the Plates and their Projections on z Direction .....	37
Figure 3.2 Definition of out of Plane Internal Forces of the Plates .....	38
Figure 3.3 Directional Cosines .....	43
Figure 3.4 Calculations of $f_{ij}$ Coefficients in Boussinesq Formula. ....	65
Figure 4.1 Domain and Boundary Nodes .....	67
Figure 4.2 Flow Chart for the W-F Program .....	77
Figure 4.3 Flow Chart for the W-U-V Program .....	81
Figure 4.4 Plate Nodes Loads and Settlement .....	82
Figure 5.1 Nodes Distribution and Boundary Sides of Plates. a) Rectangular Plate, and b) Circular Plate .....	85
Figure 5.2 Average Errors % vs Shape Variable for SQ-CC-IM and SQ-SS-IM.....	86
Figure 5.3 Average Errors % vs Shape Variable for SQ-CC-MO and SQ-SS-MO .....	87
Figure 5.4 Average Errors % vs Shape Variable for SQ-CF-IM and SQ-SF-IM.....	87
Figure 5.5 Average Errors % vs Shape Variable for SQ-CF-MO and SQ-SF-MO.....	88
Figure 5.6 Average Errors % vs Shape Variable for CI-CC-IM and CI-SS-IM (WOF) ..	88
Figure 5.7 Average Errors % vs Shape Variable for CI-CC-IM and CI-SS-IM (WF) .....	89
Figure 5.8 Average Errors % vs Shape Variable for CI-CC-MO and CI-SS-MO (WOF).....	89
Figure 5.9 Average Errors % vs Shape Variable for CI-CC-MO and CI-SS-MO (WF) ..	90
Figure 5.10 Average Errors % vs Shape Variable for CI-CF-IM and CI-SF-IM .....	90
Figure 5.11 Average Errors % vs Shape Variable for CI-CF-MO and CI-SF-MO .....	91

Figure 6.1 Nodes Distribution and Boundary Sides of Plates. a) Square Plate, and b)	
Circular Plate .....	95
Figure 7.1 $\bar{w}$ vs $\bar{q}$ on Different Foundations for SQCCIM.....	114
Figure 7.2 $\bar{\sigma}_b$ vs $\bar{q}$ on Different Foundations for SQCCIM.....	115
Figure 7.3 $\bar{\sigma}_m$ vs $\bar{q}$ on Different Foundations for SQCCIM.....	115
Figure 7.4 $\bar{w}$ vs $\bar{q}$ on Different Foundations for SQSSIM.....	117
Figure 7.5 $\bar{\sigma}_b$ vs $\bar{q}$ on Different Foundations for SQSSIM.....	118
Figure 7.6 $\bar{\sigma}_m$ vs $\bar{q}$ on Different Foundations for SQSSIM.....	118
Figure 7.7 $\bar{w}$ vs $\bar{q}$ on Different Foundations for SQCF1IM.....	120
Figure 7.8 $\bar{\sigma}_b$ vs $\bar{q}$ on Different Foundations for SQCF1IM.....	121
Figure 7.9 $\bar{\sigma}_m$ vs $\bar{q}$ on Different Foundations for SQCF1IM.....	121
Figure 7.10 $\bar{w}$ vs $\bar{q}$ on Different Foundations for SQSF1IM.....	123
Figure 7.11 $\bar{\sigma}_b$ vs $\bar{q}$ on Different Foundations for SQSF1IM.....	124
Figure 7.12 $\bar{\sigma}_m$ vs $\bar{q}$ on Different Foundations for SQSF1IM.....	124
Figure 7.13 $\bar{w}$ vs $\bar{q}$ on Different Foundations for SQCFIM.....	126
Figure 7.14 $\bar{\sigma}_b$ vs $\bar{q}$ on Different Foundations for SQCFIM.....	127
Figure 7.15 $\bar{\sigma}_m$ vs $\bar{q}$ on Different Foundations for SQCFIM.....	127
Figure 7.16 $\bar{w}$ vs $\bar{q}$ on Different Foundations for SQSFIM.....	129
Figure 7.17 $\bar{\sigma}_b$ vs $\bar{q}$ on Different Foundations for SQSFIM.....	130
Figure 7.18 $\bar{\sigma}_m$ vs $\bar{q}$ on Different Foundations for SQSFIM.....	130
Figure 7.19 $\bar{w}$ vs $\bar{q}$ on Different Foundations for SQSSMO.....	132
Figure 7.20 $\bar{\sigma}_b$ vs $\bar{q}$ on Different Foundations for SQSSMO.....	133
Figure 7.21 $\bar{\sigma}_m$ vs $\bar{q}$ on Different Foundations for SQSSMO.....	133



Figure 7.22 $\bar{w}$ vs $\bar{q}$ on Different Foundations for SQCCMO .....	135
Figure 7.23 $\bar{\sigma}_b$ vs $\bar{q}$ on Different Foundations for SQCCMO .....	136
Figure 7.24 $\bar{\sigma}_m$ vs $\bar{q}$ on Different Foundations for SQCCMO .....	136
Figure 7.25 $\bar{w}$ vs $\bar{q}$ on Different Foundations for SQSF1MO .....	138
Figure 7.26 $\bar{\sigma}_b$ vs $\bar{q}$ on Different Foundations for SQSF1MO .....	139
Figure 7.27 $\bar{w}$ vs $\bar{q}$ on Different Foundations for SQCF1MO.....	141
Figure 7.28 $\bar{\sigma}_b$ vs $\bar{q}$ on Different Foundations for SQCF1MO.....	141
Figure 7.29 $\bar{\sigma}_m$ vs $\bar{q}$ on Different Foundations for SQCF1MO.....	142
Figure 7.30 $\bar{w}$ vs $\bar{q}$ on Different Foundations for SQSFMO .....	144
Figure 7.31 $\bar{\sigma}_b$ vs $\bar{q}$ on Different Foundations for SQSFMO .....	144
Figure 7.32 $\bar{w}$ vs $\bar{q}$ on Different Foundations for SQCFMO.....	146
Figure 7.33 $\bar{\sigma}_b$ vs $\bar{q}$ on Different Foundations for SQCFMO.....	147
Figure 7.34 $\bar{\sigma}_m$ vs $\bar{q}$ on Different Foundations for SQCFMO.....	147
Figure 7.35 $\bar{w}$ vs $\bar{q}$ on Different Foundations for CICCIM.....	149
Figure 7.36 $\bar{\sigma}_b$ vs $\bar{q}$ on Different Foundations for CICCIM.....	150
Figure 7.37 $\bar{\sigma}_m$ vs $\bar{q}$ on Different Foundations for CICCIM.....	150
Figure 7.38 $\bar{w}$ vs $\bar{q}$ on Different Foundations for CICFIM .....	152
Figure 7.39 $\bar{\sigma}_b$ vs $\bar{q}$ on Different Foundations for CICFIM .....	153
Figure 7.40 $\bar{\sigma}_m$ vs $\bar{q}$ on Different Foundations for CICFIM .....	153
Figure 7.41 $\bar{w}$ vs $\bar{q}$ on Different Foundations for CISF1IM.....	155
Figure 7.42 $\bar{\sigma}_b$ vs $\bar{q}$ on Different Foundations for CISF1IM.....	156
Figure 7.43 $\bar{\sigma}_m$ vs $\bar{q}$ on Different Foundations for CISF1IM.....	156
Figure 7.44 $\bar{w}$ vs $\bar{q}$ on Different Foundations for CICCMO .....	158

Figure 7.45 $\bar{\sigma}_b$ vs $\bar{q}$ on Different Foundations for CICCMO .....	159
Figure 7.46 $\bar{\sigma}_m$ vs $\bar{q}$ on Different Foundations for CICCMO .....	159
Figure 7.47 $\bar{w}$ vs $\bar{q}$ on Different Foundations for CISSMO .....	161
Figure 7.48 $\bar{\sigma}_b$ vs $\bar{q}$ on Different Foundations for CISSMO .....	162
Figure 7.49 $\bar{\sigma}_m$ vs $\bar{q}$ on Different Foundations for CISSMO .....	162
Figure 7.50 $\bar{w}$ vs $\bar{q}$ on Different Foundations for CICFMO.....	164
Figure 7.51 $\bar{\sigma}_b$ vs $\bar{q}$ on Different Foundations for CICFMO.....	165
Figure 7.52 $\bar{\sigma}_m$ vs $\bar{q}$ on Different Foundations for CICFMO.....	165
Figure 7.53 $\bar{w}$ vs $\bar{q}$ on Different Foundations for CISFMO .....	167
Figure 7.54 $\bar{\sigma}_b$ vs $\bar{q}$ on Different Foundations for CISFMO .....	168
Figure 7.55 $\bar{w}$ vs $\bar{q}$ on Different Foundations for CISF1MO .....	170
Figure 7.56 $\bar{\sigma}_b$ vs $\bar{q}$ on Different Foundations for CISF1MO .....	170
Figure 7.57 $\bar{\sigma}_m$ vs $\bar{q}$ on Different Foundations for CISF1MO .....	171
Figure 7.58 Comparison between Small Deflection (S) and Large Deflection (L) Formulations for the Central Deflection of SQCCIM Plate on Different Foundations.....	172
Figure 7.59 Comparison between Small Deflection (S) and Large Deflection (L) Formulations for the Maximum Bending Stress in SQCCIM Plate on Different Foundations .....	173
Figure 7.60 Comparison between Small Deflection (S) and Large Deflection (L) Formulations for the Central Deflection of CICCMO Plate on Different Foundations.....	173

Figure 7.61 Comparison between Small Deflection (S) and Large Deflection (L) Formulations for the Maximum Bending Stress in CICC MO Plate on Different Foundations .....	174
Figure 8.1 3D FEM Square Plate on Elastic Half Space Soil Model .....	177
Figure 8.2 Load-Central Deflections for SQCF1IM Plate on Continuous Foundation ..	180
Figure 8.3 Loads-Central Bending Stresses for SQCF1IM Plate on Continuous Foundation .....	181
Figure 8.4 Loads-Central Membrane Stresses for SQCF1IM Plate on Continuous Foundation .....	181
Figure 8.5 Loads-Central Deflections for SQCFIM Plate on Continuous Foundation...	183
Figure 8.6 Loads-Central Bending Stresses for SQCFIM Plate on Continuous Foundation .....	183
Figure 8.7 Loads-Central Membrane Stresses for SQCFIM Plate on Continuous Foundation .....	184
Figure 8.8 Loads-Central Deflections for CICF1IM Plate on Continuous Foundation..	186
Figure 8.9 Loads-Central Bending Stresses for CICF1IM Plate on Continuous Foundation .....	187
Figure 8.10 Loads-Central Membrane Stresses for CICF1IM Plate on Continuous Foundation .....	187
Figure 8.11 Loads-Central Deflections for CICFIM Plate on Continuous Foundation..	189
Figure 8.12 Loads-Central Bending Stresses for CICFIM Plate on Continuous Foundation .....	189

Figure 8.13 Loads-Central Membrane Stresses for CICFIM Plate on Continuous Foundation .....	190
Figure 9.1 $K$ vs $E_s$ (L-W).....	195
Figure 9.2 $K$ vs $E_s$ (NL-W).....	197
Figure 9.3 $K_1$ vs $E_s$ (NL-W).....	198
Figure 9.4 $K$ vs $E_s$ (P) .....	199
Figure 9.5 $G_1$ vs $E_s$ (P).....	199
Figure 9.6 $\bar{w}$ vs $\bar{q}$ for Continuous and L-W Models .....	201
Figure 9.7 $\bar{w}$ vs $\bar{q}$ for Continuous and NL-W Models.....	202
Figure 9.8 $\bar{w}$ vs $\bar{q}$ for Continuous and Pasternak (P) Models.....	202
Figure 9.9 $\bar{w}$ vs $\bar{q}$ for Continuous and W- P Models.....	203
Figure 9.10 $\bar{w}$ vs $\bar{q}$ for all Models ( $E_s = 1000$ ).....	203
Figure 9.11 $\bar{w}$ vs $\bar{q}$ for all Models ( $E_s = 3000$ ).....	204
Figure 9.12 $\bar{w}$ vs $\bar{F}$ for all Models ( $E_s = 5000$ ) due to a Point Load .....	204
Figure 10.1 Steel Tanks. a) Bolted, b) Welded, and c) Construction .....	208
Figure 10.2 Typical Tank Section and Static Systems. a) Typical Tank Cross Section, b) Fixed Connection, and c) Simple Connection .....	209
Figure 10.3 $\bar{w}$ vs $\bar{q}$ for the Fixed Connection Case.....	212
Figure 10.4 $\bar{\sigma}_b$ vs $\bar{q}$ for the Fixed Connection Case .....	212
Figure 10.5 $\bar{\sigma}_m$ vs $\bar{q}$ for the Fixed Connection Case .....	213
Figure 10.6 $\bar{w}$ along the Radial Directions of Different Foundation Models for the Fixed Connection Case .....	213
Figure 10.7 $\bar{w}$ vs $\bar{q}$ for the Pinned Connection Case.....	215

Figure 10.8 $\bar{\sigma}_b$ vs $\bar{q}$ for the Pinned Connection Case .....	215
Figure 10.9 $\bar{\sigma}_m$ vs $\bar{q}$ for the Pinned Connection Case .....	216
Figure 10.10 $\bar{w}$ along the Radial Directions of Different Foundation Models for the Pinned Connection Case .....	216

## LIST OF SYMBOLS

$a$	:	Dimension of Plate in x Direction
$b$	:	Dimension of Plate in y Direction
$t$	:	Thickness of Plate
$\nu$	:	Poisson Ratio of Plate
$E$	:	Young's Modulus of Plate
$\nu_s$	:	Poisson Ratio of Soil
$E_s$	:	Young's Modulus of Soil
$\alpha$	:	Plate Aspect Ratio
$\beta$	:	Plate Length-to-Thickness Ratio
$\sigma_b$	:	Bending Stress
$\sigma_m$	:	Membrane Stress
$\bar{\sigma}_b$	:	Dimensionless Bending Stress
$\bar{\sigma}_m$	:	Dimensionless Membrane Stress
$w$	:	Deflection of Plate in z Direction
$u$	:	Deflection of Plate in x Direction
$v$	:	Deflection of Plate in y Direction
$\bar{w}$	:	Dimensionless Deflection of Plate in z Direction
$k$	:	Linear Winkler Parameter
$k_1$	:	Non-Linear Winkler Parameter
$g_p$	:	Pasternak Shear Parameter

$K$	:	Dimensionless Linear Winkler Parameter
$K_1$	:	Dimensionless Non-Linear Winkler Parameter
$G_1$	:	Dimensionless Pasternak Shear Parameter
$q$	:	Uniformly Distributed Transverse Loads
$\bar{q}$	:	Dimensionless Uniformly Distributed Transverse Loads
$P$	:	Supporting Soil Reaction
$F$	:	Stress Function
$V_n$	:	Internal Shear Forces
$M_n$	:	Internal Bending Moment
$N_x$	:	In-Plane Internal Forces in x Direction
$N_y$	:	In-Plane Internal Forces in y Direction
$N_{xy}$	:	In-Plane Internal Shear Forces

# **DISSERTATION ABSTRACT**

**NAME: MOHAMMED MOHAMMED HUSSEIN AL-THOLAIA**

**TITLE: RBF-BASED MESHLESS METHOD FOR LARGE DEFLECTION  
OF PLATES ON NONLINEAR FOUNDATIONS**

**Major Field: CIVIL ENGINEERING**

**DATE of Degree: January, 2015**

Modeling the interaction between the soil and the structural foundation is a major concern in many engineering applications. The soil foundations very often represent a complex medium and therefore it is extremely difficult to obtain analytical-based solutions for this interaction. The problem becomes more difficult if the structure is undergoing large deformation. Numerical methods are powerful alternative tools to solve such complicated problems. There are two main categories of these methods: element-based methods such as the finite element (FEM) and the boundary element (BEM) and element free-based or mesh-less methods like radial basis functions (RBF). The FEM and BEM have been studied extensively so far, whereas the RBF still needs to be investigated for the use in various engineering application areas.

Free-element or free-mesh methods are advantageous for problems that require frequent re-meshing such as those arising in non-linear analysis. In this work, the use of multi-quadratic radial basis function (MQ-RBF) is proposed to solve the problem of large deflection of thin elastic plates resting on nonlinear foundations. The study covers several variables, including the plate shape, the loading type, the boundary conditions, the



foundation type and the foundation parameter. Two types of foundation models (discrete and continuous) are adopted. The discrete foundation model consists of Winkler, non-linear Winkler, Pasternak and non-linear Winkler-Pasternak model whereas the Boussinesq model is used to represent interaction of the plate with the continuous foundation.

WALFRAM MATHEMATICA software was utilized for the development of the computer codes. The accuracy and efficiency of the method is demonstrated by comparing the obtained solution with readily available and corresponding numerical solutions. From the comparison, the obtained results from MQ-RBF method are close to the ones obtained from FEM. As a main conclusion, the proposed meshless-based method (MQ-RBF) can be utilized as a good alternative numerical method for the element based numerical methods such as FEM and BEM in the solution of the large deflection of thin elastic plates on nonlinear foundations. The developed computer codes have been utilized to generate correlations between discrete and continuous foundation parameters. The obtained correlations of the foundation parameters have been verified through several examples which revealed that the Pasternak and non-linear Winkler-Pasternak discrete models are the most in agreement with the continuous foundation model.

**DOCTOR OF PHILOSOPHY IN CIVIL ENGINEERING  
KING FAHD UNIVERSITY OF PETROLEUM AND MINERALS  
DHAHRAN, SAUDI ARABIA**

## ملخص الأطروحة

**الإسم :** محمد محمد حسين الثلثيا  
**عنوان الرسالة:** طريقة الـ RBF خالية الشبكة لتحليل الإنحراف العالي لإلواح الأساسات على الأساسات الغير خطيه  
**التخصص :** الهندسة المدنية  
**تاريخ التخرج :** يناير 2015

تعتبر نمذجة التفاعل بين التربة والأساس الإنشائي مصدر قلق كبير في العديد من التطبيقات الهندسية. تربة الأساسات في كثير من الأحيان تمثل أوساط معقدة، وبالتالي فإنه من الصعب للغاية الحصول على الحلول ذات الطبعه التحليلية لهذا التفاعل. هذا وتصبح المشكلة أكثر صعوبة إذا كانت ألواح الأساسات يحصل لها إنحراف كبير . وعليه, تعتبر الطرق العددية أفضل طرق الحل المستخدمه لحل مثل هذه المسائل المعقده حيث يوجد نوعين رئيسيين من هذه الطرق هما: النوع الأول هي الطرق التي تعتمد على العناصر المتناهية الصغر المحدوده (FEM) وكذلك العناصر المتناهية الصغر على الاطراف او الحدود (BEM) والنوع الثاني هي الطرق الخالية الشبكة اوبدون العناصر المتناهية الصغر مثل الداله قطرية الأساس (RBF).

النوع الأول من الطرق المستخدمه ( FEM و BEM) قد تم دراستهم بشكل مكثف منذ زمن بعيد حتى اليوم في حين أن النوع الثاني (RBF) لا تزال بحاجة إلى الدراسة والفحص لإستخدامها في مختلف مجالات التطبيق الهندس يقي الطرق الخالية من العناصر أو الخالية من الشبكة تعتبر مفيدة وجيده للمسائل التي تتطلب اعادة تكوين الشبكة مثل أولئك اللاتي يظهرن في حالة التحليلات الغير خطيه

في هذه الدراسة، تم إقتراح إستخدام الداله قطرية الأساس ال متعددة من الدرجة الثانية ( MQ-RBF) لحل مشكلة الإنحراف الكبير لألواح الأساسات الرقيقه المرنه المستنده على اساسات غير خطيه . حيث قد شملت الدراسة العديد

من المتغيرات، بما في ذلك شكل ألواح الاساسات، طرق تثبيت ألواح الأساسات من الأطراف , نوع التحميل ، انواع الأساسات المختلفه وكذلك معاملات الأساسات . تم اعتبار نوعين رئيسيين من نماذج الأساسات وهما المنفصل او المتقطع والمتصل او المستمر. النموذج المتقطع يتكون من اربعة نماذج هي : Winkler, Winkler الغير خطي و Pasternak و Winkler-Pasternak الغير خطي , بينما تم استخدام نموذج Boussinesq في تمثيل التفاعل بين لوح الأساس والأساس المتصل.

هذا وقد تم استخدام البرنامج الخاص بمسائل الرياضيات (WALFRAM MATHEMATICA) لإعداد شفرات لوغاريتيميه لتنفيذ الحل المقترح لهذه المسائل باستخدام الحاسوب الآلي . وللتأكد من دقة الشفرات اللوغاريتيميه والطريقه المقترحه في هذه الدراسه فقد تم مقارنة النتائج بالنتائج المشابهه والتي تم الحصول عليها من النوع الاول للطرق العدديه التي تم ذكرها سابقا وهي طريقة العناصر المتناهية الصغر ( FEM ) حيث أظهرت المقارنه مدى تقارب النتائج ببعضها مما يؤكد على ان الطريقه المقترحه هنا يمكن استخدامها كبديل جيد للنوع الأول من الطرق العدديه مثل ( BEM,FEM ) من حيث السهوله في التنفيذ وكذلك الدقه في النتائج. هذا وتم استخدام الشفرات اللوغاريتيميه المحققه في إيجاد علاقات بين معاملات نماذج الأساسات المتقطعه والمتصله حيث تم التحقق من هذه العلاقات عن طريق الكثير من الامثله وثبت ان Pasternak و Winkler-Pasternak الغير خطي هما الأكثر اتفاقا مع الأساس المتصل.

**درجة الدكتوراة في الفلسفه في الهندسه المدنيه**

**جامعة الملك فهد للبترول والمعادن**

**الظهران – المملكه العربيه السعوديه**

# CHAPTER ONE

## INTRODUCTION

### 1.1 General

The problem of interaction between structural foundations and supporting soil is of fundamental importance in foundation design and therefore, it has attracted the attention of many researchers and engineers. The interaction is often represented by the classical problem of plate on elastic foundation. The main difficulty in the modeling of a plate on an elastic foundation is the determination of the contact pressure. The problem becomes more difficult if the plate is undergoing large deformation. The governing equations become coupled and nonlinear. Furthermore, the layer of soil in contact with the plate behaves nonlinearly. The available analytical methods are based on simplified assumptions and are limited to simple loading and boundary conditions. For such complicated problems, numerical methods offer convenient and reliable solutions.

The ideal numerical method for the solution of nonlinear partial differential equations (PDEs) such as the one considered here should be high-order accurate, flexible with respect to the geometry, computationally efficient, and easy to implement. The conventional numerical methods that are commonly used usually fulfill one or two of these criteria, but not all. Finite difference methods (FDM), finite element methods (FEM) and boundary element methods (BEM) have been the dominating methods for the

numerical solution of PDEs. Referring to the most dominant approach, i.e. FEM, it is highly flexible, but it is hard to achieve high-order accuracy and both coding and mesh generation become increasingly difficult as the problem dimension increases. The use of a mesh implies that specific procedures have to be devised just to define the mesh. Also, and to keep the order of the local approximation within reasonable limits, the element size has to be reduced, whenever better approximations are pursued. The extraordinary amount of work, which has been put into FEM research, has circumvented these and other problems associated with the existence of a mesh and made FEM the dominant approach for most problems in computational mechanics. Accordingly, many sophisticated powerful codes (e.g. ANSYS, ABACUS, COMSOL, etc.) have been established and have proven to be reliable in solving almost any computational mechanics problem.

FDM can be made high-order accurate in resolving PDEs, but require a structured grid (or a collection of structured grids), which makes it difficult to model features of irregular domain. Furthermore, solutions of PDEs using FDM can be derived from the assumptions of the local interpolation schemes and require a mesh to support the localized approximations, however, the construction of a mesh in two or more dimensions is a non-trivial problem. In recent years, BEM has become a powerful alternative to FEM and FDM, especially for problems involving high gradients and stress concentrations. It has been successfully applied to solve the problems of large deflection of thin elastic plates. However, this was possible by devising some techniques to

overcome the inherent deficiency of BEM as a self-standing numerical method in handling nonlinearities.

Nevertheless, the possibility of obtaining numerical solutions for PDFs without resorting to element frame, that is mesh-less technique, has been the goal of many researchers throughout the computational mechanics community for the past two decades. Radial Basis Function (RBF)-based collocation method, as one of the most recently developed numerical techniques, so-called mesh free or meshless methods, has attracted attention in recent years especially in the area of computational mechanics. This method does not require mesh generation which makes them advantageous for 3-D problems as well as problems that require frequent re-meshing such as those arising in nonlinear analysis. Due to its simplicity to implement, it represents an attractive alternative to FEM, FDM and BEM as a solution method of nonlinear PDEs. However, it is only recently that the RBFs have been used to approximate solutions to PDEs and therefore this area is still relatively unexplored. In this work, RBF-based meshless model, multi-quadratic RBF (MQ-RBF), is developed for the solution of large deflection of thin elastic plates resting on nonlinear foundations. The study covers several variables, including the plate shape, the boundary condition and the foundation type and parameter.

Two types of foundation models (discrete and continuous) are adopted. The discrete foundation model consists of Winkler, non-linear Winkler, Pasternak and non-linear Winkler-Pasternak model whereas the Boussinesq model approach is used for the continuous foundation.

WALFRAM MATHEMATICA software has been utilized for the development of the computer codes. The accuracy and efficiency of the method has been demonstrated by comparing the obtained solution with FEM solution. From the comparison, the obtained results by MQ-RBF method are close to the ones obtained by FEM. As a main conclusion, the proposed meshless-based method (MQ-RBF) can be utilized as a good alternative numerical method to the element based numerical methods such as FEM and BEM for the solution of large deflection of thin elastic plates on nonlinear foundations. The developed computer codes have been utilized to generate correlations between discrete and continuous foundation parameters. The obtained correlations of the foundation parameters are verified through several examples which revealed that Pasternak and non-linear Winkler-Pasternak discrete models are the most in agreement with the continuous foundation.

## 1.2 Problem Statement

The nonlinear behavior of a thin elastic plate undergoing large deflection is governed by the well known von Karman equations [Timoshenko and Kreiger, 1959]:

$$\nabla^4 F = NLW \quad (1.1)$$

$$\nabla^4 w = NLWF + \frac{q}{D} \quad (1.2)$$

$$NLW = E \left[ \left( \frac{\partial^2 w}{\partial x \partial y} \right)^2 - \left( \frac{\partial^2 w}{\partial x^2} \right) \left( \frac{\partial^2 w}{\partial y^2} \right) \right] \quad (1.3)$$

$$NLWF = \frac{t}{D} \left[ \left( \frac{\partial^2 F}{\partial y^2} \right) \left( \frac{\partial^2 w}{\partial x^2} \right) + \left( \frac{\partial^2 F}{\partial x^2} \right) \left( \frac{\partial^2 w}{\partial y^2} \right) - 2 \left( \frac{\partial^2 F}{\partial x \partial y} \right) \left( \frac{\partial^2 w}{\partial x \partial y} \right) \right] \quad (1.4)$$

Where;  $w$  is the lateral deflection,  $F$  is a stress function,  $q$  is the distributed load,  $t$  is the plate thickness,  $D = \frac{Et^3}{12(1-\nu^2)}$  is the flexural rigidity of the plate and  $E$  and  $\nu$  are Young's modulus and Poisson's ratio of the plate. The above equations along with the given lateral boundary conditions can be used to obtain the solution for the case of movable edges.

In the case of immovable edges, the large deflection of the plates should be expressed in terms of the three displacements  $u$ ,  $v$ , and  $w$ . The details of the resulted equations are given in Naffa and Al-Gahtani (2006). For convenience, the final equations are presented here:



$$L_{11}(u) + L_{12}(v) = NL_1(w) \quad (1.5)$$

$$L_{12}(u) + L_{22}(v) = NL_2(w) \quad (1.6)$$

$$\nabla^4 w = \frac{q}{D} + NL_3(u, v, w) \quad (1.7)$$

Where,

$$L_{11} = \frac{2 \partial_{xx} + (1 - \nu) \partial_{yy}}{2(1 - \nu^2)} \quad (1.8)$$

$$L_{12} = \frac{2 \partial_{xy}}{2(1 - \nu)} \quad (1.9)$$

$$L_{22} = \frac{2 \partial_{yy} + (1 - \nu) \partial_{xx}}{2(1 - \nu^2)} \quad (1.10)$$

$$NL_1(w) = - \frac{(1 + \nu)w_{xy}w_y + w_x(2w_{xx} + (1 - \nu)w_{yy})}{2(1 - \nu^2)} \quad (1.11)$$

$$NL_2(w) = - \frac{(1 + \nu)w_{xy}w_x + w_y(2w_{yy} + (1 - \nu)w_{xx})}{2(1 - \nu^2)} \quad (1.12)$$

$$NL_3(u, v, w)$$

$$\begin{aligned} &= \frac{Etw_{xy}}{D(1 + \nu)}(u_y + v_x + w_x w_y) + \frac{Etw_{xx}}{2D(1 - \nu^2)}(2u_x + w_x^2 + \nu(2v_y + w_y^2)) \\ &+ \frac{Etw_{yy}}{2D(1 - \nu^2)}(2v_y + w_y^2 + \nu(2u_x + w_x^2)) \end{aligned} \quad (1.13)$$

Where; the subscripts indicate derivatives with the respective coordinates. The reaction at the plate-foundation interface can be accounted for by adding the following terms to the plate load:

$$-kw - k_1 w^3 + g_p \nabla^2 w \quad (1.14)$$

Where:  $k$  is the Winkler foundation stiffness,  $k_1$  is the nonlinear Winkler foundation modulus, and  $g_p$  is the interaction parameter due to shear action among the spring elements. The above approach of modeling the plate-foundation interface suffers from the drawback that the parameters are difficult to determine. To overcome this difficulty, the foundation (soil) can be modeled as continuous elastic continua. The results of the continuum model can then be used to estimate the above three parameters for a given soil type. The solution of the above coupled and highly nonlinear equations will be attempted by the use of RBF method as mentioned earlier. In general, RBF-based collocation method expands the solution of a problem in terms of radial basis functions and chooses expansion coefficients such that the governing equations and boundary conditions are satisfied at some selected domain and boundary points. However, one of the most challenging issues in applying this technique is the determination of the proper form of radial basis function for a given differential equation. Once the RBF function is selected, its shape factor needs to be optimized for the considered problem. Another challenging issue is related to the enforcement of zero shears on the free boundary of the plate. In large deflection, analysis, the shear force is a highly nonlinear function of the deflection derivatives as given by the following equation:

$$\begin{aligned}
V_n = \frac{Et}{12(-1 + \nu^2)} & \left( -n_x^3 t^2 w_{xyy} (-1 + \nu) + n_x^2 n_y t^2 (2w_{xxy} - w_{yyy}) (-1 + \nu) \right. \\
& + n_y (t^2 w_{xxy} + n_y^2 t^2 w_{xxy} - 12v_y w_y - 6w_x^2 w_y - 6w_y^3 + t^2 w_{yyy} \\
& + 6u_y w_x (-1 + \nu) + 6v_x w_x (-1 + \nu) - n_y^2 t^2 w_{xxy} \nu - 12u_x w_y \nu) \\
& + n_x \left( -12u_x w_x - 6w_x^3 + t^2 w_{xxx} + n_y^2 t^2 w_{xxx} + t^2 w_{xyy} - 2n_y^2 t^2 w_{xyy} - 6u_y w_y \right. \\
& - 6v_x w_y - n_y^2 t^2 w_{xxx} \nu + 2n_y^2 t^2 w_{xyy} \nu + 6u_y w_y \nu + 6v_x w_y \nu \\
& \left. \left. - 6w_x (w_y^2 + 2v_y \nu) \right) \right) \tag{1.15}
\end{aligned}$$

Where;  $w$ ,  $u$  and  $v$  are the components of displacements;  $n_x$  and  $n_y$  are the components of the unit normal to the boundary and the subscripts indicate derivatives with the respective coordinates.

### 1.3 Motivation and Objectives

From the reviewed literature, it can be concluded that there is still a gap in the available solutions for the large deflection of plates on nonlinear foundations. Most of these solutions are limited to simplified foundation models and/or boundary conditions. In particular, the important case of plates with free edges has not been addressed by almost all of the surveyed literature. In addition, the interaction between the plate and the foundation was not covered in a comprehensive way to include all foundation models.

The main objective of this study is to develop a meshless method for the analysis of large deflection of thin elastic plates on non-linear foundation with general geometries,

boundary conditions and foundation parameters. The model is based on the method of collocation with RBFs. The specific objectives are to:

1. Develop a meshless model for the large deflection of thin elastic plates using collocation method with multi-quadric radial basis functions (MQ-RBF).
2. Extend the model to account for the plate-foundation interface employing Winkler, nonlinear Winkler, Pasternak, non-linear Winkler Pasternak and continuous models.
3. Implement the developed models into computer codes using *MATHEMATICA* software.
4. Verify the accuracy of the developed codes by comparing the obtained solution with readily available analytical or numerical solutions for practical cases.
5. Utilize the computer codes in carrying out a detailed parametric investigation to compare various models in terms of their capabilities in modeling the plate-foundation behavior.

## **1.4 Outline of the Dissertation**

The dissertation consists of eleven chapters. Chapter 1 contains the introduction of the dissertation describes the problem, and states the objectives. Chapter 2 gives a comprehensive literature review on the topics relevant to the subject of the work. The review includes: available analytical and numerical solutions for the analysis of plates, plates resting on soil and undergoing large deflection; introduction of RBF, its

development and its application; soil foundation models. Chapter 3 contains the derivations of the governing differential equations for the large deflection of the thin plates (immovable and movable) in both dimensional and non-dimensional forms. The formulations of the supporting soil reaction are covered in this chapter. Chapter 4 describes the proposed multi-quadric RBF (MQ-RBF) method formulations and its application to the current problem. The chapter also contains the computer algorithms for the implementing the RBF formulations into Mathematica.

In Chapter 5, the optimization of the shape variable  $c$  of the proposed multi-quadric radial basis function method (MQ-RBF) is conducted. The optimization includes the plates with and without foundation. The developed Mathematica codes are verified in Chapters 6, 7, and 8 for the cases of plates without foundation, with discrete foundation models and with continuous foundation model, respectively.

Chapter 9 contains the development of relationships between the discrete foundation models parameters and the continuous model parameters. In Chapter 10, a real practical example, mainly bottom plates of large storage tank, has been analyzed and verified by comparing the results obtained from the continuous foundation model and the corresponding discrete foundation models based on the developed relationships. Finally, Chapter 11 summarizes conclusions from this work and states some recommendations for future work.

## CHAPTER TWO

### LITERATURE REVIEW

The results of the literature survey on the available analytical and numerical methods for the analysis of large deflection of plates on foundations along with the available foundation models describing their interactions are summarized below.

#### 2.1 General

For large deflection of thin isotropic plates, some approximate analytical solutions have been proposed in [Timoshenko & Woinowsky–Krieger, 1959]. Under different of support conditions, the deflections of rectangular plates were evaluated using mainly the equilibrium approach which involves the direct integration of the governing differential equations. The equilibrium approach was employed by assuming shape functions (the most challenging part to be in satisfactory shape in such approach) by Ye (1994), Little (1999), Ramachandra and Roy (2001), Wang et al (2002), and Wang & El-Sheikh, (2005).

The analytical solution methods are limited to cases involving simple plate geometries, boundary and supporting conditions. As a result of the huge development in the computing facilities (hardware and software), the researchers have directed their attentions to solve more complicated problems using the numerical methods which are summarized as: 1) Finite Difference Methods, 2) Gridwork Methods, 3) Finite Element

Methods (FEM), 4) Finite Strip methods, 5) Boundary Element Methods, and 6) Meshfree or Meshless Methods.

The finite difference method (FDM) is the oldest one and it is still valuable especially for plate problems. It is based on discretizing mathematically the plate continuum. The boundary conditions and the governing partial differential equations of the plate are expressed by corresponding finite difference proportion at each point in the mesh. After that, the whole resulted equations are solved as algebraic equations together. Such method gives accurate solution when the discretization is small. More details about FDM can be found in Forsyth and Wasow (1960), Hildebrand (1968), Ames (1977), Levy and Lessman,(1992), Papakaliatakis and Simos (1997), and Szilard (2004).

The second method is the grid-work method (GWM) which is a very good method for surface structures such as shells and plates. In this method, the plate continuum is replaced by an equivalent grid-work of beams. It is based on the physical discretization which needs to find the bending and torsional stiffness of these beams. It can be determined by strain energy of the plate and its replaced system or by stress conditions between the continuum and its grid-work beams. For the solution of the replaced system (grid-work beams), the matrix displacement method of the 3D framed structure is used. More information and details can be found in Hrennikoff (1941), Benard (1965), Saloner (1969), Yettram and Hussain (1971), Avram (1993), and Szilard (2004).

The most commonly used numerical method for solving the structural-mechanical problems is the finite element method (FEM). It follows the physical discretization by

dividing the continuum into elements called finite elements connected to each other by nodes in two or three dimensional structure. The FEM has numerous kinds that are used to analyze the plate problems. The most common types are: (1) displacement-based FEM, (2) hybrid FEM, and (3) equilibrium-based FEM.

Among the three FEM's types, the displacement-based FEM is used in engineering fields frequently because it is the most natural. In FEM, the properties of the load deformations of each element should be known in order to get the load deflection behavior of the structure by assembling the whole elements. In general, the analysis of the plate using FEM goes through the following steps: discretization of the plate, formulation of the element stiffness matrix, assembly all elements, applying the boundary conditions (prescribed boundary), the equations matrix of the displacement is then solved, and then evaluation of the results. It should be noted that the shape function which describes the displacement state must be chosen during the stiffness matrix formulation Szilard (2004).

As the matrix displacement is easy to be programmed and used in the computer applications, lots of programs and subroutines are available everywhere. Several types of commercial software are available like ADINA, ANSYS, ASKA, COMSOL, ABAQUS, etc. Examples of the research involving the application of FEM to the large deflection of plates can be found in the following references: Zienkiewicz (1965), Dhatt et al. (1969), Kawai and Yoshima (1969), Kikuchi (1975), Zienkiewicz (1978), Batoz et al. (1980), Batoz (1982), Batoz and Tahar (1982), Dhatt et al. (1986), Voyiadjis and Pecquet (1987), Jianqiao (1994), Soh et al. (1996), Turvey and Salehi (1997 and 1998), Amdahl



and Byklum (2002), Xue et al.(2003), Luo and Mote (2003), Yoo et al.(2004), Duan and Mahendran (2004), and Szilard (2004).

The fourth numerical method is the finite strip method (FSM) which is known as a particular case of FEM. It reduces the number of needed equations for the solution because it divides the plate into little number of strip divisions. Initially, it was used only for simply supported plate and then has been improved to cover other boundary condition in the longitudinal direction. Recently, it has been modified to handle stability and analysis of thin and moderately thick plates Szilard (2004).

The fifth numerical method is the boundary element method (BEM). The main difference between the BEM and both FDM and FEM is the discretization aspect. BEM is classified into two main different types: indirect and direct boundary element methods. The direct BEM deals with the clear meaningful physical variables in the formulation which makes it more reliable and meaningful while the indirect one uses singularities distribution over the body boundary and calculates this distribution by getting the solution of integral equation. Accordingly, the direct BEM is the most preferable and useful in the engineering fields.

To convert the governing differential equations of the plate into integral equations on the boundary, the Galerkin's variational approach is used. The resulted integral equations are then discretized by employing the field equation fundamental solutions to generate a certain number of elements on the boundary of the plate. The created elements have unknown variables which must be determined through the analysis. To accomplish

the analysis by the BEM, the prescribed boundary conditions are used to connect the unknown variables to the known ones on the boundary.

Several advantages are drawn from the use of the direct boundary element method compared to the other numerical methods (FDM, and FEM) such as reduction of the size of the problem which in turns simplifies the analysis of the whole problem. It also facilitates the representation and simulation of the infinite and semi-infinite domain such as plate-soil interaction. The key issue of this method is that it is still under development, i.e. it is not popular and general-purpose numerical method right now Szilard (2004).

There are several studies and research that have been conducted to cover the theory, algorithms, programs and applications of the BEM indifferent fields, including plate problems. A representing sample of BEM research can be found in Brebbia (1978), Tottenham (1979), Banerjee and Butterfield (1981), Du et al. (1984), Balas et al.(1989), Beer and waston (1992), Qin (1993), Qiao and Hua (1993), Kane (1994), Katsilkadelis and Nerantzaki(1994), El-Zarany et al. (1995), and Szilard (2004).

The main advantage of mesh-based methods when applied for large deformation problems is the mesh distortion and the need for re-meshing especially for structures of complex geometries. Both re-meshing and meshing distortion can be overcome by using the mesh-less methods as the interpolation in such methods is based on scattered nodes instead of mesh. One of the important mesh-less methods is the radial basis function method (RBF). It was used first in the early 1970s for fitting the scattered data by Hardy (1971). More details about RBF are given in Section 2.4.

Another mesh-less method is smooth particle hydrodynamics (SPH) which was proposed by Gingold (1977) and Lucy (1977), to model astrophysical phenomenon.

A third type of mesh-less methods is the Diffuse element method (DEM) which was introduced by Nayroles et al. (1992) based on moving least square approximations. A modification of the method has been proposed by Belytschko et al. (1994 and 1996) to enhance its accuracy.

A modification on the smooth particle hydrodynamics (SPH) was carried out by Liu (1995) by including a function to correct the kernel approximation in SPH to be compatible with the conditions of reproducing to come out with a new mesh-free method known as a reproducing kernel particle method (RKPM) which then was used for the analysis of large deformation problems Chen et al. (1996). Another mesh-less method was introduced by Liu and Belytschko (1997) which is known as moving least-square reproducing kernel method (MLSRK) by employing the moving least square interpolation function.

More recently, other types of meshless methods were developed by many researchers. Partition of unity method has been proposed by Babuska and Melenk(1996) and EFG and RKPM hp-cloud methods by Duarte and Oden (1996). Both of the hp-cloud and partition of unity methods are based mainly on the partition of unity concept. The local Petrov-Galerkin method which is based on local weak forms was introduced for nonlinear problems and computational mechanics by Atluri and Zhu(1998). Several different methods have been proposed such as the dual reciprocity boundary element method (DRBEM) by Chen et al.(2000), and Florez et al. (2000), the local boundary

integral equation (LBIE) by Atluri and Zhu (2000), and the method of collocation with RBF's by Pollandt (1997), Mikhailov (2000), Jumarchon et al.(2000), Zhang et al. (2000).

The above mesh-less methods have several advantages over mesh-based methods Liew et al. (2011) which can be summarized as follows: a) easier when applied to problems with complex geometries, b) for problems with large deformation and moving discontinuities, they provide efficient and more accurate results, c) additional nodes can be added easily in case of refinement to get more accurate solution at critical parts of the domain, d) they can be easily coupled with BEM or FEM to eliminate the disadvantage of each. For more details about the mesh-less, one can refer to Liu et al (1996), Li and Liu 2002, and Nguyen et al. (2008).

## **2.2 Analysis of Plates with Large Deflection**

### **2.2.1 Analytical Solutions**

Large deflection of plates has been studied by many researchers. Voyiadjis and Sarkan (1984) presented for the bending of plates with moderately large deflection a new theory which is an extension of small strains of plate theory. Their proposed theory took into consideration the transverse normal strain and it was used in an infinite plate to solve the problem of straight-crested waves.

Gorji (1989) has employed the equivalent load concept to develop a method which was used in the solution of the large deflection problems of orthotropic annular

plate according to the Von Karman governing equations. Simply of that he transformed the nonlinear terms into sets of loads in addition to the applied loads to the plate. By this transformation, the large displacement was converted to equivalent small deformation and then the equations were solved accordingly. Clamped and simply outer supported edges with free inner edges of plates were considered as numerical examples to ensure the accuracy and efficiency of the proposed method which have proved that it is accurate and efficient as well for such problems.

He (2003) has provided an approximate analytical solution to be used for the solution of the large deflection of thin circular plate utilizing the direct variational method. He presented a full theoretical basis for the finite element application and direct variational methods like Ritz method. In his method, the semi-inverse mesh was used to derive the variational principle.

Li et al. (2004) provided a new technique (incremental load technique) which was suitable for the solution of bending large deflection of an axi-symmetric simply supported plate. They have used the linear theory of thin plates for developing their method. In their method, the loads were divided into small steps at each of them the plate stress behavior is simplified to linear.

Bakker et al. (2009) provided analytical method in approximate form for the solution of thin rectangular plate with large deformation and simply supported exposed to transverse loading. The deflected shape of the first in-plane loading (compression) buckling mode was used as trail function to describe the total deflection of the plate. According to their method, the large deflection behavior of the plate under transverse

loading was formulated in-terms of the ratio of the pre-to-post-buckling in-plane stiffness of the plate.

Shufrin et al. (2010) proposed a semi-analytical method to be utilized in the solution of nonlinear analysis of trapezoidal and skew plates exposed to transverse loading. The nonlinear Van Karman strains combined with the thin elastic plate theory was used to the formulation of the large deformation of the plate. The method of multi-term extended Kantorovich was utilized to reduce the solution of the governing equations to the solution of ordinary differential equations instead of the partial differential equations. The non-rectangular geometry was switched to a rectangular computational domain.

Paik et al. (2012) provided analytical method to solve the elastic large deformation of metal plate under non-uniformly distributed lateral pressure with in-plane loads by applying the Galerkin method. Their method can be used as a better alternative method in the maritime industry for the plate design methods in the case of loads (high non-uniformity of lateral pressure).

Robert and Gorder (2012) introduced a method which is used to get perturbation solution for the Foppl-Von Karman equations that govern the large deformation of thin plate. His approach was created by the combination of Homotopy analysis method (to transform the nonlinear system of coupled PDE's into linear PDE's) and Fourier analysis to solve the resulted linear PDE's. His method makes the solution to be in few terms and perturbation solution does not depend on any parameters. The method was checked for

clamped and thickness goes to zero cases. The author of the method (Gorder) reported that his method can be modified to be used for other boundary conditions.

He et al. (2012) developed the Von Karman equation that describes the large deformation of the plate with different moduli in compression and tension and then used both the variational and displacement methods to solve the problem. Their method was created based on the flexural stiffness for a bi-modular thin plate in small deflection bending. The perturbation solution according to the deflection in the centre of the plate is valid based on the outcome from their study.

He et al. (2013) introduced a general analytical solution for the large deflection of thin plate (circular) with different moduli in compression and tension. With four boundary conditions (clamped, clamped-free to slip, simply supported and simply hinged) using the perturbation technique. They used the numerical results comparison with their method which has proved that the perturbation solution is valid.

A new approach was developed by Ibearugbulem et al. (2013) in which the direct integration of the governing differential equations of isotropic rectangular plate was carried out to get the suitable shape functions in two dimensional Taylor's series form. It used the principle of equilibrium of work developed by the action (load) and the reaction (plate) to get the equations of the deflection and the bending moments.

### **2.2.2 Numerical Solutions**

Turvey and Salehi (1990) developed a numerical solution method by using interlacing central finite difference discretization coupled with the dynamic relaxation

(DR) algorithm scheme to solve the large deflection of sector plates loaded uniformly. They verified the accuracy of their method through the use of the finite element results (ANSYS software) for clamped and simply sector plates.

Tanaka et al.(1996) presented an incremental formulation for the finite deflection of thin plates under the Von-Karman nonlinearity. They have obtained integral equations which then were numerically solved using the boundary domain element method. Their method was checked and validated by implementing several examples and comparing the results with known exact solution.

For orthotropic rectangular thin plate, Yeh et al. (2007) provided analysis of large deflection with two different boundary conditions, clamped and simply supported by utilizing approach called hybrid approach. Their approach uses combination form both differential transformation and finite difference method in order to reduce the governing equation of the large deflection of the orthotropic plate to a simple set of algebraic equations. They found that the accuracy of the solution for the clamped orthotropic plate is more or better than the simply supported ones. From the provided numerical examples, their method can be applied into the solution of the orthotropic plate large deformation problems with accepted accuracy.

Shahid et al. (2007) presented a mathematical method to analyze very large deformation of thin plates under nonlinear static loadings. Their model was developed according to the elastic Cosserat theory and virtual work principle by appropriate interpolation for the displacement and rotation fields on all domains satisfied the boundary conditions. In their work, square computational domain was created after



converting an arbitrary quadrilateral plate through a linear mapping. Important advantages for their method such as no need for mesh discretization which leads to minimal input data for the numerical computation.

Naffa and Al-Gahtani (2007) provided a numerical mesh-less method for the solution of large deflection of thin plate. In their method, the fifth order polynomial radial basis function was utilized to solve the two coupled nonlinear differential governing equation of thin plate incrementally. The used method in their study was verified by implementing several numerical examples for the movable edges (free to move in the in-plane directions of the plate).

Al-Gahtani and Naffa'a (2009) developed mesh-less formulation for the solution of the large deflection problems of immovable thin plates. They have used the fifth order polynomial radial basis function for the solution of the governing equations which were formulated in-terms of three displacement components  $u$ ,  $v$ , and  $w$ . The generated couple nonlinear system of equations was solved incrementally by iterative procedure.

Andakhshideh et al. (2010) have presented an approach based on the generalized differential quadrature to be utilized for the solution of large deformation analysis problems of laminated sector plates. The advantage of their method is that it can handle such problems under several boundary conditions such as clamped, simply and free edges or even combination of them. They have used the Newton-Raphson method for the solution of the resulting nonlinear equations iteratively. As they have concluded from their study after implementing several examples, their method is accurate and quick convergent method.

## **2.3 Analysis of Plates on Foundations**

### **2.3.1 Analytical Solutions**

In 1998, Shen provided large deflection analysis for Reissner-Mindlin plates with free edge on Pasternak foundation under the combined action of the temperature and transverse load. He used Reissner-Mindlin formulations and the mixed Galerkin-Perturbation analysis technique. Several variables were taken in consideration in his study such as foundation stiffness, transverse shear deformation, loaded area, and etc.

Yang and Zhang (2000) have provided a semi-analytical approach for the analysis of large deformation for the plate foundation interaction problem including the post-buckling plate response. The perturbation technique, Galerkin procedure, and 1D approximation were utilized in their method to simulate the nonlinear behavior of the plates under different boundary conditions (simple, clamp, and elastic rotational).

Muthurajan et al. (2005) have proposed a procedure based on the Von Karman's large deformation equations and Galerkin's method to study the response of laminated thin plate rested on elastic foundation and subjected to both out of plane and in-plane forces. The boundary conditions considered were simple and clamped supports.

Civalek (2007) presented a method for the solution of nonlinear dynamic and static problems of thin rectangular plate resting on two parameter (Winkler-Pasternak) foundations. He has used the discrete singular convolution (DSC) to discrete the plate nonlinear partial differential equations in space domain whereas the harmonic differential

quadrature (HDQ) method was used to discrete the plate equations in the time domain. The two different boundary conditions, simply and clamped immovable rectangular plates were investigated in his study.

Alamatian and Golmakani (2013) have provided a dynamic kinetic relaxation-based technique for the solution of laminated plates resting on nonlinear foundation. Their proposed method can be used for the analysis of the large deflection problems of general theta ply laminated plates on nonlinear foundation under different boundary conditions including the free and movable.

### **2.3.2 Numerical Solutions**

Dumir (1988) has carried out a large deformation analysis of annular thin plates (cylindrical orthotropic) resting on annular foundation and subjected to uniform distributed. He utilized the combined orthogonal point collocation method with the Newmark- $\beta$  scheme to solve the plate formulations based on the Van Karman equations. He proved that the static analysis is enough to get the maximum response of the plate of any load step instead of the transient solution.

Dumir and Bhaskar (1988) presented a method called orthogonal point collocation method which can be used for the analysis of the moderately large deflection of rectangular plates resting on the Winkler and Pasternak foundations and subjected to static loads. Their formulation was based on Von-Karman equations and the solutions were obtained for simply and clamped immovable plates.

Katsikadelis (1991) employed the boundary element method (BEM) to solve thin plates resting on elastic foundation and undergoing large deformation. The plate-foundation interaction was represented by linear and non linear Winkler models. The proposed method is applicable for plates with arbitrary boundary conditions and shapes. Both the nonlinearities and the foundation reactions were considered as domain forces in order to justify the use of the fundamental solution of the linear plate theory.

Qin (1993) has suggested a special boundary element method for the analysis of large deflection of plates resting on elastic foundations. The proposed boundary element method is based on the fundamental solutions derived from Hu's functions and the resolution method of the differential operator.

El-Zafrany and Fadhi (1996) provided a boundary element analysis for thin plate on elastic foundation (two-parameter). The method was based on a modified Kirchhoff theory and 3 degrees of freedom were considered at the boundary node. The complex Bessel functions were utilized to explicitly express the kernel functions. The free edge conditions were also covered in their study. The conclusion from their study is that the 3 degrees of freedom are enough for obtaining accurate results.

Rashed et al. (1998) solved the problem of thick plate on Winkler foundation using the boundary element method. Their formulation is based on Reissner plate bending theory.

In 2001, Horibe and Asano presented a boundary integral method to calculate the large deflection of a rectangular plate on a Pasternak foundation. Their formulation was

based on nonlinear Berger equation and the solution was obtained by transforming the partial differential equations to ordinary differential. Huang and Thambiratnam (2001) utilized the finite strip method to analyze the plates resting on elastic foundations and supports.

Saygun and Celik (2003) used the ring sector plate element to obtain a solution for a circular plate with a variable thickness and resting on a two-parameter foundation. Xia et al. (2004) analyzed a moderately thick rectangular plate with four free edges on two-parameter foundation using Galerkin method by including the transverse shear deformation.

Malekzadeh and Setoodeh (2007) studied the behavior of thin to moderately thick elastic rectangular laminated plates resting on nonlinear elastic foundations using the differential quadrature method (DQM).

A thick plate resting on Pasternak foundation was studied using the mesh-less radial point interpolation method by Hu et al (2009). Their formulation was based on Mindlin plate theory and the minimum total potential energy principle.

## **2.4 RBF Methods**

RBF was first introduced by Hardy in 1971 for fitting scattered data. RBF was coupled with the boundary element method (BEM) to develop new method called dual reciprocity-boundary element method by Nardini and Brebbia in 1982 for the solution of free vibration problems. In that method, the purpose of RBF was to transform the domain

integrals into boundary integrals. The coupling of RBF with boundary element method was carried out by several researchers to solve different types of problems.

However, the direct use of RBF to solve partial differential equation was due to Kansa (1990). He presented two different researches: first one was for the investigation of the accuracy of using multi-quadratic radial basis function (MQ) in estimation of the interpolation and partial derivative for 2D function. He has concluded that MQ is extremely accurate. Second one was about the use of MQ as the spatial approximation scheme for hyperbolic, parabolic and the elliptic Poisson's equation. The outcome of the second research was that the MQ is more efficient than finite difference scheme. In 1992, Kansa and Carlson introduced the variable shape parameters concept in the RBF.

Although RBF is accurate, it suffers from the stability and ill-conditioning problems, especially with dense and irregular spaces. Some researchers have conducted different studies to theoretically ensure the convergence and stability of RBF interpolation such as Schaback (1995), Wendland (1998).

Combination the RBF's with the dual reciprocity boundary element method DRBEM was studied in details by Golberg (1999). The solution of Poisson's equation by iterative RBF-DRBEM was introduced by Cheng, Young and Tsia (2000) for the solution of two-dimensional fluid dynamics represented by Navier-Stokes equations. Another Multi-domain DRBEM method has been introduced by Florez, Power and Chejne (2000) to solve Navier-Stokes equations.

To overcome ill conditioning problem particularly in the large scale problems, several types of RBF's were developed such as multilevel, compactly supported, preconditioned, truncated RBF, domain decomposition, Knot optimization method and RBF with variable shape parameter (Kansa and Hon (2000)).

Wen et al. (2000) have presented a dual reciprocity method to transform integrals to boundary integrals for shear deformable plate and shell bending problems in which the radial basis functions were employed to approximate the force terms in the equations.

Several researchers have proposed various versions of RBF for the solution of different problems. Examples are those by Driscoll (2002), and Ferreira (2003) for the analysis of laminated composite plates.

Sladek and Sladek (2003) have combined local boundary integral equation (LBIE) method with a mesh-less approximation to be used in the solution of bending of thin elastic plates with large deflections governed by the Berger equation.

The functionally graded material (FGM) plates dynamic and static analyses based on the point interpolation method (PIM) were provided by Dia et al. (2004).

Ferreira et al. (2004) utilized RBF-based collocation method with MQ function in the structural analysis of symmetric and isotropic laminated composite thick beams and plates and in the Timoshenko beams and Mindlin plates free vibration analysis by Ferreira (2005).

Larson and Fornberg (2003) have reported that the errors in RBF approximations tend to be largest near boundaries. Fedoseyev, Friedman and Kansa (2002) have provided

the formulation for an approach which collocates both with the PDE at the boundary points and the boundary condition in order to overcome the errors at the boundaries and they have added additional functions in order to have corresponding number of unknowns and equations.

In general, the solution of RBF-based collocation method is obtained by expanding the solution in terms of the radial basis functions whose coefficients are obtained by the application of both the governing equations and the boundary conditions of the problem at boundary and some selected domain points. As a consequence, it is vital issue to select the most appropriate form of radial basis function for the governing differential equations. The use of the Multi-quadrics (MQ) is preferred according to the literature Frank (1982) and Kansa (1990). This has been verified by Ferreira (2003) who has used it to solve the problem of small deflection of moderately thick rectangular laminated composite plates..

Zhou et al. (2011) have proposed a quadratic shape parameter variation scheme for the variable shaped multi-quadric (MQ). The proposed scheme with the variable shaped MQ gave better accuracy and stability than the constant shaped MQ.

In general, a typical radial basis function is dependent on the Euclidian radial distance  $r$  with or without a shape parameter  $c$ . Some of the widely used RBF functions are listed below:

❖ Poly-harmonic Spline RBF

- $\phi(r) = \phi(\|X - X_i\|) = r^k, k = 1, 3 \dots$



- $\phi(r) = \phi(\|X - X_i\|) = r^k \ln(r)$ ,  $k = 2, 4, \dots$

❖ Thin plate Spline RBF

- $\phi(r) = \phi(\|X - X_i\|) = r^2 \ln(r)$

❖ Multi-quadric RBF

- $\phi(r) = \phi(\|X - X_i\|) = \sqrt{r^2 + c^2}$

❖ Inverse of Multi-quadric RBF

- $\phi(r) = \phi(\|X - X_i\|) = \frac{1}{\sqrt{r^2 + c^2}}$

❖ Inverse quadratic RBF

- $\phi(r) = \phi(\|X - X_i\|) = \frac{1}{r^2 + c^2}$

## 2.5 Models of Soil–Foundation Interaction

Several models have been proposed for simulating the soil–foundation interaction. However, for practical considerations and applications, some models are so complex which limit their uses. On the other hand, there are simple and suitably truthful models still accepted with researchers and engineers. Some examples of such models are the Winkler model, the two parameter model, non-linear Winkler-Pasternak model, and the elastic continuum model Wang et. al (2005).

### 2.5.1 Winkler Model

The simplest foundation model is the so called Winkler model Winkler (1867) which represents the foundation reaction by a reaction  $p$  distributed perpendicularly to the plate, and therefore

$$p(x) = kw \quad (2.1)$$

Where;  $k$  is known as the Winkler parameter.

### 2.5.2 Two-Parameter Model (Pasternak Model)

The second popular model is due to Pasternak [1954 ] which counts for the effect of deformation of the shear for the foundation and it can be represented by:

$$p(x) = kw - g_p \nabla^2 w \quad (2.2)$$

Where;  $g_p$  is the shear foundation parameter.

### 2.5.3 Three-Parameter Model (Nonlinear Winkler-Pasternak Model)

The reaction for a non-linear Winkler-Pasternak foundation involves three parameters  $k$ ,  $k_1$  and  $g_p$  Kerr (1964), i.e.

$$p(x) = kw + k_1 w^3 - g_p \nabla^2 w \quad (2.3)$$

For generality, the non-linear Winkler-Pasternak model will be assumed in all subsequent formulations.

## 2.5.4 Elastic Continuous Models

The 3D continuous elastic solids are used to idealize the media of soil. The first attempt for the continuum simulation of soil media was found from the work of Boussinesq (1885) “who analyzed the problem of a semi- infinite homogeneous isotropic linear elastic half-space subjected to a concentrated force acting normal to the boundary” Wang et. al (2005). In addition, different solutions which have considered other models for the soil media were provided. They included the non-homogeneous elastic continuum, anisotropic elastic continuum, and layered elastic medium.

a) Isotropic elastic half-space. Stress-displacement relationship was first derived by Boussinesq (1885) due to the action of a normal force  $P$  (concentrated) for an isotropic elastic half-space on its boundary. As a result, the vertical direction displacement at the surface is given by  $\frac{P(1-\nu_s)}{2\pi G_s r}$  in which  $r$  is the distance between the force  $P$  and the point of interest, and  $\nu_s$  &  $G_s$  are Poisson’s ratio and the shear modulus of the elastic material.

b) Non-homogeneous elastic half-space. The overburden pressure increases with depth for the soil deposits which in turns an increase in the stiffness. Thus, the non-homogeneous medium’s Young’s modulus is expressed by Stark and Booker (1997) as follows:

$$E(z) = m_E Z^\alpha \quad (0 < \alpha < 1) \quad (2.4)$$

Where;  $m_E$  is a constant and if  $z = 0$ , it is equivalent to the Young’s modulus, and  $\alpha$  is the non-homogeneity index. To calculate the vertical settlement from a load,  $P$ , acting a point

on the surface of the non-homogeneous half-space, Booker et. al (1985) is utilized as follows:

$$w = \frac{PB}{m_E r^{1+\alpha}} \quad (2.5)$$

$$\text{where; } B = \frac{b\Gamma\left(\frac{\alpha+1}{2}\right)}{\Gamma\left(\frac{1}{2}\right)\Gamma\left(\frac{\alpha}{2}\right)} \quad ; \quad b = \frac{1-\nu_s^2}{\alpha} \sin\left(\frac{\beta\pi}{2}\right) \frac{\beta}{\alpha+1} F_{\alpha\beta} \quad ;$$

$$\beta = \sqrt{(1+\alpha)\left(1 - \frac{\alpha\nu_s}{1-\nu_s}\right)} \quad ; \quad F_{\alpha\beta} = \frac{2^{\alpha+1}}{\pi} (\alpha+2) \frac{\Gamma\left(\frac{3+\alpha+\beta}{2}\right)\Gamma\left(\frac{3+\alpha-\beta}{2}\right)}{\Gamma(3+\alpha)}$$

Where;  $\Gamma$  denotes the gamma function.

c) Cross-anisotropic foundation. The elastic vertical displacement surface  $w$  resulted from a load  $P$  at point on a cross-anisotropic soil can be calculated in Nayak (1973) by this formula:

$$w = \frac{P}{r} \left( \frac{1-\mu^2}{\pi E_z} \right) I_w \quad (2.6)$$

Where;  $r$  is the distance between the loading point and settlement point, and

$$I_w = \frac{(m_1 + m_2 s_2^2)(1 - a s_1^2) - (m_1 + m_2 s_1^2)(1 - a s_2^2)}{2n(1 - \mu^2)[s_1(c - d s_1^2)(1 - a s_2^2) - s_2(c - d s_2^2)(1 - a s_1^2)]} \quad (2.7)$$

The other variables of Eqs (2.6) and (2.7) are given as

$$m_1 = -cn - (1 + b)\mu_{rz} \quad ; \quad m_2 = dn + 2a\mu_{rz} \quad (2.8)$$

$$s_1, s_2 = \left\{ \frac{(a+c) \pm [(a+c)^2 - 4d]^{\frac{1}{2}}}{2d} \right\} \quad (2.9)$$

$$a = -\frac{\mu_{rz}(1 + \mu_{rr})}{n - \mu_{rz}^2}, \quad b = \frac{(1 - 2\beta)\mu_{rz}^2 - \beta(1 + n)\mu_{rz} + n\mu_{rr}}{n - \mu_{rz}^2},$$

$$c = \frac{(2\beta - 1)\mu_{rz} - \mu_{rr}\mu_{rz} + \beta(1 + n)}{n - \mu_{rz}^2}, \quad d = \frac{1 - \mu_{rr}^2}{n - \mu_{rz}^2} \quad (2.10)$$

d) Layered elastic media. Wang and Ishikawa (2001) provided the solution for layered soils Sennon (1951) by utilizing the Hankel transformation. The same approach was employed by Yin et al.(2001). Sennon (1951) can be expressed as

$$w(r, 0) = \frac{P}{2\pi} \int_0^\infty \frac{B_{21}B_{13} - B_{11}B_{23}}{B_{11}B_{22} - B_{21}B_{12}} \xi J_0(\xi, r) d\xi \quad (2.11)$$

Where;  $r$  is the distance between the loading point and the settlement point; the integration parameter for the Hankel transform is defined by  $\xi$ ;  $B_{ij}$  are the elements of the transformed displacements and stresses matrix. Analysis of plates on layered soil was provided by Wang et.al (2003) using semi-analytical and semi-numerical methods employing Eq.(2.11).

From the reviewed literature, it can be concluded that there is still a gap in the available solutions for the large deflection of plates on nonlinear foundations. Most of these solutions are limited to simplified foundation models and/or boundary conditions. In particular, the important case of plates with free edges has not been addressed by

almost all of the surveyed literature. In addition, the interaction between the plate and the foundation was not covered in a comprehensive way to include all foundation models.

## CHAPTER THREE

### GOVERNING EQUATIONS

In this chapter, the derivation of partial differential equations governing the behavior of thin elastic plates undergoing large deflection is presented. The derivation of equations for the plates without foundation is given, first followed by the case with foundation. For both cases, two types of formulations are considered: 1) w-F formulation which addresses the movable edge condition and 2) u-v-w formulation which addresses the immovable edge condition.

#### 3.1 Large Deflection of a Thin Plate

For the large deflection of thin plates, the governing differential equations are derived in two different approaches according to the edge conditions (movable or immovable). Timoshenko (1959) book covers the details of the derivation of equations governing the thin plate's finite deflection. The equations are provided here in a summarized form.

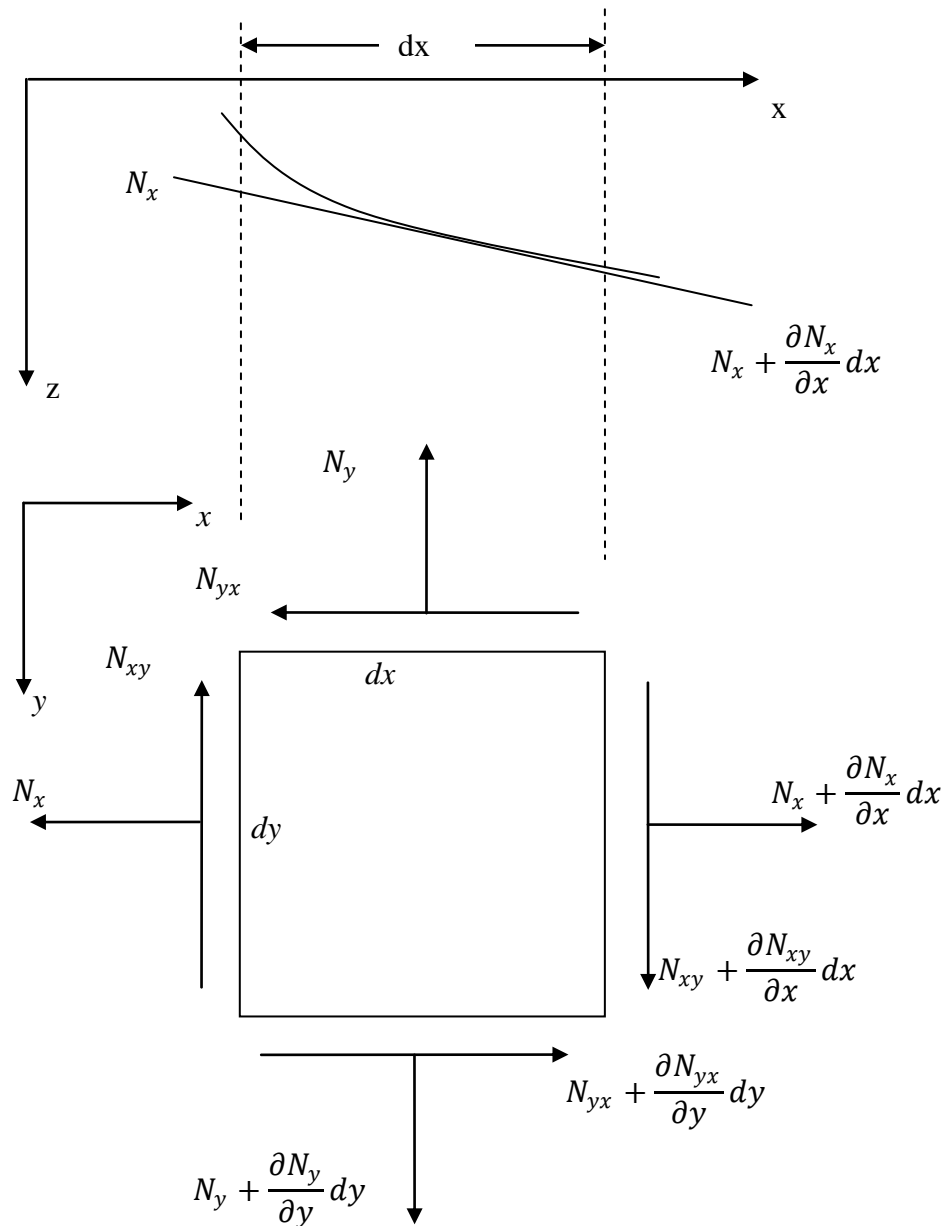


Figure 3.1 Definition of in-Plane Internal Forces of the Plates and their Projections on  $z$  Direction

(Timoshenko 1959).



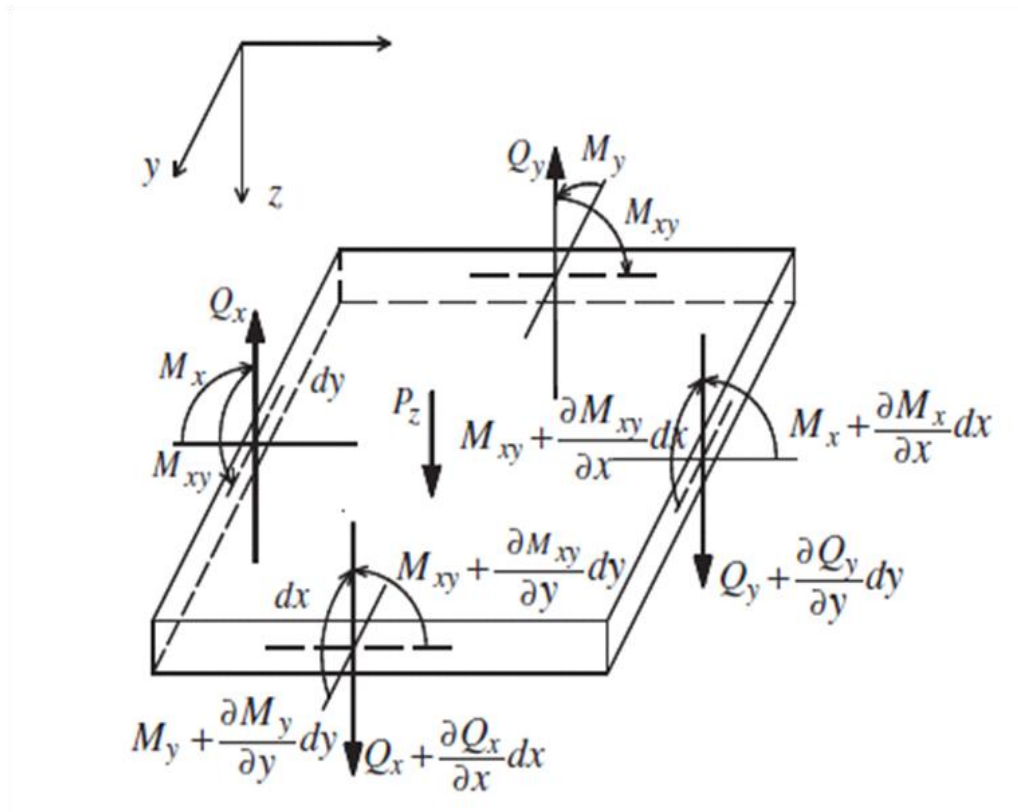


Figure 3.2 Definition of out of Plane Internal Forces of the Plates

From Figures 3-1 and 3-2, the summation of internal forces and moments in both in-plane and out of plane plates must equal to zero to achieve the equilibrium condition.

The equilibrium equations along x and y in the absence of the body forces are given by:

$$\frac{\partial N_x}{\partial x} + \frac{\partial N_{yx}}{\partial y} = 0 ; \quad (3.1)$$

$$\frac{\partial N_{xy}}{\partial x} + \frac{\partial N_y}{\partial y} = 0 ; \quad (3.2)$$

For the summation of forces in z direction, the projection of the in-plane forces  $N_x$ ,  $N_y$  and  $N_{xy}$  on the z axis must be included as shown in Figure 3-1. The bending of the

plate and the small angles between the forces  $N_x$ , and  $N_y$  which act on the opposite sides of the element must be taken in to account. As a consequence, the equation of equilibrium along  $z$  is given by:

$$-p_z + \frac{\partial Q_x}{\partial x} + \frac{\partial Q_y}{\partial y} + N_x \frac{\partial^2 w}{\partial x^2} + \frac{\partial N_x}{\partial x} \frac{\partial w}{\partial x} + N_y \frac{\partial^2 w}{\partial y^2} + \frac{\partial N_y}{\partial y} \frac{\partial w}{\partial y} + 2N_{xy} \frac{\partial^2 w}{\partial x \partial y} + \frac{\partial N_{xy}}{\partial x} \frac{\partial w}{\partial y} + \frac{\partial N_{xy}}{\partial y} \frac{\partial w}{\partial x} = 0 ; \quad (3.3)$$

Where:

$$Q_x = \frac{\partial M_x}{\partial x} - \frac{\partial M_{yx}}{\partial y} + N_x \frac{\partial w}{\partial x} + N_{xy} \frac{\partial w}{\partial y} \quad (3.4)$$

$$Q_y = \frac{\partial M_y}{\partial y} - \frac{\partial M_{xy}}{\partial x} + N_y \frac{\partial w}{\partial y} + N_{xy} \frac{\partial w}{\partial x} \quad (3.5)$$

From the in-plane forces, the strain formulas are presented as follows:

$$\varepsilon_x = \frac{N_x - N_y \nu}{Et} \quad (3.6)$$

$$\varepsilon_y = \frac{N_y - N_x \nu}{Et} \quad (3.7)$$

$$\gamma_{xy} = \frac{N_{xy}}{Gt} \quad (3.8)$$

The strain formulas during bending are as follows:

$$\varepsilon_x = \frac{\partial u(x, y)}{\partial x} + \frac{1}{2} \left( \frac{\partial w(x, y)}{\partial x} \right)^2 \quad (3.9)$$

$$\varepsilon_y = \frac{\partial v(x, y)}{\partial y} + \frac{1}{2} \left( \frac{\partial w(x, y)}{\partial y} \right)^2 \quad (3.10)$$

$$\gamma_{xy} = \frac{\partial u(x, y)}{\partial y} + \frac{\partial v(x, y)}{\partial x} + \frac{\partial w(x, y)}{\partial x} \frac{\partial w(x, y)}{\partial y} \quad (3.11)$$

### 3.1.1 w-F Formulations

In order to find  $N_x$ ,  $N_y$ , and  $N_{xy}$ , a third equation is needed to Equations 3.1 and 3.2. The required third equation can be obtained by employing the middle surface strain of the plate during the bending. The relevant strain components are as mentioned in the Equations 3.9, 3.10 and 3.11. By taking the second derivative of these expressions and combining the resulting equations, it can be shown that:

$$\frac{\partial^2 \varepsilon_x}{\partial y^2} + \frac{\partial^2 \varepsilon_y}{\partial x^2} - \frac{\partial^2 \gamma_{xy}}{\partial x \partial y} = \left( \frac{\partial^2 w(x, y)}{\partial x \partial y} \right)^2 - \frac{\partial^4 w(x, y)}{\partial x^2 \partial y^2} \quad (3.12)$$

Using the Equations 3.6, 3.7 and 3.8 for the strain components in Equations 3.12 one can get the third equation in terms of  $N_x$ ,  $N_y$ , and  $N_{xy}$ . For the solution of the resulting three equations, let us use stress function  $F$ , function of  $x$  and  $y$ , such as the Equations 3.1 and 3.2 are satisfied. To accomplish this purpose, the expressions of the  $N_x$ ,  $N_y$ , and  $N_{xy}$  are as follows:

$$\frac{N_x}{t} = \frac{\partial^2 F}{\partial y^2}; \Rightarrow N_x = t \frac{\partial^2 F}{\partial y^2} \quad (3.13)$$

$$\frac{N_y}{t} = \frac{\partial^2 F}{\partial x^2}; \Rightarrow N_y = t \frac{\partial^2 F}{\partial x^2} \quad (3.14)$$

$$\frac{N_{xy}}{t} = -\frac{\partial^2 F}{\partial x \partial y}; \Rightarrow N_{xy} = -t \frac{\partial^2 F}{\partial x \partial y} \quad (3.15)$$

By substitution Equations (3.13 - 3.15) into Equations (3.6 - 3.8), the results will be as follows:

$$\varepsilon_x = \frac{1}{E} \left( \frac{\partial^2 F}{\partial y^2} - \frac{\partial^2 F}{\partial x^2} \nu \right) \quad (3.16)$$

$$\varepsilon_y = \frac{1}{E} \left( \frac{\partial^2 F}{\partial x^2} - \nu \frac{\partial^2 F}{\partial y^2} \right) \quad (3.17)$$

$$\gamma_{xy} = -\frac{2(1+\nu)}{E} \frac{\partial^2 F}{\partial x \partial y} \quad (3.18)$$

Substitution expressions (3.16 - 3.18) into Equation (3.12), one can get the first equation relating  $w$  and  $F$  as follows:

$$\nabla^4 F = E \left[ \left( \frac{\partial^2 w}{\partial x \partial y} \right)^2 - \left( \frac{\partial^2 w}{\partial x^2} \right) \left( \frac{\partial^2 w}{\partial y^2} \right) \right] \quad (3.19)$$

$$L_f = Nl w \quad (3.20)$$

The necessary second equation to determine  $F$  and  $w$  is derived from the bending action as described in Timoshenko book (1959) which is presented here as follows:

$$\begin{aligned} \frac{\partial^4 w}{\partial x^4} + 2 \frac{\partial^4 w}{\partial x^2 \partial y^2} + \frac{\partial^4 w}{\partial y^4} \\ = \frac{t}{D} \left[ \frac{p_z}{t} + \left( \frac{\partial^2 F}{\partial y^2} \right) \left( \frac{\partial^2 w}{\partial x^2} \right) + \left( \frac{\partial^2 F}{\partial x^2} \right) \left( \frac{\partial^2 w}{\partial y^2} \right) \right. \\ \left. - 2 \left( \frac{\partial^2 F}{\partial x \partial y} \right) \left( \frac{\partial^2 w}{\partial x \partial y} \right) \right] \end{aligned} \quad (3.21)$$

$$Lw_f = \frac{p_z}{D} + Nl w_f \quad (3.22)$$

Where  $D = \frac{Et^3}{12(1-\nu^2)}$ .

From the w-F equations, the moment, shear, and stresses expressions are as follows:

$$M_n = \frac{Et^3}{12(-1+v^2)} \left( -2n_x n_y \frac{\partial^2 w(x,y)}{\partial x \partial y} (-1+v) + n_y^2 \left( \frac{\partial^2 w(x,y)}{\partial y^2} + \frac{\partial^2 w(x,y)}{\partial x^2} v \right) + n_x^2 \left( \frac{\partial^2 w(x,y)}{\partial x^2} + \frac{\partial^2 w(x,y)}{\partial y^2} v \right) \right) \quad (3.23)$$

$$V_n = \frac{et}{12(-1+v^2)} \left[ n_x t^2 (1 - n_y^2 (-1+v)) \frac{\partial^3 w}{\partial x^3} + (n_y t^2 - n_x^2 n_y t^2 (-1+v)) \frac{\partial^3 w}{\partial y^3} + (n_y t^2 (1 - n_y^2 (-1+v)) + 2n_x^2 n_y t^2 (-1+v)) \frac{\partial^3 w}{\partial x^2 \partial y} + (n_x^3 t^2 (1-v) + n_x t^2 (1 + 2n_y^2 (-1+v))) \frac{\partial^3 w}{\partial x \partial y^2} + n_y t \frac{\partial^2 F}{\partial x^2} \frac{\partial w}{\partial y} - n_y t \frac{\partial^2 F}{\partial x \partial y} \frac{\partial w}{\partial x} + n_x t \frac{\partial^2 F}{\partial y^2} \frac{\partial w}{\partial x} - n_x t \frac{\partial^2 F}{\partial x \partial y} \frac{\partial w}{\partial y} \right] \quad (3.24)$$

By reorganizing the shear formula to be in terms of linear and nonlinear terms, the shear force is written as  $V_n = V_n^L + V_n^{NL}$ ;

$$V_n^L = \frac{Et}{12(-1+v^2)} \left[ n_x t^2 (1 - n_y^2 (-1+v)) \frac{\partial^3 w}{\partial x^3} + (n_y t^2 - n_x^2 n_y t^2 (-1+v)) \frac{\partial^3 w}{\partial y^3} + (n_y t^2 (1 - n_y^2 (-1+v)) + 2n_x^2 n_y t^2 (-1+v)) \frac{\partial^3 w}{\partial x^2 \partial y} + (n_x^3 t^2 (1-v) + n_x t^2 (1 + 2n_y^2 (-1+v))) \frac{\partial^3 w}{\partial x \partial y^2} \right] \quad (3.25)$$

$$V_n^{NL} = \frac{Et}{12(-1 + \nu^2)} \left[ n_y t \frac{\partial^2 F}{\partial x^2} \frac{\partial w}{\partial y} - n_y t \frac{\partial^2 F}{\partial x \partial y} \frac{\partial w}{\partial x} + n_x t \frac{\partial^2 F}{\partial y^2} \frac{\partial w}{\partial x} - n_x t \frac{\partial^2 F}{\partial x \partial y} \frac{\partial w}{\partial y} \right] \quad (3.26)$$

Where;  $n_x$  and  $n_y$  are the components of the unit normal to the boundary and the subscripts indicate derivatives with the respective coordinates as shown in Figure 3.3.

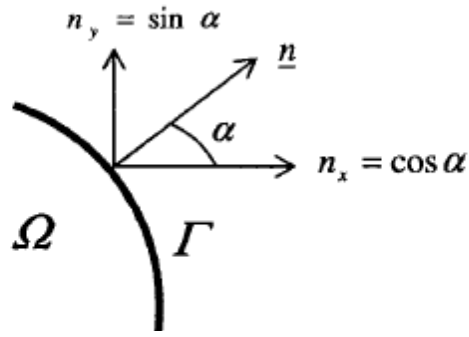


Figure 3.3 Directional Cosines

The bending stresses are obtained from Equation 3.23 as follows:

$$\sigma_x^b = -\frac{Et}{2(1 - \nu^2)} \left( \frac{\partial^2 w(x, y)}{\partial x^2} + \nu \frac{\partial^2 w(x, y)}{\partial y^2} \right) \quad (3.27)$$

$$\sigma_y^b = -\frac{Et}{2(1 - \nu^2)} \left( \nu \frac{\partial^2 w(x, y)}{\partial x^2} + \frac{\partial^2 w(x, y)}{\partial y^2} \right) \quad (3.28)$$

$$\sigma_{xy}^b = \frac{Et}{2(1 + \nu)} \frac{\partial^2 w(x, y)}{\partial x \partial y} \quad (3.29)$$

And membrane stresses are obtained from the in-plane forces as follows:

$$\sigma_x^m = \frac{\partial^2 F(x, y)}{\partial x^2} \quad (3.30)$$

$$\sigma_y^m = \frac{\partial^2 F(x, y)}{\partial y^2} \quad (3.31)$$

$$\sigma_{xy}^m = -\frac{\partial^2 F(x, y)}{\partial x \partial y} \quad (3.32)$$

### 3.1.2 w-u-v Formulations

By equating the strain equations (3.6 - 3.8 and 3.9 - 3.11) and solving the resulting formulas, the  $N_x$ ,  $N_y$ , and  $N_{xy}$  are determined and then substituted into Equations 3.1 3.2 and 3.3, the following equations are found and given by:

$$\begin{aligned} & \frac{Et}{2(v+1)} \left( \frac{\partial^2 v(x, y)}{\partial x \partial y} + \frac{\partial w(x, y)}{\partial y} \frac{\partial^2 w(x, y)}{\partial x \partial y} + \frac{\partial^2 u(x, y)}{\partial y^2} + \frac{\partial w(x, y)}{\partial x} \frac{\partial^2 w(x, y)}{\partial y^2} \right) \\ & - \frac{Et}{(v^2-1)} \left( v \frac{\partial^2 v(x, y)}{\partial x \partial y} + v \frac{\partial w(x, y)}{\partial y} \frac{\partial^2 w(x, y)}{\partial x \partial y} + \frac{\partial^2 u(x, y)}{\partial x^2} \right. \\ & \left. + \frac{\partial w(x, y)}{\partial x} \frac{\partial^2 w(x, y)}{\partial x^2} \right) = 0 \end{aligned} \quad (3.33)$$

$$\begin{aligned} & \frac{Et}{2(v+1)} \left( \frac{\partial^2 u(x, y)}{\partial x \partial y} + \frac{\partial w(x, y)}{\partial x} \frac{\partial^2 w(x, y)}{\partial x \partial y} + \frac{\partial^2 v(x, y)}{\partial x^2} + \frac{\partial w(x, y)}{\partial y} \frac{\partial^2 w(x, y)}{\partial x^2} \right) \\ & - \frac{Etv}{(v^2-1)} \left( \frac{\partial^2 u(x, y)}{\partial x \partial y} + \frac{\partial w(x, y)}{\partial x} \frac{\partial^2 w(x, y)}{\partial x \partial y} \right) \\ & - \frac{Et}{(v^2-1)} \left( \frac{\partial^2 v(x, y)}{\partial y^2} + \frac{\partial w(x, y)}{\partial y} \frac{\partial^2 w(x, y)}{\partial y^2} \right) \\ & = 0 \end{aligned} \quad (3.34)$$

$$\begin{aligned}
& -\frac{Et^3(1-v)}{6(1-v^2)} \frac{\partial^4 w(x,y)}{\partial x^2 \partial y^2} - \frac{Et^3}{12(1-v^2)} \left( v \frac{\partial^4 w(x,y)}{\partial x^2 \partial y^2} + \frac{\partial^4 w(x,y)}{\partial y^4} \right) \\
& - \frac{Et^3}{12(1-v^2)} \left( v \frac{\partial^4 w(x,y)}{\partial x^2 \partial y^2} + \frac{\partial^4 w(x,y)}{\partial x^4} \right) \\
& + \frac{Et}{v+1} \frac{\partial^2 w(x,y)}{\partial x \partial y} \left( \frac{\partial u(x,y)}{\partial y} + \frac{\partial v(x,y)}{\partial x} + \frac{\partial w(x,y)}{\partial x} \frac{\partial w(x,y)}{\partial y} \right) \\
& - \frac{Et}{2(v^2-1)} \frac{\partial^2 w(x,y)}{\partial x^2} \left( 2 \frac{\partial u(x,y)}{\partial x} + 2v \frac{\partial v(x,y)}{\partial y} + v \left( \frac{\partial w(x,y)}{\partial y} \right)^2 \right. \\
& \left. + \left( \frac{\partial w(x,y)}{\partial x} \right)^2 \right) \\
& - \frac{Et}{2(v^2-1)} \frac{\partial^2 w(x,y)}{\partial y^2} \left( 2v \frac{\partial u(x,y)}{\partial x} + 2 \frac{\partial v(x,y)}{\partial y} + v \left( \frac{\partial w(x,y)}{\partial x} \right)^2 \right. \\
& \left. + \left( \frac{\partial w(x,y)}{\partial y} \right)^2 \right) - p_z = 0 \tag{3.35}
\end{aligned}$$

From Equations 3.33, 3.34, and 3.35, the linear and nonlinear parts are put on the left and right hand sides respectively as follows:

$$\begin{aligned}
& \frac{Et}{2(v+1)} \frac{\partial^2 u(x,y)}{\partial y^2} - \frac{Et}{(v^2-1)} \frac{\partial^2 u(x,y)}{\partial x^2} - \frac{Et}{2(v-1)} \frac{\partial^2 v(x,y)}{\partial x \partial y} \\
& = \frac{Et}{2(v+1)} \left( \frac{\partial w(x,y)}{\partial x} \frac{\partial^2 w(x,y)}{\partial y^2} \right) - \frac{Et}{2(v-1)} \left( \frac{\partial w(x,y)}{\partial y} \frac{\partial^2 w(x,y)}{\partial x \partial y} \right) \\
& - \frac{Et}{(v^2-1)} \frac{\partial w(x,y)}{\partial x} \frac{\partial^2 w(x,y)}{\partial x^2} - p_x \tag{3.36}
\end{aligned}$$



$$\begin{aligned}
& \frac{Et}{2(v+1)} \frac{\partial^2 v(x,y)}{\partial x^2} - \frac{Et}{(v^2-1)} \frac{\partial^2 v(x,y)}{\partial y^2} - \frac{Et}{2(v-1)} \frac{\partial^2 u(x,y)}{\partial x \partial y} \\
&= \frac{Et}{2(v+1)} \left( \frac{\partial w(x,y)}{\partial y} \frac{\partial^2 w(x,y)}{\partial x^2} \right) - \frac{Et}{2(v-1)} \left( \frac{\partial w(x,y)}{\partial x} \frac{\partial^2 w(x,y)}{\partial x \partial y} \right) \\
& - \frac{Et}{(v^2-1)} \frac{\partial w(x,y)}{\partial y} \frac{\partial^2 w(x,y)}{\partial y^2} - p_y
\end{aligned} \tag{3.37}$$

$$\begin{aligned}
& - \frac{Et^3}{12(1-v^2)} \left( \frac{2 \partial^4 w(x,y)}{\partial x^2 \partial y^2} + \frac{\partial^4 w(x,y)}{\partial y^4} + \frac{\partial^4 w(x,y)}{\partial x^4} \right) \\
&= - \frac{Et}{v+1} \frac{\partial^2 w(x,y)}{\partial x \partial y} \left( \frac{\partial u(x,y)}{\partial y} + \frac{\partial v(x,y)}{\partial x} + \frac{\partial w(x,y)}{\partial x} \frac{\partial w(x,y)}{\partial y} \right) \\
& + \frac{Et}{2(v^2-1)} \frac{\partial^2 w(x,y)}{\partial x^2} \left( 2 \frac{\partial u(x,y)}{\partial x} + 2v \frac{\partial v(x,y)}{\partial y} + v \left( \frac{\partial w(x,y)}{\partial y} \right)^2 \right. \\
& \left. + \left( \frac{\partial w(x,y)}{\partial x} \right)^2 \right) \\
& + \frac{1}{2(v^2-1)} \frac{\partial^2 w(x,y)}{\partial y^2} \left( 2Etv \frac{\partial u(x,y)}{\partial x} + 2Et \frac{\partial v(x,y)}{\partial y} + Etv \left( \frac{\partial w(x,y)}{\partial x} \right)^2 \right. \\
& \left. + Et \left( \frac{\partial w(x,y)}{\partial y} \right)^2 \right) + p_z
\end{aligned} \tag{3.38}$$

The Equations 3.36, 3.37, and 3.38 are rearranged to be as follows:

$$Luv_{11} + Luv_{12} = Nlw_1 \tag{3.39}$$

$$Luv_{21} + Luv_{22} = Nlw_2 \tag{3.40}$$

$$Lw = NLuvw + pz \tag{3.41}$$

In which;

$$Luv_{11} = \frac{Et}{2(v+1)} \frac{\partial^2 u(x,y)}{\partial y^2} - \frac{Et}{(v^2-1)} \frac{\partial^2 u(x,y)}{\partial x^2} \quad (3.42)$$

$$Luv_{12} = -\frac{Et}{2(v-1)} \frac{\partial^2 v(x,y)}{\partial x \partial y} \quad (3.43)$$

$$Luv_{21} = -\frac{et}{2(v-1)} \frac{\partial^2 u(x,y)}{\partial x \partial y} \quad (3.44)$$

$$Luv_{22} = \frac{Et}{2(v+1)} \frac{\partial^2 v(x,y)}{\partial x^2} - \frac{Et}{(v^2-1)} \frac{\partial^2 v(x,y)}{\partial y^2} \quad (3.45)$$

$$\begin{aligned} Nlw_1 = & \frac{Et}{2(v+1)} \left( \frac{\partial w(x,y)}{\partial x} \frac{\partial^2 w(x,y)}{\partial y^2} \right) - \frac{Et}{2(v-1)} \left( \frac{\partial w(x,y)}{\partial y} \frac{\partial^2 w(x,y)}{\partial x \partial y} \right) \\ & - \frac{Et}{(v^2-1)} \frac{\partial w(x,y)}{\partial x} \frac{\partial^2 w(x,y)}{\partial x^2} - p_x \end{aligned} \quad (3.46)$$

$$\begin{aligned} Nlw_2 = & \frac{Et}{2(v+1)} \left( \frac{\partial w(x,y)}{\partial y} \frac{\partial^2 w(x,y)}{\partial x^2} \right) - \frac{Et}{2(v-1)} \left( \frac{\partial w(x,y)}{\partial x} \frac{\partial^2 w(x,y)}{\partial x \partial y} \right) \\ & - \frac{Et}{(v^2-1)} \frac{\partial w(x,y)}{\partial y} \frac{\partial^2 w(x,y)}{\partial y^2} - p_y \end{aligned} \quad (3.47)$$

$$Lw = -\frac{Et^3}{12(1-v^2)} \left( \frac{2 \partial^4 w(x,y)}{\partial x^2 \partial y^2} + \frac{\partial^4 w(x,y)}{\partial y^4} + \frac{\partial^4 w(x,y)}{\partial x^4} \right) \quad (3.48)$$

NLuvv

$$\begin{aligned}
&= -\frac{Et}{\nu + 1} \frac{\partial^2 w(x, y)}{\partial x \partial y} \left( \frac{\partial u(x, y)}{\partial y} + \frac{\partial v(x, y)}{\partial x} + \frac{\partial w(x, y)}{\partial x} \frac{\partial w(x, y)}{\partial y} \right) \\
&+ \frac{Et}{2(\nu^2 - 1)} \frac{\partial^2 w(x, y)}{\partial x^2} \left( 2 \frac{\partial u(x, y)}{\partial x} + 2\nu \frac{\partial v(x, y)}{\partial y} + \nu \left( \frac{\partial w(x, y)}{\partial y} \right)^2 + \left( \frac{\partial w(x, y)}{\partial x} \right)^2 \right) \\
&+ \frac{Et}{2(\nu^2 - 1)} \frac{\partial^2 w(x, y)}{\partial y^2} \left( 2\nu \frac{\partial u(x, y)}{\partial x} + 2 \frac{\partial v(x, y)}{\partial y} + \nu \left( \frac{\partial w(x, y)}{\partial x} \right)^2 \right. \\
&\left. + \left( \frac{\partial w(x, y)}{\partial y} \right)^2 \right) \tag{3.49}
\end{aligned}$$

For a general curved boundary, the bending moment and the shear forces of the normal to the plate edges as follows:

$$\begin{aligned}
M_n &= \frac{Et^3}{12(-1 + \nu^2)} \left( -2n_x n_y \frac{\partial^2 w(x, y)}{\partial x \partial y} (-1 + \nu) + n_y^2 \left( \frac{\partial^2 w(x, y)}{\partial y^2} + \frac{\partial^2 w(x, y)}{\partial x^2} \nu \right) \right. \\
&\left. + n_x^2 \left( \frac{\partial^2 w(x, y)}{\partial x^2} + \frac{\partial^2 w(x, y)}{\partial y^2} \nu \right) \right) \tag{3.50}
\end{aligned}$$

$$\begin{aligned}
V_n = & \frac{Et}{12(-1+v)} \left[ (n_x n_y^2 t^2 (1-v) + n_x t^2) \frac{\partial^3 w(x,y)}{\partial x^3} \right. \\
& + (n_y n_x^2 t^2 (1-v) + n_y t^2) \frac{\partial^3 w(x,y)}{\partial y^3} \\
& + \left( 2n_y n_x^2 t^2 (v-1) + n_y t^2 + n_y^3 t^2 (1-v) \right) \frac{\partial^3 w(x,y)}{\partial x^2 \partial y} \\
& + \left( 2n_x n_y^2 t^2 (v-1) + n_x t^2 + n_x^3 t^2 (1-v) \right) \frac{\partial^3 w(x,y)}{\partial x \partial y^2} \\
& - 12n_y \frac{\partial v(x,y)}{\partial y} \frac{\partial w(x,y)}{\partial y} - 6n_y \left( \frac{\partial w(x,y)}{\partial x} \right)^2 \frac{\partial w(x,y)}{\partial y} - 6n_y \left( \frac{\partial w(x,y)}{\partial y} \right)^3 \\
& + 6n_y (-1+v) \frac{\partial u(x,y)}{\partial y} \frac{\partial w(x,y)}{\partial x} + 6n_y (-1+v) \frac{\partial v(x,y)}{\partial x} \frac{\partial w(x,y)}{\partial x} \\
& - 12n_y v \frac{\partial u(x,y)}{\partial x} \frac{\partial w(x,y)}{\partial y} - 12n_x \frac{\partial u(x,y)}{\partial x} \frac{\partial w(x,y)}{\partial x} - 6n_x \left( \frac{\partial w(x,y)}{\partial x} \right)^3 \\
& + 6n_x (-1+v) \frac{\partial u(x,y)}{\partial y} \frac{\partial w(x,y)}{\partial y} + 6n_x (-1+v) \frac{\partial v(x,y)}{\partial x} \frac{\partial w(x,y)}{\partial y} \\
& \left. - 6n_x \left( \frac{\partial w(x,y)}{\partial y} \right)^2 \frac{\partial w(x,y)}{\partial x} - 12n_x v \frac{\partial v(x,y)}{\partial y} \frac{\partial w(x,y)}{\partial x} \right] \tag{3.51}
\end{aligned}$$

The shear force  $V_n$  can be divided into two parts, linear ( $V_n^L$ ) and nonlinear ( $V_n^{NL}$ ) as

follows:

$$v_n = V_n^L + V_n^{NL}$$

$$\begin{aligned}
V_n^L = & \frac{Et}{12(-1+v)} \left[ (n_x n_y^2 t^2 (1-v) + n_x t^2) \frac{\partial^3 w(x,y)}{\partial x^3} \right. \\
& + (n_y n_x^2 t^2 (1-v) + n_y t^2) \frac{\partial^3 w(x,y)}{\partial y^3} \\
& + \left( 2n_y n_x^2 t^2 (v-1) + n_y t^2 + n_y^3 t^2 (1-v) \right) \frac{\partial^3 w(x,y)}{\partial x^2 \partial y} \\
& \left. + \left( 2n_x n_y^2 t^2 (v-1) + n_x t^2 + n_x^3 t^2 (1-v) \right) \frac{\partial^3 w(x,y)}{\partial x \partial y^2} \right] \quad (3.52)
\end{aligned}$$

$$\begin{aligned}
V_n^{NL} = & \frac{Et}{12(-1+v)} \left[ -12n_y \frac{\partial v(x,y)}{\partial y} \frac{\partial w(x,y)}{\partial y} - 6n_y \left( \frac{\partial w(x,y)}{\partial x} \right)^2 \frac{\partial w(x,y)}{\partial y} \right. \\
& - 6n_y \left( \frac{\partial w(x,y)}{\partial y} \right)^3 + 6n_y (-1+v) \frac{\partial u(x,y)}{\partial y} \frac{\partial w(x,y)}{\partial x} \\
& + 6n_y (-1+v) \frac{\partial v(x,y)}{\partial x} \frac{\partial w(x,y)}{\partial x} - 12n_y v \frac{\partial u(x,y)}{\partial x} \frac{\partial w(x,y)}{\partial y} \\
& - 12n_x \frac{\partial u(x,y)}{\partial x} \frac{\partial w(x,y)}{\partial x} - 6n_x \left( \frac{\partial w(x,y)}{\partial x} \right)^3 + 6n_x (-1+v) \frac{\partial u(x,y)}{\partial y} \frac{\partial w(x,y)}{\partial y} \\
& + 6n_x (-1+v) \frac{\partial v(x,y)}{\partial x} \frac{\partial w(x,y)}{\partial y} - 6n_x \left( \frac{\partial w(x,y)}{\partial y} \right)^2 \frac{\partial w(x,y)}{\partial x} \\
& \left. - 12n_x v \frac{\partial v(x,y)}{\partial y} \frac{\partial w(x,y)}{\partial x} \right] \quad (3.53)
\end{aligned}$$

Where;  $n_x$  and  $n_y$  are the components of the unit normal to the boundary and the subscripts indicate derivatives with the respective coordinates as shown in Figure 3.3.

The bending stresses are obtained from Equation 3.50 as follows:

$$\sigma_x^b = -\frac{Et}{2(1-\nu^2)} \left( \frac{\partial^2 w(x,y)}{\partial x^2} + \nu \frac{\partial^2 w(x,y)}{\partial y^2} \right) \quad (3.54)$$

$$\sigma_y^b = -\frac{Et}{2(1-\nu^2)} \left( \nu \frac{\partial^2 w(x,y)}{\partial x^2} + \frac{\partial^2 w(x,y)}{\partial y^2} \right) \quad (3.55)$$

$$\sigma_{xy}^b = \frac{Et}{2(1+\nu)} \frac{\partial^2 w(x,y)}{\partial x \partial y} \quad (3.56)$$

The membrane stresses are obtained from the in-plane forces as follows:

$$\begin{aligned} \sigma_x^m = & -\frac{E}{2(\nu^2-1)} \left( 2 \frac{\partial u(x,y)}{\partial x} + 2\nu \frac{\partial v(x,y)}{\partial y} + \nu \left( \frac{\partial w(x,y)}{\partial y} \right)^2 \right. \\ & \left. + \left( \frac{\partial w(x,y)}{\partial x} \right)^2 \right) \end{aligned} \quad (3.57)$$

$$\begin{aligned} \sigma_y^m = & -\frac{E}{2(\nu^2-1)} \left( 2\nu \frac{\partial u(x,y)}{\partial x} + 2 \frac{\partial v(x,y)}{\partial y} + \nu \left( \frac{\partial w(x,y)}{\partial x} \right)^2 \right. \\ & \left. + \left( \frac{\partial w(x,y)}{\partial y} \right)^2 \right) \end{aligned} \quad (3.58)$$

$$\sigma_{xy}^m = \frac{E}{2(\nu+1)} \left( \frac{\partial u(x,y)}{\partial y} + \frac{\partial v(x,y)}{\partial x} + \frac{\partial w(x,y)}{\partial x} \frac{\partial w(x,y)}{\partial y} \right) \quad (3.59)$$

To generalize the solution, the previously derived governing equations and relationships need to be non-dimensionalized.

For a rectangular domain (a x b), and thickness of t, one can define the following non-dimensionalized quantities:

$$X = \frac{x}{a}; \quad Y = \frac{y}{b}; \quad U = \frac{ua}{t^2}; \quad V = \frac{va}{t^2}; \quad W = \frac{w}{t}; \quad F = \frac{f}{et^2};$$

$$\alpha = \frac{a}{b}; \quad \beta = \frac{a}{t}; \quad P_X = \frac{(-1 + \nu^2) p_x \beta^3}{E};$$

$$P_Y = \frac{(-1 + \nu^2) p_y \beta^3}{E}; \quad P_Z = \frac{12(1 - \nu^2) p_z \beta^4}{E};$$

$$\frac{\partial u(x, y)}{\partial x} = \frac{t^2}{a^2} \frac{\partial U(X, Y)}{\partial X}; \quad \frac{\partial u(x, y)}{\partial y} = \frac{t^2}{ab} \frac{\partial U(X, Y)}{\partial Y};$$

$$\frac{\partial v(x, y)}{\partial x} = \frac{t^2}{ab} \frac{\partial V(X, Y)}{\partial X}; \quad \frac{\partial v(x, y)}{\partial y} = \frac{t^2}{b^2} \frac{\partial V(X, Y)}{\partial Y};$$

$$\frac{\partial^2 u(x, y)}{\partial x^2} = \frac{t^2}{a^3} \frac{\partial^2 U(X, Y)}{\partial X^2}; \quad \frac{\partial^2 u(x, y)}{\partial y^2} = \frac{t^2}{ab^2} \frac{\partial^2 U(X, Y)}{\partial Y^2};$$

$$\frac{\partial^2 v(x, y)}{\partial x^2} = \frac{t^2}{a^2 b} \frac{\partial^2 V(X, Y)}{\partial X^2}; \quad \frac{\partial^2 v(x, y)}{\partial y^2} = \frac{t^2}{b^3} \frac{\partial^2 V(X, Y)}{\partial Y^2};$$

$$\frac{\partial^2 u(x, y)}{\partial x \partial y} = \frac{t^2}{a^2 b} \frac{\partial^2 U(X, Y)}{\partial X \partial Y}; \quad \frac{\partial^2 v(x, y)}{\partial x \partial y} = \frac{t^2}{ab^2} \frac{\partial^2 V(X, Y)}{\partial X \partial Y};$$

$$\frac{\partial w(x, y)}{\partial x} = \frac{t}{a} \frac{\partial W(X, Y)}{\partial X}; \quad \frac{\partial w(x, y)}{\partial y} = \frac{t}{b} \frac{\partial W(X, Y)}{\partial Y};$$

$$\frac{\partial^2 w(x, y)}{\partial x \partial y} = \frac{t}{ab} \frac{\partial^2 W(X, Y)}{\partial X \partial Y}; \quad \frac{\partial^2 w(x, y)}{\partial x^2} = \frac{t}{a^2} \frac{\partial^2 W(X, Y)}{\partial X^2};$$

$$\frac{\partial^2 w(x, y)}{\partial y^2} = \frac{t}{b^2} \frac{\partial^2 W(X, Y)}{\partial Y^2}; \quad \frac{\partial^3 w(x, y)}{\partial x^3} = \frac{t}{a^3} \frac{\partial^3 W(X, Y)}{\partial X^3};$$

$$\frac{\partial^3 w(x, y)}{\partial x^2 \partial y} = \frac{t}{a^2 b} \frac{\partial^3 W(X, Y)}{\partial X^2 \partial Y}; \quad \frac{\partial^3 w(x, y)}{\partial x \partial y^2} = \frac{t}{ab^2} \frac{\partial^3 W(X, Y)}{\partial X \partial Y^2};$$

$$\frac{\partial^3 w(x, y)}{\partial y^3} = \frac{t}{b^3} \frac{\partial^3 W(X, Y)}{\partial Y^3}; \quad \frac{\partial^4 w(x, y)}{\partial x^4} = \frac{t}{a^4} \frac{\partial^4 W(X, Y)}{\partial X^4};$$

$$\frac{\partial^4 w(x, y)}{\partial x^2 \partial y^2} = \frac{t}{a^2 b^2} \frac{\partial^4 W(X, Y)}{\partial X^2 \partial Y^2}; \quad \text{and} \quad \frac{\partial^4 w(x, y)}{\partial y^4} = \frac{t}{b^4} \frac{\partial^4 W(X, Y)}{\partial Y^4}$$

### 3.1.3 Non-Dimensional W-F Formulations

The resulting non-dimensional W-F formulas are as follows:

$$\nabla^4 F = \left[ \left( \frac{\partial^2 W}{\partial X \partial Y} \right)^2 - \left( \frac{\partial^2 W}{\partial X^2} \right) \left( \frac{\partial^2 W}{\partial Y^2} \right) \right] \quad (3.60)$$

$$LF = NLW \quad (3.61)$$

$$\begin{aligned} \nabla^4 W = P_z & \\ & + 12(1 - \nu^2) \left[ \left( \frac{\partial^2 F}{\partial Y^2} \right) \left( \frac{\partial^2 W}{\partial X^2} \right) + \left( \frac{\partial^2 F}{\partial X^2} \right) \left( \frac{\partial^2 W}{\partial Y^2} \right) \right. \\ & \left. - 2 \left( \frac{\partial^2 F}{\partial X \partial Y} \right) \left( \frac{\partial^2 W}{\partial X \partial Y} \right) \right] \quad (3.62) \end{aligned}$$

$$LWF = P_z + NLWF \quad (3.63)$$



For the bending moment, shear, and stresses, the following are the non-dimensional expressions:

$$M_N = \frac{1}{12(-1 + \nu^2)} \left( -2n_x n_y (-1 + \nu) \alpha \frac{\partial^2 W(X, Y)}{\partial X \partial Y} + n_y^2 \left( \frac{\partial^2 W(X, Y)}{\partial X^2} \nu \right. \right. \\ \left. \left. + \alpha^2 \frac{\partial^2 W(X, Y)}{\partial Y^2} \right) + n_x^2 \left( \frac{\partial^2 W(X, Y)}{\partial X^2} + \alpha^2 \nu \frac{\partial^2 W(X, Y)}{\partial Y^2} \right) \right) \quad (3.64)$$

$$V_N = \frac{1}{12(-1 + \nu^2)} \left[ n_x \left( 1 - n_y^2 (-1 + \nu) \right) \frac{\partial^3 W}{\partial X^3} + \left( n_y \alpha^3 - n_x^2 n_y \alpha^3 (-1 + \nu) \right) \frac{\partial^3 W}{\partial Y^3} \right. \\ \left. + \left( n_y \alpha \left( 1 - n_y^2 (-1 + \nu) \right) + 2n_x^2 n_y \alpha (-1 + \nu) \right) \frac{\partial^3 W}{\partial X^2 \partial Y} \right. \\ \left. + \left( n_x^3 \alpha^2 (1 - \nu) + n_x \alpha^2 \left( 1 + 2n_y^2 (-1 + \nu) \right) \right) \frac{\partial^3 W}{\partial X \partial Y^2} + n_y \alpha \frac{\partial^2 F}{\partial X^2} \frac{\partial W}{\partial Y} \right. \\ \left. - n_y \frac{\partial^2 F}{\partial X \partial Y} \frac{\partial W}{\partial X} + n_x \frac{\partial^2 F}{\partial Y^2} \frac{\partial W}{\partial X} - n_x \alpha \frac{\partial^2 F}{\partial X \partial Y} \frac{\partial W}{\partial Y} \right] \quad (3.65)$$

Shear Force;  $V_N = V_N^L + V_N^{NL}$

$$V_N^L = \frac{1}{12(-1 + \nu^2)} \left[ n_x \left( 1 - n_y^2 (-1 + \nu) \right) \frac{\partial^3 W}{\partial X^3} + \left( n_y \alpha^3 - n_x^2 n_y \alpha^3 (-1 + \nu) \right) \frac{\partial^3 W}{\partial Y^3} \right. \\ \left. + \left( n_y \alpha \left( 1 - n_y^2 (-1 + \nu) \right) + 2n_x^2 n_y \alpha (-1 + \nu) \right) \frac{\partial^3 W}{\partial X^2 \partial Y} + \left( n_x^3 \alpha^2 (1 - \nu) \right. \right. \\ \left. \left. + n_x \alpha^2 \left( 1 + 2n_y^2 (-1 + \nu) \right) \right) \frac{\partial^3 W}{\partial X \partial Y^2} \right] \quad (3.66)$$

$$V_N^{NL} = \frac{1}{12(-1 + \nu^2)} \left[ n_y \alpha \frac{\partial^2 F}{\partial X^2} \frac{\partial W}{\partial Y} - n_y \frac{\partial^2 F}{\partial X \partial Y} \frac{\partial W}{\partial X} + n_x \frac{\partial^2 F}{\partial Y^2} \frac{\partial W}{\partial X} - n_x \alpha \frac{\partial^2 F}{\partial X \partial Y} \frac{\partial W}{\partial Y} \right] \quad (3.67)$$

The stresses relationships for bending and membrane are as follows:

$$\sigma_X^B = -\frac{1}{2(1 - \nu^2)} \left( \frac{\partial^2 W(X, Y)}{\partial X^2} + \nu \alpha^2 \frac{\partial^2 W(X, Y)}{\partial Y^2} \right) \quad (3.68)$$

$$\sigma_Y^B = -\frac{1}{2(1 - \nu^2)} \left( \nu \frac{\partial^2 W(X, Y)}{\partial X^2} + \frac{\partial^2 W(X, Y)}{\partial Y^2} \alpha^2 \right) \quad (3.69)$$

$$\sigma_{XY}^B = \frac{\alpha}{2(1 + \nu)} \frac{\partial^2 W(X, Y)}{\partial X \partial Y} \quad (3.70)$$

$$\sigma_X^M = \frac{\partial^2 F(X, Y)}{\partial X^2} \quad (3.71)$$

$$\sigma_Y^M = \frac{\partial^2 F(X, Y)}{\partial Y^2} \quad (3.72)$$

$$\sigma_{XY}^M = -\frac{\partial^2 F(X, Y)}{\partial X \partial Y} \quad (3.73)$$

### 3.1.4 Non-Dimensional W-U-V Formulations

Applying those non-dimensional quantities, and multiplying sides of Equations 3.36 and 3.37 by  $(a^3/t^2)$  and Equation 3.38 by  $(a^4/t)$ , we get the final form of non-dimensional partial differential equations are as follows:

$$LUV_{11} + LUV_{12} = NLW_1 \quad (3.74)$$

$$LUV_{21} + LUV_{22} = NLW_2 \quad (3.75)$$

$$LW = NLUVW + PZ \quad (3.76)$$

In which;

$$LUV_{11} = \frac{\alpha^2(-1 + \nu)}{2} \frac{\partial^2 U(X, Y)}{\partial Y^2} + \frac{\partial^2 U(X, Y)}{\partial X^2} \quad (3.77)$$

$$LUV_{12} = \frac{\alpha^2(1 + \nu)}{2} \frac{\partial^2 V(X, Y)}{\partial X \partial Y} \quad (3.78)$$

$$LUV_{21} = \frac{\alpha(1 + \nu)}{2} \frac{\partial^2 U(X, Y)}{\partial X \partial Y} \quad (3.79)$$

$$LUV_{22} = \frac{\alpha(1 - \nu)}{2} \frac{\partial^2 V(X, Y)}{\partial X^2} + \alpha^3 \frac{\partial^2 V(X, Y)}{\partial Y^2} \quad (3.80)$$

$$\begin{aligned} NLW_1 = & \frac{\alpha^2(-1 + \nu)}{2} \left( \frac{\partial W(X, Y)}{\partial X} \frac{\partial^2 W(X, Y)}{\partial Y^2} \right) - \frac{\alpha^2(1 + \nu)}{2} \left( \frac{\partial W(X, Y)}{\partial Y} \frac{\partial^2 W(X, Y)}{\partial X \partial Y} \right) \\ & - \frac{\partial W(X, Y)}{\partial X} \frac{\partial^2 W(X, Y)}{\partial X^2} + P_x \end{aligned} \quad (3.81)$$

$$\begin{aligned} NLW_2 = & \frac{\alpha(-1 + \nu)}{2} \left( \frac{\partial W(X, Y)}{\partial Y} \frac{\partial^2 W(X, Y)}{\partial X^2} \right) - \frac{\alpha(1 + \nu)}{2} \left( \frac{\partial W(X, Y)}{\partial X} \frac{\partial^2 W(X, Y)}{\partial X \partial Y} \right) \\ & - \alpha^3 \frac{\partial W(X, Y)}{\partial Y} \frac{\partial^2 W(X, Y)}{\partial Y^2} + P_y \end{aligned} \quad (3.82)$$

$$LW = \frac{\partial^4 W(X, Y)}{\partial X^4} + 2\alpha^2 \frac{\partial^4 W(X, Y)}{\partial X^2 \partial Y^2} + \alpha^4 \frac{\partial^4 W(X, Y)}{\partial Y^4} \quad (3.83)$$

NLUVW

$$\begin{aligned}
&= -12\alpha^2(-1 + \nu) \frac{\partial^2 W(X, Y)}{\partial X \partial Y} \left( \frac{\partial U(X, Y)}{\partial Y} + \frac{\partial V(X, Y)}{\partial X} + \frac{\partial W(X, Y)}{\partial X} \frac{\partial W(X, Y)}{\partial Y} \right) \\
&+ 6 \frac{\partial^2 W(X, Y)}{\partial X^2} \left( 2 \frac{\partial U(X, Y)}{\partial X} + 2\alpha^2 \nu \frac{\partial V(X, Y)}{\partial Y} + \alpha^2 \nu \left( \frac{\partial W(X, Y)}{\partial Y} \right)^2 + \left( \frac{\partial W(X, Y)}{\partial X} \right)^2 \right) \\
&+ 6\alpha^2 \frac{\partial^2 W(X, Y)}{\partial Y^2} \left( 2\nu \frac{\partial U(X, Y)}{\partial X} + 2\alpha^2 \frac{\partial V(X, Y)}{\partial Y} + \nu \left( \frac{\partial W(X, Y)}{\partial X} \right)^2 \right) \\
&+ \alpha^2 \left( \frac{\partial W(X, Y)}{\partial Y} \right)^2 \tag{3.84}
\end{aligned}$$

The non-dimensional formulas bending moment, membrane forces, bending stresses and the membrane stresses become;

$$M_x = -\frac{1}{12(1 - \nu^2)} \left( \frac{\partial^2 W(X, Y)}{\partial X^2} + \alpha^2 \nu \frac{\partial^2 W(X, Y)}{\partial Y^2} \right) \tag{3.85}$$

$$M_y = -\frac{1}{12(1 - \nu^2)} \left( \nu \frac{\partial^2 W(X, Y)}{\partial X^2} + \alpha^2 \frac{\partial^2 W(X, Y)}{\partial Y^2} \right) \tag{3.86}$$

$$M_{xy} = \frac{\alpha}{12(1 + \nu)} \frac{\partial^2 W(X, Y)}{\partial X \partial Y} \tag{3.87}$$

$$\begin{aligned}
N_x = &-\frac{Ea}{2\beta^3(\nu^2 - 1)} \left( 2 \frac{\partial U(X, Y)}{\partial X} + 2\nu\alpha^2 \frac{\partial V(X, Y)}{\partial Y} + \nu\alpha^2 \left( \frac{\partial W(X, Y)}{\partial Y} \right)^2 \right. \\
&\left. + \left( \frac{\partial W(X, Y)}{\partial X} \right)^2 \right) \tag{3.88}
\end{aligned}$$

$$N_Y = -\frac{Ea}{2\beta^3(v^2 - 1)} \left( 2v \frac{\partial U(X, Y)}{\partial X} + 2\alpha^2 \frac{\partial V(X, Y)}{\partial Y} + v \left( \frac{\partial W(X, Y)}{\partial X} \right)^2 + \alpha^2 \left( \frac{\partial W(X, Y)}{\partial Y} \right)^2 \right) \quad (3.89)$$

$$N_{XY} = \frac{Ea\alpha}{2\beta^3(v + 1)} \left( \frac{\partial U(X, Y)}{\partial Y} + \frac{\partial V(X, Y)}{\partial X} + \frac{\partial W(X, Y)}{\partial X} \frac{\partial W(X, Y)}{\partial Y} \right) \quad (3.90)$$

$$\sigma_X^B = -\frac{1}{2(1 - v^2)} \left( \frac{\partial^2 W(X, Y)}{\partial X^2} + \alpha^2 v \frac{\partial^2 W(X, Y)}{\partial Y^2} \right) \quad (3.91)$$

$$\sigma_Y^B = -\frac{1}{2(1 - v^2)} \left( v \frac{\partial^2 W(X, Y)}{\partial X^2} + \alpha^2 \frac{\partial^2 W(X, Y)}{\partial Y^2} \right) \quad (3.92)$$

$$\sigma_{XY}^B = \frac{\alpha}{2(1 + v)} \frac{\partial^2 W(X, Y)}{\partial X \partial Y} \quad (3.93)$$

$$\sigma_X^M = -\frac{1}{2(v^2 - 1)} \left( 2 \frac{\partial U(X, Y)}{\partial X} + 2v\alpha^2 \frac{\partial V(X, Y)}{\partial Y} + \alpha^2 v \left( \frac{\partial W(X, Y)}{\partial Y} \right)^2 + \left( \frac{\partial W(X, Y)}{\partial X} \right)^2 \right) \quad (3.94)$$

$$\sigma_Y^M = -\frac{1}{2(v^2 - 1)} \left( 2v \frac{\partial U(X, Y)}{\partial X} + 2\alpha^2 \frac{\partial V(X, Y)}{\partial Y} + v \left( \frac{\partial W(X, Y)}{\partial X} \right)^2 + \alpha^2 \left( \frac{\partial W(X, Y)}{\partial Y} \right)^2 \right) \quad (3.95)$$

$$\sigma_{XY}^M = \frac{\alpha}{2(v + 1)} \left( \frac{\partial U(X, Y)}{\partial Y} + \frac{\partial V(X, Y)}{\partial X} + \frac{\partial W(X, Y)}{\partial X} \frac{\partial W(X, Y)}{\partial Y} \right) \quad (3.96)$$

$$\begin{aligned}
M_N = & -\frac{1}{12(1-\nu^2)} \left( -2n_X n_Y (-1 + \nu) \alpha \frac{\partial^2 W(X, Y)}{\partial X \partial Y} + n_Y^2 \left( \frac{\partial^2 W(X, Y)}{\partial X^2} \nu \right. \right. \\
& \left. \left. + \alpha^2 \frac{\partial^2 W(X, Y)}{\partial Y^2} \right) + n_X^2 \left( \frac{\partial^2 W(X, Y)}{\partial X^2} + \alpha^2 \nu \frac{\partial^2 W(X, Y)}{\partial Y^2} \right) \right) \quad (3.97)
\end{aligned}$$

$$\begin{aligned}
V_N = & \frac{1}{12(-1 + \nu)} \left[ (n_x n_y^2 (1 - \nu) + n_x) \frac{\partial^3 W(X, Y)}{\partial X^3} + (n_y n_x^2 (1 - \nu) + n_y \alpha^3) \frac{\partial^3 W(X, Y)}{\partial Y^3} \right. \\
& + \left( 2n_y n_x^2 \alpha (\nu - 1) + \alpha n_y + \alpha n_y^3 (1 - \nu) \right) \frac{\partial^3 W(X, Y)}{\partial X^2 \partial Y} \\
& + \left( 2n_x n_y^2 \alpha^2 (\nu - 1) + \alpha^2 n_x + \alpha^2 n_x^3 (1 - \nu) \right) \frac{\partial^3 W(X, Y)}{\partial X \partial Y^2} \\
& - 12n_y \alpha^3 \frac{\partial V(X, Y)}{\partial Y} \frac{\partial W(X, Y)}{\partial Y} - 6n_y \alpha \left( \frac{\partial W(X, Y)}{\partial X} \right)^2 \frac{\partial W(X, Y)}{\partial Y} \\
& - 6n_y \alpha^3 \left( \frac{\partial W(X, Y)}{\partial Y} \right)^3 + 6n_y (-1 + \nu) \alpha \frac{\partial U(X, Y)}{\partial Y} \frac{\partial W(X, Y)}{\partial X} \\
& + 6n_y (-1 + \nu) \alpha \frac{\partial V(X, Y)}{\partial X} \frac{\partial W(X, Y)}{\partial X} - 12n_y \nu \alpha \frac{\partial U(X, Y)}{\partial X} \frac{\partial W(X, Y)}{\partial Y} \\
& - 12n_x \frac{\partial U(X, Y)}{\partial X} \frac{\partial W(X, Y)}{\partial X} - 6n_x \left( \frac{\partial W(X, Y)}{\partial X} \right)^3 \\
& + 6n_x (-1 + \nu) \alpha^2 \frac{\partial U(X, Y)}{\partial Y} \frac{\partial W(X, Y)}{\partial Y} + 6n_x (-1 + \nu) \alpha^2 \frac{\partial V(X, Y)}{\partial X} \frac{\partial W(X, Y)}{\partial Y} \\
& - 6n_x \alpha^2 \left( \frac{\partial W(X, Y)}{\partial Y} \right)^2 \frac{\partial W(X, Y)}{\partial X} \\
& \left. - 12n_x \nu \alpha^2 \frac{\partial V(X, Y)}{\partial Y} \frac{\partial W(X, Y)}{\partial X} \right] \tag{3.98}
\end{aligned}$$

The shear force becomes  $V_N = V_N^L + V_N^{NL}$

$$\begin{aligned}
V_N^L = & \frac{1}{12(-1+u)} \left[ (n_x n_y^2 (1-u) + n_x) \frac{\partial^3 W(X, Y)}{\partial X^3} \right. \\
& + (n_y n_x^2 \alpha^3 (1-u) + n_y \alpha^3) \frac{\partial^3 W(X, Y)}{\partial Y^3} \\
& + (2n_y n_x^2 \alpha (u-1) + \alpha n_y + \alpha n_y^3 (1-u)) \frac{\partial^3 W(X, Y)}{\partial X^2 \partial Y} \\
& + (2n_x n_y^2 \alpha^2 (u-1) + \alpha^2 n_x \\
& \left. + \alpha^2 n_x^3 (1-u)) \frac{\partial^3 W(X, Y)}{\partial X \partial Y^2} \right] \tag{3.99}
\end{aligned}$$

$$\begin{aligned}
V_N^{NL} = & \frac{1}{12(-1+u)} \left[ -12n_y \alpha^3 \frac{\partial V(X, Y)}{\partial Y} \frac{\partial W(X, Y)}{\partial Y} - 6n_y \alpha \left( \frac{\partial W(X, Y)}{\partial X} \right)^2 \frac{\partial W(X, Y)}{\partial Y} \right. \\
& - 6n_y \alpha^3 \left( \frac{\partial W(X, Y)}{\partial Y} \right)^3 + 6n_y (-1+u) \alpha \frac{\partial U(X, Y)}{\partial Y} \frac{\partial W(X, Y)}{\partial X} \\
& + 6n_y (-1+u) \alpha \frac{\partial V(X, Y)}{\partial X} \frac{\partial W(X, Y)}{\partial X} - 12n_y u \alpha \frac{\partial U(X, Y)}{\partial X} \frac{\partial W(X, Y)}{\partial Y} \\
& - 12n_x \frac{\partial U(X, Y)}{\partial X} \frac{\partial W(X, Y)}{\partial X} - 6n_x \left( \frac{\partial W(X, Y)}{\partial X} \right)^3 \\
& + 6n_x (-1+u) \alpha^2 \frac{\partial U(X, Y)}{\partial Y} \frac{\partial W(X, Y)}{\partial Y} + 6n_x (-1+u) \alpha^2 \frac{\partial V(X, Y)}{\partial X} \frac{\partial W(X, Y)}{\partial Y} \\
& - 6n_x \alpha^2 \left( \frac{\partial W(X, Y)}{\partial Y} \right)^2 \frac{\partial W(X, Y)}{\partial X} \\
& \left. - 12n_x u \alpha^2 \frac{\partial V(X, Y)}{\partial Y} \frac{\partial W(X, Y)}{\partial X} \right] \tag{3.100}
\end{aligned}$$



## 3.2 Large Deflection of Thin Plates on Foundations

In this section, the governing equations derived in the previous section are modified to include the effect of the foundation. Both discrete and continuous foundation models are considered.

### 3.2.1 Governing Equations for Plates on Discrete Foundations

#### 3.2.1.1 Updated w-f Equations

$$Lwf = NLwf + \frac{1}{D} \left( p_z - kw(x, y) - k_1 w^3(x, y) + g_p \nabla^2 w(x, y) \right) \quad (3.101)$$

Where  $Lwf$  is  $\nabla^4 w$ ,  $NLwf$  is defined in the right hand side of Equation (3.22),  $p_z$  is the transverse external loads, and  $k$ ,  $k_1$  and  $g_p$  are the discrete foundation model parameters.

The updated non-dimensional W-F equation becomes:

$$LWF = NLWF + P_z - KW(X, Y) - K_1 W^3(X, Y) + G_1 \nabla^2 W(X, Y) \quad (3.102)$$

Where;

$LWF$  is  $\nabla^4 W$ ,

$NLWF$  is defined in Equation 3.62,  $P_z$  is  $\frac{12(1 - \nu^2)p_z a^4}{Et^4}$ , and  $K$ ,  $K_1$  and  $G_1$  are the non

– dimensional foundation parameters and defined by:

$$K = \frac{ka^4}{D} ; K_1 = \frac{k_1 a^4 t^2}{D} ; \text{ and } G_1 = \frac{g_p a^2}{D}$$

a and t are the side dimension and the thickness of the plate respectively.

### 3.2.1.2 Updated w-u-v Equations

The updated dimensional w-u-v Equation (3.57) becomes

$$Lw = NLuvw + p_z - kw(x, y) - k_1 w^3(x, y) + g_p \nabla^2 w(x, y) \quad (3.103)$$

In which Lw is defined by Equation (3.48), and NLuvw is defined by Equation (3.49),  $p_z$  is the transverse external loads.

Dividing Equation (3.103) by  $D = \frac{Et^3}{12(1-\nu^2)}$  ;

$$\nabla^4 w = \frac{1}{D} (NLuvw + p_z - kw(x, y) - k_1 w^3(x, y) + g_p \nabla^2 w(x, y)) \quad (3.104)$$

The updated non-dimensional W-U-V Equation becomes

$$LW = NLUVW + P_z - KW(X, Y) + K_1 W^3(X, Y) - G_1 \nabla^2 W(X, Y) \quad (3.105)$$

In which LW is defined by Equation (3.83), and NLUVW is defined by Equation (3.84).

## 3.2.2 Elastic Continuous Model

In this model, the supporting soil is assumed to be elastic, isotropic, homogeneous and semi-infinite continuous characterized by the two constants: elastic modulus,  $E_s$ , and Poisson's ratio,  $\nu_s$ . The model is based on Boussinesq's solution of the elastic half-space

problem. The deflections of the plate-soil contact surface at arbitrary point  $x_j$  are given by:

$$w(x_j) = \sum_{i=1}^{n_p} \frac{P_i(1-\nu_s^2)}{\pi E_s r_{ij}} ; \quad u(x_j) = \sum_{i=1}^{n_p} -\frac{P_i(1-2\nu_s)(1+\nu_s)}{2\pi E_s r_{ij}} \quad (3.106)$$

Where  $P_i$  is the soil reaction at point  $x_i$  and  $r_{ij}$  is the distance between points  $j$  and  $i$ . Applying the above equation at all points  $j = 1, n_p$ , the developed equations are as follows:

$$\begin{Bmatrix} w_1 \\ \vdots \\ w_{n_p} \end{Bmatrix} = \begin{bmatrix} f_{w11} & \cdots & f_{w1n_p} \\ \vdots & \ddots & \vdots \\ f_{wn_p1} & \cdots & f_{wn_p n_p} \end{bmatrix} \begin{Bmatrix} P_1 \\ \vdots \\ P_{n_p} \end{Bmatrix}$$

$$\begin{Bmatrix} u_1 \\ \vdots \\ u_{n_p} \end{Bmatrix} = \begin{bmatrix} f_{u11} & \cdots & f_{u1n_p} \\ \vdots & \ddots & \vdots \\ f_{un_p1} & \cdots & f_{un_p n_p} \end{bmatrix} \begin{Bmatrix} P_1 \\ \vdots \\ P_{n_p} \end{Bmatrix} \quad (3.107)$$

$$\text{Where: } f_{wij} = \frac{(1-\nu_s^2)}{\pi E_s r_{ij}} \text{ and } f_{uij} = -\frac{(1-2\nu_s)(1+\nu_s)}{2\pi E_s r_{ij}}$$

Or:

$$\{W\} = [f_w]\{P\} ; \quad \{U\} = [f_u]\{P\} \quad (3.108)$$

As noticed, the elements of the coefficient matrix  $F$  can be easily computed directly at the points where  $i \neq j$ . For  $i = j$ , however  $r_{ij} \rightarrow 0$  and therefore  $f_{ii}$  becomes singular and needs to be computed indirectly using the following procedure: to find  $f_{ii}$ ,

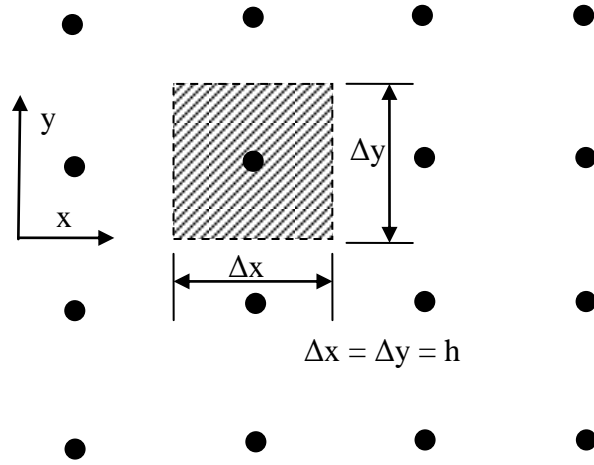


Figure 3.4 Calculations of  $f_{ij}$  Coefficients in Boussinesq Formula.

From Figure 3.4,

$$\begin{aligned}
 f_{wii} &= \frac{(1 - \nu_s^2)}{h^2 \pi E_s} \int_{-\frac{h}{2}}^{\frac{h}{2}} \int_{-\frac{h}{2}}^{\frac{h}{2}} \frac{1}{\sqrt{x^2 + y^2}} dx dy \\
 &= \frac{(1 - \nu_s^2)}{h \pi E_s} \log(17 + 12\sqrt{2}) \\
 &= 3.525 \frac{(1 - \nu_s^2)}{h \pi E_s}
 \end{aligned}$$

So that;

$$f_{wii} = 3.525 \frac{(1 - \nu_s^2)}{h \pi E_s} \text{ and similar formula for } f_{uii} = -3.525 \frac{(1 - 2\nu_s)(1 + \nu_s)}{h 2 \pi E_s};$$

Where; h is the mesh size.

The implementation of the above model in RBF formulation will be explained in the next chapter.

## CHAPTER FOUR

# RBF FORMULATIONS AND COMPUTER IMPLEMENTATION

In this chapter, the formulation of multi-quadric radial basis function (MQ-RBF) is provided in details. In addition, the program codes for implementing the RBF formulations are presented.

### 4.1 RBF Formulation

In this work, the multi-quadric radial basis function MQ-RBF is used. Consider the 2-D computational domain (Figure 4.1) that represents the plate geometry. For collocation, we use node points distributed both along the boundary ( $\underline{x}_B^j, j = 1, \dots, N_B$ ), and over the interior ( $\underline{x}_D^j, j = 1, \dots, N_D$ ). Let  $x_p = \{X_B, X_D\}$ , so that the total number of points called poles is  $N_p = N_B + N_D$ .

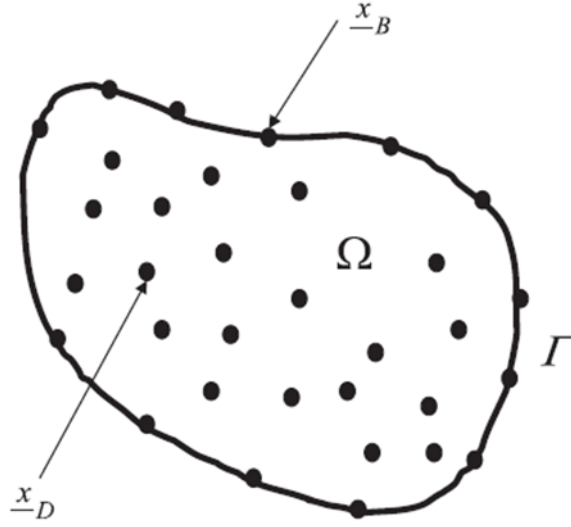


Figure 4.1 Domain and Boundary Nodes

The transverse deflections  $w$ , the in plane deflections,  $u$  and  $v$ , and the stress function  $F$  are interpolated linearly by MQ-RBF. The MQ-RBF formulations are written into two types (a and b) to be suitable for the different boundary conditions including the free-edge ones. Type a is used in all boundary conditions except the free edge whereas Type b is suitable for all. The disadvantage of Type b is the need for extra nodes rather than the domain and boundary nodes. Both MQ-RBF formulations types are given as follows:

$$\begin{aligned}
 w(\underline{x}) = & \sum_{j=1}^{N_B} a_w^j BC_{w1} \left( \phi(\|\underline{x} - \underline{x}_B^j\|) \right) + \sum_{j=1}^{N_B} a_w^{j+N_B} BC_{w2} \left( \phi(\|\underline{x} - \underline{x}_B^j\|) \right) \\
 & + \sum_{j=1}^{N_D} a_w^{j+2N_B} \phi(\|\underline{x} - \underline{x}_D^j\|)
 \end{aligned} \tag{4-1a}$$

$$\begin{aligned}
F(\underline{x}) &= \sum_{j=1}^{N_B} \alpha_F^j BC_{F1} \left( \phi(\|\underline{x} - \underline{x}_B^j\|) \right) + \sum_{j=1}^{N_B} \alpha_F^{j+N_B} BC_{F2} \left( \phi(\|\underline{x} - \underline{x}_B^j\|) \right) \\
&\quad + \sum_{j=1}^{N_D} \alpha_F^{j+2N_B} \phi(\|\underline{x} - \underline{x}_D^j\|)
\end{aligned} \tag{4-2a}$$

$$u(\underline{x}) = \sum_{j=1}^{N_B} \alpha_u^j BC_u \left( \phi(\|\underline{x} - \underline{x}_B^j\|) \right) + \sum_{j=1}^{N_D} \alpha_u^{j+N_B} \left( \phi(\|\underline{x} - \underline{x}_B^j\|) \right) \tag{4-3a}$$

$$v(\underline{x}) = \sum_{j=1}^{N_B} \alpha_v^j BC_v \left( \phi(\|\underline{x} - \underline{x}_B^j\|) \right) + \sum_{j=1}^{N_D} \alpha_v^{j+N_B} \left( \phi(\|\underline{x} - \underline{x}_B^j\|) \right) \tag{4-4a}$$

$$w(\underline{x}) = \sum_{j=1}^{N_B+N_P} \alpha_w^j \left( \phi(\|\underline{x} - \underline{x}_B^j\|) \right) \tag{4-1b}$$

$$F(\underline{x}) = \sum_{j=1}^{N_B+N_P} \alpha_F^j \left( \phi(\|\underline{x} - \underline{x}_B^j\|) \right) \tag{4-2b}$$

$$u(\underline{x}) = \sum_{j=1}^{N_P} \alpha_u^j \left( \phi(\|\underline{x} - \underline{x}_B^j\|) \right) \tag{4-3b}$$

$$v(\underline{x}) = \sum_{j=1}^{N_P} \alpha_v^j \left( \phi(\|\underline{x} - \underline{x}_B^j\|) \right) \tag{4-4b}$$

Where;

- $\phi(\|\underline{x} - \underline{x}^j\|) = \sqrt{(x - x^j)^2 + (y - y^j)^2 + c^2}$  is a multi-quadric RBF ,
- $c$  is the shape factor, and

- $a_w^j, a_u^j, a_v^j$  and  $a_F^j$  are unknown coefficients to be determined by applying the governing equations at the domain points and satisfying the boundary conditions at the boundary points.
- $BC_{w1}, BC_{w2}, BC_{F1}, BC_{F2}, BC_u$  and  $BC_v$  are the differential operators of the boundary conditions corresponding to w, F, u and v, respectively.

The summary of the governing equations as derived in Chapter 3 are given below followed by their corresponding RBF matrix equations. W-F formulas and matrices:

$$\nabla^4 F = NLW \quad (4 - 5)$$

$$\nabla^4 w = \frac{q}{D} - \frac{p}{D} + NLWF \quad (4 - 6)$$

Where;

$$NLW = E \left[ \left( \frac{\partial^2 w}{\partial x \partial y} \right)^2 - \left( \frac{\partial^2 w}{\partial x^2} \right) \left( \frac{\partial^2 w}{\partial y^2} \right) \right]$$

$$NLWF = \frac{t}{D} \left[ \left( \frac{\partial^2 F}{\partial y^2} \right) \left( \frac{\partial^2 w}{\partial x^2} \right) + \left( \frac{\partial^2 F}{\partial x^2} \right) \left( \frac{\partial^2 w}{\partial y^2} \right) - 2 \left( \frac{\partial^2 F}{\partial x \partial y} \right) \left( \frac{\partial^2 w}{\partial x \partial y} \right) \right]$$

The corresponding RBF equations are:

$$[A_f] \{a_f\} = \{R_f\} \quad (4 - 7)$$



$$\begin{aligned}
& \begin{bmatrix} BC_{F1}(BC_{F1}(\emptyset)) & BC_{F1}(BC_{F2}(\emptyset)) & BC_{F1}(\emptyset) \\ BC_{F2}(BC_{F1}(\emptyset)) & BC_{F2}(BC_{F2}(\emptyset)) & BC_{F2}(\emptyset) \\ \nabla^4(BC_{F1}(\emptyset)) & \nabla^4(BC_{F2}(\emptyset)) & \nabla^4(\emptyset) \end{bmatrix} \begin{Bmatrix} \alpha_F^j, j = 1, N_B \\ \alpha_F^{j+N_B}, j = 1, N_B \\ \alpha_F^{j+2N_B}, j = 1, N_D \end{Bmatrix} \\
& = \begin{Bmatrix} F \\ \frac{\partial F(x, y)}{\partial n} \\ \text{NLW} \end{Bmatrix} \tag{4-7a}
\end{aligned}$$

$$\begin{bmatrix} BC_{F1}(\emptyset) \\ BC_{F2}(\emptyset) \\ \nabla^4(\emptyset) \end{bmatrix} \{ \alpha_F^j, j = 1, N_B + N_P \} = \begin{Bmatrix} F \\ \frac{\partial F(x, y)}{\partial n} \\ \text{NLW} \end{Bmatrix} \tag{4-7b}$$

$$[A_w] \{ a_w \} = \{ R_w \} \tag{4-8}$$

$$\begin{aligned}
& \begin{bmatrix} BC_{w1}(BC_{w1}(\emptyset)) & BC_{w1}(BC_{w2}(\emptyset)) & BC_{w1}(\emptyset) \\ BC_{w2}(BC_{w1}(\emptyset)) & BC_{w2}(BC_{w2}(\emptyset)) & BC_{w2}(\emptyset) \\ \nabla^4(BC_{w1}(\emptyset)) & \nabla^4(BC_{w2}(\emptyset)) & \nabla^4(\emptyset) \end{bmatrix} \begin{Bmatrix} \alpha_w^j, j = 1, N_B \\ \alpha_w^{j+N_B}, j = 1, N_B \\ \alpha_w^{j+2N_B}, j = 1, N_D \end{Bmatrix} \\
& = \begin{Bmatrix} w \text{ or } V_n + V_n^{NL} \\ \frac{\partial w(x, y)}{\partial n} \text{ or } Mn \\ \text{NLWF} + \frac{q}{D} - \frac{p}{D} \end{Bmatrix} \tag{4-8a}
\end{aligned}$$

$$\begin{bmatrix} BC_{w1}(\emptyset) \\ BC_{w2}(\emptyset) \\ \nabla^4(\emptyset) \end{bmatrix} \{ \alpha_w^j, j = 1, N_B + N_P \} = \begin{Bmatrix} w \text{ or } V_n + V_n^{NL} \\ \frac{\partial w(x, y)}{\partial n} \text{ or } Mn \\ \text{NLWF} + \frac{q}{D} - \frac{p}{D} \end{Bmatrix} \tag{4-8b}$$

W-U-V formulas and matrices:

$$L_{11}(u) + L_{12}(v) = NL_1(w) \quad (4-9)$$

$$L_{21}(u) + L_{22}(v) = NL_2(w) \quad (4-10)$$

$$\nabla^4 w = \frac{q}{D} - \frac{p}{D} + NL_3(u, v, w) \quad (4-11)$$

Where,

$$L_{11} = \frac{2\partial_{xx} + (1-v)\partial_{yy}}{2(1-v^2)}, \quad L_{12} = L_{21} = \frac{2\partial_{xy}}{2(1-v)}, \quad L_{22} = \frac{2\partial_{yy} + (1-v)\partial_{xx}}{2(1-v^2)}$$

$$NL_1(w) = -\frac{(1+v)w_{xy}w_y + w_x(2w_{xx} + (1-v)w_{yy})}{2(1-v^2)}$$

$$NL_2(w) = -\frac{(1+v)w_{xy}w_x + w_y(2w_{yy} + (1-v)w_{xx})}{2(1-v^2)}$$

$$NL_3(u, v, w)$$

$$\begin{aligned} &= \frac{Etw_{xy}}{D(1+v)}(u_y + v_x + w_x w_y) + \frac{Etw_{xx}}{2D(1-v^2)}(2u_x + w_x^2 + v(2v_y + w_y^2)) \\ &+ \frac{Etw_{yy}}{2D(1-v^2)}(2v_y + w_y^2 + v(2u_x + w_x^2)) \end{aligned}$$

The corresponding RBF equations are:

$$[A_{uv}]\{a_{uv}\} = \{R_{uv}\} \quad (4-12)$$

$$\begin{aligned}
& \begin{bmatrix} BC_u(BC_u(\emptyset)) & BC_u(\emptyset) & 0 & 0 \\ L_{11}(BC_u(\emptyset)) & L_{11}(\emptyset) & L_{12}(BC_v(\emptyset)) & L_{12}(\emptyset) \\ 0 & 0 & BC_v(BC_v(\emptyset)) & BC_v(\emptyset) \\ L_{21}(BC_u(\emptyset)) & L_{21}(\emptyset) & L_{22}(BC_v(\emptyset)) & L_{22}(\emptyset) \end{bmatrix} * \begin{Bmatrix} a_u^j, j = 1, N_B \\ a_u^{j+N_B}, j = 1, N_D \\ a_v^j, j = 1, N_B \\ a_v^{j+N_B}, j = 1, N_D \end{Bmatrix} \\
& = \begin{Bmatrix} u \text{ or } Tx \\ NL_1(w) \\ v \text{ or } Ty \\ NL_2(w) \end{Bmatrix} \tag{4-12a}
\end{aligned}$$

$$\begin{aligned}
& \begin{bmatrix} BC_u(\emptyset) & 0 \\ L_{11}(\emptyset) & L_{12}(\emptyset) \\ 0 & BC_v(\emptyset) \\ L_{21}(\emptyset) & L_{22}(\emptyset) \end{bmatrix} * \begin{Bmatrix} a_u^j, j = 1, N_P \\ a_v^j, j = 1, N_P \end{Bmatrix} = \begin{Bmatrix} u \text{ or } Tx \\ NL_1(w) \\ v \text{ or } Ty \\ NL_2(w) \end{Bmatrix} \tag{4-12b}
\end{aligned}$$

$$[A_w]\{a_w\} = \{R_w\} \tag{4-13}$$

$$\begin{aligned}
& \begin{bmatrix} BC_{w1}(BC_{w1}(\emptyset)) & BC_{w1}(BC_{w2}(\emptyset)) & BC_{w1}(\emptyset) \\ BC_{w2}(BC_{w1}(\emptyset)) & BC_{w2}(BC_{w2}(\emptyset)) & BC_{w2}(\emptyset) \\ \nabla^4(BC_{w1}(\emptyset)) & \nabla^4(BC_{w2}(\emptyset)) & \nabla^4(\emptyset) \end{bmatrix} * \begin{Bmatrix} a_w^j, j = 1, N_B \\ a_w^{j+N_B}, j = 1, N_B \\ a_w^{j+2N_B}, j = 1, N_D \end{Bmatrix} \\
& = \begin{Bmatrix} w \text{ or } V_n + V_n^{NL} \\ \frac{\partial w(x, y)}{\partial n} \text{ or } M_n \\ \frac{q}{D} - \frac{p}{D} + NL_3(u, v, w) \end{Bmatrix} \tag{4-13a}
\end{aligned}$$

$$\begin{bmatrix} BC_{w1}(\emptyset) \\ BC_{w2}(\emptyset) \\ \nabla^4(\emptyset) \end{bmatrix} * \{a_w^j, j = 1, N_B + N_P\} = \left\{ \begin{array}{l} w \text{ or } V_n + V_n^{NL} \\ \frac{\partial w(x, y)}{\partial n} \text{ or } M_n \\ \frac{q}{D} - \frac{p}{D} + NL_3(u, v, w) \end{array} \right\} \quad (4 - 13b)$$

## 4.2 Computer Implementation

All symbolic and numerical computations have been performed using Mathematica. The procedure for programming the RBF matrices for both W-F and U-V-W formulations are explained below.

### 4.2.1 Mathematica Code for W-F Formulation

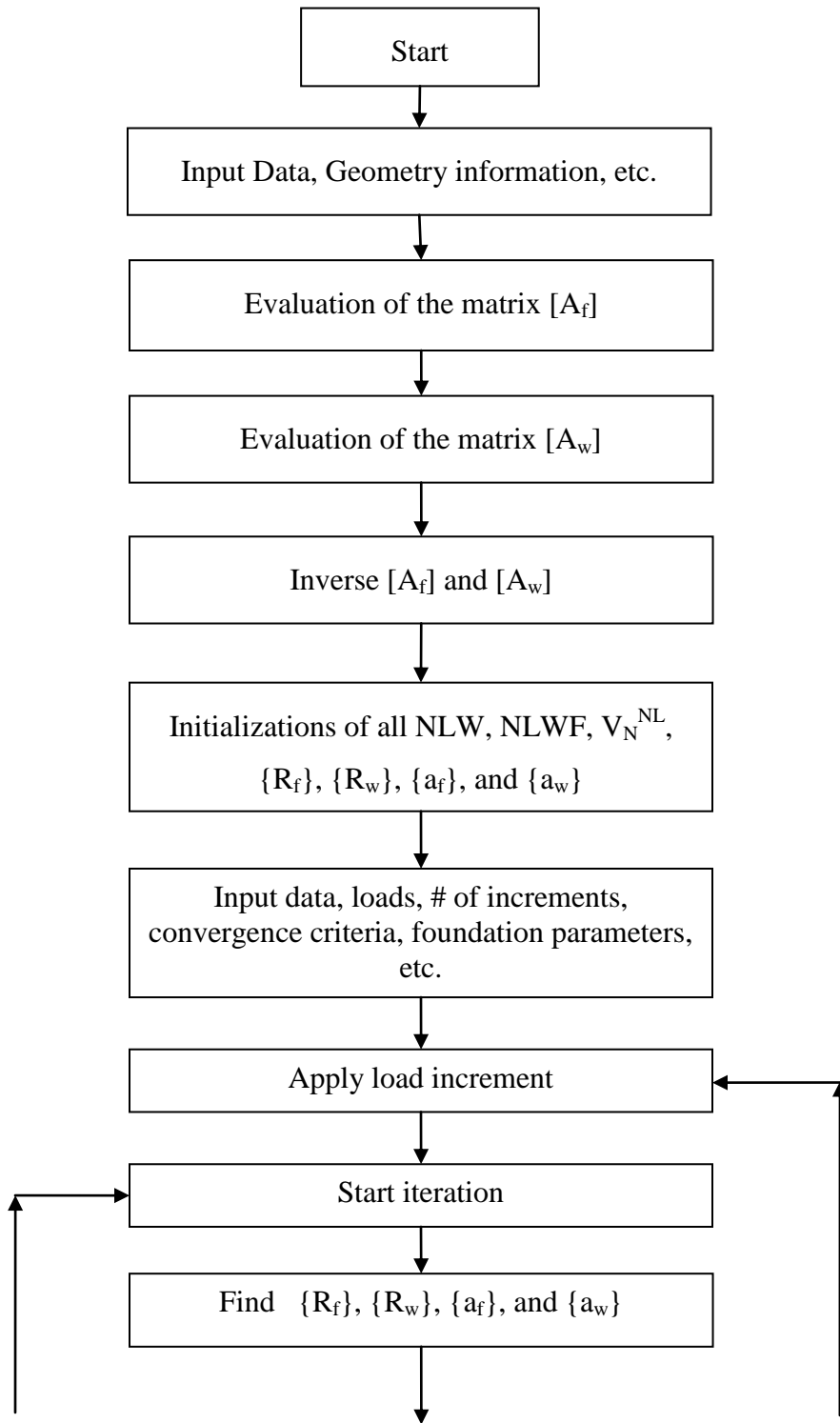
To solve the Equations (4-7) and (4-8), the following steps are followed:

- 1) Modeling geometry
- 2) Boundary conditions information
- 3) Radial Basis Function (RBF) definition
- 4) Governing Partial differential equations definitions
- 5) Definitions of boundary condition equations
- 6) Evaluation of the matrix  $[A_f]$  in Equation (4-7)
- 7) Evaluation of the matrix  $[A_w]$  in Equation (4-8)
- 8) Determination the Inverses of both matrices  $[A_f]$ , and  $[A_w]$

- 9) Initializations of all NLW, NLWF,  $V_n^{NL}$ ,  $\{R_f\}$ ,  $\{R_w\}$ ,  $\{a_f\}$ , and  $\{a_w\}$
- 10) Definitions of loads and their increments, convergence criteria, etc.
- 11) Definitions of the foundation models parameters
- 12) Start with first incremental load
- 13) Start with first iteration
- 14) Evaluation the  $\{R_f\}$ , and  $\{R_w\}$ ,
- 15) Calculation of  $\{a_f\}$  , and  $\{a_w\}$
- 16) Evaluation of all  $w$ , and  $F$  using the Equations (4-1a or 4-1b, and 4-2a or 4-2b) respectively
- 17) Evaluation of the foundation reaction  $P$  and the New of NLW, NLWF, and  $V_n^{NL}$ .
- 18) Evaluation the vertical displacement  $w$  at the centre of the plate.
- 19) Repeating the steps from 13 up to 18
- 20) Calculation of the  $error = Abs\left(\frac{Abs(w_{19})-Abs(w_{18})}{Abs(w_{18})}\right)$
- 21) If the error is not less than the convergence error criteria defined in step 10, repeating the steps from 13 up to 19 with the new iterations.

- 22) If the error is less than the convergence error criteria defined in step 10, writing the results of this incremental load step and then starting new incremental load by repeating the steps from 12 up to 19. Repeat all steps from 12 up to 21 for all incremental loads
- 23) Writing summarized report for the results containing, deflections, stresses, etc.
- 24) Stop

The above steps are shown in the flow chart (Figure 4-2).



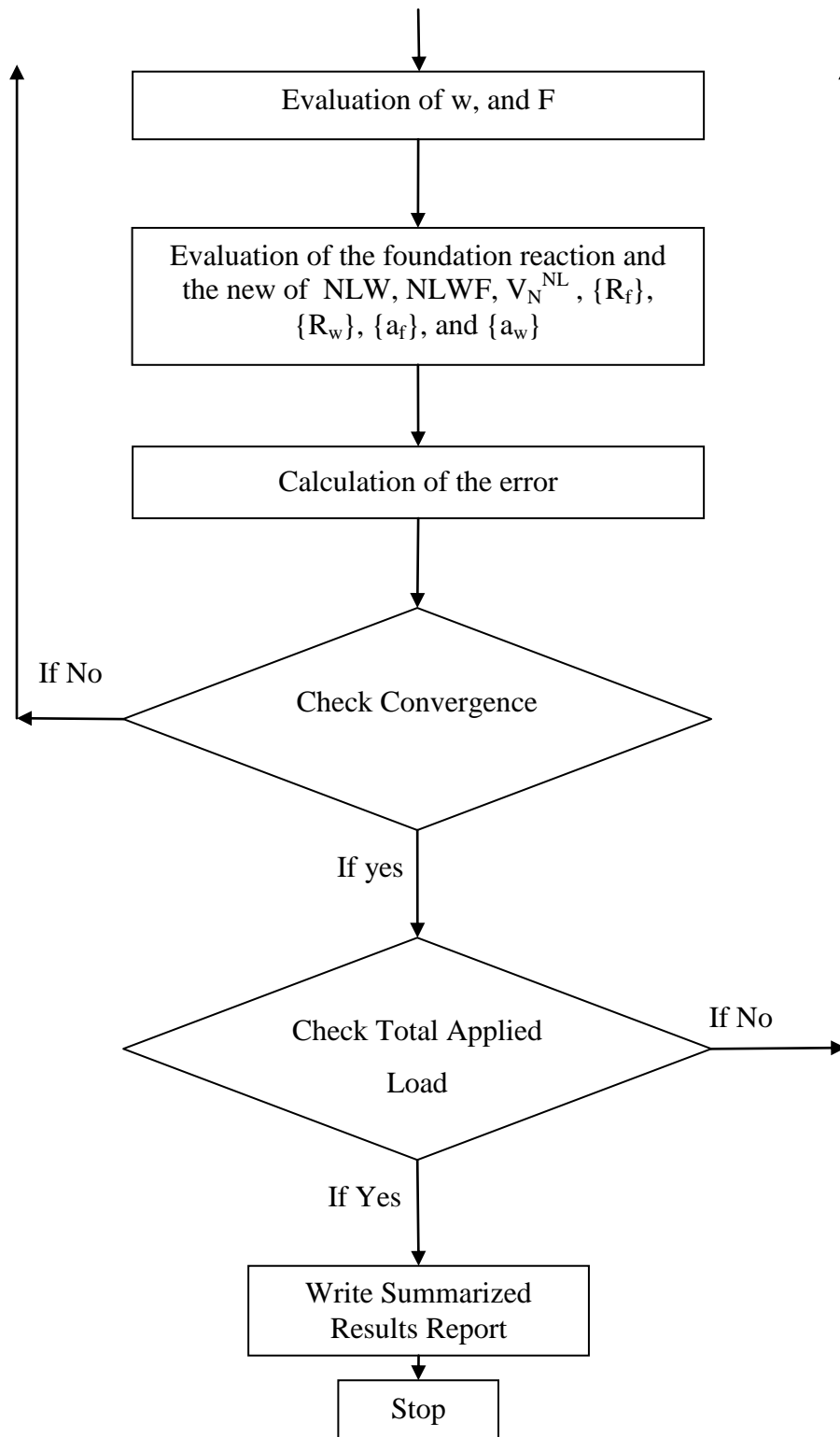


Figure 4.2 Flow Chart for the W-F Program



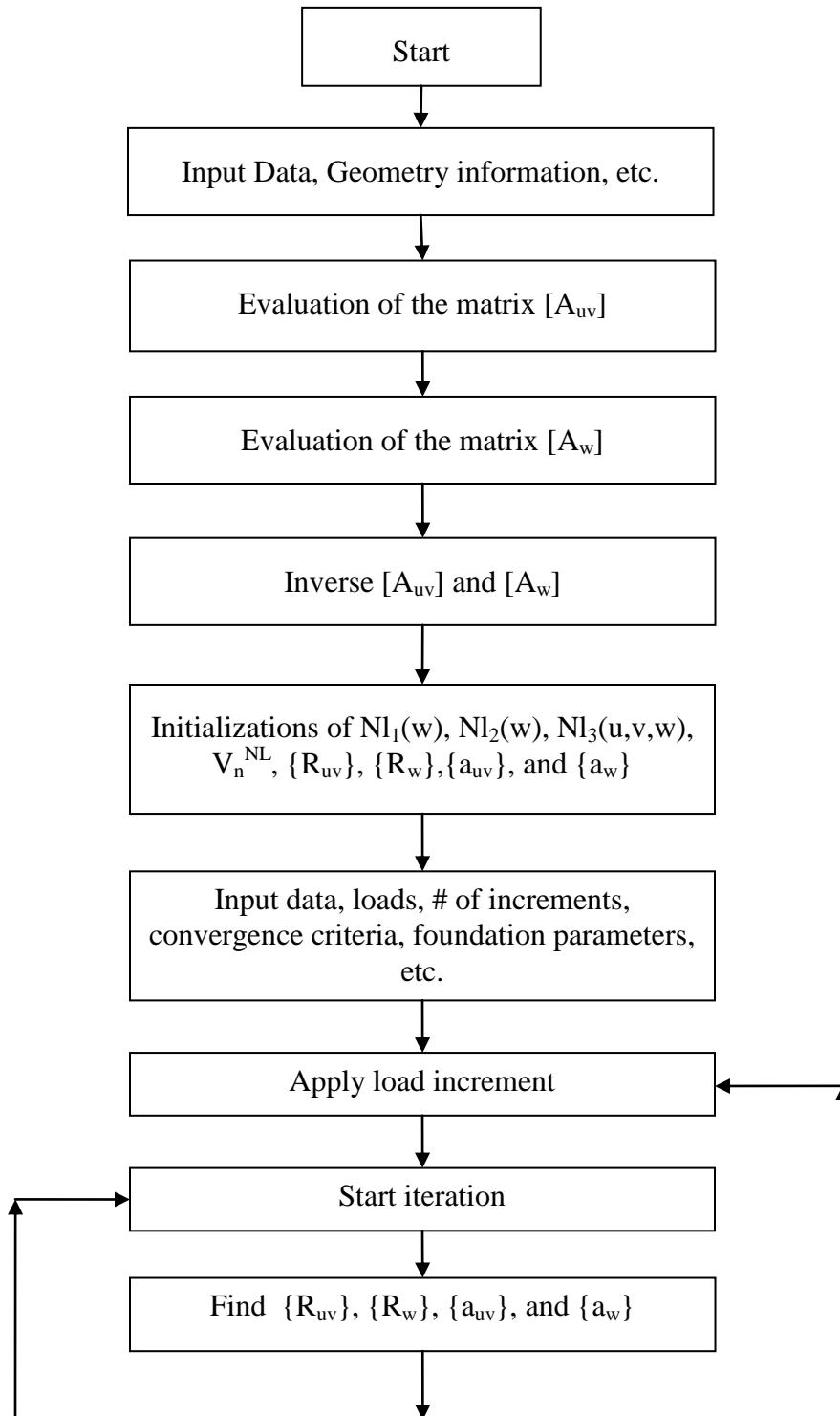
## 4.2.2 Mathematica Code for W-U-V Formulations

To solve the Equations (4-12) and (4-13), the following steps are followed:

- 1) Modeling geometry
- 2) Boundary conditions information
- 3) Radial Basis Function (RBF) definition
- 4) Governing Partial differential equations definitions
- 5) Definitions of boundary condition equations
- 6) Evaluation of the matrix  $[A_{uv}]$  in Equation (4-12)
- 7) Evaluation of the matrix  $[A_w]$  in Equation (4-13)
- 8) Determination of the Inverses of both matrices  $[A_{uv}]$ , and  $[A_w]$
- 9) Initializations of  $Nl_1(w)$ ,  $Nl_2(w)$ ,  $Nl_3(u,v,w)$ ,  $V_n^{NL}$ ,  $\{R_{uv}\}$ ,  $\{R_w\}$ ,  $\{a_{uv}\}$ , and  $\{a_w\}$
- 10) Definitions of loads and their increments, convergence criteria, etc.
- 11) Definitions of the foundation models parameters
- 12) Start with first increment load
- 13) Start with first iteration
- 14) Evaluation the  $\{R_{uv}\}$ , and  $\{R_w\}$

- 15) Calculation of  $\{a_{uv}\}$ , and  $\{a_w\}$
- 16) Evaluation of all  $w$ ,  $u$ , and  $v$  using the Equations (4-1a or 4-1b, 4-3a or 4-3b, and 4-4a or 4-4b) respectively.
- 17) Evaluation of foundation reaction  $p$  and the New  $Nl_1(w)$ ,  $Nl_2(w)$ ,  $Nl_3(u,v,w)$ , and  $V_n^{NL}$
- 18) Evaluation the vertical displacement  $w$  at the centre of the plate.
- 19) Repeating the steps from 13 up to 18
- 20) Calculation of the  $error = Abs\left(\frac{Abs(w_{19})-Abs(w_{18})}{Abs(w_{18})}\right)$
- 21) If the error is not less than the convergence error criteria defined in step 10, repeating the steps from 13 up to 19 with the new iteration.
- 22) If the error is less than the convergence error criteria defined in step 10, writing the results of this incremental load step and then starting new incremental load by repeating the steps from 12 up to 19.
- 23) Repeating all steps from 12 up to 22 for all incremental loads
- 24) Writing summarized report for the results containing, deflections, stresses, etc.
- 25) Stop

The above steps are shown in the flow chart (Figure 4-3) while the code in Mathematica is given in the Appendix A.



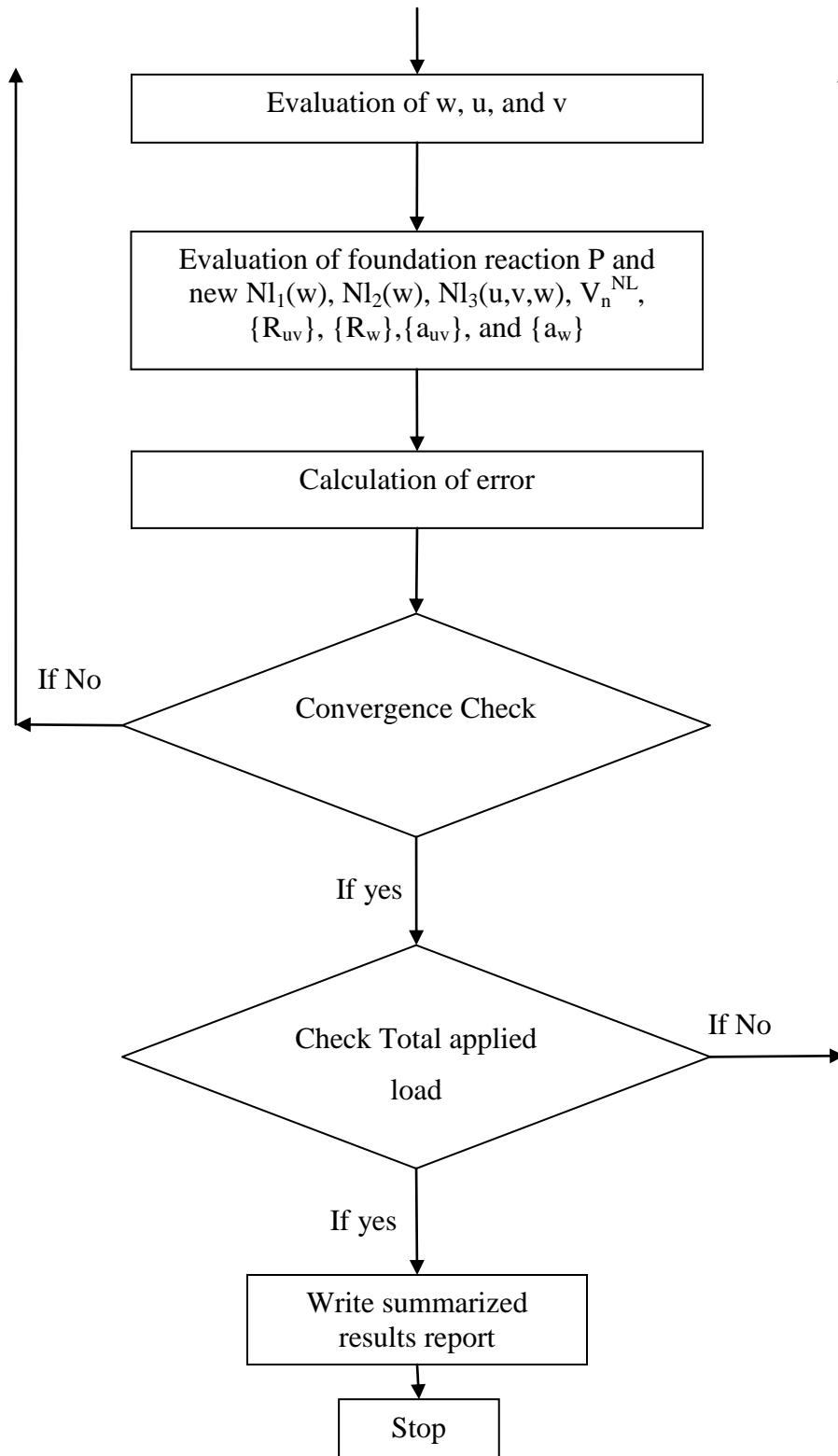


Figure 4.3 Flow Chart for the W-U-V Program

To calculate the response of the supporting soil media when using the elastic continuous models, a specific procedure sequence is adopted. From the analysis, each node has a corresponding settlement and a consequence point force. The configuration of the plate is shown in Figure (4.4).

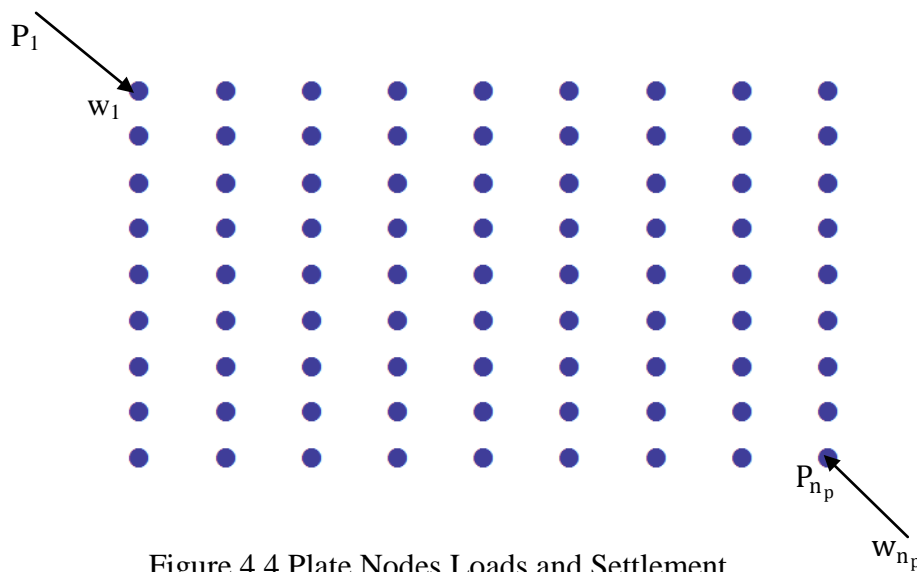


Figure 4.4 Plate Nodes Loads and Settlement

According to the continuous media concept, each point load on the domain will affect all other points and causes settlement depending on the radial distance between them. As a result, the total settlement at each point will be the summation of all nodes forces effects. Considering the Boussinesq elastic half space model (1885) formulas, the resulting equations can be represented by the following:

For the vertical displacements,

$$w_1 = \left( \frac{1 - v_s^2}{\pi E_s} \right) \left[ \frac{P_1}{h} f_{11} + \frac{P_2}{r_{12}} + \dots + \frac{P_{n_p}}{r_{1n_p}} \right]$$

$$w_2 = \left( \frac{1 - v_s^2}{\pi E_s} \right) \left[ \frac{P_1}{r_{21}} + \frac{P_2}{h} f_{22} + \frac{P_3}{r_{23}} + \dots + \frac{P_{n_p}}{r_{2n_p}} \right]$$

.

.

.

$$w_{n_p} = \left( \frac{1 - v_s^2}{\pi E_s} \right) \left[ \frac{P_1}{r_{n_p 1}} + \frac{P_2}{r_{n_p 2}} + \dots + \frac{P_{n_p}}{h} f_{n_p n_p} \right]$$

For the horizontal displacements,

$$w_1 = \left( \frac{1 - v_s^2}{\pi E_s} \right) \left[ \frac{P_1}{h} f_{11} + \frac{P_2}{r_{12}} + \dots + \frac{P_{n_p}}{r_{1n_p}} \right]$$

$$w_2 = \left( \frac{1 - v_s^2}{\pi E_s} \right) \left[ \frac{P_1}{r_{21}} + \frac{P_2}{h} f_{22} + \frac{P_3}{r_{23}} + \dots + \frac{P_{n_p}}{r_{2n_p}} \right]$$

.

.

.

$$w_{n_p} = \left( \frac{1 - v_s^2}{\pi E_s} \right) \left[ \frac{P_1}{r_{n_p 1}} + \frac{P_2}{r_{n_p 2}} + \dots + \frac{P_{n_p}}{h} f_{n_p n_p} \right] \quad (4 - 14)$$

As the deflections of the nodes are known from the analysis of the plates, the only unknowns in the Equations 4-14 are the resulting reaction forces P's. By solving the resulting linear algebra equations, the values of P's can be determined and taken as the average of the calculated from both the vertical and the horizontal displacements. The calculated forces P's are then considered as a contact soil pressure in the Equations (4-8), and (4-13).

## CHAPTER FIVE

### OPTIMIZATION OF RBF SHAPE VARIABLE C

The multi-quadric radial basis function MQ RBF proposed here is given by:

$$\phi(\|\underline{x} - \underline{x}^j\|) = \sqrt{(x - x^j)^2 + (y - y^j)^2 + c^2}, \text{ where } c \text{ is the shape variable.}$$

In order to obtain the optimum value of the shape variable  $c$ , it was necessary to perform a parametric investigation in which  $c$  was varied from a low value of 0.1 to a high value of 0.8 with an increment of 0.02. The analysis was carried out for both plates on and without foundation. Two shapes of the plate considered: square and circular. Several boundary conditions were considered, namely: clamped, free, simply, movable and immovable).

A summary of cases studied are given in Table 5-1. The boundary indications and the nodal distribution are given in Figure 5-1. The total cases of studies which have been carried out to get the optimal values of  $c$  are 1120 cases ( $16*2*35$ ). The analysis of similar cases was carried out using the finite element method (FEM) by COMSOL software. Dimensionless units were used and the  $(w/t)$  at the center of the plate results were used for the comparison of MQ-RBF and FEM and then the errors were calculated.

For each case of study, the loads were applied incrementally as described in Chapter 3. The relaxation factor,  $relf = 0.65$ , was used in all. The average error was calculated by

$$Error \% = Abs \left( \frac{(\bar{W})_{RBF} - (\bar{W})_{FEM}}{(\bar{W})_{FEM}} \right) * 100;$$

where:  $\bar{W}$  is  $\frac{w}{t}$  at the center of the plate. The results of the parametric study are given in Figures 5-2 to 5-11.

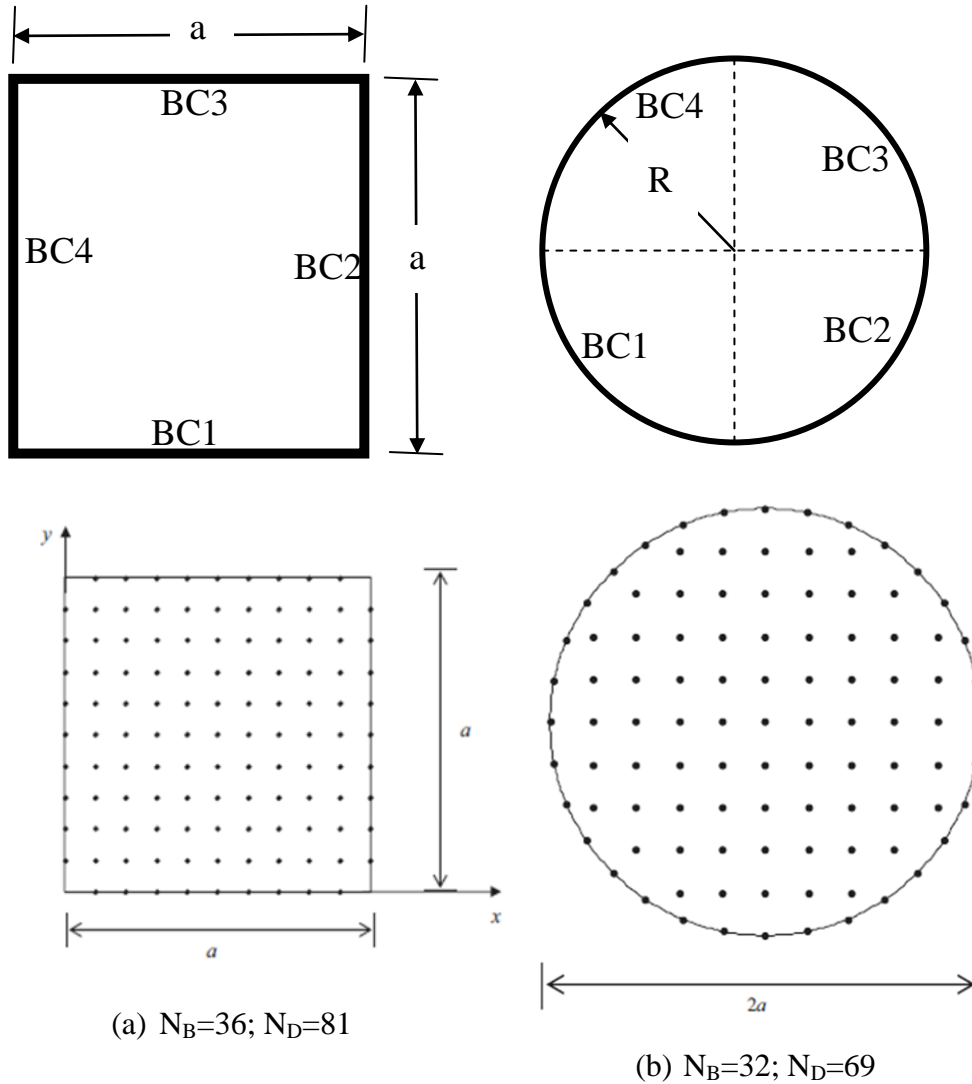


Figure 5.1 Nodes Distribution and Boundary Sides of Plates. a) Rectangular Plate, and b) Circular Plate



Table 5.1 Designated and Description of Plates Cases of Studies

Number #	Designated Name	BC1	BC2	BC3	BC4
1	SQ-CC-IM	C & IM	C & IM	C & IM	C & IM
2	SQ-CC-MO	C & MO	C & MO	C & MO	C & MO
3	SQ-SS-IM	S & IM	S & IM	S & IM	S & IM
4	SQ-SS-MO	S & MO	S & MO	S & MO	S & MO
5	SQ-CF-IM	F & IM	C & IM	F & IM	C & IM
6	SQ-CF-MO	F & MO	C & MO	F & MO	C & MO
7	SQ-SF-IM	F & IM	S & IM	F & IM	S & IM
8	SQ-SF-MO	F & MO	S & MO	F & MO	S & MO
9	CI-CC-IM	C & IM	C & IM	C & IM	C & IM
10	CI-CC-MO	C & MO	C & MO	C & MO	C & MO
11	CI-SS-IM	S & IM	S & IM	S & IM	S & IM
12	CI-SS-MO	S & MO	S & MO	S & MO	S & MO
13	CI-CF-IM	F & IM	C & IM	F & IM	C & IM
14	CI-CF-MO	F & MO	C & MO	F & MO	C & MO
15	CI-SF-IM	F & IM	S & IM	F & IM	S & IM
16	CI-SF-MO	F & MO	S & MO	F & MO	S & MO

Where;

SQ: Square or Rectangle ; CI: Circle ; C: Clamped ; S: Simple ; F: Free ; IM: Immovable ; MO: Movable.

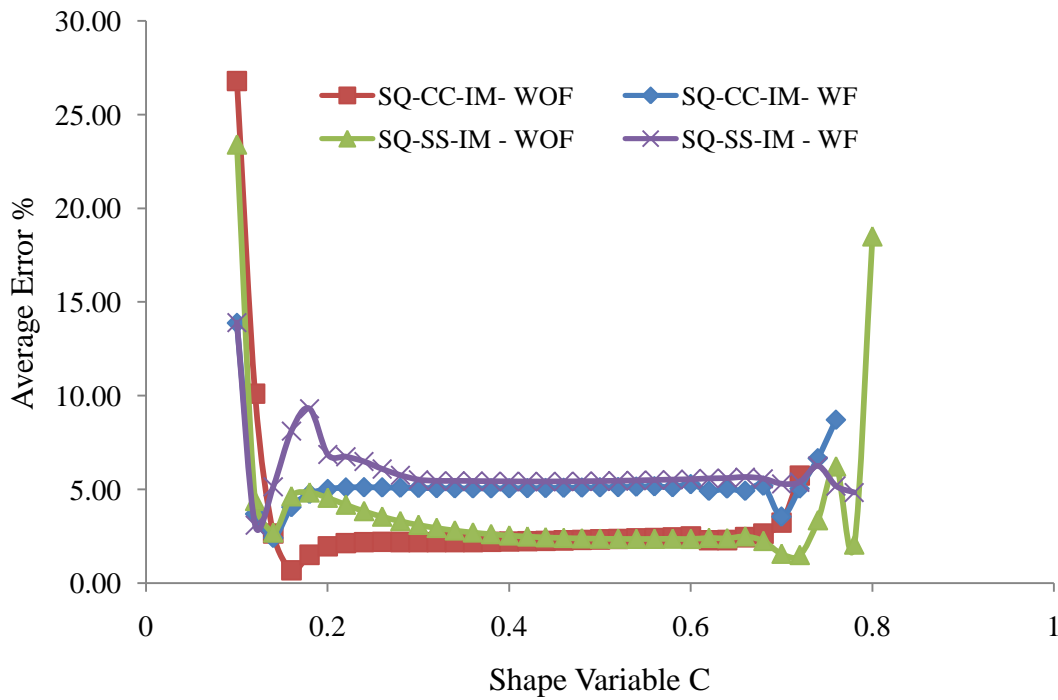


Figure 5.2 Average Errors % vs Shape Variable for SQ-CC-IM and SQ-SS-IM

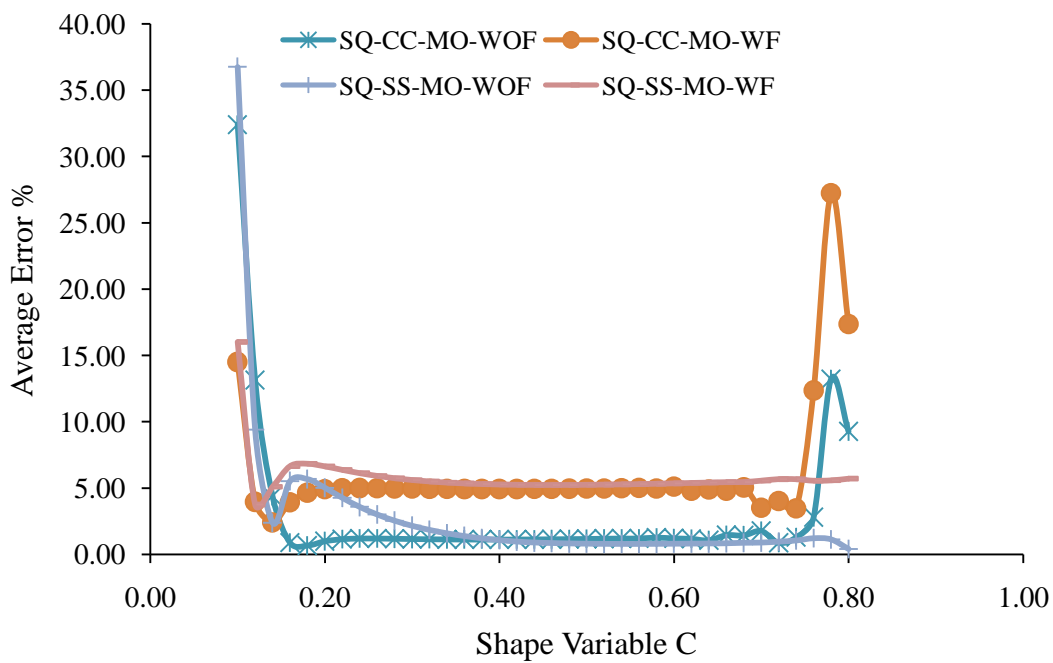


Figure 5.3 Average Errors % vs Shape Variable for SQ-CC-MO and SQ-SS-MO

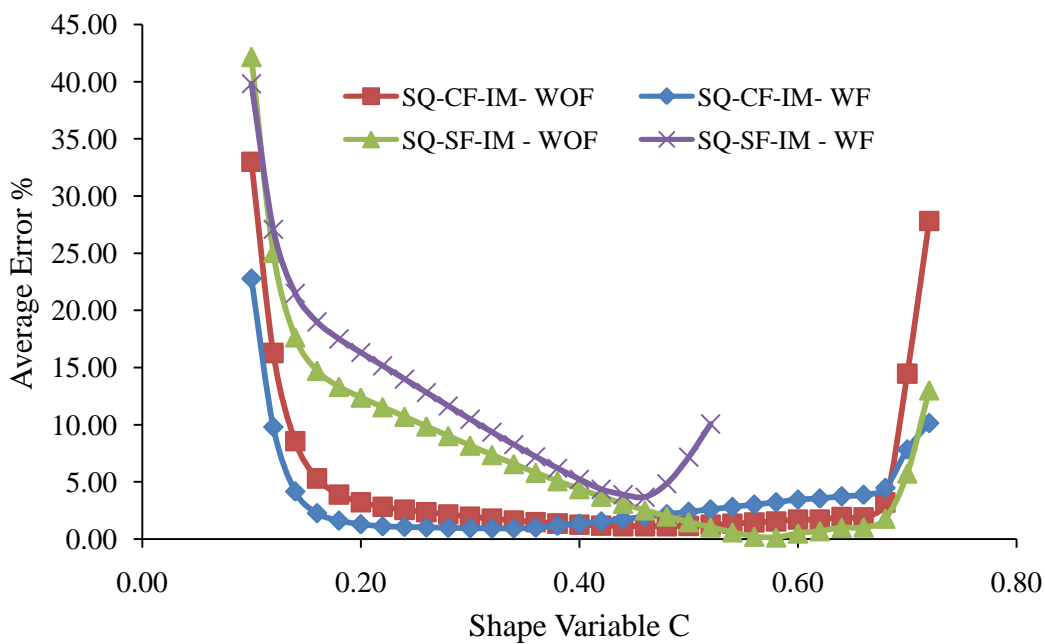


Figure 5.4 Average Errors % vs Shape Variable for SQ-CF-IM and SQ-SF-IM

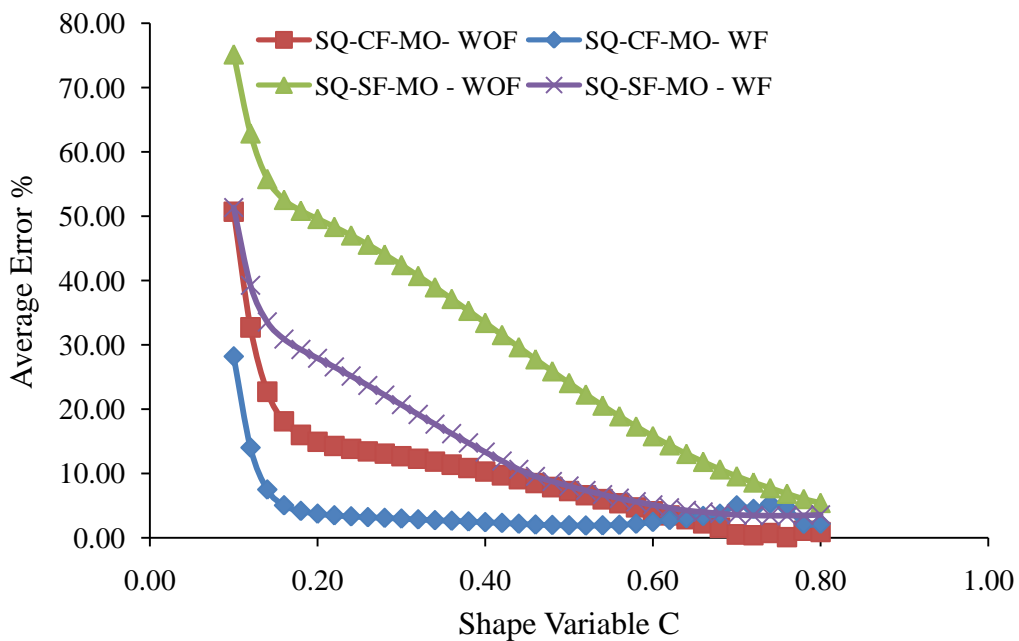


Figure 5.5 Average Errors % vs Shape Variable for SQ-CF-MO and SQ-SF-MO

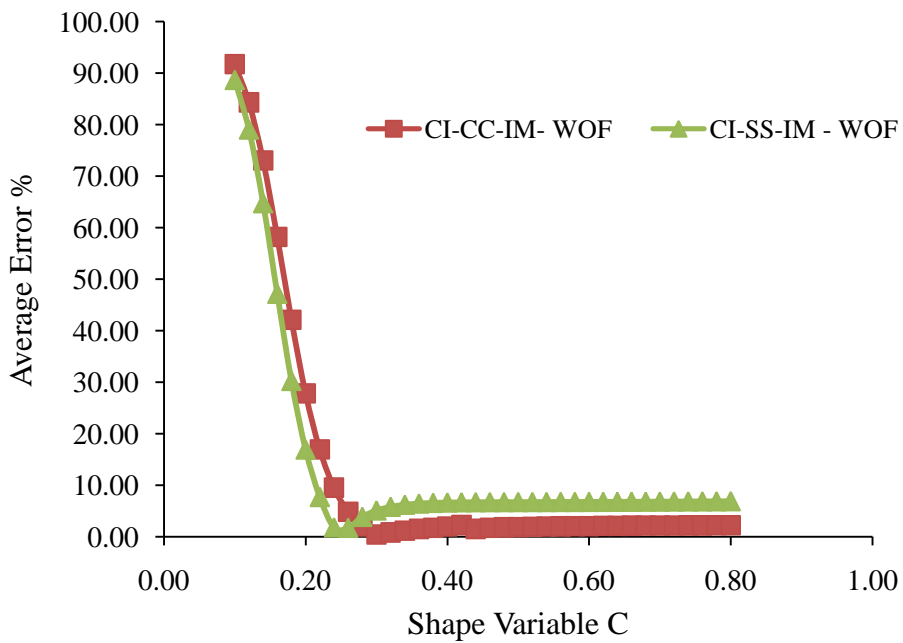


Figure 5.6 Average Errors % vs Shape Variable for CI-CC-IM and CI-SS-IM (WOF)

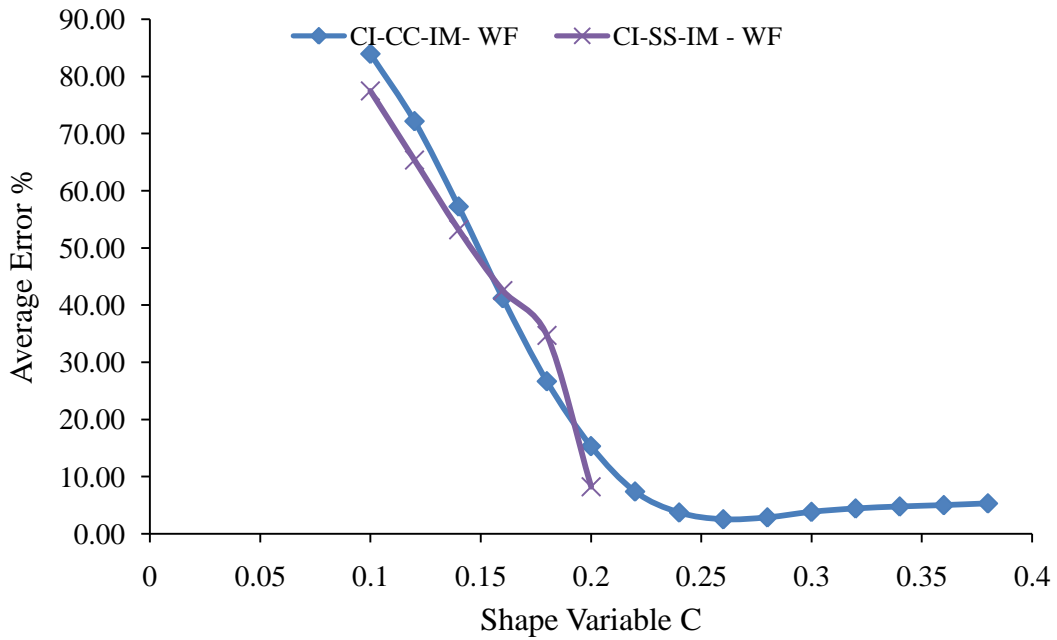


Figure 5.7 Average Errors % vs Shape Variable for CI-CC-IM and CI-SS-IM (WF)

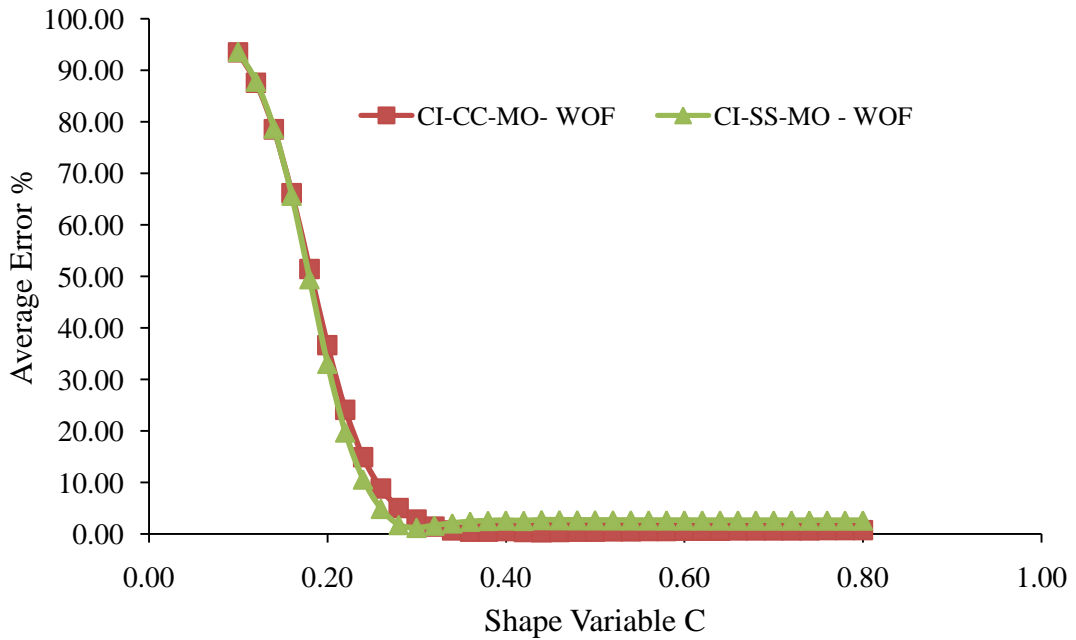


Figure 5.8 Average Errors % vs Shape Variable for CI-CC-MO and CI-SS-MO (WOF)

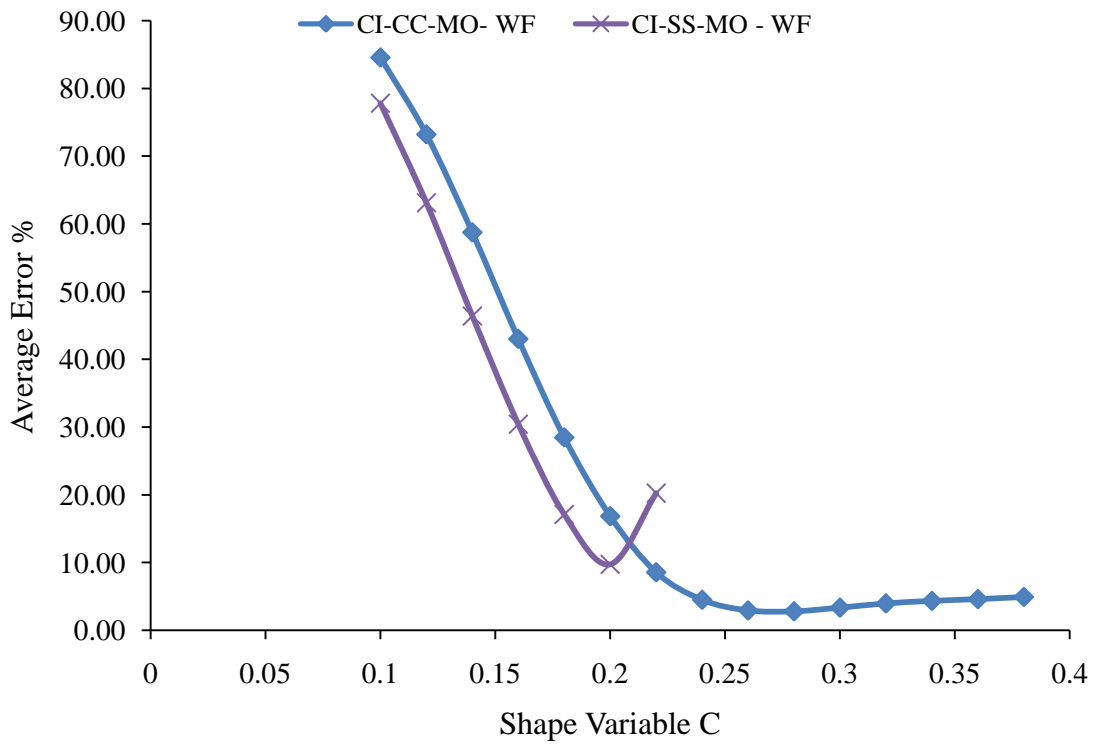


Figure 5.9 Average Errors % vs Shape Variable for CI-CC-MO and CI-SS-MO (WF)

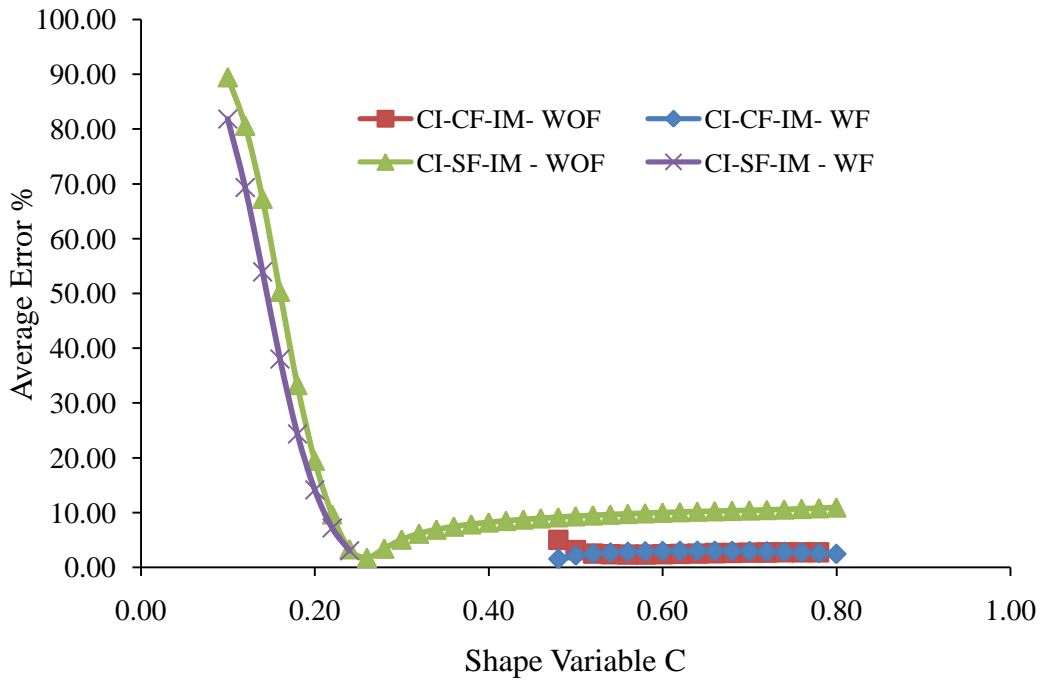


Figure 5.10 Average Errors % vs Shape Variable for CI-CF-IM and CI-SF-IM

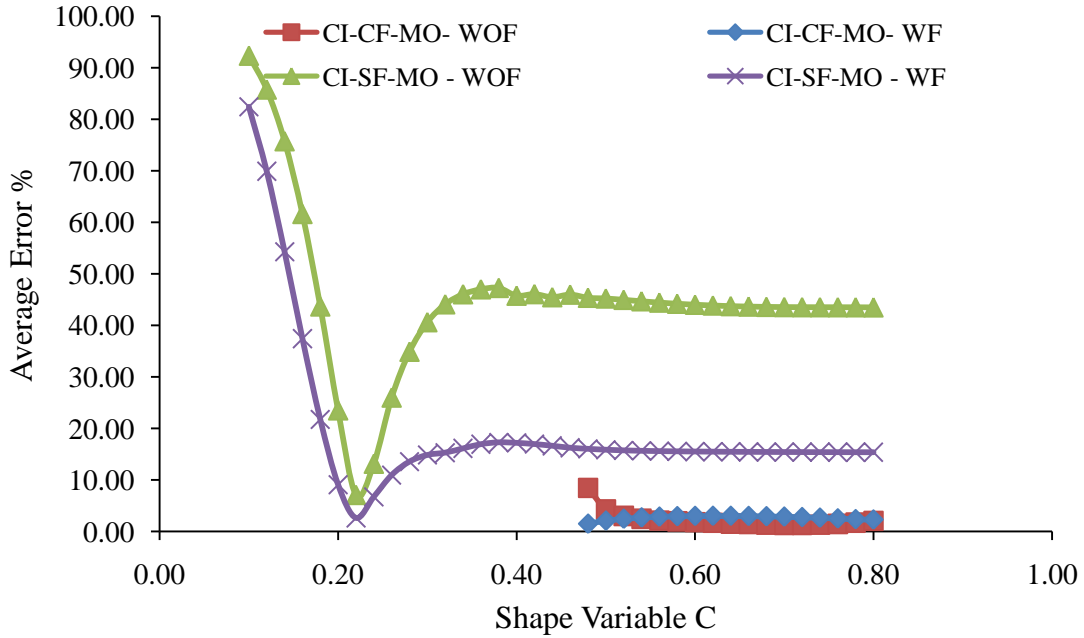


Figure 5.11 Average Errors % vs Shape Variable for CI-CF-MO and CI-SF-MO

The parametric study results for the square plate are given by Figures 5.2 to 5.5 and the Tables B-1 and B-2 in Appendix B. The shown results show that there exists a range of  $c$  for which the error of RBF solution as compared to FEM is less than 5% and 2.5% for plates on and without foundation respectively. The range of optimum  $c$  is between 0.2 and 0.7 for most of the cases. It should be noted that the range of  $c$  gets narrower for few of the cases corresponding to plates on foundations.

Moreover, when the free edge boundary condition comes to the picture, the observations are different for both the immovable and movable edges as they are shown in Tables (B-3 and B-4) in Appendix B and Figures (5.4 and 5.5) respectively. For the free movable cases, the minimum errors are observed when the  $c$  changes from 0.6 to more than 0.8 for all cases. For the simply-free immovable cases, the minimum errors are

within 5% when  $c$  changes from 0.4 to 0.45 for WF case and within 2% when  $c$  changes from 0.5 to 0.65 for WOF (Figure 5.4).

The average errors and corresponding  $c$  values for the circular cases are as shown in Tables B-5 to B-8 in Appendix B and Figures 5.6 to 5.11. The non-free circular cases, the more sensitive cases are the ones with foundation (WF) on the simply supported boundary conditions (both immovable and movable ) in which the average errors are less than 10 % in almost one value of  $c$  which is 0.2 as it is shown in both Tables B-5 and B-6. However, the clamped ones are sensitive only at  $c$  values of 0.1 to 0.2 and from 0.4 to 0.46 in both movable and immovable edges cases. Unlike the WF, the WOF produces small errors when  $c$  changes from 0.25 to more than 0.8 for all boundary conditions (movable, immovable, clamped and simple).

The circular free edges plate as shown in Tables B-7 and B-8 and Figures 5.10 and 5.11 behave different from all the previous cases where the simply boundary conditions give minimum errors (less than 5%) at  $c$  changes from 0.2 to 0.25 for immovable edges and 0.22 for movable ones. Whereas for the clamped free, the minimum errors (less than 3 %) are obtained when  $c$  changes between 0.5 to more than 0.8 for both WF and WOF movable and immovable conditions.

As a conclusion of the above discussion, it can be observed that when the shape variable  $c$  changes from 0.6 to 0.65 all square plate, not free circular, and circular clamped free cases without foundation in both movable and immovable conditions produce minimum average error less than 5 %. However, the other remaining cases are provided with their  $c$  values as follows: square plate simply free immovable with

foundation (SQ-SF-IM-WF) gives minimum error when  $c$  ranging from 0.4 to 0.45 whereas the circular clamped movable and immovable (CI-CC-MO and IM) with foundation produce minimum average error when  $c$  either changes from 0.22 to 0.38 or from 0.48 to 0.8. But the minimum error  $c$  value for the circular simply movable and immovable with foundation is 0.2 and 0.22 for the circular simply free movable and immovable boundary conditions in both WOF and WF cases. These conclusions are tabulated in Table 5.2 below.

Table 5.2 Range of Optimum  $c$  for all Cases

Range of C values	Cases	
	WOF	WF
0.6 – 0.65	SQ-CC-IM, SQ-SS-IM, SQ-CC-MO, SQ-SS-MO, SQ-CF-MO, SQ-SF-MO, SQ-SF-IM, CI-CC-IM, CI-SS-IM, CI-CC-MO, CI-SS-MO, CI-CF-IM, CI-CF-MO	SQ-CC-IM, SQ-SS-IM, SQ-CC-MO, SQ-SS-MO, SQ-CF-MO, SQ-SF-MO, CI-CF-IM, CI-CF-MO
0.4 - 0.45	-----	SQ-SF-IM
0.22-0.38	-----	CI-CC-MO, CI-CC-IM
0.48-0.8	-----	CI-CC-MO, CI-CC-IM
0.22	CI-SF-IM, CI-SF-MO	CI-SF-IM, CI-SF-MO
0.2	-----	CI-SS-MO, CI-SS-IM



## CHAPTER SIX

# VERIFICATION OF THE COMPUTER CODE FOR LARGE DEFLECTION OF THIN PLATE WITHOUT FOUNDATION (WOF)

### 6.1 General

In order to examine the effectiveness of the proposed RBF method, the following several numerical examples are considered. In all examples, the load is assumed to be uniformly distributed =  $q$ , Poisson ratio  $\nu$  is assumed 0.3 and the analysis was performed for several combinations of boundary conditions. For generality of the solutions, all results are made dimensionless, so that the coordinates, the load, the deflection, and the stress are represented by  $\bar{x} = \frac{x}{a}, \bar{y} = \frac{y}{a}, \bar{q} = \frac{qa^4}{Et^4}, \bar{w} = \frac{w}{t}, \bar{\sigma} = \frac{\sigma a^2}{Et^2}$ , respectively. The shape factor,  $c$ , of the RBF was changed according to the boundary conditions, and the geometry. Its optimum value ranged between 0.1 and 0.8.

Two plate shapes are considered: square and circular, while the boundary conditions include clamped, simply supported, free, movable and immovable. The definitions, node distributions, and designation of all considered cases are shown in Figure 6.1 and Table 6.1 below.

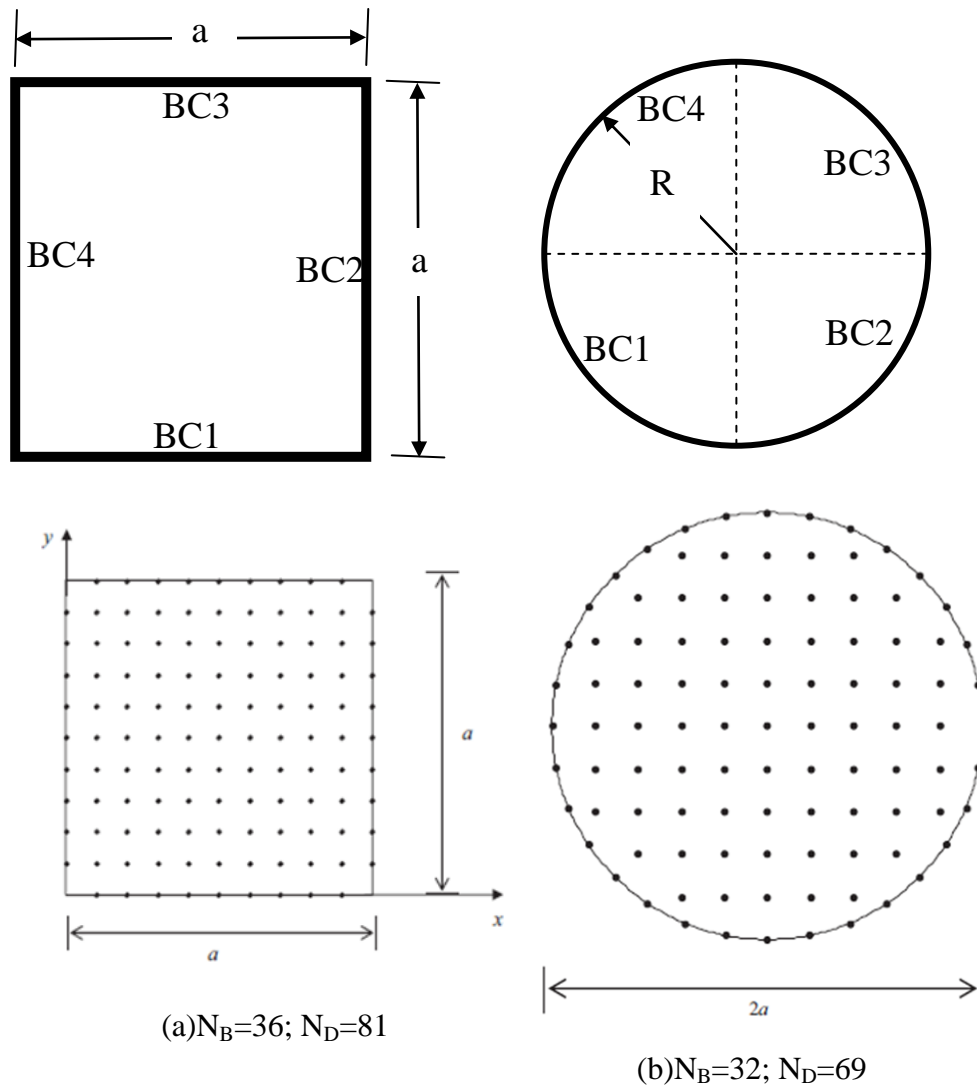


Figure 6.1 Nodes Distribution and Boundary Sides of Plates. a) Square Plate, and b) Circular Plate

Table 6.1 Designated and Description of Plates Cases of Studies

Number #	Designated Name	BC1	BC2	BC3	BC4
1	SQ-CC-IM	C & IM	C & IM	C & IM	C & IM
2	SQ-CC-MO	C & MO	C & MO	C & MO	C & MO
3	SQ-SS-IM	S & IM	S & IM	S & IM	S & IM
4	SQ-SS-MO	S & MO	S & MO	S & MO	S & MO
5	SQ-CF1-IM	C & IM	C & IM	C & IM	F & IM
6	SQ-CF1-MO	C & MO	C & MO	C & MO	F & MO
7	SQ-SF1-IM	S & IM	S & IM	S & IM	F & IM
8	SQ-SF1-MO	S & MO	S & MO	S & MO	F & MO
9	CI-CC-IM	C & IM	C & IM	C & IM	C & IM
10	CI-CC-MO	C & MO	C & MO	C & MO	C & MO
11	CI-SS-IM	S & IM	S & IM	S & IM	S & IM
12	CI-SS-MO	S & MO	S & MO	S & MO	S & MO
13	CI-CF1-IM	C & IM	C & IM	C & IM	F & IM
14	CI-CF1-MO	C & MO	C & MO	C & MO	F & MO
15	CI-SF1-IM	S & IM	S & IM	S & IM	F & IM
16	CI-SF1-MO	S & MO	S & MO	S & MO	F & MO

Where;

SQ: Square; CI: Circle ; C: Clamped ; S: Simple ; F: Free ; IM: Immovable ; MO: Movable

The results of RBF solution were compared with FEM results using the commercial software COMSOL and the error was calculated using the following formula:

$$\text{Error \%} = \text{Abs} \left( \frac{(\text{result})_{\text{RBF}} - (\text{result})_{\text{FEM}}}{(\text{result})_{\text{FEM}}} \right) * 100 \quad (6 - 1)$$

The results of the numerical examples are provided in Section 6.2 followed by their discussion in Section 6.3.

## 6.2 WOF Numerical Examples

### 6.2.1 WOF Immovable Square Plates

The square plates are subjected to uniformly distributed load and modeled by 36 nodes in the boundary ( $N_b$ ), and 81 nodes in the domain ( $N_d$ ) with a uniform spacing of  $h = 0.1$  as shown in Figure 6-1.

For this type of edge condition ( $u = v = 0$ ), the code developed based on w-u-v formulation is used. The analysis is repeated for different boundary conditions in the transverse direction. The results of the transverse deflection  $\bar{w}$ , the bending stress  $\bar{\sigma}_b$  and membrane stress  $\bar{\sigma}_m$  are presented for each case at different levels of applied load.

- SQ-CC-IM

A clamped supported square plate with immovable edges, ( $w = \frac{\partial w}{\partial n} = u = v = 0$ ) is subjected to a uniform dimensionless total load,  $\bar{q} = 180$  which is applied incrementally at a rate of 15 per increment. The summary of the results at the center of the plate is shown in Table 6-2 below.

Table 6.2 Summary of the Results of SQ-CC-IM without Foundation

$\bar{q}$	$\bar{w}$		Error %	$\bar{\sigma}_b$		Error %	$\bar{\sigma}_m$		Error %
	FEM	RBF		FEM	RBF		FEM	RBF	
15	0.2033	0.1969	3.1500	2.0267	1.9465	3.9568	0.1366	0.1313	3.8743
30	0.3852	0.3744	2.7994	3.7704	3.6426	3.3891	0.4889	0.4726	3.3285
45	0.5396	0.5261	2.5064	5.1597	5.0114	2.8743	0.9556	0.9319	2.4762
60	0.6701	0.6550	2.2637	6.2513	6.1002	2.4181	1.4678	1.4399	1.9006
75	0.7821	0.7651	2.1739	7.1220	6.9686	2.1534	1.9915	1.9670	1.2324
90	0.8797	0.8623	1.9682	7.8279	7.6926	1.7293	2.5113	2.4889	0.8919

105	0.9662	0.9484	1.8466	8.4152	8.2955	1.4230	3.0210	3.0036	0.5766
120	1.0440	1.0247	1.8528	8.9127	8.7946	1.3253	3.5183	3.5104	0.2250
135	1.1147	1.0956	1.7210	9.3402	9.2471	0.9967	4.0023	4.0011	0.0299
150	1.1797	1.1579	1.8501	9.7140	9.6083	1.0880	4.4735	4.4915	0.4016
165	1.2398	1.2186	1.7107	10.0445	9.9670	0.7714	4.9326	4.9534	0.4225
180	1.2958	1.2736	1.7114	10.3400	10.2712	0.6653	5.3802	5.4139	0.6268

- SQ-SS-IM

A simply supported square plate with immovable edges, ( $w = M_n = u = v = 0$ ) is subjected to a uniform total load,  $\bar{q} = 90$  which is applied incrementally at a rate of 10 per increment. The summary of the results at the center of the plate is shown in Table 6-3 below.

Table 6.3 Summary of the Results of SQ-SS-IM without Foundation

$\bar{q}$	$\bar{w}$		Error %	$\bar{\sigma}_b$		Error %	$\bar{\sigma}_m$		Error %
	FEM	RBF		FEM	RBF		FEM	RBF	
10	0.3713	0.3770	1.5450	2.3604	2.3988	1.6272	0.4183	0.4031	3.634
20	0.5897	0.5969	1.2254	3.6413	3.6915	1.3791	1.0587	0.9954	5.9796
30	0.7379	0.7440	0.8325	4.4461	4.4900	0.9870	1.6627	1.6057	3.4274
40	0.8513	0.8566	0.6256	5.0266	5.0664	0.7917	2.2193	2.1651	2.4408
50	0.9442	0.9490	0.5109	5.4808	5.5188	0.6935	2.7368	2.6838	1.9369
60	1.0235	1.0281	0.4475	5.8545	5.8924	0.6471	3.2227	3.1700	1.6347
70	1.0930	1.0976	0.4123	6.1731	6.2119	0.6287	3.6830	3.6299	1.4416
80	1.1552	1.1599	0.4042	6.4514	6.4921	0.6307	4.1215	4.0680	1.2983
90	1.2117	1.2266	1.2352	6.6995	6.8055	1.5818	4.5419	4.4688	1.6093

- SQ-CF1-IM

A clamped free-at-one-edge supported square plate with immovable edges, ( $w = \frac{\partial w}{\partial n} = (V_n \text{ and } M_n \text{ at the free edge}) = u = v = 0$ ) is subjected to a uniform dimensionless total load,  $\bar{q} = 120$  which is applied incrementally at a rate of 10 per

increment. The summary of the results at the free edge of the plate is shown in Table 6-4 below.

Table 6.4 Summary of the Results of SQ-CF1-IM without Foundation

$\bar{q}$	$\bar{w}$		Error %	$\bar{\sigma}_b$		Error %	$\bar{\sigma}_m$		Error %
	FEM	RBF		FEM	RBF		FEM	RBF	
10	0.3016	0.313456	3.9198	0.0296	0.0285	3.7719	0.0845	0.0804	4.8521
20	0.5291	0.548298	3.6242	0.0566	0.0547	3.4975	0.2854	0.2739	4.0554
30	0.6971	0.717273	2.8958	0.0817	0.0794	2.8144	0.5381	0.5235	2.6982
40	0.8285	0.848015	2.3611	0.1055	0.1031	2.3066	0.8105	0.7948	1.9312
50	0.9367	0.955335	1.9893	0.1288	0.1262	1.9505	1.0887	1.0734	1.4038
60	1.0292	1.04703	1.7275	0.1515	0.1490	1.6982	1.3662	1.3525	1.0048
70	1.1106	1.12758	1.5333	0.1740	0.1714	1.5102	1.6401	1.6288	0.6894
80	1.1833	1.19975	1.3938	0.1962	0.1935	1.3746	1.9090	1.9009	0.4226
90	1.2494	1.26539	1.2829	0.2181	0.2154	1.2666	2.1724	2.1680	0.1996
100	1.3101	1.32577	1.1941	0.2399	0.2371	1.1800	2.4302	2.4301	0.0059
110	1.3665	1.38183	1.1224	0.2614	0.2585	1.1099	2.6826	2.6870	0.1648
120	1.4192	1.43425	1.0625	0.2827	0.2798	1.0513	2.9297	2.9390	0.3172

- SQ-SF1-IM

A simply free-at-one-edge supported square plate with immovable edges, ( $w = M_n = V_n$  and  $M_n$  at the free edge =  $u = v = 0$ ) is subjected to a uniform dimensionless total load  $\bar{q} = 28$  which is applied incrementally at a rate of 4 per increment. The summary of the results at the free edge of the plate is shown in Table 6-5 below.

Table 6.5 Summary of the Results of SQ-SF1-IM without Foundation

$\bar{q}$	$\bar{w}$		Error %	$\bar{\sigma}_b$		Error %	$\bar{\sigma}_m$		Error %
	FEM	RBF		FEM	RBF		FEM	RBF	
4	0.4023	0.412392	2.5025	0.0114	0.0112	2.4414	0.1381	0.1303	5.648
8	0.5895	0.596317	1.1552	0.0220	0.0217	1.1420	0.3393	0.3238	4.5682
12	0.7102	0.714666	0.6282	0.0322	0.0320	0.6243	0.5394	0.5098	5.4958

16	0.8014	0.80465	0.4072	0.0424	0.0422	0.4056	0.7325	0.7004	4.3804
20	0.8759	0.87856	0.3082	0.0524	0.0522	0.3073	0.9179	0.8842	3.6681
24	0.9395	0.942073	0.2711	0.0624	0.0622	0.2703	1.0960	1.0613	3.1703
28	0.9956	1.04562	5.0286	0.0722	0.0688	4.7878	1.2676	1.2595	0.6385

## 6.2.2 WOF Movable Square Plates

For this type of edge condition ( $\frac{\partial F}{\partial n} = F = 0$ ), the code developed based on w-F formulation is used. The analysis is repeated for different boundary conditions in the transverse direction. The results of the transverse deflection  $\bar{w}$ , the bending stress  $\bar{\sigma}_b$  and membrane stress  $\bar{\sigma}_m$  are presented for each case at different levels of applied load.

- SQ-CC-MO

A clamped supported square plate with movable edges, ( $w = \frac{\partial w}{\partial n} = \frac{\partial F}{\partial n} = F = 0$ ) is subjected to a uniform dimensionless total load,  $\bar{q} = 180$  which is applied incrementally with at a rate of 15 per increment. The summary of the results at the center of the plate is shown in Table 6-6 below.

Table 6.6 Summary of the Results of SQ-CC-MO without Foundation

$\bar{q}$	$\bar{w}$		Error %	$\bar{\sigma}_b$		Error %	$\bar{\sigma}_m$		Error %
	FEM	RBF		FEM	RBF		FEM	RBF	
15	0.2098	0.2068	1.4430	2.0438	2.0627	0.9257	0.0726	0.0695	4.270
30	0.4113	0.4114	0.0088	3.9601	4.0907	3.2980	0.2763	0.2704	2.135
45	0.5992	0.5856	2.2593	5.6698	5.6473	0.3984	0.5786	0.5681	1.8145
60	0.7717	0.7529	2.4342	7.1537	7.1038	0.6980	0.9446	0.9256	2.0085
75	0.9294	0.9054	2.5907	8.4252	8.3433	0.9720	1.3466	1.3089	2.7981
90	1.0740	1.0612	1.1953	9.5146	9.6562	1.4884	1.7662	1.7250	2.3357
105	1.2072	1.1957	0.9554	10.4523	10.6536	1.9261	2.1919	2.1594	1.4848
120	1.3307	1.3205	0.7660	11.2661	11.5224	2.2748	2.6170	2.6016	0.5882
135	1.4456	1.4363	0.6482	11.9748	12.2714	2.4771	3.0365	3.0491	0.4136

150	1.5535	1.5192	2.2081	12.6009	12.5506	0.3991	3.4493	3.4036	1.3255
165	1.6552	1.6131	2.5438	13.1572	13.0192	1.0488	3.8538	3.7928	1.5822
180	1.7516	1.7035	2.7429	13.6554	13.4609	1.4246	4.2495	4.1517	2.3022

- SQ-SS-MO

A simply supported square plate with movable edges, ( $w = M_n = \frac{\partial F}{\partial n} = F = 0$ ) is subjected to a uniform dimensionless total load  $\bar{q} = 60$  which is applied incrementally at a rate of 5 per increment. The summary of the results at the center of the plate is shown in Table 6-7 below.

Table 6.7 Summary of the Results of SQ-SS-MO without Foundation

$\bar{q}$	$\bar{w}$		Error %	$\bar{\sigma}_b$		Error %	$\bar{\sigma}_m$		Error %
	FEM	RBF		FEM	RBF		FEM	RBF	
5	0.2216	0.2223	0.3028	1.4214	1.4389	1.2297	0.0488	0.0459	5.9426
10	0.4322	0.4290	0.7254	2.7411	2.7335	0.2782	0.1838	0.1836	0.1484
15	0.6255	0.6192	0.9953	3.9033	3.8761	0.6965	0.3802	0.3790	0.3222
20	0.8003	0.7897	1.3221	4.8999	4.8409	1.2044	0.6132	0.6051	1.3213
25	0.9580	0.9585	0.0562	5.7472	5.8007	0.9309	0.8647	0.8499	1.7106
30	1.1008	1.1049	0.3715	6.4692	6.5613	1.4238	1.1236	1.1131	0.9289
35	1.2314	1.2390	0.6183	7.0898	7.2187	1.8178	1.3835	1.3845	0.0725
40	1.3515	1.3616	0.7412	7.6275	7.7804	2.0045	1.6406	1.6611	1.2490
45	1.4630	1.4448	1.2412	8.0982	7.9982	1.2353	1.8932	1.8737	1.0278
50	1.5670	1.5396	1.7482	8.5139	8.3344	2.1074	2.1402	2.1068	1.5595
55	1.6646	1.6303	2.0621	8.8841	8.6488	2.6481	2.3812	2.3162	2.7298
60	1.7568	1.7374	1.1044	9.2163	9.1148	1.1017	2.6162	2.5894	1.0267

- SQ-CF1-MO

A clamped free-at-one-edge supported square plate with movable edges, ( $w = V_n$  and  $M_n$  at the free edge =  $F = \frac{\partial F}{\partial n} = 0$ ) is subjected to a uniform dimensionless total



load,  $\bar{q} = 40$  which is applied incrementally at a rate of 5 per increment. The summary of the results at the free edge of the plate is shown in Table 6-8 below.

Table 6.8 Summary of the Results of SQ-CF1-MO without Foundation

$\bar{q}$	$\bar{w}$		Error %	$\bar{\sigma}_b$		Error %
	FEM	RBF		FEM	RBF	
5	0.1302	0.134332	3.1698	0.0157	0.0153	3.0725
10	0.2605	0.268664	3.1310	0.0316	0.0306	3.0360
15	0.3910	0.402996	3.0712	0.0475	0.0461	2.9797
20	0.5218	0.537326	2.9825	0.0636	0.0618	2.8961
25	0.6529	0.671648	2.8781	0.0799	0.0777	2.7976
30	0.7843	0.805947	2.7572	0.0964	0.0938	2.6833
35	0.9162	0.940196	2.6210	0.1131	0.1102	2.5541
40	1.0484	1.07436	2.4728	0.1299	0.1268	2.4132

- SQ-SF1-MO

A simply free-at-one-edge supported square plate with movable edges, ( $w = M_n = V_n$  and  $M_n$  at the free edge =  $F = 0$ ) is subjected to a uniform dimensionless total load,  $\bar{q} = 12$  which is applied incrementally at a rate of 1 per increment. The summary of the results at the free edge of the plate is shown in Table 6-9 below.

Table 6.9 Summary of the Results of SQ-SF1-MO without Foundation

$\bar{q}$	$\bar{w}$		Error %	$\bar{\sigma}_b$		Error %
	FEM	RBF		FEM	RBF	
1	0.1409	0.146377	3.9094	0.0010	0.0010	3.7623
2	0.2817	0.292733	3.9033	0.0020	0.0020	3.7567
3	0.4227	0.438995	3.8660	0.0030	0.0029	3.7221
4	0.5636	0.585079	3.8133	0.0040	0.0038	3.6732
5	0.7045	0.730904	3.7441	0.0049	0.0047	3.6090
6	0.8455	0.876394	3.6482	0.0057	0.0055	3.5198
7	0.9866	1.02148	3.5387	0.0064	0.0062	3.4178

8	1.1276	1.16608	3.4133	0.0070	0.0068	3.3006
9	1.2673	1.31015	3.3778	0.0075	0.0073	3.2674
10	1.4097	1.45362	3.1168	0.0078	0.0075	3.0226
11	1.5506	1.59644	2.9567	0.0079	0.0077	2.8718
12	1.6915	1.73858	2.7848	0.0079	0.0077	2.7093

### 6.2.3 WOF Immovable Circular Plates

The circular plates are subjected to uniformly distributed load and modeled by 36 nodes in the boundary ( $N_b$ ), and 69 nodes in the domain ( $N_d$ ), with a uniform spacing of  $h = 0.2$  as shown in Figure 6-1.

- CI-CC-IM

A clamped supported circular plate with immovable edges, ( $w = \frac{\partial w}{\partial n} = u = v = 0$ ) is subjected to a uniform dimensionless total load,  $\bar{q} = 12$  which is applied incrementally at a rate of 1 per increment. The summary of the results at the center of the plate is shown in Table 6-10 below.

Table 6.10 Summary of the Results of CI-CC-IM without Foundation

$\bar{q}$	$\bar{w}$		Error %	$\bar{\sigma}_b$		Error %	$\bar{\sigma}_m$		Error %
	FEM	RBF		FEM	RBF		FEM	RBF	
1	0.1686	0.1692	0.3418	0.4785	0.4852	1.3962	0.0277	0.0285	2.889
2	0.3239	0.3212	0.8180	0.9075	0.9051	0.2667	0.1019	0.1023	0.3836
3	0.4602	0.4562	0.8576	1.2674	1.2627	0.3699	0.2051	0.2046	0.2499
4	0.5783	0.5703	1.3880	1.5627	1.5436	1.2202	0.3230	0.3308	2.4340
5	0.6812	0.6716	1.4064	1.8053	1.7798	1.4135	0.4469	0.4514	1.0117
6	0.7719	0.7694	0.3238	2.0074	2.0214	0.6968	0.5724	0.5761	0.6533
7	0.8529	0.8469	0.6969	2.1780	2.1794	0.0662	0.6971	0.7042	1.0255
8	0.9259	0.9272	0.1384	2.3241	2.3540	1.2840	0.8200	0.8164	0.4323
9	0.9925	0.9902	0.2400	2.4510	2.4680	0.6917	0.9405	0.9451	0.4868
10	1.0538	1.0242	2.8062	2.5625	2.4725	3.5131	1.0585	1.1181	5.6243
11	1.1106	1.0963	1.2889	2.6615	2.6471	0.5416	1.1740	1.2012	2.3142

12	1.1636	1.1562	0.6383	2.7508	2.7562	0.1938	1.2871	1.3054	1.4185
----	--------	--------	--------	--------	--------	--------	--------	--------	--------

- CI-SS-IM

A clamped supported circular plate with immovable edges, ( $w = M_n = u = v = 0$ ) is subjected to a uniform dimensionless total load,  $\bar{q} = 6$  which is applied incrementally at a rate of 0.5 per increment. The summary of the results at the center of the plate is shown in Table 6-11 below.

Table 6.11 Summary of the Results of CI-SS-IM without Foundation

$\bar{q}$	$\bar{w}$		Error %	$\bar{\sigma}_b$		Error %	$\bar{\sigma}_m$		Error %
	FEM	RBF		FEM	RBF		FEM	RBF	
0.5	0.2977	0.3062	2.8594	0.5227	0.5432	3.9222	0.0806	0.0776	3.722
1	0.4809	0.5001	3.9873	0.8284	0.8742	5.5259	0.2110	0.1991	5.639
1.5	0.6069	0.6237	2.7680	1.0277	1.0703	4.1459	0.3370	0.3134	6.9937
2	0.7039	0.7182	2.0328	1.1744	1.2131	3.2946	0.4545	0.4336	4.5879
2.5	0.7834	0.7958	1.5867	1.2903	1.3259	2.7615	0.5643	0.5451	3.4017
3	0.8513	0.8623	1.2916	1.3863	1.4195	2.3981	0.6678	0.6498	2.7058
3.5	0.9110	0.9208	1.0720	1.4684	1.4997	2.1283	0.7663	0.7489	2.2656
4	0.9643	0.9732	0.9298	1.5401	1.5699	1.9349	0.8602	0.8435	1.9349
4.5	1.0127	1.0209	0.8136	1.6041	1.6326	1.7777	0.9504	0.9342	1.6984
5	1.0572	1.0648	0.7221	1.6618	1.6892	1.6512	1.0373	1.0216	1.5149
5.5	1.0983	1.1055	0.6514	1.7144	1.7409	1.5463	1.1213	1.1060	1.3662
6	1.1368	1.1435	0.5917	1.7629	1.7886	1.4556	1.2029	1.1879	1.2450

- CI-CF1-IM

A clamped free-at-one-edge supported circular plate with immovable edges, ( $w = \frac{\partial w}{\partial n} = V_n$  and  $M_n$  at the free edge =  $u = v = 0$ ) is subjected to a uniform dimensionless total load,  $\bar{q} = 8.4$  which is applied incrementally at a rate of 0.7 per increment. The summary of the results at the free edge of the plate is shown in Table 6-12 below.

Table 6.12 Summary of the Results of CI-CF1-IM without Foundation

$\bar{q}$	$\bar{w}$		Error %	$\bar{\sigma}_b$		Error %	$\bar{\sigma}_m$		Error %
	FEM	RBF		FEM	RBF		FEM	RBF	
0.7	0.1567	0.162903	3.9585	0.2788	0.2640	5.3085	0.0176	0.0176	0.1661
1.4	0.2972	0.326712	9.9435	0.5263	0.4787	9.0442	0.0652	0.0639	1.8637
2.1	0.4167	0.451067	8.2408	0.7330	0.6772	7.6134	0.1323	0.1282	3.0775
2.8	0.5182	0.548623	5.8754	0.9041	0.8539	5.5493	0.2103	0.2045	2.7430
3.5	0.6055	0.643579	6.2829	1.0475	0.9855	5.9115	0.2937	0.2837	3.4196
4.2	0.6821	0.729828	6.9973	1.1699	1.0934	6.5397	0.3796	0.3646	3.9276
4.9	0.7503	0.796854	6.2026	1.2764	1.2019	5.8403	0.4660	0.4488	3.6988
5.6	0.8119	0.842201	3.7278	1.3707	1.3215	3.5939	0.5521	0.5323	3.5942
6.3	0.8682	0.879819	1.3415	1.4552	1.4359	1.3237	0.6373	0.6328	0.7119
7	0.9201	0.958761	4.2066	1.5320	1.4701	4.0368	0.7214	0.6936	3.8573
7.7	0.9683	1.0331	6.6945	1.6023	1.5018	6.2744	0.8042	0.7734	3.8278
8.4	1.0134	1.0524	3.8495	1.6674	1.6056	3.7068	0.8857	0.8537	3.6068

- CI-SF1-IM

A simply free-at-one-edge supported circular plate with immovable edges, ( $w = M_n = V_n$  and  $M_n$  at the free edge =  $u = v = 0$ ) is subjected to a uniform dimensionless total load,  $\bar{q} = 4.8$  which is applied incrementally at a rate of 0.4 per increment. The summary of the results at the center of the plate is shown in Table 6-13 below.

Table 6.13 Summary of the Results of CI-SF1-IM without Foundation

$\bar{q}$	$\bar{w}$		Error %	$\bar{\sigma}_b$		Error %	$\bar{\sigma}_m$		Error %
	FEM	RBF		FEM	RBF		FEM	RBF	
0.4	0.2717	0.2763	1.7124	0.4335	0.4235	2.3068	0.0576	0.0558	3.1250
0.8	0.4507	0.4538	0.6863	0.7060	0.6890	2.4079	0.1581	0.1539	2.6565
1.2	0.5765	0.5788	0.3926	0.8884	0.8675	2.3525	0.258	0.2486	3.6434
1.6	0.6739	0.6763	0.3576	1.0242	0.9957	2.7827	0.3521	0.342	2.8685
2	0.7541	0.7571	0.4021	1.1325	1.1077	2.1898	0.4406	0.4258	3.3591
2.4	0.8228	0.8266	0.4670	1.2228	1.2013	1.7583	0.5242	0.5103	2.6517

2.8	0.8830	0.8878	0.5419	1.3004	1.2623	2.9299	0.6036	0.5911	2.0709
3.2	0.9371	0.9428	0.6103	1.3686	1.3338	2.5427	0.6797	0.6688	1.6036
3.6	0.9862	0.9928	0.6726	1.4296	1.3979	2.2174	0.7527	0.7437	1.1957
4	1.0313	1.0388	0.7288	1.4849	1.4560	1.9463	0.8232	0.8161	0.8625
4.4	1.0731	1.0815	0.7823	1.5355	1.5093	1.7063	0.8914	0.8863	0.5721
4.8	1.1121	1.1213	0.8289	1.5822	1.5585	1.4979	0.9576	0.9545	0.3237

## 6.2.4 WOF Movable Circular Plates

- CI-CC-MO

A clamped supported circular plate with movable edges, ( $w = \frac{\partial w}{\partial n} = \frac{\partial F}{\partial n} = F = 0$ ) is subjected to a uniform dimensionless total load,  $\bar{q} = 9.6$  which is applied incrementally at a rate of 0.8 per increment. The summary of the results at the center of the plate is shown in Table 6-14 below.

Table 6.14 Summary of the Results of CI-CC-MO without Foundation

$\bar{q}$	$\bar{w}$		Error %	$\bar{\sigma}_b$		Error %	$\bar{\sigma}_m$		Error %
	FEM	RBF		FEM	RBF		FEM	RBF	
0.8	0.1365	0.1359	0.4511	0.3886	0.3899	0.3377	0.0093	0.0091	2.1505
1.6	0.2704	0.2711	0.2816	0.7655	0.7768	1.4679	0.0362	0.0373	3.0387
2.4	0.3993	0.3959	0.8483	1.1215	1.1186	0.2597	0.0786	0.0785	0.1411
3.2	0.5220	0.5297	1.4753	1.4506	1.4991	3.3404	0.1334	0.1388	4.0479
4	0.6377	0.6313	1.0095	1.7507	1.7420	0.5001	0.1976	0.1965	0.5418
4.8	0.7464	0.7380	1.1354	2.0222	2.0082	0.6947	0.2684	0.2668	0.5809
5.6	0.8484	0.8380	1.2338	2.2665	2.2474	0.8444	0.3436	0.3401	1.0159
6.4	0.9442	0.9318	1.3166	2.4865	2.4624	0.9661	0.4217	0.4152	1.5373
7.2	1.0344	1.0318	0.2455	2.6846	2.7068	0.8258	0.5014	0.4972	0.8418
8	1.1193	1.1176	0.1556	2.8634	2.8917	0.9888	0.5818	0.5792	0.4360
8.8	1.1996	1.1989	0.0633	3.0254	3.0604	1.1590	0.6622	0.6617	0.0823
9.6	1.2758	1.2759	0.0033	3.1726	3.2134	1.2841	0.7424	0.7448	0.3152

- CI-SS-MO

A simply supported circular plate with movable edges, ( $w = M_n = \frac{\partial F}{\partial n} = F = 0$ ) is subjected to a uniform dimensionless total load,  $\bar{q} = 2$  which is applied incrementally at a rate of 0.2 per increment. The summary of the results at the center of the plate is shown in Table 6-15 below.

Table 6.15 Summary of the Results of CI-SS-MO without Foundation

$\bar{q}$	$\bar{w}$		Error %	$\bar{\sigma}_b$		Error %	$\bar{\sigma}_m$		Error %
	FEM	RBF		FEM	RBF		FEM	RBF	
0.2	0.1385	0.1391	0.4678	0.2459	0.2476	0.6923	0.0057	0.0055	3.509
0.4	0.2727	0.2771	1.6211	0.4820	0.4925	2.1843	0.0219	0.0207	5.4795
0.6	0.3995	0.3984	0.2796	0.7013	0.6994	0.2731	0.0468	0.0472	0.7473
0.8	0.5173	0.5148	0.4739	0.9003	0.8956	0.5302	0.0781	0.0785	0.5787
1	0.6259	0.6216	0.6901	1.0789	1.0701	0.8171	0.1137	0.1137	0.0107
1.2	0.7260	0.7195	0.8933	1.2384	1.2250	1.0840	0.1520	0.1508	0.8116
1.4	0.8180	0.8215	0.4309	1.3805	1.3902	0.7028	0.1918	0.1909	0.4769
1.6	0.9031	0.9084	0.5845	1.5079	1.5218	0.9192	0.2323	0.2324	0.0193
1.8	0.9821	0.9893	0.7261	1.6224	1.6406	1.1207	0.2731	0.2745	0.5338
2	1.0558	1.0644	0.8147	1.7258	1.7473	1.2481	0.3137	0.3172	1.1345
2.2	1.1248	1.1174	0.6629	1.8197	1.8051	0.8002	0.3539	0.3545	0.1652
2.4	1.1897	1.1783	0.9614	1.9053	1.8820	1.2228	0.3937	0.3939	0.0549

- CI-CF1-MO

A clamped free-at-one-edge supported circular plate with movable edges, ( $w = V_n$  and  $M_n$  at the free edge =  $F = \frac{\partial F}{\partial n} = 0$ ) is subjected to a uniform dimensionless total load,  $\bar{q} = 7.2$  which is applied incrementally at a rate of 0.6 per increment. The summary of the results at the center of the plate is shown in Table 6-16 below.

Table 6.16 Summary of the Results of CI-CF1-MO without Foundation

$\bar{q}$	$\bar{w}$		Error %	$\bar{\sigma}_b$		Error %
	FEM	RBF		FEM	RBF	
0.6	0.1293	0.1261	2.4883	0.3024	0.3041	0.5604
1.2	0.2578	0.2519	2.2983	0.6009	0.6068	0.9872
1.8	0.3847	0.3762	2.2184	0.8919	0.9030	1.2468
2.4	0.5096	0.4922	3.4114	1.1730	1.1621	0.9336
3	0.6321	0.6163	2.5051	1.4428	1.4571	0.9917
3.6	0.7523	0.7198	4.3118	1.7008	1.6594	2.4343
4.2	0.8700	0.8439	3.0089	1.9471	1.9538	0.3467
4.8	0.9856	0.9328	5.3520	2.1822	2.0898	4.2359
5.4	1.0991	1.0586	3.6847	2.4071	2.3906	0.6847
6	1.2107	1.1354	6.2222	2.6224	2.4698	5.8209
6.6	1.3207	1.2651	4.2041	2.8293	2.7869	1.4962
7.2	1.4291	1.3311	6.8558	3.0284	2.8153	7.0350

- CI-SF1-MO

A simply free-at-one-edge supported circular plate with movable edges, ( $w = M_n = V_n$  and  $M_n$  at the free edge  $= \frac{\partial F}{\partial n} = F = 0$ ) is subjected to a uniform dimensionless total load,  $\bar{q} = 2.4$  which is applied incrementally at a rate of 0.2 per increment. The summary of the results at the center of the plate is shown in Table 6-17 below.

Table 6.17 Summary of the Results of CI-SF1-MO without Foundation

$\bar{q}$	$\bar{w}$		Error %	$\bar{\sigma}_b$		Error %
	FEM	RBF		FEM	RBF	
0.2	0.1529	0.14875	2.7142	0.2464	0.2423	1.6616
0.4	0.3022	0.29692	1.7483	0.4839	0.4828	0.2260
0.6	0.4451	0.4425	0.5841	0.7063	0.7156	1.3238
0.8	0.5805	0.57417	1.0910	0.9104	0.9057	0.5066

1	0.7081	0.72075	1.7865	1.0960	1.0719	2.1989
1.2	0.8287	0.83467	0.7200	1.2645	1.2793	1.1710
1.4	0.9430	0.95642	1.4228	1.4179	1.4401	1.5626
1.6	1.0518	1.07467	2.1741	1.5583	1.5915	2.1265
1.8	1.1560	1.18758	2.7318	1.6876	1.7165	1.7125
2	1.2564	1.29875	3.3707	1.8078	1.8597	2.8701
2.2	1.3536	1.386	2.3936	1.9201	1.9759	2.91
2.4	1.4479	1.49883	3.5177	2.0257	2.0412	0.7621

### 6.3 Discussion of Results

For the SQCCIM case, the maximum errors are 3.15%, 4%, and 3.9% for the non-dimensional deflection,  $\bar{w}$ , bending stresses,  $\bar{\sigma}_b$ , and membrane stresses,  $\bar{\sigma}_m$  respectively, at the center of the square plate (Table 6.2). The maximum errors for the simply supported square immovable plate (SQSSIM) are 1.5%, 1.6% and 6% for  $\bar{w}$  and  $\bar{\sigma}_b$  and larger in  $\bar{\sigma}_m$ , respectively (Table 6.3).

For clamped and simply free immovable supported plates (SQCF1IM and SQSF1IM), the maximum errors are close to 5% (Tables 6.4 & 6.5). In general, the calculated deflections and stresses at the boundary are less accurate than at any other location in the square plate.

Similar results are obtained for the square plates with movable edges but with less values of the maximum error. The maximum errors for SQCCMO for  $\bar{w}$ ,  $\bar{\sigma}_b$  and  $\bar{\sigma}_m$  are 2.8%, 3.3% and 4.3% respectively (Tables 6.6 to 6.9). Similar order of errors are obtained for SQSSMO, SQCF1MO and SQSF1MO cases.



From the square plate results, it can be observed that the analysis of the movable plates is more accurate than the immovable ones utilizing the proposed MQ-RBF method in this work. In addition, the method is less accurate at the free edge for both movable and immovable boundary conditions which is an expected challenge for any numerical method.

The circular shape plate behaves a little different from the square one. For CICCIM and CISSIM cases, the maximum error occurs in the membrane stresses with values of less than 7% and 5.6% for both CICCIM and CISSIM (Tables 6.10 and 6.11).

For the immovable free circular cases (CICF1IM and CISF1IM), the maximum errors take place at the free edge. The maximum errors are 10%, 9% and 4% for  $\bar{w}$ ,  $\bar{\sigma}_b$  and  $\bar{\sigma}_m$ , respectively (Table 6.12 and 6.13). The errors at the center of the plate are reasonably small within the value of 3% as given in Table 6.13.

The movable circular cases produce less error values for all the boundary conditions as compared with the immovable ones as given in Tables 6.14 to 6.17. For the non-free edge cases, CICCMO and CISSMO, the errors are small within the range of 1.5% to 3.3% for the deflection and bending stresses respectively and 4% to 5.5% for the membrane stresses where the highest values correspond to the clamped plates and the lowest values being for the simply supported plates.

For CICF1MO and CISF1MO plates, the values of the errors are relatively higher with maximum values of 7% and 4% for simply-free and clamped-free movable plates, respectively (Tables 6.16 and 6.17).

As main conclusions from the above discussions, the accuracy of MQ-RBF method is accurate for most cases, especially those that do not involve circular plates with free movable edges. The results are less accurate for these cases but are considered to be within reasonable limits.

## CHAPTER SEVEN

# VERIFICATION OF THE COMPUTER CODES FOR LARGE DEFLECTION OF THIN PLATES ON DISCRETE FOUNDATION (WPF)

### 7.1 General

In this Chapter, the verification of the proposed RBF method as applied to large deflection of thin elastic plates on elastic continuous foundations is presented. In all examples, the load is assumed to be uniformly distributed =  $q$ , Poisson ratio  $\nu$  is assumed 0.3 and the analysis is performed for several combinations of the foundation parameters and boundary conditions. For generality of the solutions, all results are made dimensionless, so that the coordinates, the load, the deflection, the Winkler foundation stiffness, the nonlinear Winkler modulus, the shear interaction parameter and the stress are represented by  $\bar{x} = \frac{x}{a}, \bar{y} = \frac{y}{a}, \bar{q} = \frac{qa^4}{Et^4}, \bar{w} = \frac{w}{t}, K = k \frac{a^4}{D}, K_1 = k_1 \frac{a^4 t^2}{D}, G_1 = g_p \frac{a^2}{D}, \bar{\sigma} = \frac{\sigma a^2}{Et^2}$ , respectively. The shape factor,  $c$ , of the RBF is changed according to the boundary conditions, the geometry, and the type of foundation models. Its optimum value ranges between 0.1 and 0.8.

The results of the solution obtained by the radial basis function MQ-RBF are compared with the results from the finite element method FEM using the commercial software COMSOL. The results are presented in two different formats (tables and charts).

The presented results are at different locations of the plates and different load levels. The computations of deflections and stresses are obtained at the critical locations of the plate.

## 7.2 WPF Numerical Examples

### 7.2.1 WPF Immovable Rectangular Plates

- SQCCIM

In this example, a clamped supported square plate with immovable edges, ( $w = \frac{\partial w}{\partial n} = u = v = 0$ ) resting on the Winkler-Pasternak foundation (WPF) is considered. The plate is subjected to uniformly distributed load  $\bar{q}$  ranging from 30 -180. Selected results of some cases representing various foundation parameters are given in Table 7-1 and Figures 7.1, 7.2, and 7.3. In Table 7-1, the RBF and FEM results with their percentage errors at the center of the plate for  $\bar{w}$ ,  $\bar{\sigma}_b$ , and  $\bar{\sigma}_m$  are presented only at load  $\bar{q} = 180$ . The results for  $\bar{q}$  versus  $\bar{w}$ ,  $\bar{\sigma}_b$ , and  $\bar{\sigma}_m$  at the center of the plate are provided in Figures 7.1, 7.2, and 7.3 respectively. All three figures show a consistent agreement between RBF and FEM solutions. The RBF results compare very well with the FEM results with maximum relative differences of 1.6%, 3 % and 3.8% for  $\bar{w}$ ,  $\bar{\sigma}_b$  and  $\bar{\sigma}_m$  respectively.

Table 7.1 SQCCIM Results of  $\bar{w}$ ,  $\bar{\sigma}_b$ ,  $\bar{\sigma}_m$  at Load  $\bar{q} = 180$

Foundation Parameters			$\bar{w}$			$\bar{\sigma}_b$			$\bar{\sigma}_m$		
K	K1	G1	RBF	FEM	Error %	RBF	FEM	Error %	RBF	FEM	Error %
0	0	0	1.2968	1.2957	0.0856	10.3987	10.3577	0.3958	5.5520	5.4039	2.7394
500	0	0	1.1548	1.1525	0.1985	9.1749	9.1240	0.5579	4.3930	4.2726	2.8182
1000	0	0	1.0240	1.0209	0.2994	7.9962	7.9385	0.7262	3.4477	3.3491	2.9425

500	500	0	1.0571	1.0546	0.2428	7.9244	7.8720	0.6662	3.6886	3.5746	3.1888
500	1000	0	0.9870	0.9844	0.2615	7.0384	6.9870	0.7353	3.2238	3.1154	3.4790
1000	500	0	0.9517	0.9487	0.3176	7.0469	6.9907	0.8037	2.9854	2.8905	3.2833
1000	1000	0	0.8054	0.8024	0.3757	5.6374	5.5816	0.9990	2.1406	2.0624	3.7878
0	0	25	1.1365	1.1345	0.1750	8.9719	8.9196	0.5871	4.2487	4.1290	2.8978
500	0	25	1.0077	1.0049	0.2812	7.8229	7.7648	0.7481	3.3349	3.2364	3.0410
1000	0	25	0.8931	0.8899	0.3670	6.7694	6.7090	0.9006	2.6169	2.5350	3.2297
0	0	50	0.9934	0.9903	0.3080	7.6754	7.6152	0.7900	3.2350	3.1361	3.1531
500	0	50	0.8811	0.8776	0.4002	6.6567	6.5947	0.9401	2.5424	2.4601	3.3466
1000	0	50	0.7836	0.7799	0.4736	5.7577	5.6960	1.0831	2.0111	1.9416	3.5804
500	500	25	0.9394	0.9366	0.3046	6.9542	6.8974	0.8233	2.9054	2.8104	3.3807
500	500	50	0.8346	0.8313	0.4068	6.0718	6.0126	0.9851	2.2878	2.2076	3.6296
500	1000	25	0.8879	0.8851	0.3165	6.3079	6.2529	0.8792	2.6026	2.5109	3.6523
500	1000	50	0.7978	0.7946	0.4103	5.6138	5.5570	1.0230	2.0960	2.0181	3.8616
1000	500	25	0.8441	0.8409	0.3755	6.1328	6.0745	0.9585	2.3440	2.2640	3.5341
1000	500	50	0.7508	0.7473	0.4712	5.3374	5.2785	1.1163	1.8514	1.7832	3.8264
1000	1000	25	0.8054	0.8024	0.3757	5.6374	5.5816	0.9990	2.1406	2.0624	3.7878
1000	1000	50	0.7320	0.7203	1.6207	5.0945	4.9377	3.1745	1.7124	1.6580	3.2831

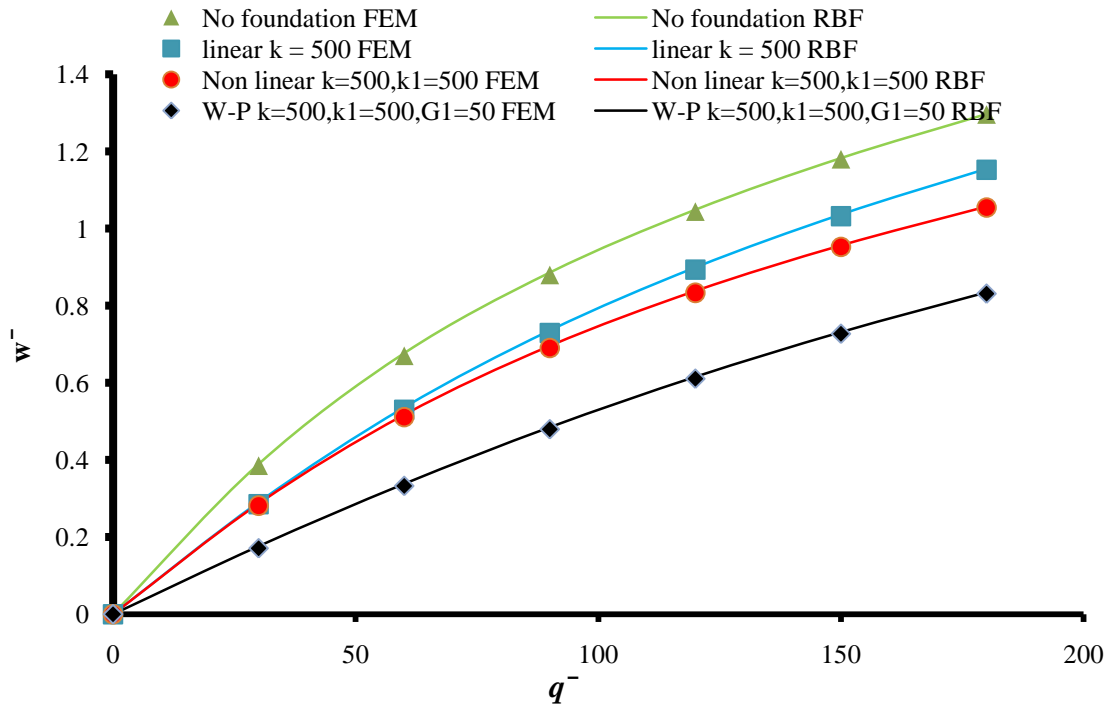


Figure 7.1  $\bar{w}$  vs  $\bar{q}$  on Different Foundations for SQCCIM

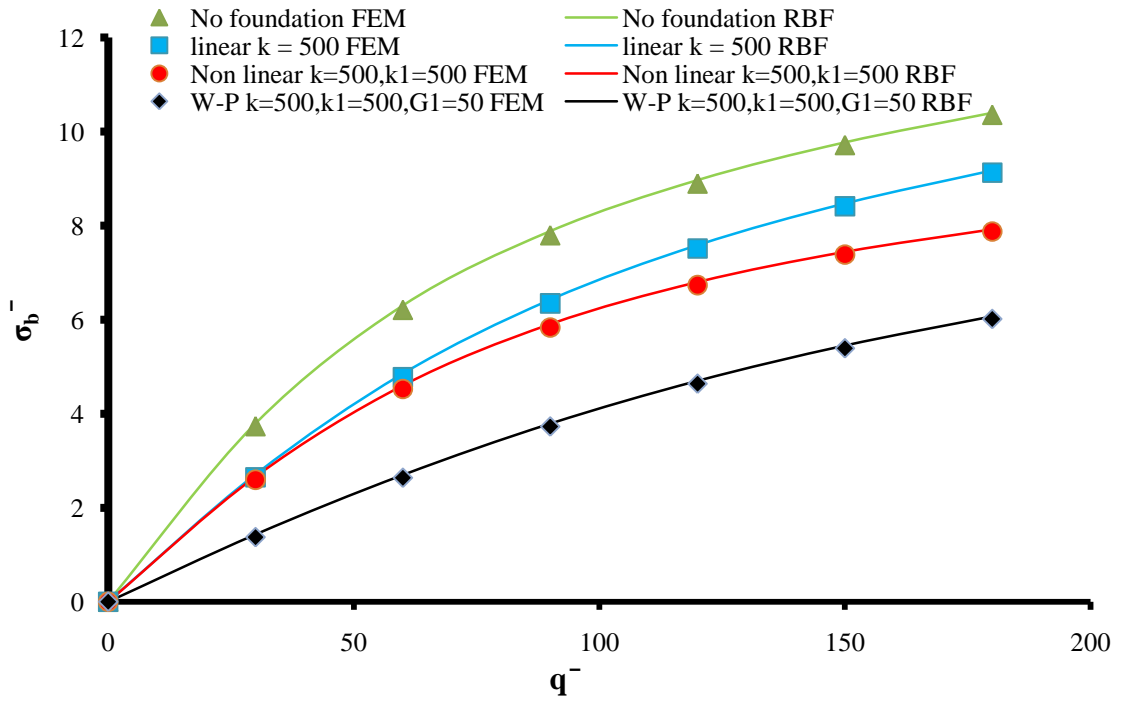


Figure 7.2  $\bar{\sigma}_b$  vs  $\bar{q}$  on Different Foundations for SQCCIM

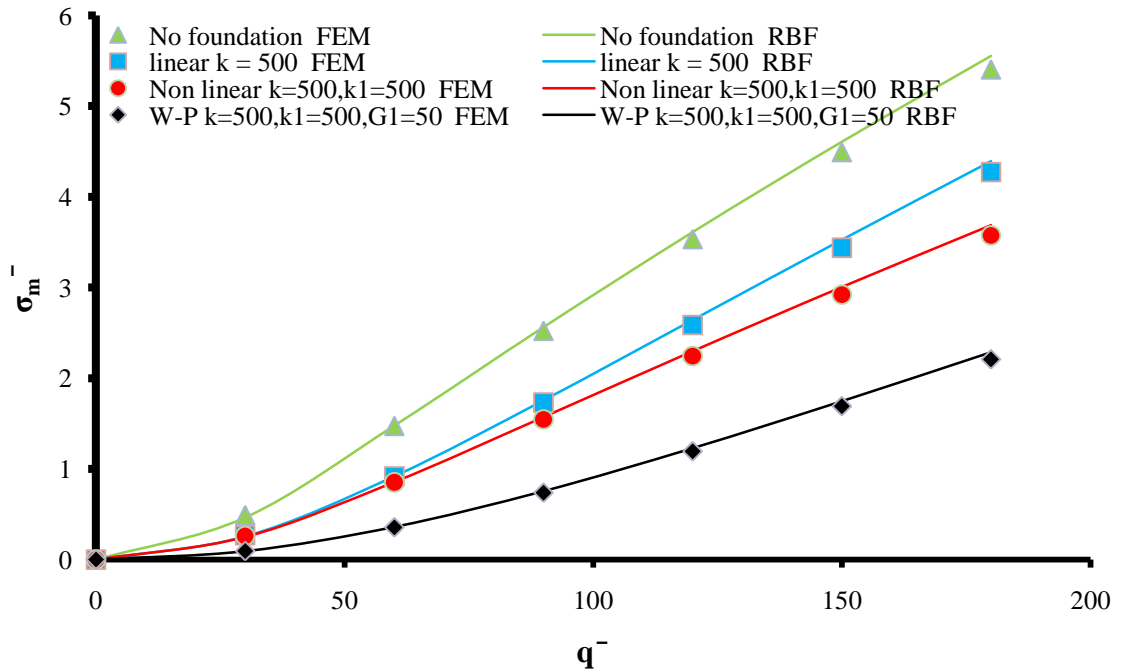


Figure 7.3  $\bar{\sigma}_m$  vs  $\bar{q}$  on Different Foundations for SQCCIM

- SQSSIM

The plate in this example is a simply supported square plate with immovable edges, ( $w = Mn = u = v = 0$ ) resting on the Winkler-Pasternak foundation and is subjected to uniformly distributed load  $\bar{q}$  ranging from 6 - 48. Selected results of some cases representing various foundation parameters are given in Table 7-2 and Figures 7.4, 7.5, and 7.6. In the shown Table 7-2, the RBF and FEM results with their percentage errors at the center of the plate for  $\bar{w}$ ,  $\bar{\sigma}_b$ , and  $\bar{\sigma}_m$  are presented only at load  $\bar{q} = 36$ . The results for  $\bar{q}$  versus  $\bar{w}$ ,  $\bar{\sigma}_b$ , and  $\bar{\sigma}_m$  at the center of the plate are provided in Figures 7.4, 7.5, and 7.6 respectively. All three figures show a consistent agreement between RBF and FEM solutions. The RBF results compare very well with the FEM results with maximum relative differences of 1%, 2.7 % and 1.11% for  $\bar{w}$ ,  $\bar{\sigma}_b$  and  $\bar{\sigma}_m$  respectively.

Table 7.2 SQSSIM Results of  $\bar{w}$ ,  $\bar{\sigma}_b$ ,  $\bar{\sigma}_m$  at Load  $\bar{q} = 36$

Foundation Parameters			$\bar{w}$			$\bar{\sigma}_b$			$\bar{\sigma}_m$		
K	K1	G1	FEM	RBF	Error %	FEM	RBF	Error %	FEM	RBF	Error %
0	0	0	0.8090	0.8160	0.8670	4.8130	4.8911	1.6221	2.0012	2.0066	0.2664
0	0	10	0.7045	0.7107	0.8867	4.1666	4.2390	1.7357	1.5193	1.5168	0.1662
0	0	20	0.6110	0.6164	0.8773	3.5821	3.6475	1.8259	1.1447	1.1375	0.6228
0	200	0	0.7672	0.7734	0.8074	4.4367	4.5169	1.8076	1.8066	1.8104	0.2112
0	200	10	0.6751	0.6808	0.8368	3.9050	3.9785	1.8812	1.3995	1.3971	0.1732
0	200	20	0.5914	0.5963	0.8423	3.4078	3.4741	1.9453	1.0747	1.0684	0.5846
0	400	0	0.7333	0.7389	0.7666	4.1350	4.2175	1.9940	1.6560	1.6589	0.1773
0	400	10	0.6506	0.6558	0.8008	3.6883	3.7631	2.0273	1.3032	1.3009	0.1729
0	400	20	0.5744	0.5791	0.8154	3.2583	3.3255	2.0629	1.0161	1.0105	0.5503
200	0	0	0.7007	0.7070	0.9048	4.0763	4.1562	1.9585	1.5064	1.5042	0.1415
200	0	10	0.6077	0.6131	0.8968	3.5033	3.5754	2.0574	1.1349	1.1281	0.5968
200	0	20	0.5279	0.5325	0.8776	3.0099	3.0745	2.1451	0.8581	0.8496	0.9951
200	200	0	0.6715	0.6772	0.8563	3.8124	3.8938	2.1344	1.3879	1.3858	0.1471
200	200	10	0.5882	0.5932	0.8630	3.3280	3.4012	2.1995	1.0658	1.0599	0.5572
200	200	20	0.5152	0.5196	0.8570	2.8964	2.9619	2.2610	0.8190	0.8114	0.9298

200	400	0	0.6471	0.6524	0.8216	3.5939	3.6769	2.3093	1.2926	1.2907	0.1464
200	400	10	0.5713	0.5761	0.8372	3.1776	3.2519	2.3385	1.0079	1.0026	0.5233
200	400	20	0.5039	0.5081	0.8405	2.7957	2.8621	2.3730	0.7849	0.7780	0.8743
400	0	0	0.6041	0.6096	0.9199	3.4140	3.4940	2.3424	1.1245	1.1182	0.5677
400	0	10	0.5248	0.5295	0.9019	2.9329	3.0044	2.4364	0.8505	0.8423	0.9642
400	0	20	0.4587	0.4628	0.8901	2.5332	2.5973	2.5312	0.6512	0.6430	1.2648
400	200	0	0.5846	0.5898	0.8875	3.2374	3.3187	2.5135	1.0563	1.0507	0.5279
400	200	10	0.5122	0.5167	0.8825	2.8188	2.8913	2.5730	0.8119	0.8046	0.8987
400	200	20	0.4506	0.4545	0.8772	2.4599	2.5248	2.6362	0.6294	0.6219	1.1920
400	400	0	0.5678	0.5727	0.8629	3.0859	3.1686	2.6799	0.9991	0.9942	0.4930
400	400	10	0.5009	0.5053	0.8669	2.7176	2.7912	2.7050	0.7782	0.7716	0.8431
400	400	20	0.4431	0.4469	0.8490	2.3931	2.4581	2.7162	0.6098	0.6030	1.1176

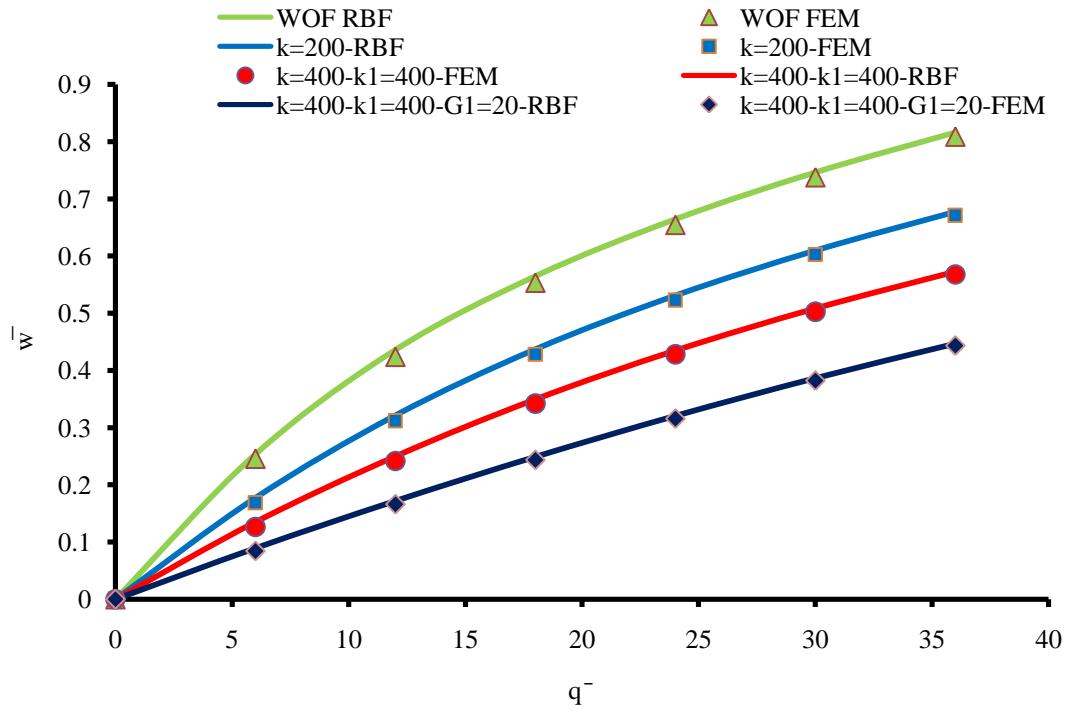


Figure 7.4  $\bar{w}$  vs  $\bar{q}$  on Different Foundations for SQSSIM



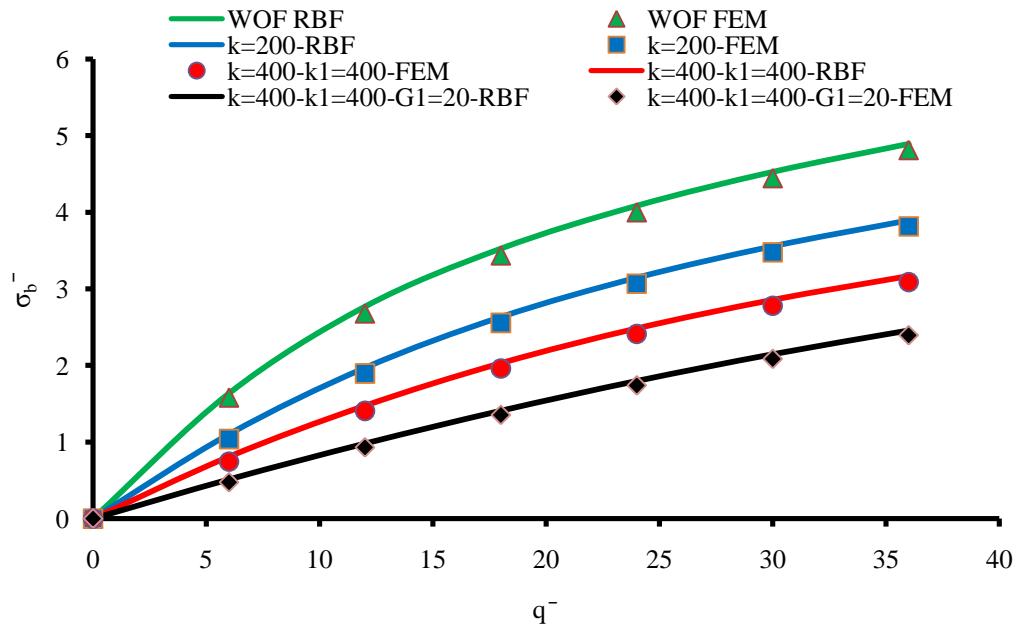


Figure 7.5  $\bar{\sigma}_b$  vs  $\bar{q}$  on Different Foundations for SQSSIM

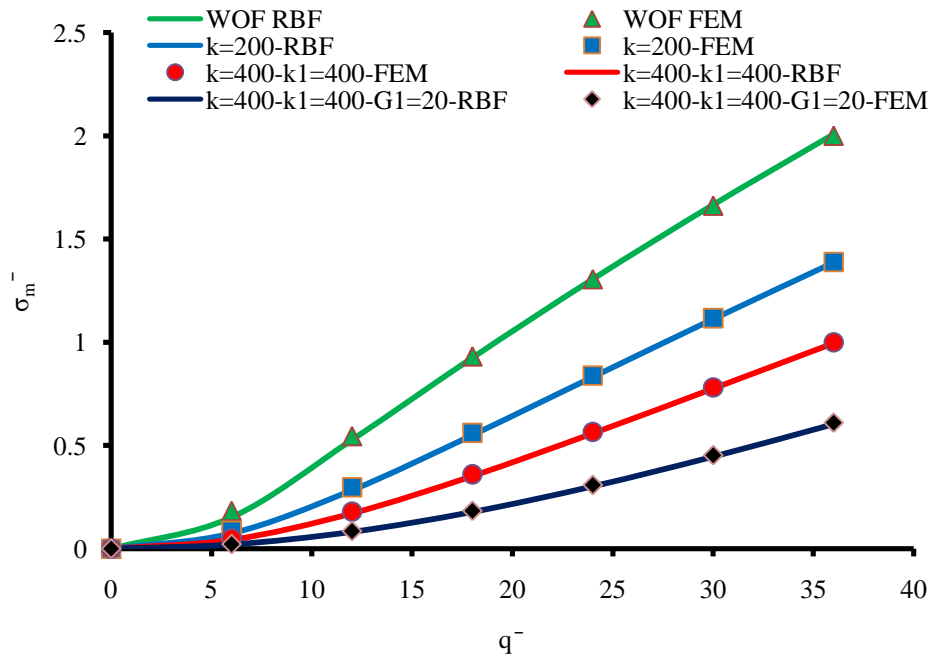


Figure 7.6  $\bar{\sigma}_m$  vs  $\bar{q}$  on Different Foundations for SQSSIM

- SQCF1IM

The plate is a clamped free at on edge square plate with immovable edges, ( $w = (V_n = M_n \text{ at free}) = u = v = 0$ ) resting on the Winkler-Pasternak foundation in this example and subjected to uniformly distributed load  $\bar{q}$  ranging from 10-80. Selected results of some cases representing various foundation parameters are given in Table 7-3 and Figures 7.7, 7.8, and 7.9. In Table 7-3, the RBF and FEM results with their percentage errors at the free edge of the plate for  $\bar{w}$ ,  $\bar{\sigma}_b$ , and  $\bar{\sigma}_m$  are presented only at load  $\bar{q} = 80$ . The results for  $\bar{q}$  versus  $\bar{w}$ ,  $\bar{\sigma}_b$ , and  $\bar{\sigma}_m$  at the free edge of the plate are provided in Figures 7.7, 7.8, and 7.9 respectively. All three figures show a good agreement between RBF and FEM solutions. The RBF results compare very well with the FEM results with maximum relative differences of 5%, 5.7 % and 5.7% for  $\bar{w}$ ,  $\bar{\sigma}_b$  and  $\bar{\sigma}_m$  respectively.

Table 7.3 SQCF1IM Results of  $\bar{w}$ ,  $\bar{\sigma}_b$ ,  $\bar{\sigma}_m$  at Load  $\bar{q} = 80$

Foundation Parameters			$\bar{w}$			$\bar{\sigma}_b$			$\bar{\sigma}_m$		
K	K1	G1	FEM	RBF	Error %	FEM	RBF	Error %	FEM	RBF	Error %
0	0	0	1.183	1.155	2.423	0.199	0.203	2.483	2.153	2.207	2.483
0	0	10	1.118	1.086	2.885	0.176	0.181	2.970	1.929	1.986	2.970
0	0	20	1.057	1.008	4.584	0.156	0.164	4.804	1.728	1.811	4.804
0	200	0	1.087	1.061	2.366	0.147	0.151	2.423	1.832	1.876	2.423
0	200	10	1.035	1.013	2.187	0.133	0.136	2.236	1.664	1.701	2.236
0	200	20	0.986	0.963	2.301	0.121	0.123	2.355	1.511	1.546	2.355
0	400	0	1.016	0.993	2.251	0.114	0.116	2.302	1.615	1.652	2.302
0	400	10	0.973	0.940	3.416	0.104	0.108	3.537	1.480	1.532	3.537
0	400	20	0.931	0.943	1.238	0.096	0.095	1.223	1.355	1.339	1.223
200	0	0	1.071	1.030	3.825	0.154	0.161	3.978	1.771	1.841	3.978
200	0	10	1.011	0.971	3.971	0.136	0.142	4.136	1.582	1.648	4.136
200	0	20	0.955	0.924	3.255	0.121	0.125	3.364	1.416	1.463	3.364
200	200	0	0.995	0.977	1.745	0.117	0.119	1.776	1.539	1.567	1.776
200	200	10	0.946	0.928	1.909	0.106	0.108	1.946	1.394	1.421	1.946

200	200	20	0.900	0.881	2.035	0.095	0.097	2.077	1.263	1.289	2.077
200	400	0	0.937	0.920	1.821	0.092	0.094	1.855	1.376	1.402	1.855
200	400	10	0.896	0.910	1.544	0.084	0.083	1.520	1.258	1.239	1.520
200	400	20	0.857	0.868	1.334	0.077	0.076	1.317	1.149	1.134	1.317
400	0	0	0.966	0.934	3.299	0.118	0.122	3.412	1.447	1.496	3.412
400	0	10	0.911	0.862	5.372	0.104	0.110	5.676	1.292	1.365	5.676
400	0	20	0.861	0.830	3.637	0.092	0.095	3.774	1.156	1.200	3.774
400	200	0	0.907	0.896	1.213	0.092	0.093	1.228	1.284	1.300	1.228
400	200	10	0.862	0.847	1.761	0.082	0.084	1.793	1.161	1.182	1.793
400	200	20	0.820	0.795	3.021	0.074	0.076	3.115	1.052	1.084	3.115
400	400	0	0.861	0.876	1.673	0.073	0.072	1.646	1.166	1.147	1.646
400	400	10	0.823	0.809	1.704	0.066	0.068	1.734	1.063	1.082	1.734
400	400	20	0.786	0.767	2.396	0.061	0.062	2.454	0.971	0.994	2.454

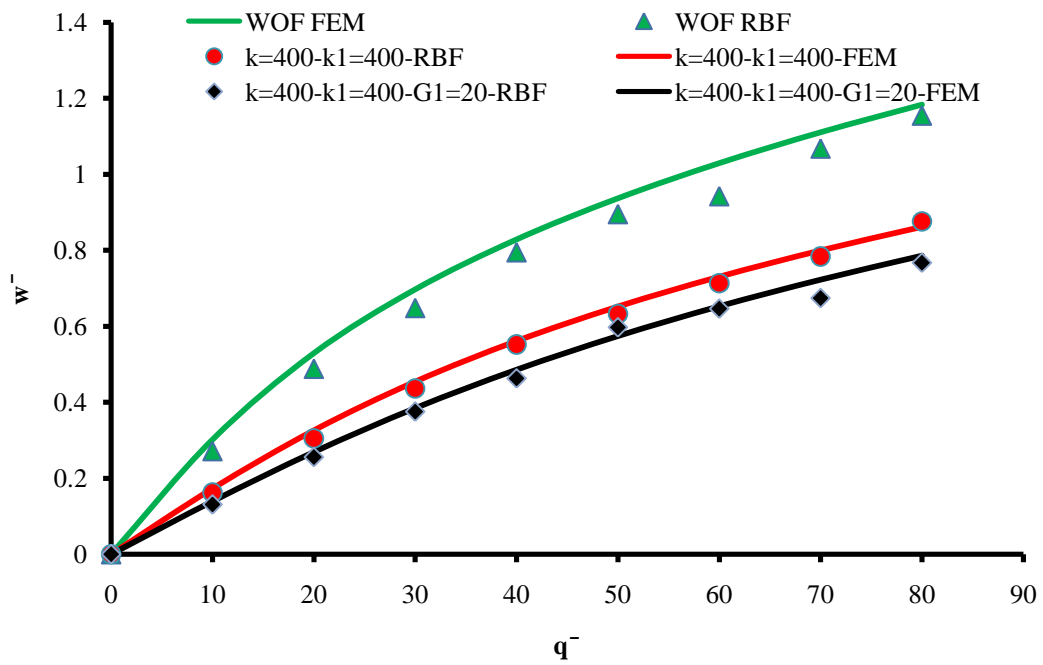


Figure 7.7  $\bar{w}$  vs  $\bar{q}$  on Different Foundations for SQCF1IM

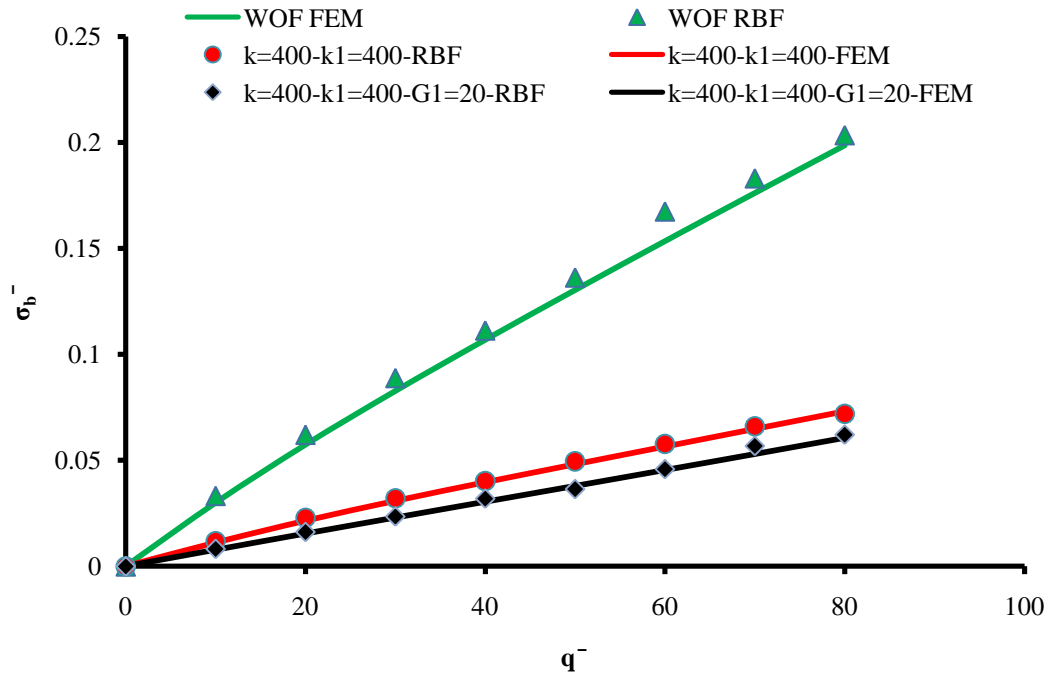


Figure 7.8  $\bar{\sigma}_b$  vs  $\bar{q}$  on Different Foundations for SQCF1IM

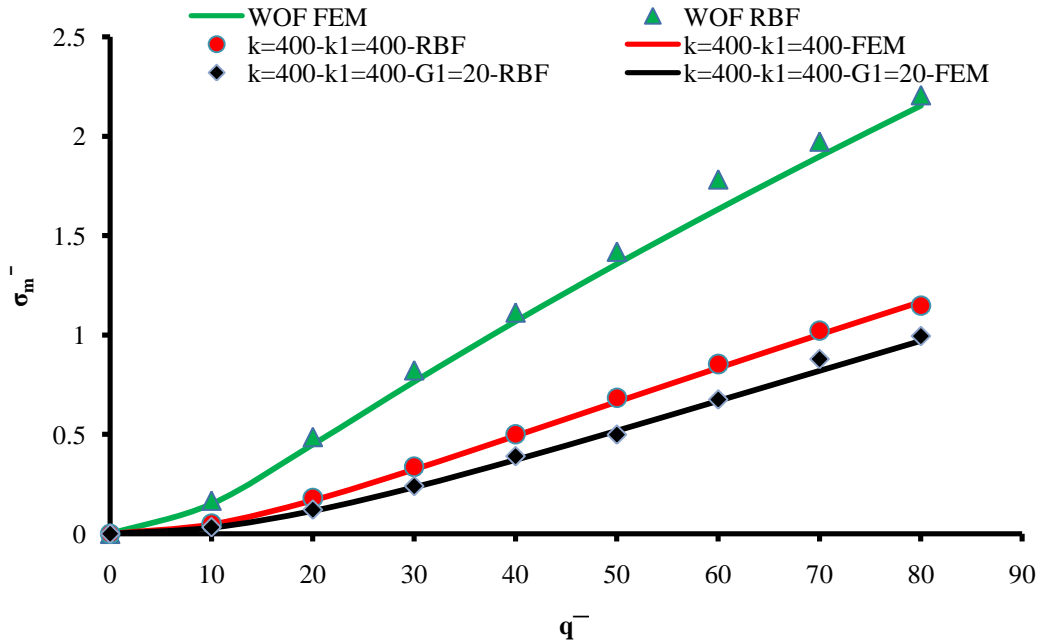


Figure 7.9  $\bar{\sigma}_m$  vs  $\bar{q}$  on Different Foundations for SQCF1IM

- SQSF1IM

A simply free at one edge supported square plate with immovable edges, ( $w = (V_n \text{ and } M_n \text{ at free} = M_n \text{ at simple}) = u = v = 0$ ) resting on the Winkler-Pasternak foundation is provided in this example and subjected to uniformly distributed load  $\bar{q}$  ranging from 3-24. The selected results of some cases representing various foundation parameters are given in Table 7-4 and Figures 7.10, 7.11, and 7.12. In the shown Table 7-4, the RBF and FEM results with their percentage errors at the free edge of the plate for  $\bar{w}, \bar{\sigma}_b$ , and  $\bar{\sigma}_m$  are presented only at load  $\bar{q} = 18$ . The results for  $\bar{q}$  versus  $\bar{w}, \bar{\sigma}_b$ , and  $\bar{\sigma}_m$  at the free edge of the plate are provided in Figures 7.10, 7.11, and 7.12 respectively. All three figures show a good agreement between RBF and FEM solutions. The RBF results compare very well with the FEM results with maximum relative differences of 4.8%, 4.6 % and 4.4% for  $\bar{w}, \bar{\sigma}_b$  and  $\bar{\sigma}_m$  respectively.

Table 7.4 SQSF1IM Results of  $\bar{w}, \bar{\sigma}_b, \bar{\sigma}_m$  at Load  $\bar{q} = 18$

Foundation Parameters			$\bar{w}$			$\bar{\sigma}_b$			$\bar{\sigma}_m$		
K	K1	G1	FEM	RBF	Error %	FEM	RBF	Error %	FEM	RBF	Error %
0	0	0	0.8402	0.8571	2.0031	0.0482	0.0473	1.9637	1.1048	1.0853	1.7677
0	0	10	0.7386	0.7550	2.2189	0.0366	0.0359	2.1707	0.8452	0.8285	1.9750
0	0	20	0.6482	0.6637	2.3990	0.0281	0.0274	2.3428	0.6472	0.6333	2.1475
0	25	0	0.8274	0.8499	2.7123	0.0449	0.0437	2.6407	1.0738	1.0476	2.4460
0	25	10	0.7296	0.7517	3.0239	0.0345	0.0335	2.9352	0.8259	0.8033	2.7410
0	25	20	0.6421	0.6633	3.2993	0.0268	0.0259	3.1939	0.6355	0.6165	3.0003
0	50	0	0.8154	0.8406	3.0951	0.0418	0.0405	3.0022	1.0451	1.0157	2.8082
0	50	10	0.7211	0.7461	3.4690	0.0325	0.0314	3.3527	0.8078	0.7823	3.1594
0	50	20	0.6363	0.6605	3.8043	0.0255	0.0246	3.6649	0.6245	0.6028	3.4722
25	0	0	0.8132	0.8453	3.9402	0.0434	0.0417	3.7908	1.0360	0.9987	3.5984
25	0	10	0.7136	0.7449	4.3797	0.0328	0.0314	4.1959	0.7897	0.7581	4.0043
25	0	20	0.6259	0.6557	4.7625	0.0251	0.0239	4.5460	0.6040	0.5777	4.3551
25	25	0	0.8014	0.8282	3.3439	0.0404	0.0391	3.2357	1.0082	0.9775	3.0422
25	25	10	0.7054	0.7317	3.7246	0.0309	0.0298	3.5909	0.7727	0.7464	3.3981

25	25	20	0.6204	0.6456	4.0606	0.0239	0.0230	3.9021	0.5939	0.5718	3.7099
25	50	0	0.7902	0.8159	3.2523	0.0376	0.0364	3.1498	0.9823	0.9533	2.9561
25	50	10	0.6976	0.7230	3.6356	0.0292	0.0281	3.5080	0.7566	0.7316	3.3151
25	50	20	0.6151	0.6400	4.0580	0.0228	0.0219	3.8997	0.5842	0.5625	3.7075
50	0	0	0.7865	0.8137	3.4575	0.0388	0.0375	3.3420	0.9701	0.9396	3.1487
50	0	10	0.6892	0.7155	3.8213	0.0292	0.0281	3.6807	0.7373	0.7116	3.4880
50	0	20	0.6043	0.6296	4.1814	0.0223	0.0214	4.0136	0.5636	0.5421	3.8216
50	25	0	0.7756	0.8016	3.3606	0.0361	0.0350	3.2513	0.9453	0.9164	3.0578
50	25	10	0.6817	0.7071	3.7293	0.0276	0.0266	3.5953	0.7223	0.6977	3.4024
50	25	20	0.5993	0.6217	3.7322	0.0213	0.0205	3.5979	0.5547	0.5358	3.4051
50	50	0	0.7652	0.7902	3.2712	0.0337	0.0326	3.1675	0.9221	0.8947	2.9739
50	50	10	0.6745	0.6991	3.6437	0.0260	0.0251	3.5156	0.7081	0.6846	3.3227
50	50	20	0.5945	0.6096	2.5539	0.0203	0.0198	2.4903	0.5462	0.5337	2.2953

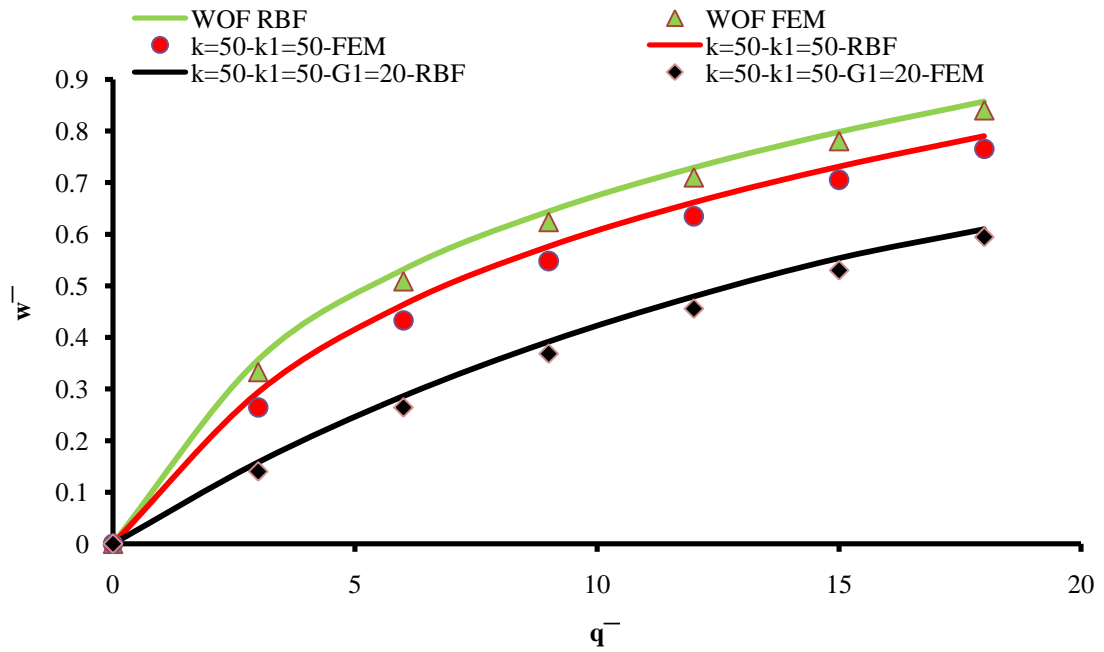


Figure 7.10  $\bar{w}$  vs  $\bar{q}$  on Different Foundations for SQSF11M

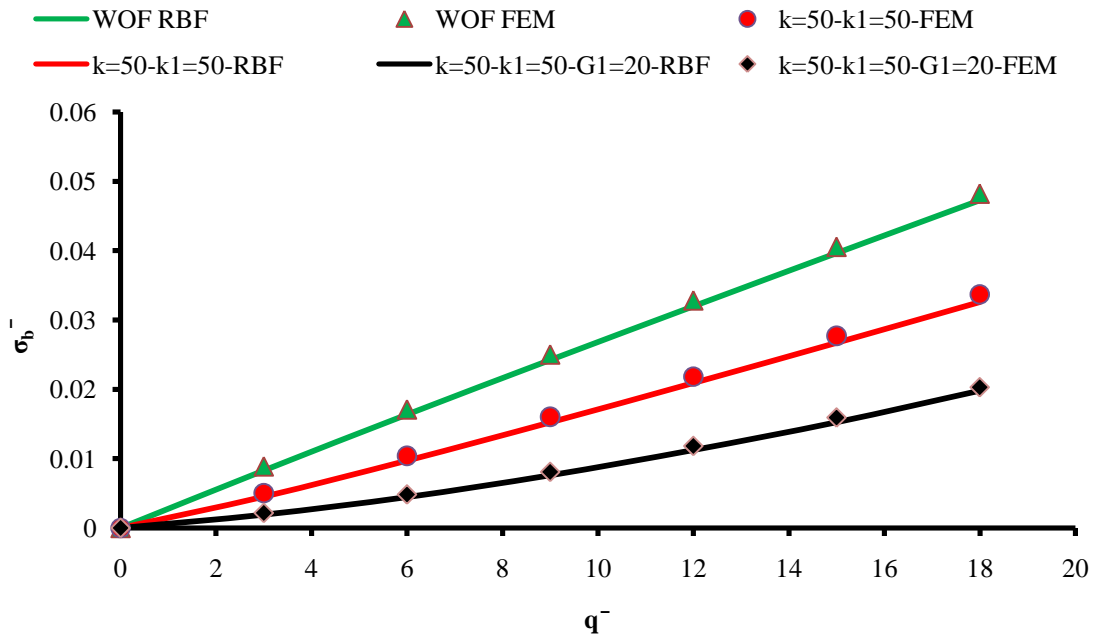


Figure 7.11  $\bar{\sigma}_b$  vs  $\bar{q}$  on Different Foundations for SQSF1IM

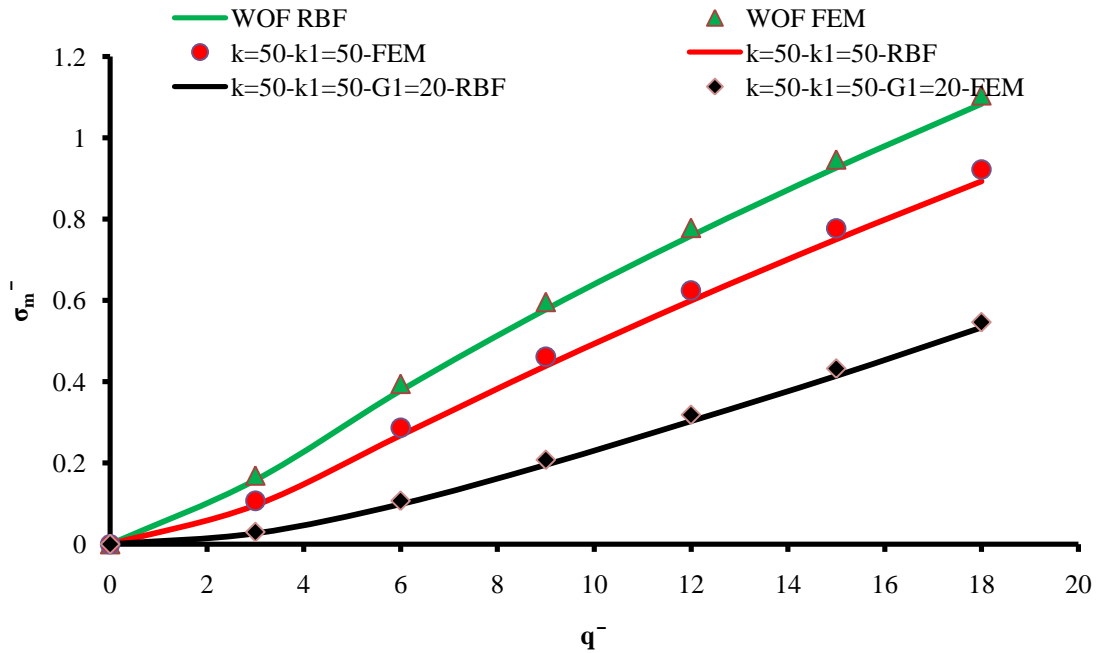


Figure 7.12  $\bar{\sigma}_m$  vs  $\bar{q}$  on Different Foundations for SQSF1IM

- SQCFIM

The plate in this example is a clamped free at two edge supported square plate with immovable edges, ( $w = (V_n = M_n \text{ at free}) = u = v = 0$ ) resting on the Winkler-Pasternak foundation and subjected to uniformly distributed load  $\bar{q}$  ranging from 10-80. The selected results of some cases representing various foundation parameters are given in Table 7-5 and Figures 7.13, 7.14, and 7.15. In the shown Table 7-5, the RBF and FEM results with their percentage errors at the free edge of the plate for  $\bar{w}$ ,  $\bar{\sigma}_b$ , and  $\bar{\sigma}_m$  are presented only at load  $\bar{q} = 80$ . The results for  $\bar{q}$  versus  $\bar{w}$ ,  $\bar{\sigma}_b$ , and  $\bar{\sigma}_m$  at the free edge of the plate are provided in Figures 7.13, 7.14, and 7.15 respectively. All three figures show a good agreement between RBF and FEM solutions. The RBF results compare very well with the FEM results with maximum relative differences of 3.4%, 3.3 % and 3% for  $\bar{w}$ ,  $\bar{\sigma}_b$  and  $\bar{\sigma}_m$  respectively.

Table 7.5 SQCFIM Results of  $\bar{w}$ ,  $\bar{\sigma}_b$ ,  $\bar{\sigma}_m$  at Load  $\bar{q} = 80$

Foundation Parameters			$\bar{w}$			$\bar{\sigma}_b$			$\bar{\sigma}_m$		
K	K1	G1	FEM	RBF	Error %	FEM	RBF	Error %	FEM	RBF	Error %
0	0	0	1.174	1.184	0.829	9.683	9.604	0.822	0.201	0.200	0.624
0	0	10	1.113	1.136	2.064	8.954	8.773	2.023	0.193	0.190	1.827
0	0	20	1.054	1.075	1.994	8.280	8.118	1.955	0.185	0.181	1.759
0	200	0	1.076	1.106	2.732	8.514	8.287	2.659	0.185	0.181	2.464
0	200	10	1.027	1.056	2.790	7.953	7.737	2.714	0.178	0.174	2.519
0	200	20	0.980	1.008	2.841	7.429	7.223	2.762	0.170	0.166	2.568
0	400	0	1.007	1.032	2.491	7.696	7.509	2.430	0.173	0.169	2.235
0	400	10	0.965	0.990	2.548	7.238	7.058	2.485	0.166	0.163	2.290
0	400	20	0.925	0.949	2.600	6.808	6.635	2.534	0.159	0.156	2.339
200	0	0	1.061	1.095	3.248	8.555	8.286	3.146	0.173	0.168	2.953
200	0	10	1.004	1.037	3.284	7.888	7.638	3.180	0.166	0.161	2.986
200	0	20	0.950	0.982	3.308	7.281	7.048	3.202	0.158	0.153	3.009
200	200	0	0.984	1.013	2.893	7.651	7.436	2.812	0.161	0.157	2.617
200	200	10	0.938	0.966	2.939	7.125	6.922	2.856	0.154	0.150	2.661



200	200	20	0.894	0.921	2.976	6.640	6.448	2.890	0.147	0.143	2.696
200	400	0	0.928	0.953	2.654	6.994	6.813	2.585	0.151	0.148	2.390
200	400	10	0.888	0.912	2.703	6.559	6.387	2.631	0.145	0.142	2.437
200	400	20	0.850	0.874	2.744	6.154	5.990	2.670	0.139	0.135	2.476
400	0	0	0.955	0.987	3.366	7.520	7.275	3.256	0.148	0.144	3.063
400	0	10	0.903	0.934	3.380	6.923	6.697	3.269	0.142	0.137	3.076
400	0	20	0.856	0.885	3.380	6.388	6.179	3.270	0.135	0.130	3.076
400	200	0	0.897	0.924	3.035	6.837	6.636	2.946	0.139	0.135	2.752
400	200	10	0.854	0.880	3.066	6.354	6.165	2.974	0.133	0.129	2.780
400	200	20	0.814	0.839	3.084	5.914	5.738	2.992	0.127	0.123	2.798
400	400	0	0.852	0.876	2.804	6.321	6.149	2.728	0.132	0.128	2.533
400	400	10	0.815	0.838	2.839	5.915	5.751	2.761	0.126	0.123	2.566
400	400	20	0.780	0.802	2.864	5.541	5.387	2.784	0.120	0.117	2.589

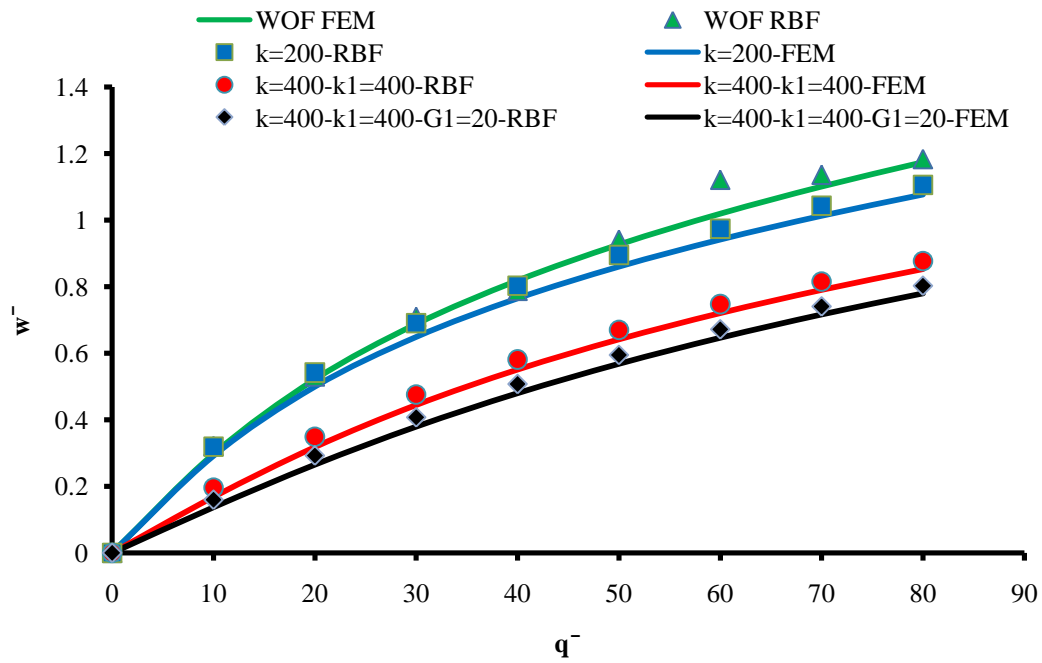


Figure 7.13  $\bar{w}$  vs  $\bar{q}$  on Different Foundations for SQCFIM

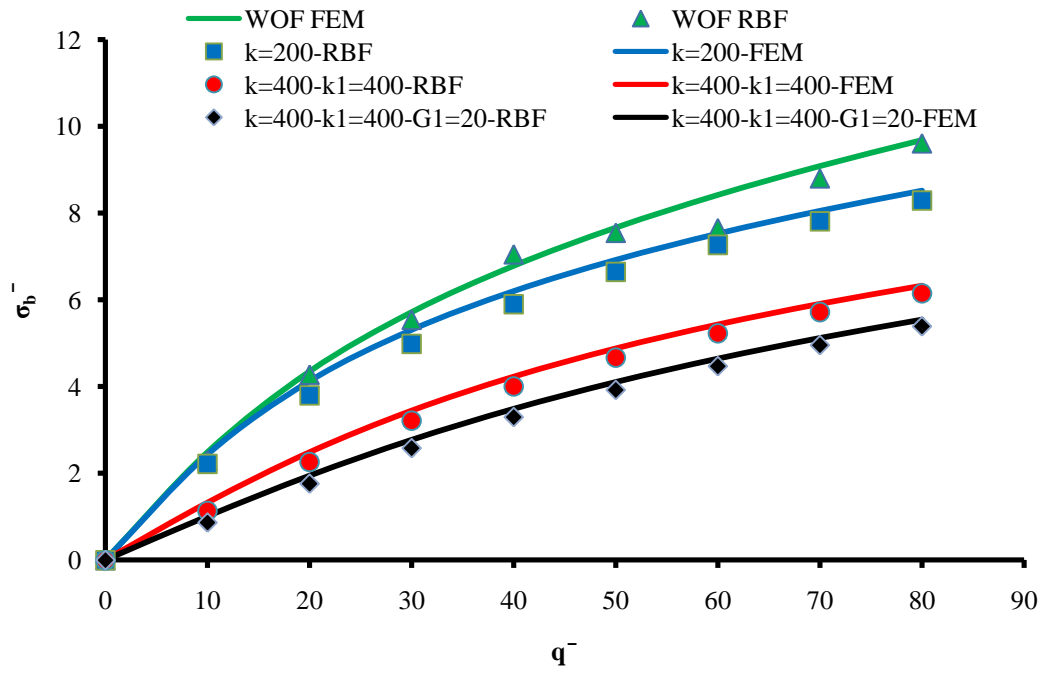


Figure 7.14  $\bar{\sigma}_b$  vs  $\bar{q}$  on Different Foundations for SQCFIM

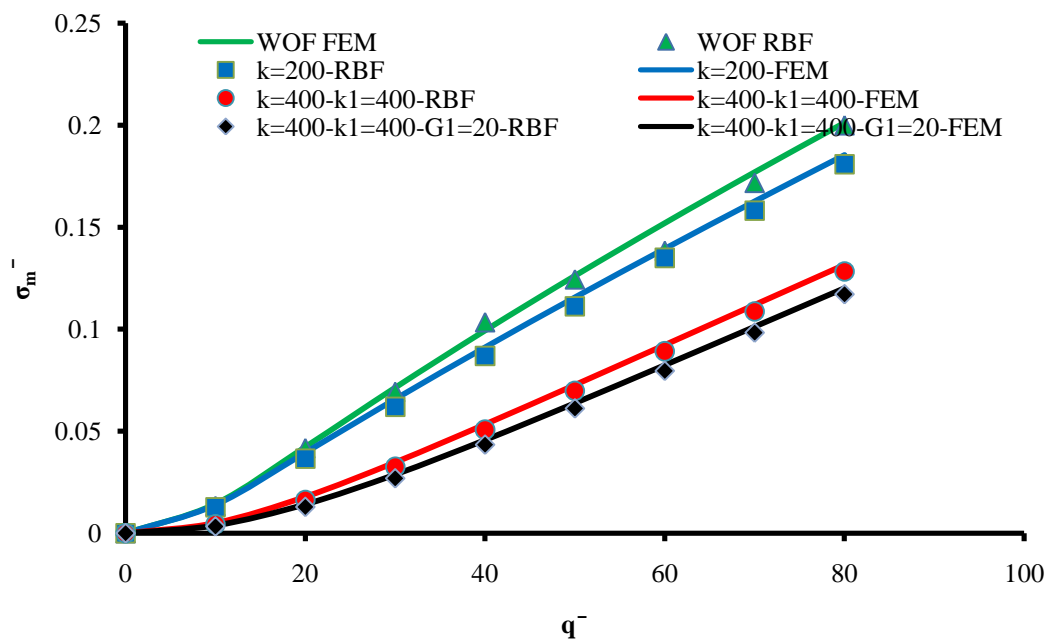


Figure 7.15  $\bar{\sigma}_m$  vs  $\bar{q}$  on Different Foundations for SQCFIM

- SQSFIM

A simply free at two edges supported square plate with immovable edges, ( $w = (V_n \text{ at free} = M_n \text{ at free and simple}) = u = v = 0$ ) resting on the Winkler-Pasternak foundation is presented in this example and subjected to uniformly distributed load  $\bar{q}$  ranging from 3-24. The selected results of some cases representing various foundation parameters are given in Table 7-6 and Figures 7.16, 7.17, and 7.18. In the shown Table 7-6, the RBF and FEM results with their percentage errors at the free edge of the plate for  $\bar{w}, \bar{\sigma}_b$ , and  $\bar{\sigma}_m$  are presented only at load  $\bar{q} = 18$ . The results for  $\bar{q}$  versus  $\bar{w}, \bar{\sigma}_b$ , and  $\bar{\sigma}_m$  at the free edge of the plate are provided in Figures 7.16, 7.17, and 7.18 respectively. All three figures show a reasonable agreement between RBF and FEM solutions. The RBF results compare very well with the FEM results with maximum relative differences of 5.8%, 5.8 % and 6% for  $\bar{w}, \bar{\sigma}_b$  and  $\bar{\sigma}_m$  respectively.

Table 7.6 SQSFIM Results of  $\bar{w}, \bar{\sigma}_b, \bar{\sigma}_m$  at Load  $\bar{q} = 18$

Foundation Parameters			$\bar{w}$			$\bar{\sigma}_b$			$\bar{\sigma}_m$		
K	K1	G1	FEM	RBF	Error %	FEM	RBF	Error %	FEM	RBF	Error %
0	0	0	0.8343	0.7964	4.5429	4.5044	4.7187	4.7591	0.1873	0.1966	4.9687
0	0	10	0.7398	0.7025	5.0398	3.8479	4.0521	5.3073	0.1514	0.1598	5.5179
0	0	20	0.6543	0.6182	5.5102	3.2912	3.4831	5.8315	0.1214	0.1288	6.0431
0	25	0	0.8205	0.7839	4.4546	4.3893	4.5940	4.6622	0.1824	0.1913	4.8716
0	25	10	0.7297	0.6936	4.9474	3.7690	3.9652	5.2049	0.1481	0.1561	5.4153
0	25	20	0.6472	0.6132	5.2466	3.2386	3.4179	5.5371	0.1192	0.1261	5.7482
0	50	0	0.8076	0.7723	4.3699	4.2830	4.4787	4.5696	0.1779	0.1865	4.7788
0	50	10	0.7202	0.6852	4.8607	3.6953	3.8841	5.1091	0.1449	0.1527	5.3193
0	50	20	0.6404	0.6085	4.9848	3.1889	3.3562	5.2463	0.1171	0.1235	5.4568
25	0	0	0.8066	0.7705	4.4842	4.3054	4.5076	4.6947	0.1766	0.1852	4.9041
25	0	10	0.7139	0.6783	4.9764	3.6722	3.8645	5.2370	0.1421	0.1499	5.4475
25	0	20	0.6308	0.5987	5.0831	3.1404	3.3086	5.3554	0.1137	0.1200	5.5661
25	25	0	0.7938	0.7589	4.3978	4.2006	4.3938	4.6001	0.1722	0.1805	4.8093
25	25	10	0.7047	0.6702	4.8895	3.6012	3.7863	5.1408	0.1391	0.1466	5.3511

25	25	20	0.6244	0.5914	5.2802	3.0935	3.2660	5.5745	0.1117	0.1182	5.7857
25	50	0	0.7819	0.7481	4.3160	4.1033	4.2884	4.5107	0.1681	0.1760	4.7197
25	50	10	0.6960	0.6625	4.8135	3.5346	3.7134	5.0569	0.1363	0.1435	5.2670
25	50	20	0.6183	0.5986	3.1862	3.0490	3.2581	3.5782	0.1099	0.1146	4.2766
50	0	0	0.7792	0.7448	4.4205	4.1114	4.3016	4.6249	0.1662	0.1743	4.8342
50	0	10	0.6885	0.6546	4.9165	3.5026	3.6837	5.1707	0.1333	0.1404	5.3810
50	0	20	0.6080	0.5815	4.3586	2.9962	3.0873	3.0406	0.1063	0.1098	3.293
50	25	0	0.7674	0.7342	4.3367	4.0162	4.1982	4.5333	0.1622	0.1699	4.7423
50	25	10	0.6801	0.6472	4.8432	3.4389	3.6139	5.0897	0.1306	0.1375	5.2999
50	25	20	0.6023	0.5759	4.3832	2.9544	3.0595	3.5574	0.1046	0.1067	2.0076
50	50	0	0.7564	0.7242	4.2572	3.9277	4.1023	4.4465	0.1585	0.1659	4.6553
50	50	10	0.6722	0.6402	4.7572	3.3790	3.5477	4.9948	0.1281	0.1348	5.2048
50	50	20	0.5967	0.5618	5.8488	2.9147	3.0705	5.3453	0.1030	0.1078	4.6602

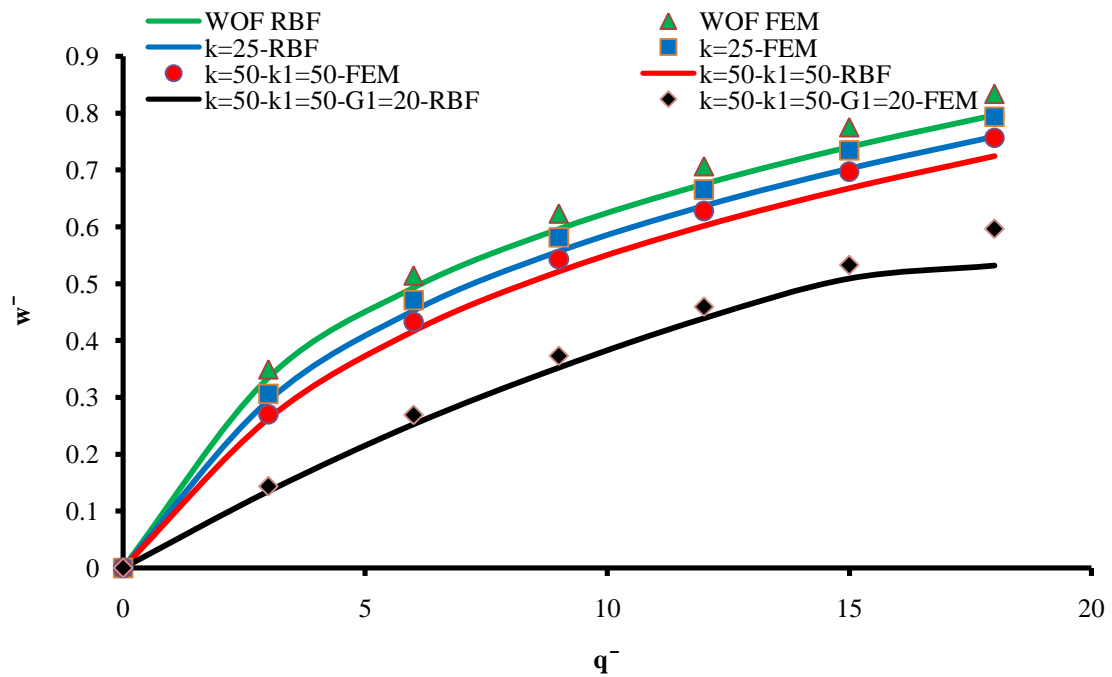


Figure 7.16  $\bar{w}$  vs  $\bar{q}$  on Different Foundations for SQSFIM

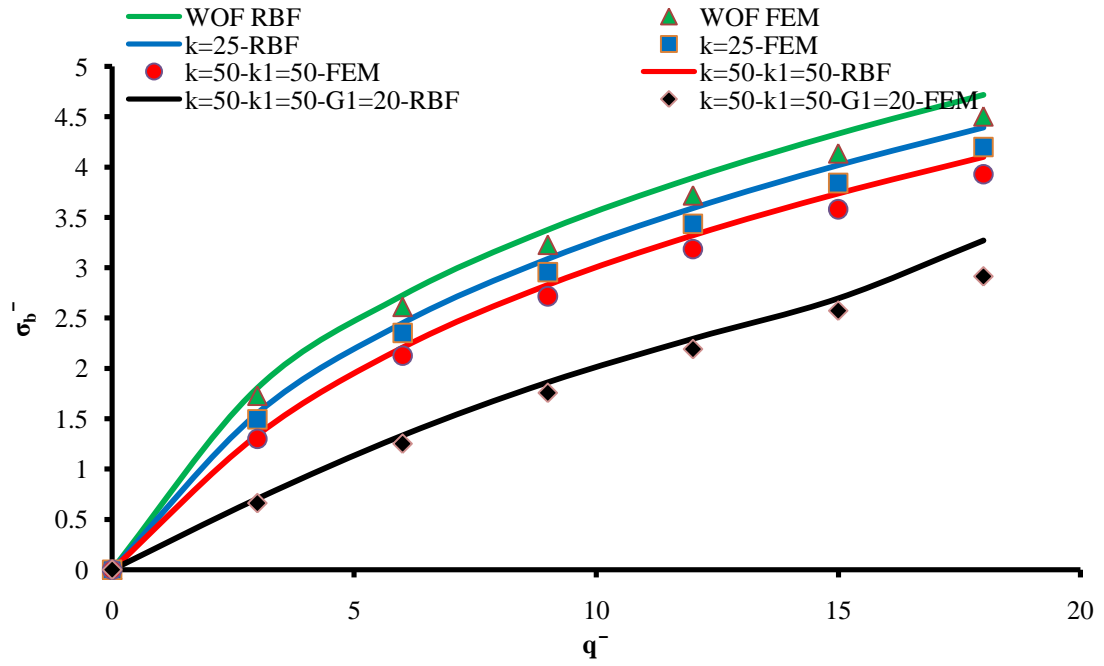


Figure 7.17  $\bar{\sigma}_b$  vs  $\bar{q}$  on Different Foundations for SQSFIM

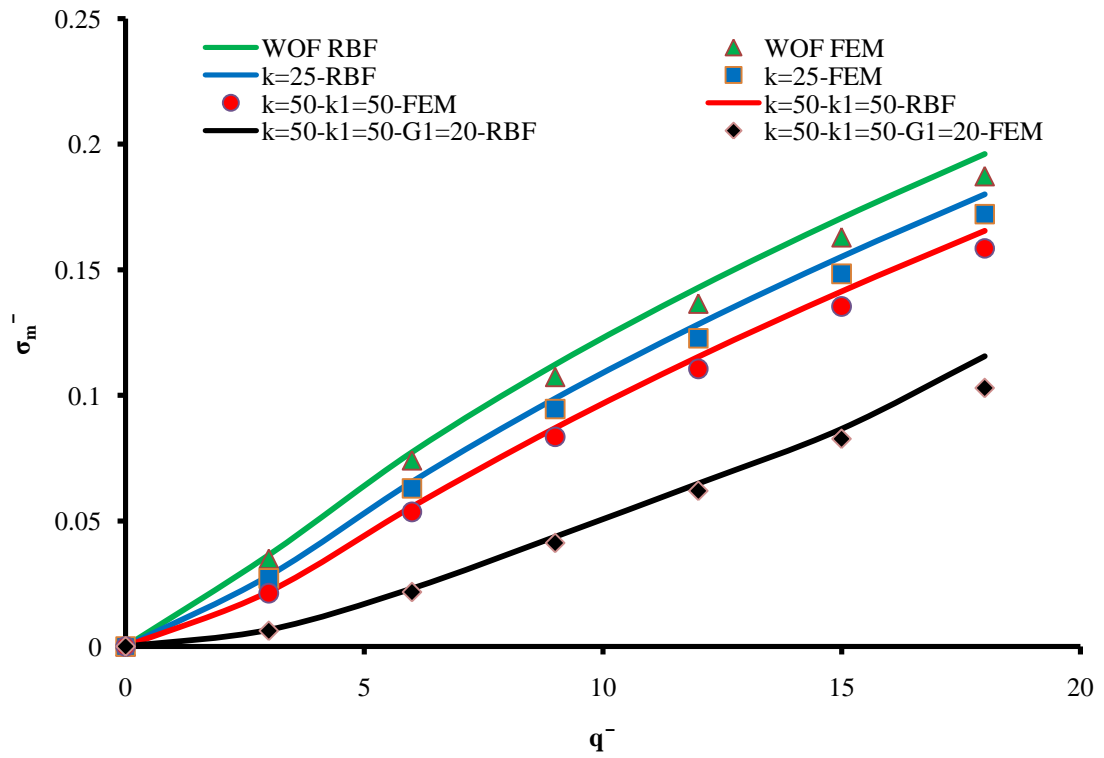


Figure 7.18  $\bar{\sigma}_m$  vs  $\bar{q}$  on Different Foundations for SQSFIM

## 7.2.2 WPF Movable Square Plates

- SQSSMO

This example is a simply supported square plate with movable edges, ( $w = M_n = F = \frac{\partial F}{\partial n} = 0$ ), resting on the Winkler-Pasternak foundation and subjected to uniformly distributed load  $\bar{q}$  ranging from 5 - 40. The selected results of some cases representing various foundation parameters are given in Table 7-7 and Figures 7.19, 7.20, and 7.21. In the shown Table 7-7, the RBF and FEM results with their percentage errors at the center of the plate for  $\bar{w}$ ,  $\bar{\sigma}_b$ , and  $\bar{\sigma}_m$  are presented only at load  $\bar{q} = 40$ . The results for  $\bar{q}$  versus  $\bar{w}$ ,  $\bar{\sigma}_b$ , and  $\bar{\sigma}_m$  at the center of the plate are provided in Figures 7.19, 7.20, and 7.21 respectively. All three figures show excellent agreement between RBF and FEM solutions. The RBF results compare very well with the FEM results with maximum relative differences of 1.8%, 1.6 % and 2.3% for  $\bar{w}$ ,  $\bar{\sigma}_b$  and  $\bar{\sigma}_m$  respectively.

Table 7.7 SQSSMO Results of  $\bar{w}$ ,  $\bar{\sigma}_b$ ,  $\bar{\sigma}_m$  at Load  $\bar{q} = 40$

Foundation Parameters			$\bar{w}$			$\bar{\sigma}_b$			$\bar{\sigma}_m$		
K	K1	G1	RBF	FEM	Error %	RBF	FEM	Error %	RBF	FEM	Error %
0	0	0	1.3619	1.3508	0.8163	7.7815	7.6551	1.6511	1.6611	1.6359	1.5383
200	0	0	1.0341	1.0312	0.2816	5.9414	5.8956	0.7771	0.9590	0.9586	0.0402
400	0	0	0.8044	0.8093	0.6027	4.5326	4.5575	0.5469	0.5896	0.5831	1.1188
200	200	0	0.9078	0.9073	0.0467	5.0130	4.9992	0.2777	0.7219	0.7252	0.4521
200	400	0	0.8347	0.8333	0.1720	4.4777	4.4571	0.4638	0.5978	0.6006	0.4683
400	200	0	0.7489	0.7488	0.0253	4.0960	4.0876	0.2060	0.4880	0.4894	0.2819
400	400	0	0.7038	0.7060	0.3151	3.7456	3.7553	0.2584	0.4287	0.4281	0.1468
0	0	10	1.0404	1.0373	0.2992	6.0838	6.0361	0.7914	0.9827	0.9822	0.0508
200	0	10	0.8095	0.8145	0.6146	4.6535	4.6798	0.5616	0.6059	0.5989	1.1756
400	0	10	0.6607	0.6604	0.0545	3.7046	3.6975	0.1931	0.3846	0.3856	0.2797
0	0	20	0.8185	0.8195	0.1196	4.7874	4.7878	0.0097	0.6127	0.6134	0.1125

200	0	20	0.6638	0.6646	0.1208	3.7934	3.7948	0.0369	0.3959	0.3959	0.0158
400	0	20	0.5537	0.5544	0.1348	3.0708	3.0732	0.0785	0.2693	0.2692	0.0296
200	200	10	0.7537	0.7535	0.0219	4.2163	4.2084	0.1869	0.5018	0.5032	0.2826
200	200	20	0.6319	0.6334	0.2369	3.5369	3.5435	0.1884	0.3553	0.3548	0.1233
200	400	10	0.7238	0.7104	1.8874	3.9810	3.8753	2.7266	0.4305	0.4407	2.2933
200	400	20	0.6089	0.6086	0.0428	3.3506	3.3447	0.1767	0.3233	0.3239	0.1909
400	200	10	0.6261	0.6294	0.5289	3.4274	3.4469	0.5665	0.3469	0.3454	0.4438
400	200	20	0.5357	0.5376	0.3613	2.9224	2.9335	0.3791	0.2512	0.2506	0.2353
400	400	10	0.6086	0.6049	0.6188	3.2800	3.2483	0.9744	0.3126	0.3151	0.7857
400	400	20	0.5255	0.5233	0.4282	2.8331	2.8142	0.6722	0.2340	0.2352	0.4879

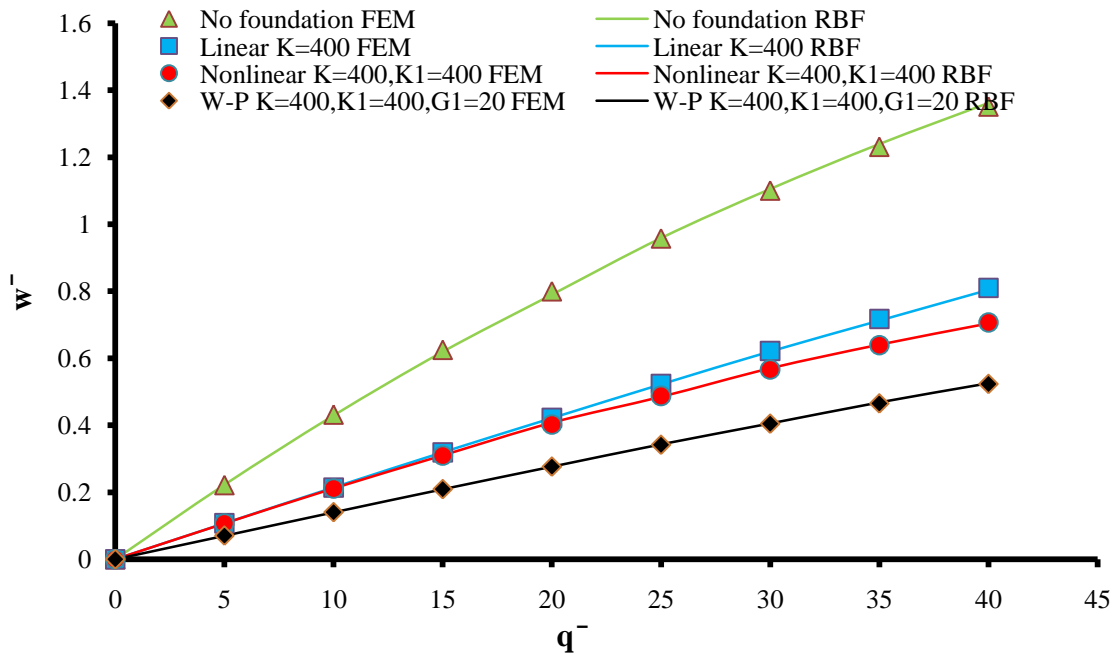


Figure 7.19  $\bar{w}$  vs  $\bar{q}$  on Different Foundations for SQSSMO

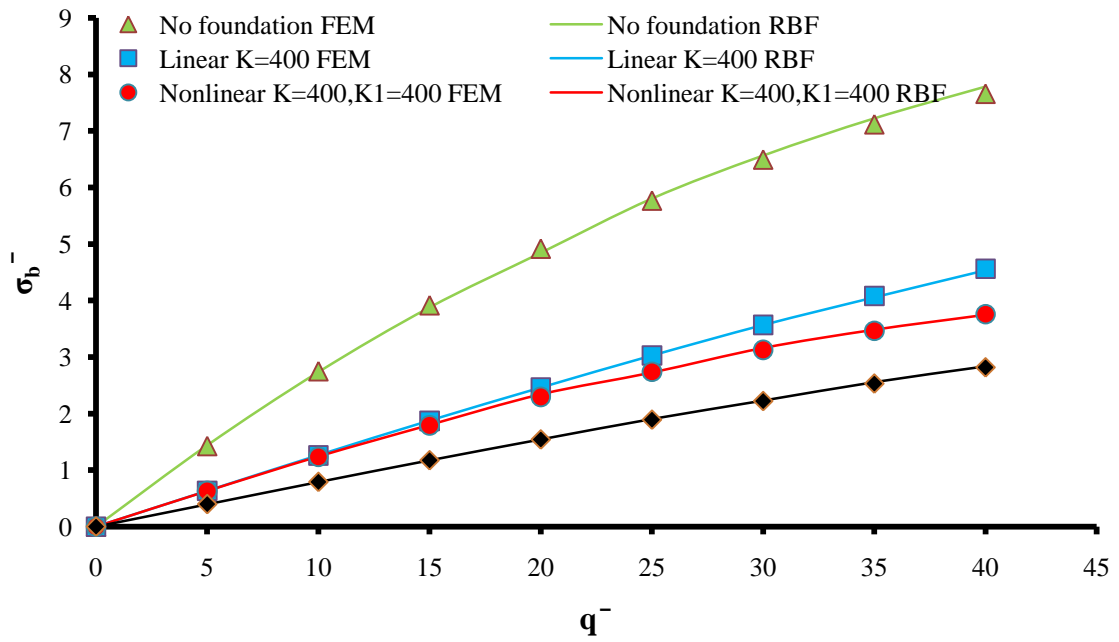


Figure 7.20  $\bar{\sigma}_b$  vs  $\bar{q}$  on Different Foundations for SQSSMO

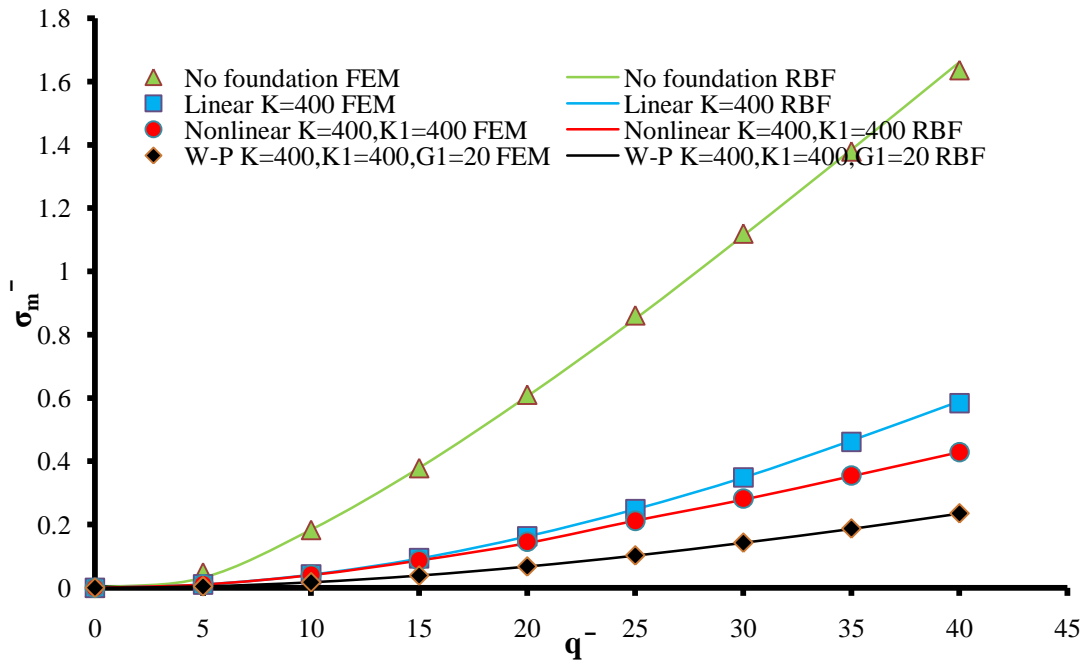


Figure 7.21  $\bar{\sigma}_m$  vs  $\bar{q}$  on Different Foundations for SQSSMO



- SQCCMO

In this example, a clamped supported square plate with movable edges, ( $w = \frac{\partial w}{\partial n} = F = \frac{\partial F}{\partial n} = 0$ ) resting on the Winkler-Pasternak foundation is considered. The plate is subjected to uniformly distributed load  $\bar{q}$  ranging from 20 -160. The selected results of some cases representing various foundation parameters are given in Table 7-8 and Figures 7.22, 7.23, and 7.24. In the shown Table 7-8, the RBF and FEM results with their percentage errors at the center of the plate for  $\bar{w}$ ,  $\bar{\sigma}_b$ , and  $\bar{\sigma}_m$  are presented only at load  $\bar{q} = 160$ . The results for  $\bar{q}$  versus  $\bar{w}$ ,  $\bar{\sigma}_b$ , and  $\bar{\sigma}_m$  at the center of the plate are provided in Figures 7.22, 7.23, and 7.24 respectively. All three figures show a good agreement between RBF and FEM solutions. The RBF results compare very well with the FEM results with maximum relative differences of 3.7%, 4.5 % and 4% for  $\bar{w}$ ,  $\bar{\sigma}_b$  and  $\bar{\sigma}_m$  respectively.

Table 7.8 SQCCMO Results of  $\bar{w}$ ,  $\bar{\sigma}_b$ ,  $\bar{\sigma}_m$  at Load  $\bar{q} = 160$

Foundation Parameters			$\bar{w}$			$\bar{\sigma}_b$			$\bar{\sigma}_m$		
K	K1	G1	FEM	RBF	Error %	FEM	RBF	Error %	FEM	RBF	Error %
0	0	0	1.602	1.573	1.818	13.039	12.740	2.297	3.692	3.655	1.014
0	0	25	1.281	1.283	0.113	10.398	10.549	1.452	2.328	2.333	0.215
0	0	50	1.040	1.033	0.677	8.237	8.252	0.182	1.492	1.475	1.108
0	500	0	1.300	1.296	0.290	9.834	9.942	1.098	2.341	2.337	0.136
0	500	25	1.108	1.114	0.549	8.426	8.639	2.527	1.679	1.643	2.143
0	500	50	0.944	0.939	0.550	7.101	7.155	0.756	1.194	1.188	0.507
0	1000	0	1.152	1.145	0.599	8.202	8.288	1.051	1.781	1.788	0.412
0	1000	25	1.008	1.016	0.768	7.281	7.532	3.434	1.353	1.333	1.475
0	1000	50	0.880	0.878	0.229	6.349	6.454	1.662	1.014	1.008	0.546
500	0	0	1.317	1.327	0.758	10.793	11.056	2.440	2.496	2.482	0.552
500	0	25	1.064	1.060	0.415	8.504	8.539	0.408	1.584	1.568	1.018
500	0	50	0.880	0.882	0.263	6.778	6.901	1.821	1.044	1.020	2.329

500	500	0	1.130	1.129	0.090	8.615	8.729	1.328	1.766	1.757	0.500
500	500	25	0.961	0.955	0.628	7.244	7.281	0.523	1.249	1.251	0.137
500	500	50	0.822	0.820	0.271	6.065	6.145	1.320	0.890	0.884	0.712
500	1000	0	1.024	1.017	0.710	7.368	7.423	0.750	1.407	1.415	0.584
500	1000	25	0.893	0.900	0.766	6.420	6.637	3.368	1.051	1.037	1.392
500	1000	50	0.779	0.780	0.127	5.543	5.673	2.351	0.784	0.778	0.836
1000	0	0	1.092	1.098	0.515	8.823	8.986	1.844	1.694	1.651	2.522
1000	0	25	0.898	0.895	0.282	6.966	7.021	0.789	1.102	1.094	0.712
1000	0	50	0.756	0.751	0.689	5.624	5.651	0.471	0.752	0.750	0.234
1000	500	0	0.979	0.974	0.542	7.410	7.456	0.614	1.313	1.319	0.390
1000	500	25	0.836	0.832	0.386	6.171	6.235	1.042	0.928	0.927	0.130
1000	500	50	0.721	0.719	0.266	5.172	5.248	1.486	0.670	0.667	0.489
1000	1000	0	0.907	0.903	0.453	6.502	6.580	1.202	1.094	1.097	0.293
1000	1000	25	0.790	0.761	3.687	5.597	5.347	4.466	0.812	0.844	3.920
1000	1000	50	0.693	0.683	1.308	4.813	4.808	0.120	0.608	0.613	0.821

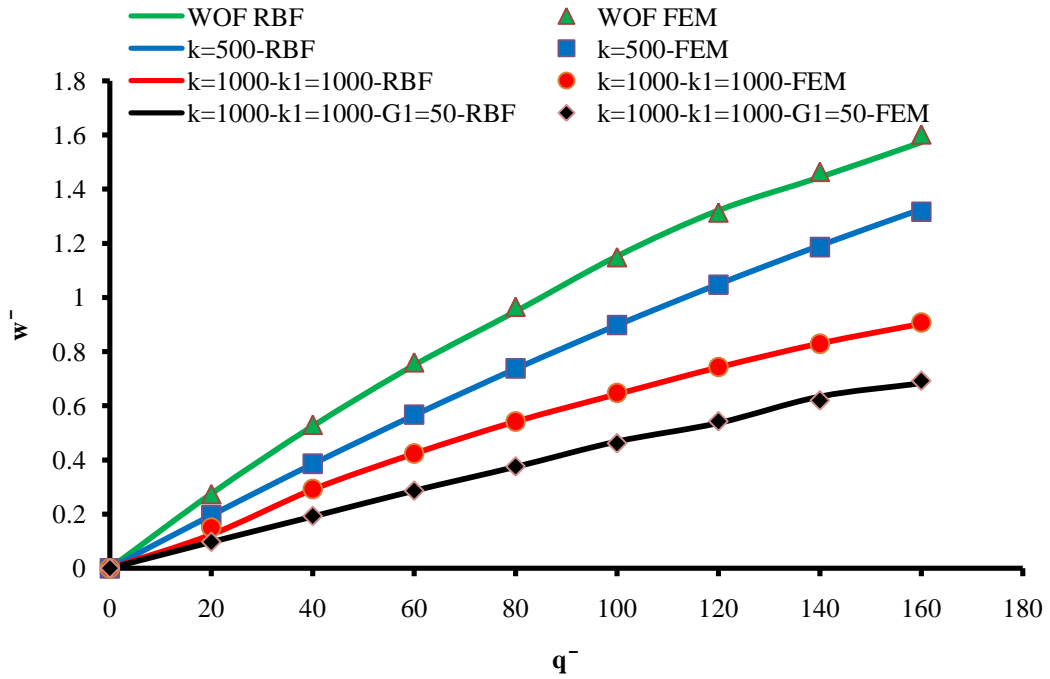


Figure 7.22  $\bar{w}$  vs  $\bar{q}$  on Different Foundations for SQCCMO

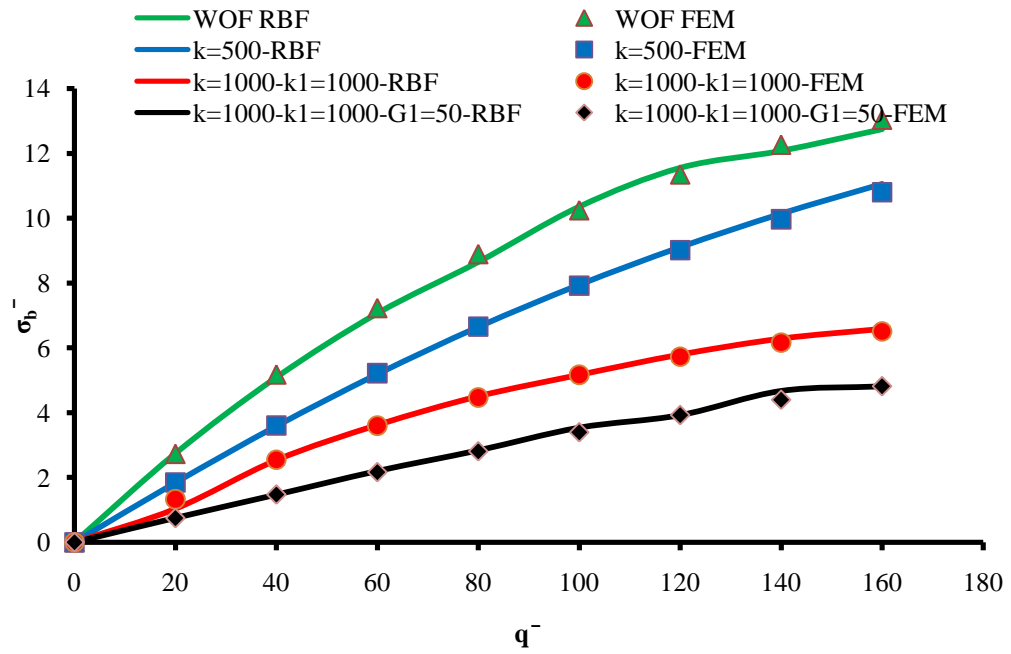


Figure 7.23  $\bar{\sigma}_b$  vs  $\bar{q}$  on Different Foundations for SQCCMO

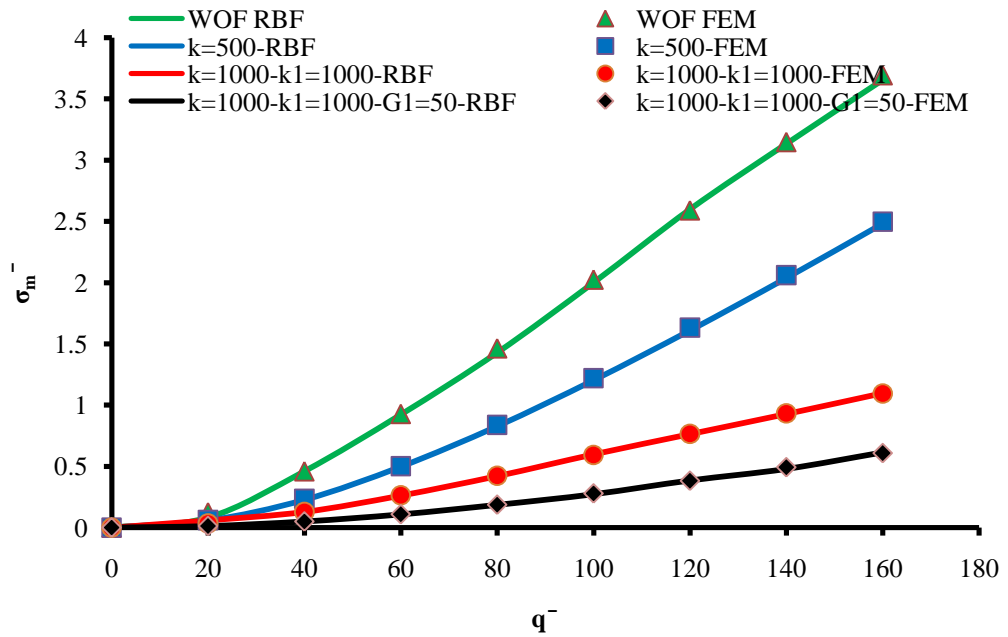


Figure 7.24  $\bar{\sigma}_m$  vs  $\bar{q}$  on Different Foundations for SQCCMO

- SQSF1MO

The plate is a simple free at on edge supported square plate with movable edges, ( $w = (V_n \text{ and } M_n \text{ at free} = M_n \text{ at simple}) = F = \frac{\partial F}{\partial n} = 0$ ) resting on the Winkler-Pasternak foundation in this example. It is subjected to uniformly distributed load  $\bar{q}$  ranging from 1.5-12. The selected results of some cases representing various foundation parameters are given in Table 7-9 and Figures 7.25, and 7.26. In the shown Table 7-9, the RBF and FEM results with their percentage errors at the free edge of the plate for  $\bar{w}$ ,  $\bar{\sigma}_b$ , and  $\bar{\sigma}_m$  are presented only at load  $\bar{q} = 12$ . The results for  $\bar{q}$  versus  $\bar{w}$ , and  $\bar{\sigma}_b$  at the free edge of the plate are provided in Figures 7.25 and 7.26 respectively. Both two figures show a good agreement between RBF and FEM solutions. The RBF results compare very well with the FEM results with maximum relative differences of 3.4%, 3.4% and 3.6% for  $\bar{w}$ ,  $\bar{\sigma}_b$  and  $\bar{\sigma}_m$  respectively.

Table 7.9 SQSF1MO Results of  $\bar{w}$ ,  $\bar{\sigma}_b$ ,  $\bar{\sigma}_m$  at Load  $\bar{q} = 12$

Foundation Parameters			$\bar{w}$			$\bar{\sigma}_b$			$\bar{\sigma}_m$		
K	K1	G1	RBF	FEM	Error %	RBF	FEM	Error %	RBF	FEM	Error %
0	0	0	1.688	1.667	1.255	0.0345	0.0349	1.2714	0.0124	0.0126	1.4739
0	0	10	0.966	0.956	1.010	0.0187	0.0189	1.0200	0.0039	0.0039	1.2221
0	0	20	0.674	0.662	1.710	0.0123	0.0125	1.7400	0.0018	0.0019	1.9435
0	20	0	1.443	1.442	0.013	0.0213	0.0213	0.0133	0.0080	0.0080	0.2134
0	20	10	0.924	0.915	0.939	0.0156	0.0158	0.9476	0.0033	0.0034	1.1495
0	20	20	0.662	0.652	1.489	0.0113	0.0115	1.5116	0.0017	0.0017	1.7146
0	40	0	1.310	1.290	1.550	0.0142	0.0144	1.5744	0.0060	0.0061	1.7775
0	40	10	0.891	0.887	0.423	0.0131	0.0132	0.4247	0.0030	0.0030	0.6255
0	40	20	0.651	0.648	0.583	0.0104	0.0104	0.5863	0.0016	0.0016	0.7875
20	0	0	1.461	1.450	0.729	0.0279	0.0281	0.7342	0.0089	0.0090	0.9356
20	0	10	0.882	0.853	3.285	0.0156	0.0161	3.3966	0.0031	0.0032	3.6034
20	0	20	0.630	0.622	1.298	0.0105	0.0107	1.3154	0.0015	0.0016	1.5180
20	20	0	1.300	1.302	0.168	0.0184	0.0184	0.1677	0.0063	0.0063	0.0319
20	20	10	0.852	0.847	0.531	0.0133	0.0133	0.5340	0.0027	0.0028	0.7351

20	20	20	0.621	0.642	3.360	0.0097	0.0094	3.2509	0.0015	0.0014	3.0574
20	40	0	1.201	1.181	1.659	0.0127	0.0129	1.6866	0.0049	0.0050	1.8900
20	40	10	0.826	0.824	0.238	0.0113	0.0113	0.2387	0.0024	0.0025	0.4391
20	40	20	0.613	0.607	0.888	0.0090	0.0090	0.8958	0.0014	0.0014	1.0976
40	0	0	1.284	1.281	0.240	0.0224	0.0224	0.2401	0.0066	0.0066	0.4406
40	0	10	0.811	0.806	0.603	0.0130	0.0130	0.6062	0.0025	0.0025	0.8074
40	0	20	0.592	0.587	0.883	0.0089	0.0090	0.8907	0.0013	0.0013	1.0924
40	20	0	1.176	1.179	0.259	0.0156	0.0156	0.2582	0.0050	0.0050	0.0587
40	20	10	0.788	0.786	0.327	0.0112	0.0112	0.3285	0.0023	0.0023	0.5291
40	20	20	0.585	0.579	0.886	0.0083	0.0084	0.8936	0.0012	0.0013	1.0954
40	40	0	1.103	1.083	1.774	0.0111	0.0113	1.8058	0.0040	0.0041	2.0094
40	40	10	0.769	0.772	0.482	0.0096	0.0096	0.4797	0.0021	0.0021	0.2807
40	40	20	0.578	0.566	2.122	0.0077	0.0078	2.1676	0.0012	0.0012	2.3719

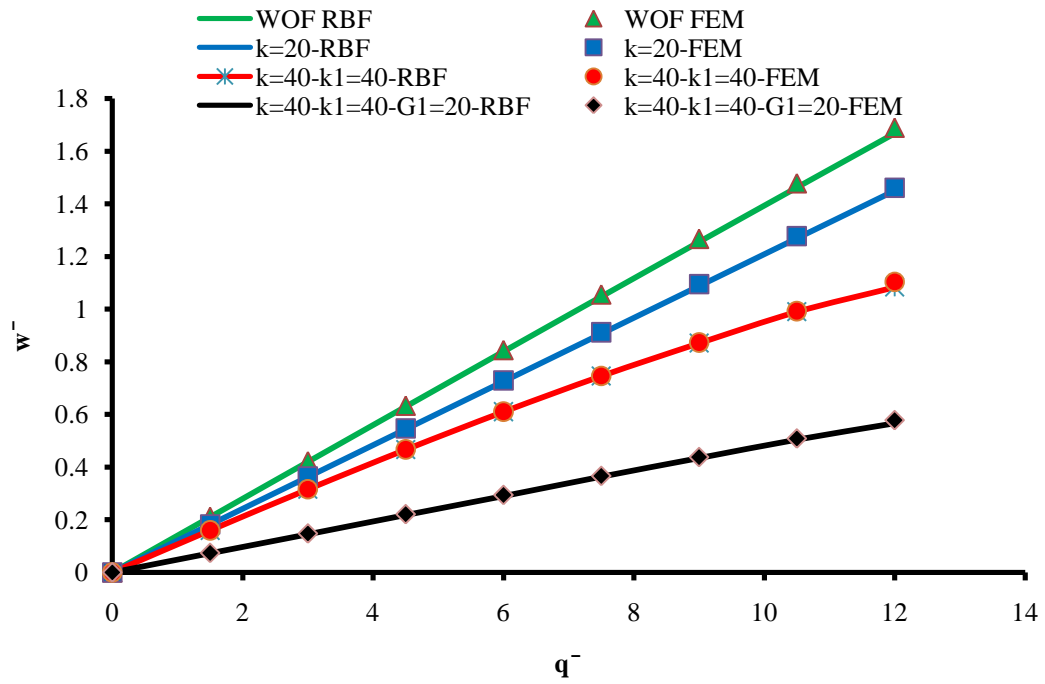


Figure 7.25  $\bar{w}$  vs  $\bar{q}$  on Different Foundations for SQSF1MO

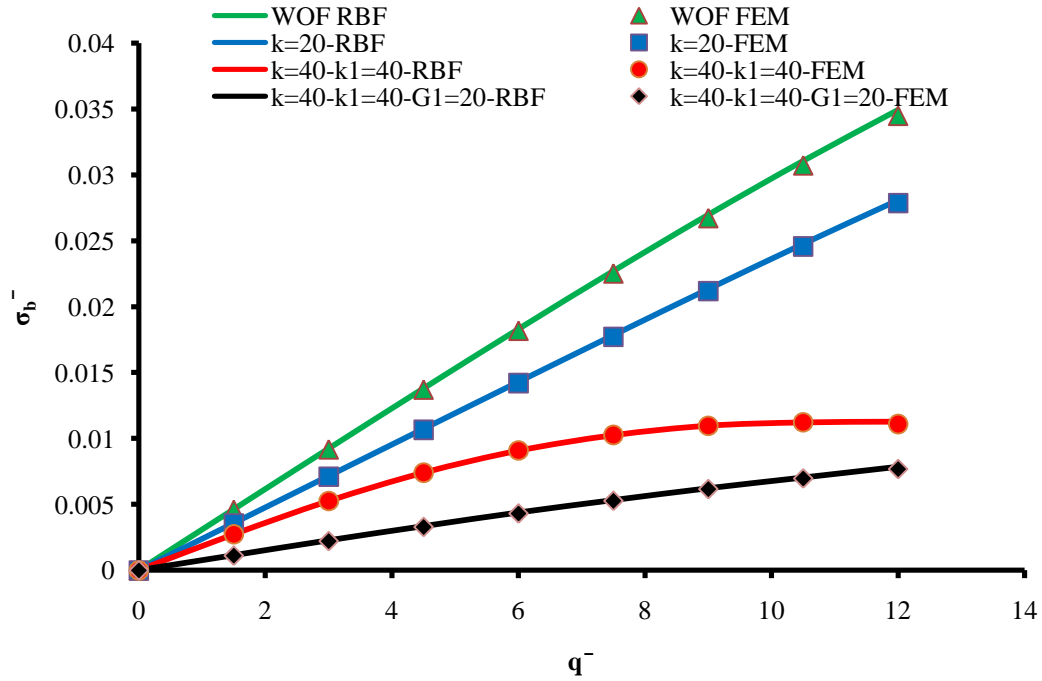


Figure 7.26  $\bar{\sigma}_b$  vs  $\bar{q}$  on Different Foundations for SQSF1MO

- SQCF1MO

A clamped free at one edge supported square plate with movable edges, ( $w = (V_n \text{ and } M_n \text{ at free}) = F = \frac{\partial F}{\partial n} = 0$ ) resting on the Winkler-Pasternak foundation is presented in this example. It is subjected to uniformly distributed load  $\bar{q}$  ranging from 5-40. The selected results of some cases representing various foundation parameters are given in Table 7-10 and Figures 7.27, 7.28, and 7.29. In Table 7-10, the RBF and FEM results with their percentage errors at the free edge of the plate for  $\bar{w}$ ,  $\bar{\sigma}_b$ , and  $\bar{\sigma}_m$  are presented only at load  $\bar{q} = 40$ . The results for  $\bar{q}$  versus  $\bar{w}$ ,  $\bar{\sigma}_b$ , and  $\bar{\sigma}_m$  at the free edge of the plate are provided in Figures 7.27, 7.28, and 7.29 respectively. All three figures show a good agreement between RBF and FEM solutions. The RBF results compare very

well with the FEM results with maximum relative differences of 5.7%, 6 % and 6.3% for  $\bar{w}$ ,  $\bar{\sigma}_b$  and  $\bar{\sigma}_m$  respectively.

Table 7.10 SQCF1MO Results of  $\bar{w}$ ,  $\bar{\sigma}_b$ ,  $\bar{\sigma}_m$  at Load  $\bar{q} = 40$

Foundation Parameters			$\bar{w}$			$\bar{\sigma}_b$			$\bar{\sigma}_m$		
K	K1	G1	RBF	FEM	Error %	RBF	FEM	Error %	RBF	FEM	Error %
0	0	0	1.302	1.282	1.543	0.129	0.133	3.100	0.0194	0.0201	3.6083
0	0	10	1.062	1.042	1.888	0.095	0.098	3.1578	0.0121	0.0126	4.1322
0	0	20	0.898	0.885	1.475	0.074	0.077	4.054	0.0082	0.0086	4.878
0	200	0	1.036	0.997	3.816	0.075	0.078	3.968	0.0096	0.0100	4.1758
0	200	10	0.910	0.872	4.230	0.064	0.066	4.417	0.0074	0.0077	4.6255
0	200	20	0.806	0.767	4.867	0.054	0.057	5.116	0.0057	0.0061	5.3258
0	400	0	0.916	0.876	4.371	0.053	0.055	4.571	0.0062	0.0065	4.7801
0	400	10	0.827	0.786	4.925	0.047	0.050	5.180	0.0053	0.0055	5.3901
0	400	20	0.748	0.719	3.875	0.043	0.044	4.031	0.0044	0.0046	4.2392
200	0	0	0.928	0.884	4.773	0.077	0.081	5.012	0.0084	0.0088	5.2218
200	0	10	0.795	0.759	4.530	0.060	0.063	4.745	0.0058	0.0061	4.9542
200	0	20	0.697	0.664	4.816	0.048	0.051	5.060	0.0043	0.0045	5.2703
200	200	0	0.824	0.796	3.412	0.055	0.057	3.533	0.0055	0.0057	3.7397
200	200	10	0.731	0.692	5.382	0.046	0.048	5.688	0.0043	0.0045	5.8996
200	200	20	0.656	0.631	3.867	0.039	0.041	4.022	0.0034	0.0035	4.2303
200	400	0	0.760	0.739	2.687	0.042	0.043	2.762	0.0040	0.0041	2.9671
200	400	10	0.687	0.669	2.634	0.037	0.038	2.706	0.0033	0.0034	2.9110
200	400	20	0.625	0.608	2.734	0.032	0.033	2.811	0.0028	0.0029	3.0170
400	0	0	0.713	0.689	3.363	0.048	0.050	3.480	0.0041	0.0042	3.6869
400	0	10	0.630	0.594	5.718	0.039	0.041	6.065	0.0031	0.0032	6.2771
400	0	20	0.566	0.550	2.985	0.032	0.033	3.077	0.0024	0.0025	3.2833
400	200	0	0.667	0.635	4.823	0.038	0.040	5.067	0.0031	0.0033	5.2775
400	200	10	0.600	0.586	2.407	0.032	0.033	2.467	0.0025	0.0026	2.6715
400	200	20	0.546	0.538	1.553	0.027	0.028	1.578	0.0020	0.0021	1.7809
400	400	0	0.633	0.622	1.738	0.031	0.032	1.768	0.0024	0.0025	1.9718
400	400	10	0.577	0.571	1.043	0.027	0.027	1.054	0.0021	0.0021	1.2558
400	400	20	0.529	0.522	1.275	0.024	0.024	1.292	0.0018	0.0018	1.4942

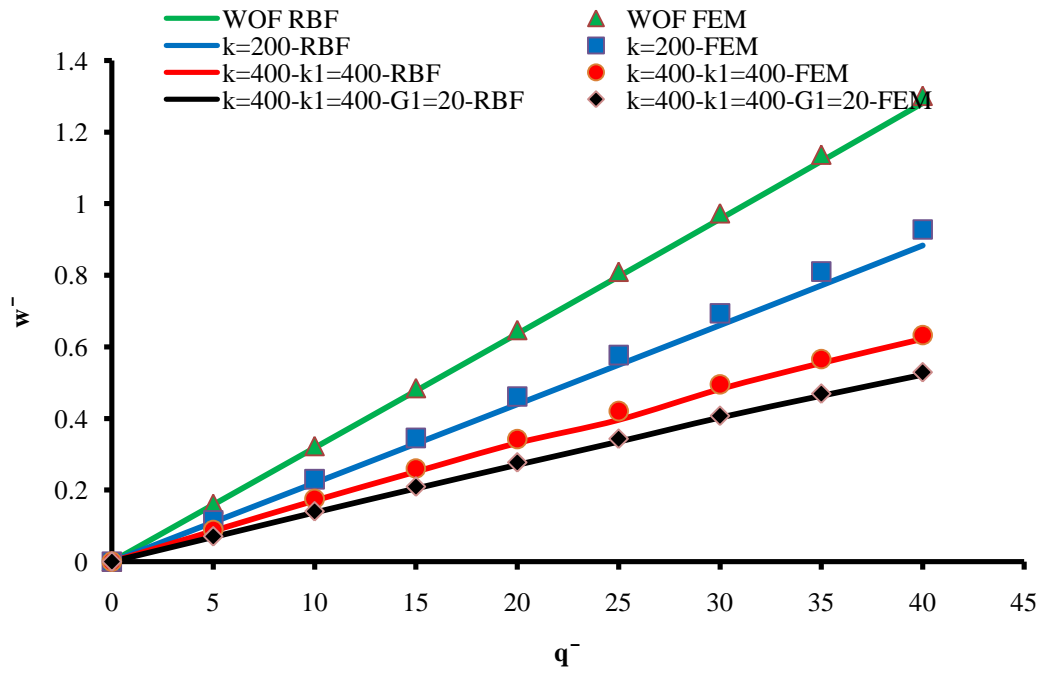


Figure 7.27  $\bar{w}$  vs  $\bar{q}$  on Different Foundations for SQCF1MO

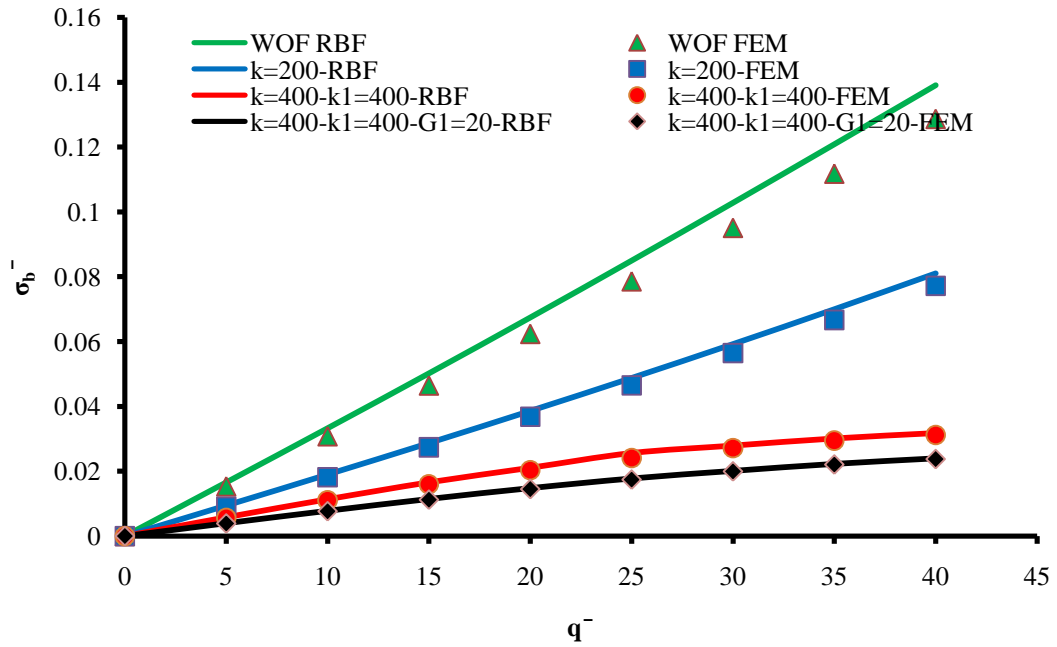


Figure 7.28  $\bar{\sigma}_b$  vs  $\bar{q}$  on Different Foundations for SQCF1MO



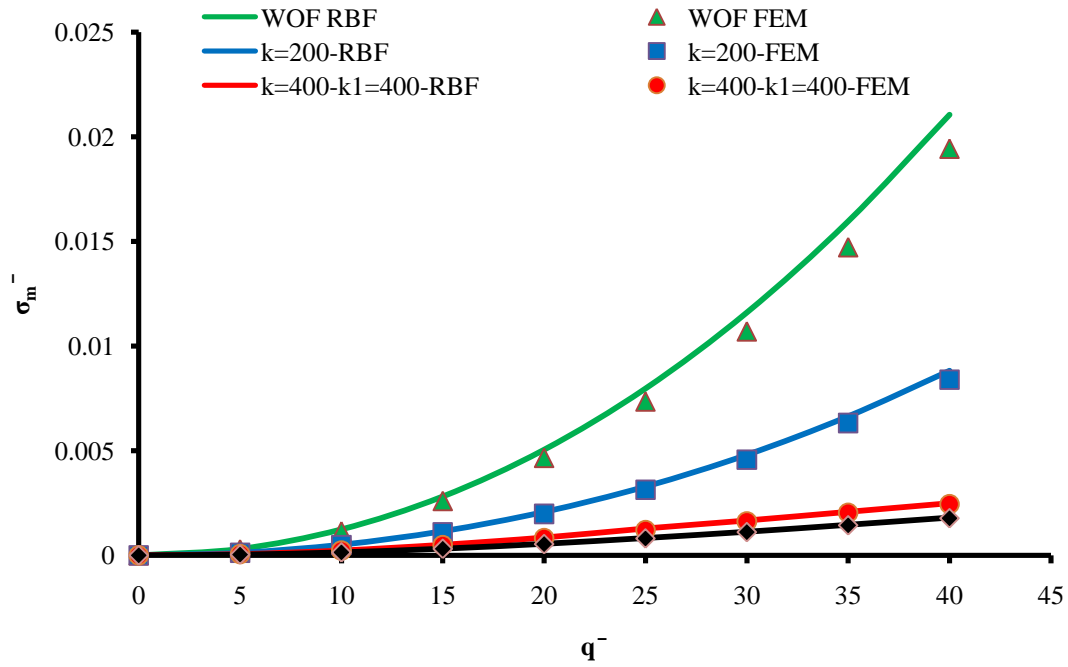


Figure 7.29  $\bar{\sigma}_m$  vs  $\bar{q}$  on Different Foundations for SQCF1MO

- SQSFMO

In this example, the plate is a simple free at two edges supported square plate with movable edges, ( $w = (V_n \text{ and } M_n \text{ at free} = M_n \text{ at simple}) = F = \frac{\partial F}{\partial n} = 0$ ) resting on the Winkler-Pasternak foundation. It is subjected to uniformly distributed load  $\bar{q}$  ranging from 1.5-12. The selected results of some cases representing various foundation parameters are given in Table 7-11 and Figures 7.30, and 7.31. In the shown Table 7-11, the RBF and FEM results with their percentage errors at the free edge of the plate for  $\bar{w}$ ,  $\bar{\sigma}_b$ , and  $\bar{\sigma}_m$  are presented only at load  $\bar{q} = 12$ . The results for  $\bar{q}$  versus  $\bar{w}$ , and  $\bar{\sigma}_b$  at the free edge of the plate are provided in Figures 7.30, and 7.31 respectively. Both two figures show a reasonable agreement between RBF and FEM solutions. The RBF results

compare very well with the FEM results with maximum relative differences of 4.6%, 4.6% and 6.5% for  $\bar{w}$ ,  $\bar{\sigma}_b$  and  $\bar{\sigma}_m$  respectively.

Table 7.11 SQSFMO Results of  $\bar{w}$ ,  $\bar{\sigma}_b$ ,  $\bar{\sigma}_m$  at Load  $\bar{q} = 12$

Foundation Parameters			$\bar{w}$			$\bar{\sigma}_b$			$\bar{\sigma}_m$		
K	K1	G1	FEM	RBF	Error	FEM	RBF	Error	FEM	RBF	Error
0	0	0	1.871	1.800	3.795	8.926	8.559	4.112	1.177	1.138	3.314
0	0	10	1.017	0.975	4.129	4.783	4.565	4.558	0.428	0.447	4.439
0	0	20	0.701	0.684	2.355	3.248	3.203	1.397	0.215	0.225	4.406
0	20	0	1.457	1.392	4.4612	6.830	6.617	3.119	0.761	0.800	5.093
0	20	10	0.954	0.932	2.277	4.453	4.376	1.728	0.375	0.394	4.853
0	20	20	0.685	0.666	2.678	3.160	3.108	1.673	0.204	0.215	5.142
0	40	0	1.292	1.241	3.977	5.992	5.784	3.468	0.608	0.632	3.947
0	40	10	0.908	0.885	2.480	4.211	4.132	1.887	0.339	0.357	5.310
0	40	20	0.670	0.651	2.832	3.083	3.028	1.779	0.195	0.206	5.507
20	0	0	1.558	1.494	4.1078	7.404	7.143	3.525	0.871	0.864	0.770
20	0	10	0.916	0.887	3.149	4.286	4.172	2.658	0.350	0.370	5.849
20	0	20	0.650	0.642	1.335	2.999	2.995	0.148	0.185	0.191	3.391
20	20	0	1.308	1.255	4.050	6.125	5.855	4.408	0.631	0.668	5.864
20	20	10	0.872	0.847	2.898	4.055	3.960	2.321	0.315	0.328	4.127
20	20	20	0.638	0.613	3.918	2.932	2.701	7.864	0.177	0.186	5.085
20	40	0	1.185	1.152	2.734	5.493	5.372	2.196	0.522	0.555	6.434
20	40	10	0.838	0.854	1.893	3.874	3.986	2.884	0.290	0.292	0.925
20	40	20	0.627	0.609	2.816	2.872	2.825	1.611	0.170	0.179	5.292
40	0	0	1.334	1.295	2.924	6.308	6.103	3.250	0.664	0.673	1.322
40	0	10	0.832	0.817	1.866	3.874	3.828	1.203	0.290	0.304	5.106
40	0	20	0.606	0.596	1.712	2.782	2.772	0.372	0.160	0.166	3.746
40	20	0	1.177	1.123	4.618	5.499	5.264	4.271	0.522	0.544	4.215
40	20	10	0.801	0.783	2.255	3.709	3.652	1.539	0.267	0.285	6.660
40	20	20	0.597	0.590	1.233	2.730	2.736	0.202	0.155	0.160	3.450
40	40	0	1.086	1.062	2.249	5.029	4.943	1.719	0.445	0.466	4.719
40	40	10	0.776	0.762	1.777	3.573	3.539	0.965	0.249	0.265	6.535
40	40	20	0.588	0.577	1.862	2.683	2.671	0.421	0.149	0.156	4.128

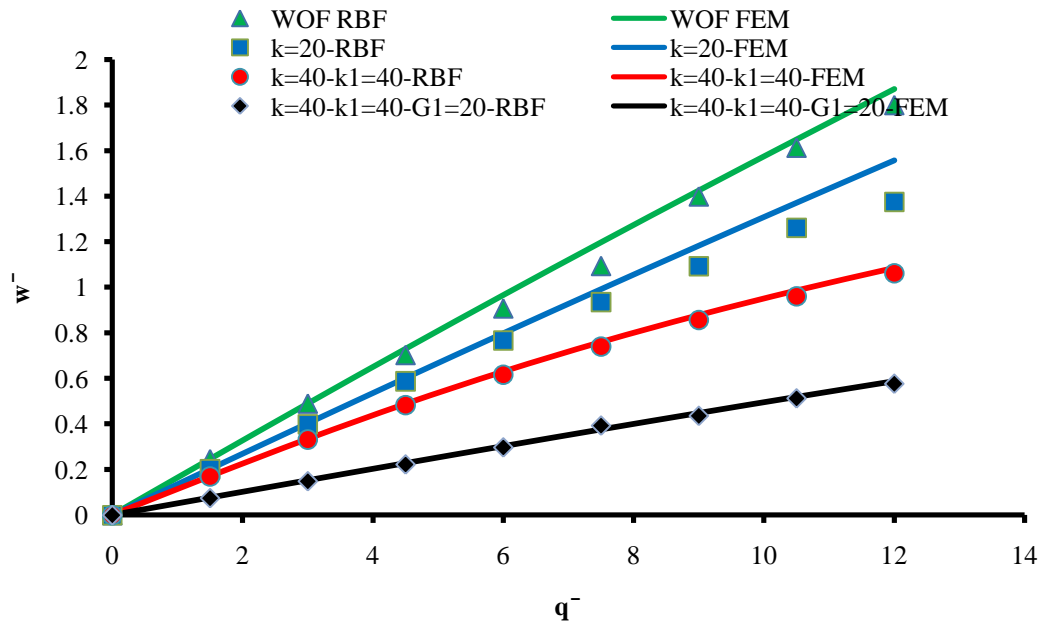


Figure 7.30  $\bar{w}$  vs  $\bar{q}$  on Different Foundations for SQSFMO

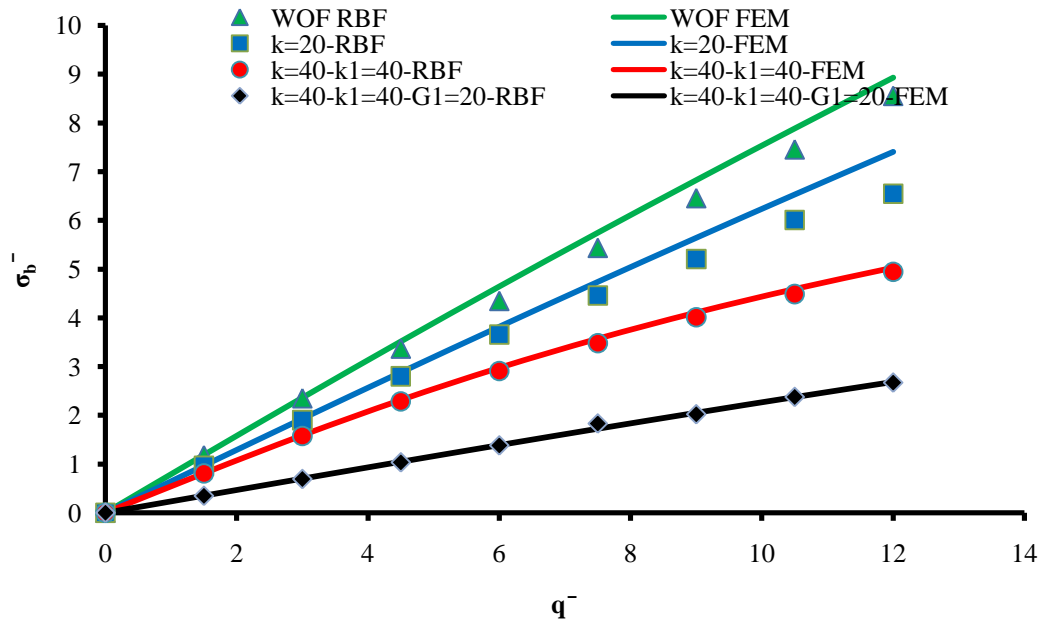


Figure 7.31  $\bar{\sigma}_b$  vs  $\bar{q}$  on Different Foundations for SQSFMO

- SQCFMO

The plate in this example is a clamped free at two edges supported square plate with movable edges, ( $w = (V_n \text{ and } M_n \text{ at free}) = F = \frac{\partial F}{\partial n} = 0$ ) resting on the Winkler-Pasternak foundation. It is subjected to uniformly distributed load  $\bar{q}$  ranging from 5-40. The selected results of some cases representing various foundation parameters are given in Table 7-12 and Figures 7.32, 7.33, and 7.34. In the shown Table 7-12, the RBF and FEM results with their percentage errors at the free edge of the plate for  $\bar{w}$ ,  $\bar{\sigma}_b$  and  $\bar{\sigma}_m$  are presented only at load  $\bar{q} = 40$ . The results for  $\bar{q}$  versus  $\bar{w}$ ,  $\bar{\sigma}_b$ , and  $\bar{\sigma}_m$  at the free edge of the plate are provided in Figures 7.32, 7.33, and 7.34 respectively. All three figures show a reasonable agreement between RBF and FEM solutions. The RBF results compare very well with the FEM results with maximum relative differences of 8%, less than 8 % and 8% for  $\bar{w}$ ,  $\bar{\sigma}_b$  and  $\bar{\sigma}_m$  respectively.

Table 7.12 SQCFMO Results of  $\bar{w}$ ,  $\bar{\sigma}_b$ ,  $\bar{\sigma}_m$  at Load  $\bar{q} = 40$

Foundation Parameters			$\bar{w}$			$\bar{\sigma}_b$			$\bar{\sigma}_m$		
K	K1	G1	FEM	RBF	Error %	FEM	RBF	Error %	FEM	RBF	Error %
0	0	0	1.242	1.340	7.880	10.346	9.590	7.304	0.861	0.799	7.119
0	0	10	1.026	1.090	6.198	8.229	7.748	5.836	0.618	0.583	5.648
0	0	20	0.877	0.930	6.009	6.797	6.411	5.668	0.464	0.438	5.480
0	200	0	0.984	1.030	4.682	7.880	7.528	4.473	0.525	0.502	4.282
0	200	10	0.876	0.918	4.833	6.813	6.499	4.610	0.433	0.414	4.419
0	200	20	0.784	0.810	3.243	5.934	5.748	3.141	0.358	0.347	2.947
0	400	0	0.875	0.909	3.947	6.834	6.575	3.797	0.403	0.388	3.605
0	400	10	0.797	0.829	4.047	6.069	5.833	3.890	0.348	0.335	3.698
0	400	20	0.727	0.750	3.138	5.406	5.241	3.043	0.299	0.290	2.849
200	0	0	0.884	0.944	6.749	7.166	6.713	6.323	0.444	0.417	6.135
200	0	10	0.768	0.816	6.285	5.995	5.640	5.913	0.343	0.324	5.725
200	0	20	0.680	0.715	5.195	5.134	4.881	4.938	0.273	0.260	4.748
200	200	0	0.787	0.828	5.164	6.215	5.910	4.911	0.339	0.323	4.721
200	200	10	0.707	0.743	5.168	5.406	5.140	4.914	0.281	0.268	4.724
200	200	20	0.640	0.675	5.506	4.751	4.503	5.219	0.235	0.223	5.029

200	400	0	0.729	0.759	4.212	5.642	5.414	4.042	0.282	0.271	3.850
200	400	10	0.665	0.693	4.181	5.004	4.803	4.013	0.242	0.233	3.821
200	400	20	0.609	0.629	3.267	4.466	4.325	3.164	0.208	0.202	2.970
400	0	0	0.683	0.720	5.419	5.374	5.097	5.140	0.259	0.246	4.951
400	0	10	0.610	0.643	5.404	4.634	4.397	5.127	0.210	0.200	4.937
400	0	20	0.553	0.580	4.958	4.064	3.872	4.724	0.174	0.167	4.534
400	200	0	0.641	0.678	5.749	4.956	4.687	5.437	0.222	0.210	5.248
400	200	10	0.582	0.607	4.298	4.358	4.179	4.121	0.187	0.179	3.929
400	200	20	0.533	0.558	4.605	3.874	3.704	4.402	0.159	0.152	4.211
400	400	0	0.610	0.640	4.954	4.648	4.428	4.720	0.196	0.187	4.530
400	400	10	0.560	0.608	8.498	4.140	3.816	7.832	0.169	0.156	7.648
400	400	20	0.517	0.530	2.505	3.716	3.626	2.443	0.147	0.143	2.248

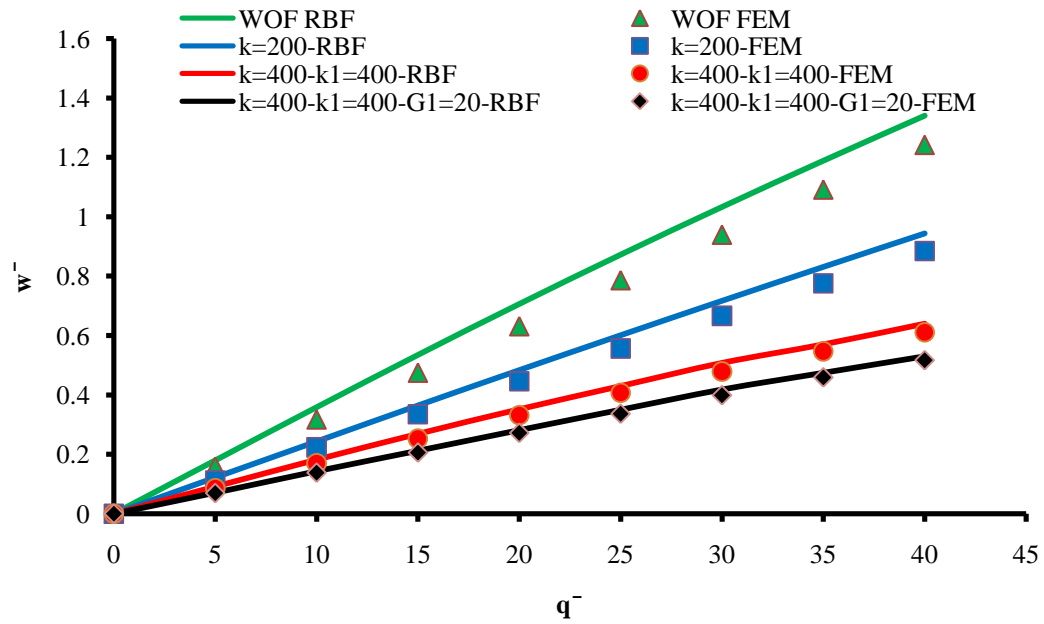


Figure 7.32  $\bar{w}$  vs  $\bar{q}$  on Different Foundations for SQCFMO

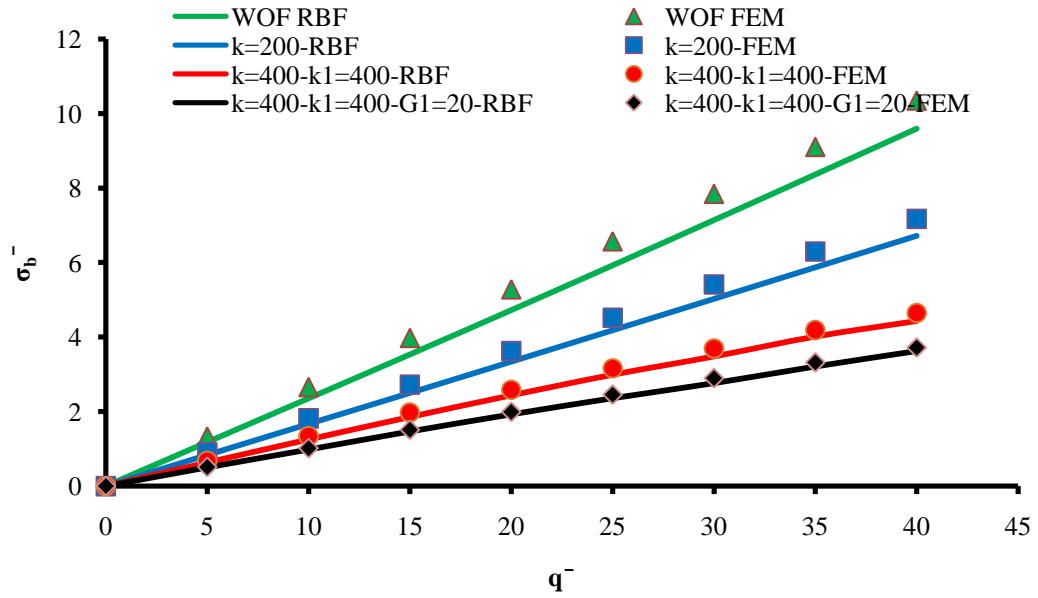


Figure 7.33  $\bar{\sigma}_b$  vs  $\bar{q}$  on Different Foundations for SQCFMO

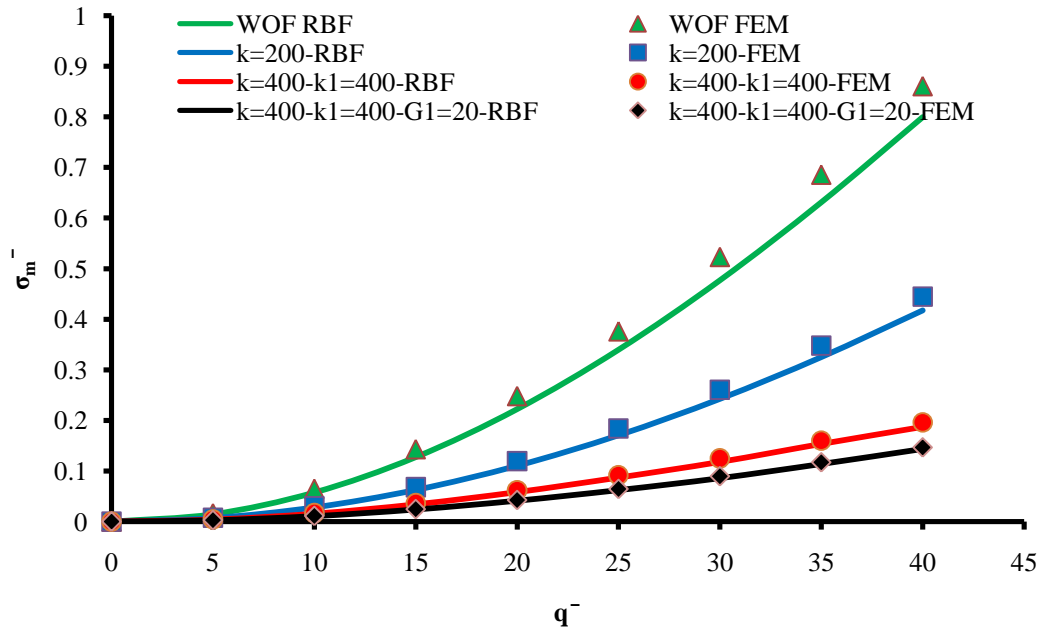


Figure 7.34  $\bar{\sigma}_m$  vs  $\bar{q}$  on Different Foundations for SQCFMO

### 7.2.3 WPF Immovable Circular Plates

- CICCIM

In this example, the plate is a clamped supported circular plate with immovable edges, ( $w = \frac{\partial w}{\partial n} = u = v = 0$ ) resting on the Winkler-Pasternak foundation. It is subjected to uniformly distributed load  $\bar{q}$  ranging from 2 -12. The selected results of some cases representing various foundation parameters are given in Table 7-13 and Figures 7.35, 7.36, and 7.37. In the shown Table 7-13, the RBF and FEM results with their percentage errors at the center of the plate for  $\bar{w}$ ,  $\bar{\sigma}_b$ , and  $\bar{\sigma}_m$  are presented only at load  $\bar{q} = 12$ . The results for  $\bar{q}$  versus  $\bar{w}$ ,  $\bar{\sigma}_b$ , and  $\bar{\sigma}_m$  at the center of the plate are provided in Figures 7.35, 7.36, and 7.37 respectively. All three figures show excellent agreement between RBF and FEM solutions. The RBF results compare very well with the FEM results with maximum relative differences of 1.4%, 2.8 % and 2.14% for  $\bar{w}$ ,  $\bar{\sigma}_b$  and  $\bar{\sigma}_m$  respectively.

Table 7.13 CICCIM Results of  $\bar{w}$ ,  $\bar{\sigma}_b$ ,  $\bar{\sigma}_m$  at Load  $\bar{q} = 12$

Foundation Parameters			$\bar{w}$			$\bar{\sigma}_b$			$\bar{\sigma}_m$		
K	K1	G1	RBF	FEM	Diff. %	RBF	FEM	Diff. %	RBF	FEM	Diff. %
0	0	0	1.1650	1.1627	0.2001	2.7976	2.7530	1.6220	1.3060	1.2868	1.4947
50	0	0	0.9846	0.9867	0.2081	2.3491	2.3052	1.9060	0.9393	0.9260	1.4347
100	0	0	0.8330	0.8346	0.1880	1.9385	1.8967	2.2014	0.6714	0.6616	1.4717
50	50	0	0.9006	0.9025	0.2106	2.0362	1.9956	2.0335	0.7877	0.7743	1.7295
50	100	0	0.8439	0.8429	0.1186	1.8107	1.7790	1.7819	0.6624	0.6756	1.9538
100	50	0	0.7911	0.7807	1.3354	1.7308	1.6916	2.3166	0.5891	0.5789	1.7688
100	100	0	0.6253	0.6238	0.2297	1.3004	1.2631	2.9527	0.3751	0.3682	1.8657
0	0	10	0.9277	0.9352	0.8029	2.1939	2.1502	2.0307	0.8368	0.8282	1.0374
50	0	10	0.7892	0.7920	0.3592	1.8127	1.7712	2.3447	0.6001	0.5934	1.1348

100	0	10	0.6731	0.6752	0.3080	1.4934	1.4541	2.6986	0.4367	0.4309	1.3551
0	0	20	0.7553	0.7545	0.1080	1.7092	1.6673	2.5129	0.5404	0.5366	0.7201
50	0	20	0.6474	0.6458	0.2400	1.4187	1.3787	2.9012	0.3969	0.3929	1.0045
100	0	20	0.5614	0.5590	0.4293	1.1608	1.1463	1.2694	0.2895	0.2944	1.6644
50	50	10	0.7456	0.7465	0.1201	1.6454	1.6052	2.5029	0.5350	0.5272	1.4734
50	50	20	0.6236	0.6219	0.2791	1.3322	1.2926	3.0617	0.3693	0.3645	1.3028
50	100	10	0.7189	0.7112	1.0723	1.5170	1.4780	2.6402	0.4871	0.4788	1.7305
50	100	20	0.6051	0.6018	0.5493	1.2501	1.2211	2.3750	0.3469	0.3416	1.5463
100	50	10	0.6551	0.6470	1.2533	1.3871	1.3489	2.8327	0.4023	0.3959	1.6392
100	50	20	0.5467	0.5441	0.4779	1.1075	1.0916	1.4566	0.2725	0.2791	2.3647
100	100	10	0.6253	0.6238	0.2297	1.3004	1.2631	2.9527	0.3751	0.3682	1.8657
100	100	20	0.5337	0.5309	0.5274	1.0607	1.0440	1.5996	0.2603	0.2660	2.1429

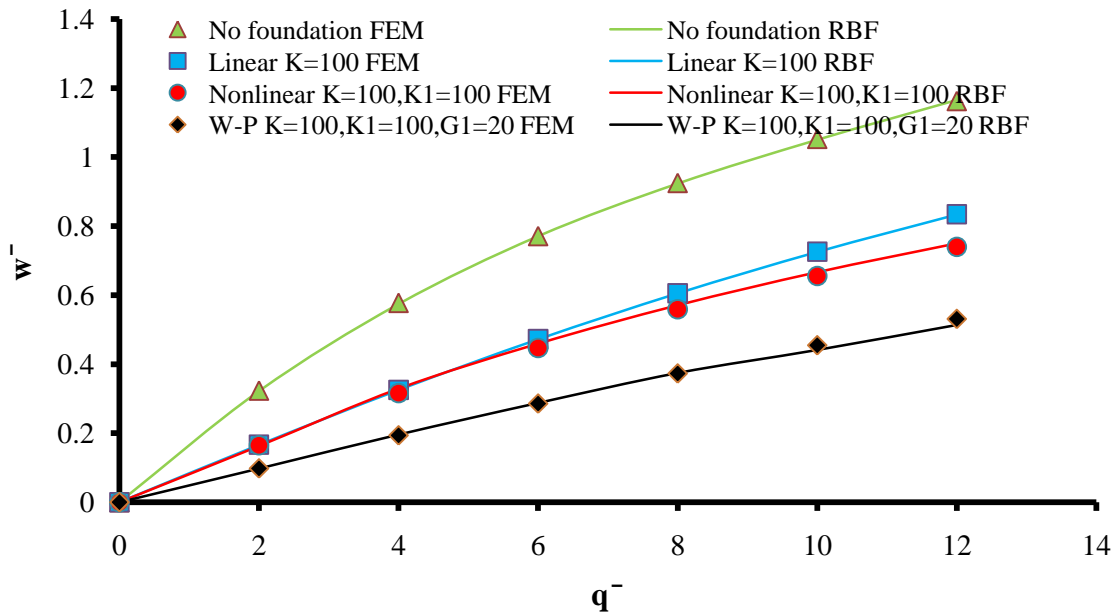


Figure 7.35  $\bar{w}$  vs  $\bar{q}$  on Different Foundations for CICCIM



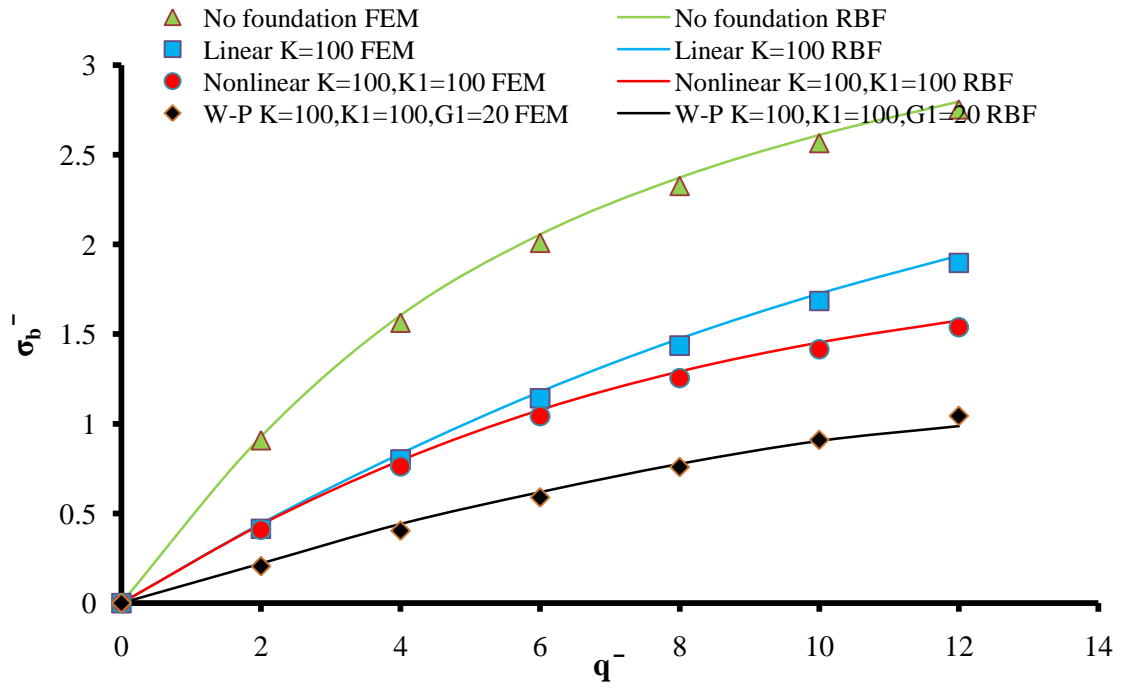


Figure 7.36  $\bar{\sigma}_b$  vs  $\bar{q}$  on Different Foundations for CICCIM

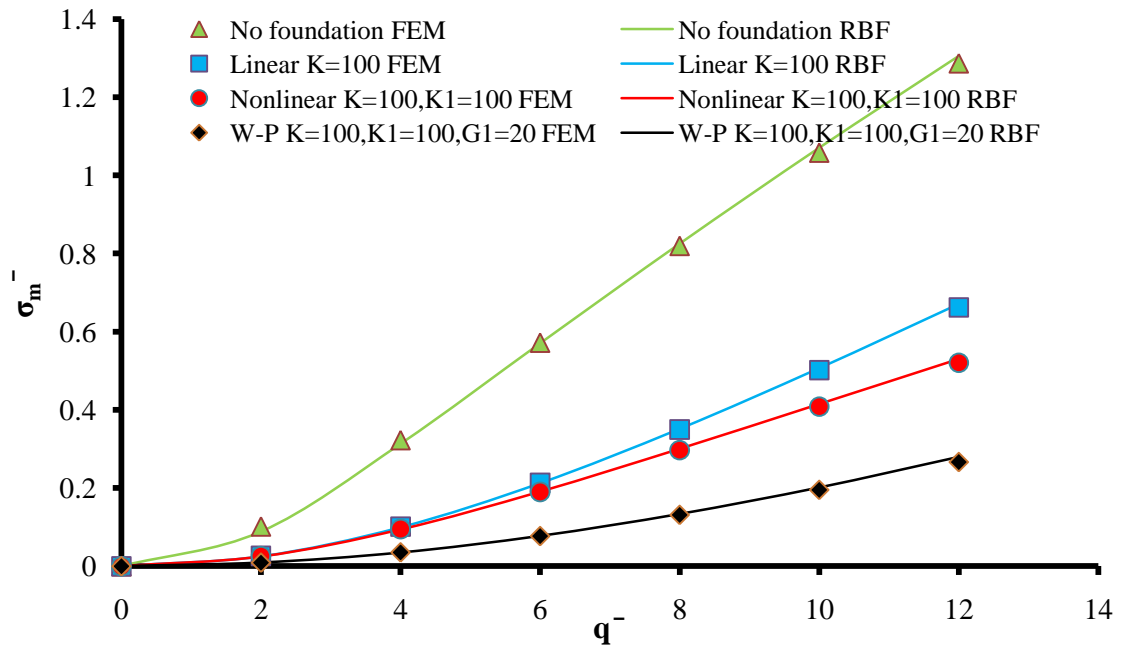


Figure 7.37  $\bar{\sigma}_m$  vs  $\bar{q}$  on Different Foundations for CICCIM

- CICFIM

The plate in this example is a clamped-two edges free supported circular plate with immovable edges, ( $w = \frac{\partial w}{\partial n} = (V_n \text{ and } M_n \text{ at the free edges}) = u = v = 0$ ) resting on the Winkler-Pasternak foundation. It is subjected to uniformly distributed load  $\bar{q}$  ranging from 0.9 -7.2. The selected results of some cases representing various foundation parameters are given in Table 7-14 and Figures 7.38, 7.39 and 7.40. In the shown Table 7-14, the RBF and FEM results with their percentage errors at the free edge of the plate for  $\bar{w}$ ,  $\bar{\sigma}_b$  and  $\bar{\sigma}_m$  are presented only at load  $\bar{q} = 7.2$ . The results for  $\bar{q}$  versus  $\bar{w}$ ,  $\bar{\sigma}_b$ , and  $\bar{\sigma}_m$  at the free edge of the plate are provided in Figures 7.38, 7.39, and 7.40 respectively. All three figures show a good agreement between RBF and FEM solutions. The RBF results compare very well with the FEM results with maximum relative differences of 5.2%, 5.1 % and 4.4% for  $\bar{w}$ ,  $\bar{\sigma}_b$  and  $\bar{\sigma}_m$  respectively.

Table 7.14 CICFIM Results of  $\bar{w}$ ,  $\bar{\sigma}_b$ ,  $\bar{\sigma}_m$  at Load  $\bar{q} = 7.2$

Foundation Parameters			$\bar{w}$			$\bar{\sigma}_b$			$\bar{\sigma}_m$		
k	K1	G1	FEM	RBF	Error %	FEM	RBF	Error %	FEM	RBF	Error %
0	0	0	0.942	0.956	1.4862	1.261	1.204	4.520	0.276	0.264	4.348
0	0	4	0.868	0.903	3.990	1.147	1.103	3.837	0.235	0.226	3.644
0	0	8	0.800	0.841	5.12	1.042	0.989	5.086	0.200	0.193	3.500
0	20	0	0.882	0.925	4.875	1.165	1.118	4.034	0.242	0.237	2.066
0	20	4	0.820	0.837	2.071	1.070	1.049	2.029	0.210	0.206	1.833
0	20	8	0.762	0.773	1.407	0.982	0.968	1.388	0.181	0.179	1.190
0	40	0	0.837	0.872	4.220	1.093	1.049	4.049	0.218	0.210	3.857
0	40	4	0.783	0.787	0.576	1.011	1.005	0.573	0.191	0.190	0.374
0	40	8	0.731	0.727	0.537	0.934	0.939	0.540	0.167	0.168	0.741
20	0	0	0.845	0.844	0.081	1.126	1.127	0.081	0.223	0.223	0.282
20	0	4	0.778	0.791	1.678	1.021	1.004	1.650	0.189	0.186	1.453
20	0	8	0.717	0.729	1.632	0.927	0.912	1.606	0.161	0.158	1.409
20	20	0	0.800	0.823	2.831	1.053	1.024	2.753	0.200	0.195	2.559
20	20	4	0.743	0.754	1.531	0.964	0.950	1.507	0.172	0.170	1.310
20	20	8	0.689	0.700	1.472	0.883	0.870	1.451	0.148	0.147	1.253
20	40	0	0.765	0.772	0.971	0.996	0.987	0.961	0.183	0.181	0.763

20	40	4	0.714	0.721	0.992	0.918	0.909	0.982	0.159	0.158	0.784
20	40	8	0.666	0.673	0.953	0.846	0.838	0.944	0.139	0.138	0.746
40	0	0	0.757	0.782	3.201	1.002	0.971	3.102	0.179	0.174	2.908
40	0	4	0.698	0.713	2.220	0.908	0.889	2.172	0.152	0.149	1.976
40	0	8	0.644	0.657	1.907	0.826	0.810	1.871	0.130	0.127	1.675
40	20	0	0.724	0.762	5.212	0.948	0.901	4.954	0.164	0.156	4.763
40	20	4	0.672	0.677	0.672	0.867	0.861	0.667	0.141	0.140	0.468
40	20	8	0.624	0.612	1.974	0.794	0.809	2.013	0.122	0.124	2.217
40	40	0	0.698	0.711	1.950	0.905	0.887	1.913	0.152	0.150	1.717
40	40	4	0.651	0.660	1.362	0.832	0.821	1.344	0.132	0.131	1.147
40	40	8	0.607	0.618	1.729	0.766	0.753	1.700	0.115	0.113	1.503

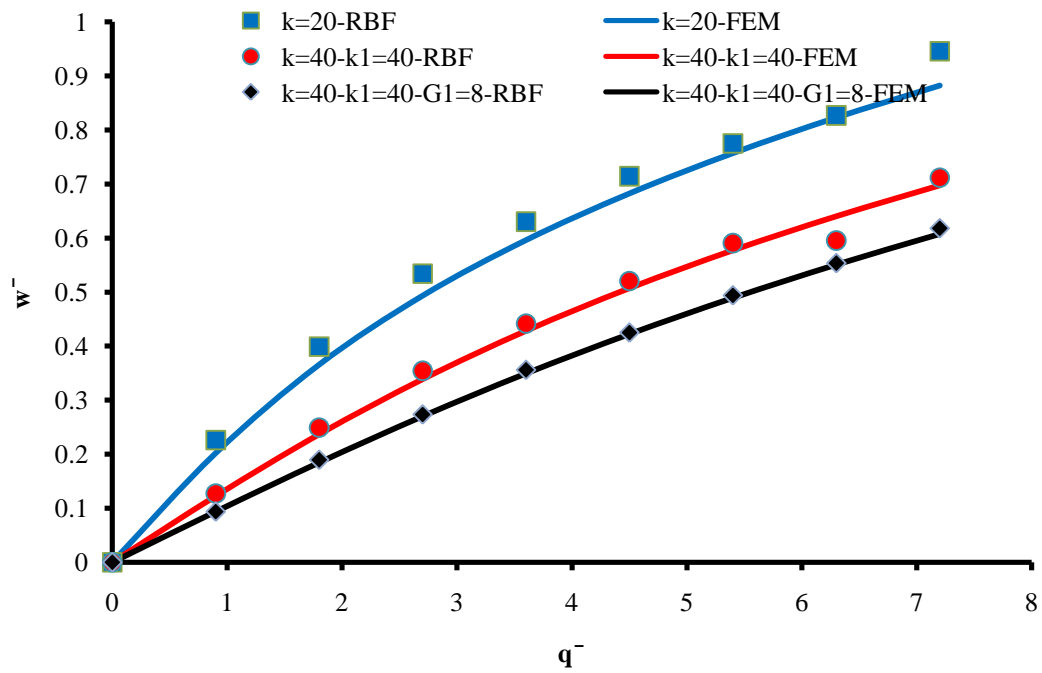


Figure 7.38  $\bar{w}$  vs  $\bar{q}$  on Different Foundations for CICFIM

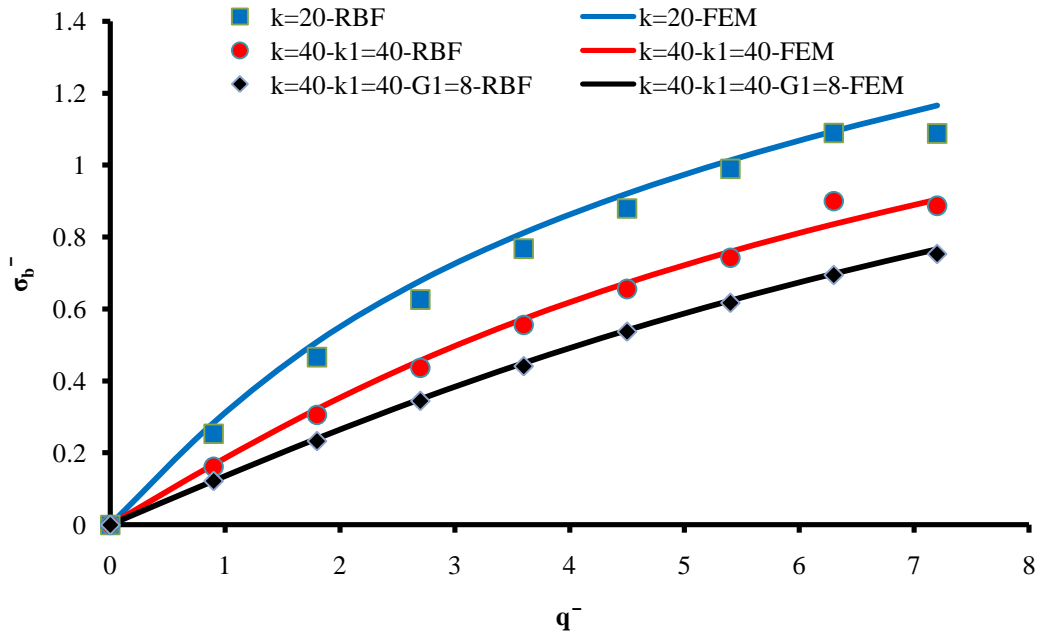


Figure 7.39  $\bar{\sigma}_b$  vs  $\bar{q}$  on Different Foundations for CICFIM

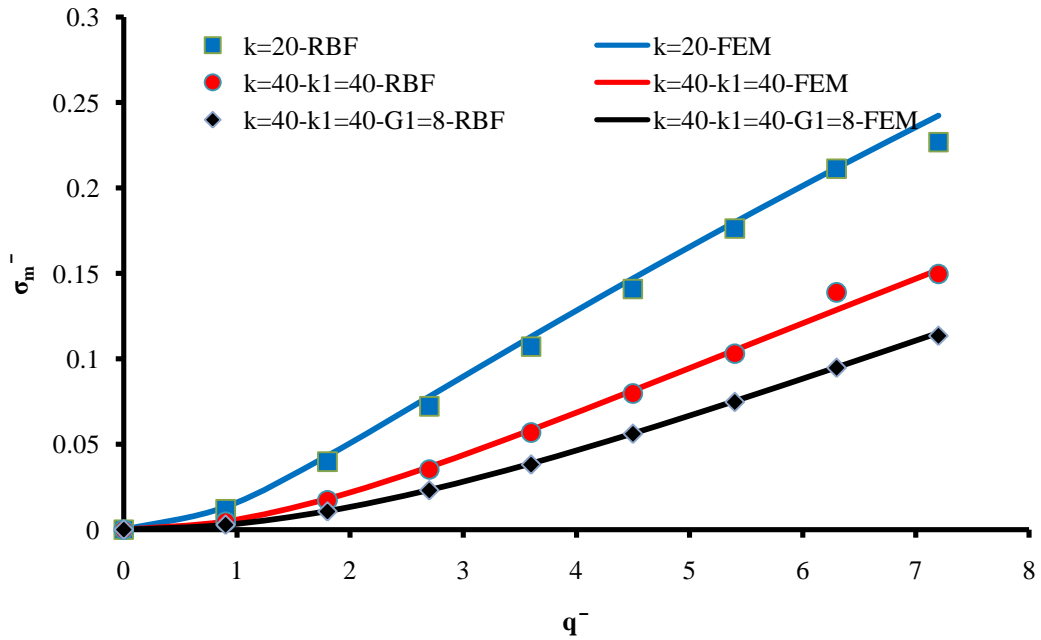


Figure 7.40  $\bar{\sigma}_m$  vs  $\bar{q}$  on Different Foundations for CICFIM

- CISF1IM

In this example, the plate is a simply with one free edge supported circular plate with immovable edges, ( $w = M_n = (V_n \text{ and } M_n \text{ at the free edge}) = u = v = 0$ ) resting on the Winkler-Pasternak foundation. It is subjected to uniformly distributed load  $\bar{q}$  ranging from 0.5 - 3.0. The selected results of some cases representing various foundation parameters are given in Table 7-15 and Figures 7.41, 7.42, and 7.43. In the shown Table 7-15, the RBF and FEM results with their percentage errors at the center of the plate for  $\bar{w}, \bar{\sigma}_b$ , and  $\bar{\sigma}_m$  are presented only at load  $\bar{q} = 3$ . The results for  $\bar{q}$  versus  $\bar{w}, \bar{\sigma}_b$ , and  $\bar{\sigma}_m$  at the center of the plate are provided in Figures 7.41, 7.42, and 7.43 respectively. All three figures show a good agreement between RBF and FEM solutions. The RBF results compare very well with the FEM results with maximum relative differences of 2.8%, 2.4 % and 4% for  $\bar{w}, \bar{\sigma}_b$  and  $\bar{\sigma}_m$  respectively.

Table 7.15 CISF1IM Results of  $\bar{w}, \bar{\sigma}_b, \bar{\sigma}_m$  at Load  $\bar{q} = 3$

Foundation Parameters			$\bar{w}$			$\bar{\sigma}_b$			$\bar{\sigma}_m$		
k	K 1	G 1	FEM	RBF	Error %	FEM	RBF	Error %	FEM	RBF	Error %
0	0	0	0.910	0.935	2.763	1.334	1.358	1.792	0.639	0.664	3.933
0	0	2	0.834	0.857	2.794	1.219	1.244	2.072	0.537	0.558	4.055
0	0	4	0.762	0.783	2.777	1.109	1.135	2.333	0.447	0.465	4.076
0	15	0	0.851	0.868	1.990	1.205	1.223	1.496	0.562	0.577	2.751
0	15	2	0.785	0.802	2.081	1.115	1.135	1.766	0.478	0.492	2.947
0	15	4	0.723	0.738	2.141	1.027	1.048	2.035	0.405	0.417	3.080
0	30	0	0.805	0.817	1.543	1.107	1.123	1.451	0.505	0.516	2.106
0	30	2	0.747	0.760	1.654	1.035	1.052	1.687	0.435	0.445	2.312
0	30	4	0.692	0.704	1.750	0.962	0.980	1.938	0.372	0.381	2.475
15	0	0	0.791	0.808	2.179	1.138	1.159	1.892	0.486	0.500	2.850
15	0	2	0.721	0.736	2.163	1.032	1.055	2.135	0.404	0.415	2.848
15	0	4	0.656	0.670	2.115	0.935	0.957	2.356	0.334	0.344	2.782
15	15	0	0.748	0.761	1.661	1.045	1.064	1.754	0.437	0.446	2.100
15	15	2	0.687	0.699	1.711	0.961	0.980	1.996	0.368	0.377	2.192

15	15	4	0.630	0.641	1.714	0.880	0.899	2.203	0.310	0.317	2.245
15	30	0	0.714	0.724	1.342	0.972	0.989	1.768	0.400	0.407	1.666
15	30	2	0.660	0.669	1.419	0.902	0.920	1.982	0.341	0.347	1.790
15	30	4	0.609	0.607	0.222	0.834	0.835	0.060	0.290	0.298	2.691
30	0	0	0.682	0.693	1.576	0.958	0.977	1.957	0.365	0.371	1.831
30	0	2	0.621	0.631	1.551	0.867	0.886	2.174	0.302	0.307	1.804
30	0	4	0.566	0.572	1.120	0.785	0.800	1.895	0.250	0.255	1.980
30	15	0	0.654	0.662	1.274	0.895	0.913	1.954	0.336	0.341	1.438
30	15	2	0.599	0.607	1.319	0.819	0.837	2.188	0.282	0.286	1.472
30	15	4	0.549	0.552	0.557	0.749	0.760	1.409	0.237	0.240	1.308
30	30	0	0.630	0.636	1.075	0.843	0.860	2.027	0.313	0.317	1.194

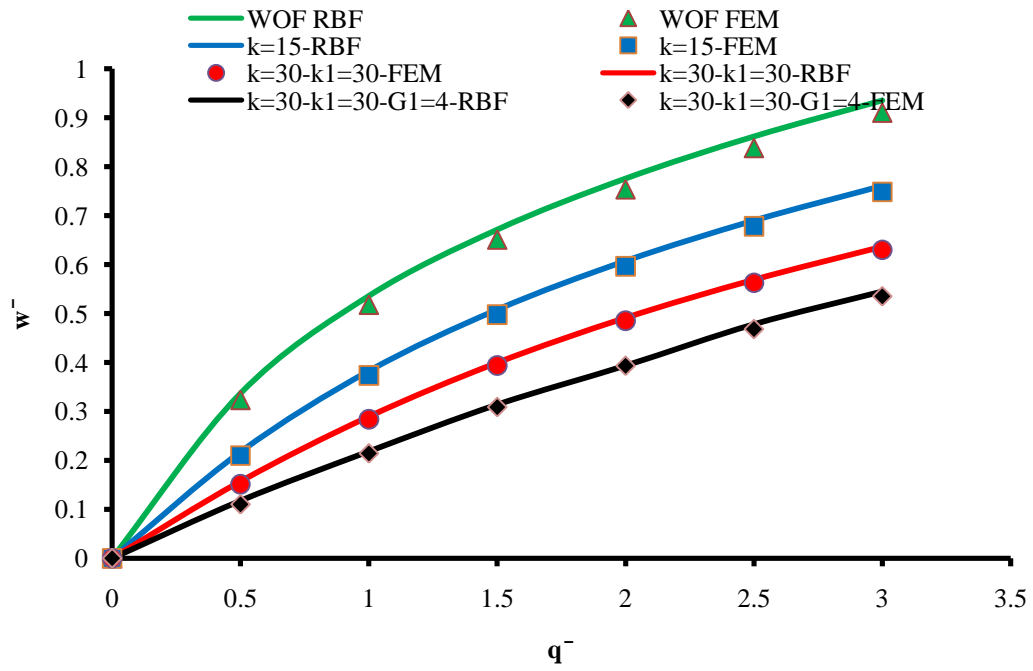


Figure 7.41  $\bar{w}$  vs  $\bar{q}$  on Different Foundations for CISF1IM

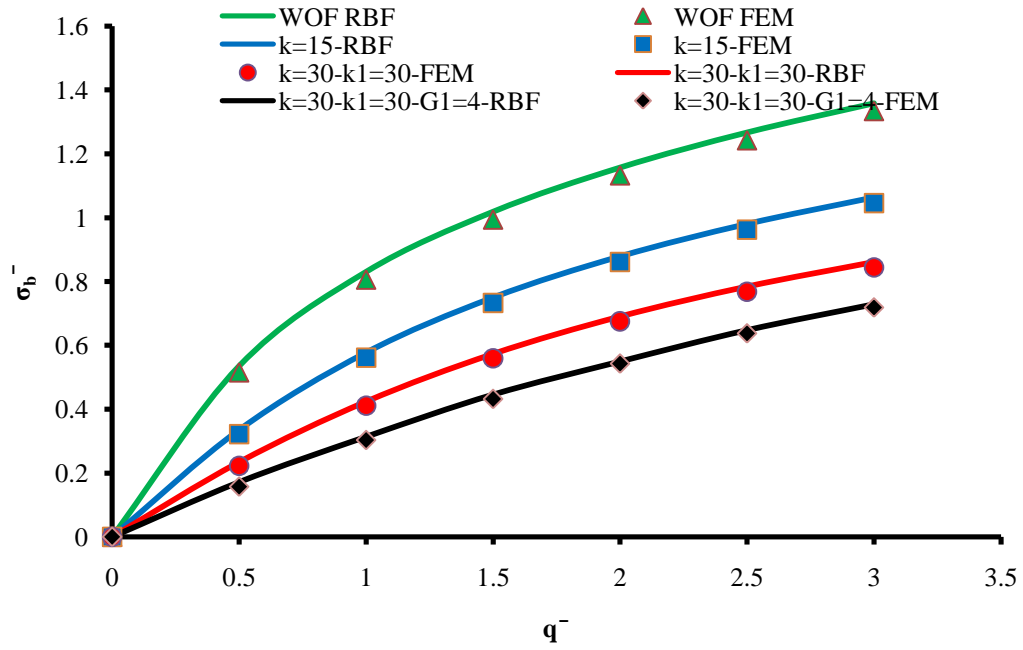


Figure 7.42  $\bar{\sigma}_b$  vs  $\bar{q}$  on Different Foundations for CISF1IM

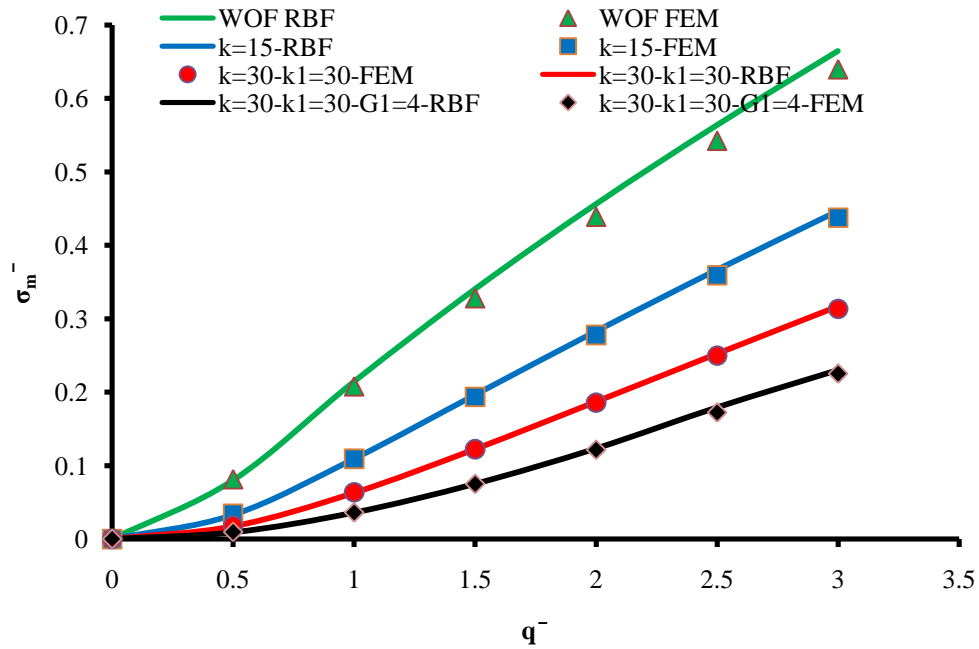


Figure 7.43  $\bar{\sigma}_m$  vs  $\bar{q}$  on Different Foundations for CISF1IM

## 7.2.4 WPF Movable Circular Plates

- CICC MO

The plate in this example is a clamped supported circular plate with movable edges,  $w = \frac{\partial w}{\partial n} = F = \frac{\partial F}{\partial n} = 0$ ) resting on the Winkler-Pasternak foundation. It is subjected to uniformly distributed load  $\bar{q}$  ranging from 1 - 8. The selected results of some cases representing various foundation parameters are given in Table 7-16 and Figures 7.44, 7.45, and 7.46. In the shown Table 7- 16 the RBF and FEM results with their percentage errors at the center of the plate for  $\bar{w}$ ,  $\bar{\sigma}_b$ , and  $\bar{\sigma}_m$  are presented only at load  $\bar{q} = 8$ . The results for  $\bar{q}$  versus  $\bar{w}$ ,  $\bar{\sigma}_b$ , and  $\bar{\sigma}_m$  at the center of the plate are provided in Figures 7.44, 7.45, and 7.46 respectively. All three figures show excellent agreement between RBF and FEM solutions. The RBF results compare very well with the FEM results with maximum relative differences of 2.14%, 4.4 % and 3% for  $\bar{w}$ ,  $\bar{\sigma}_b$  and  $\bar{\sigma}_m$  respectively.

Table 7.16 CICC MO Results of  $\bar{w}$ ,  $\bar{\sigma}_b$ ,  $\bar{\sigma}_m$  at Load  $\bar{q} = 8$

Foundation Parameters			$\bar{w}$			$\bar{\sigma}_b$			$\bar{\sigma}_m$		
K	K1	G I	RBF	FEM	Error %	RBF	FEM	Error %	RBF	FEM	Error %
0	0	0	1.120	1.118	0.199	2.888	2.865	0.819	0.584	0.582	0.388
50	0	0	0.833	0.834	0.073	2.108	2.100	0.414	0.319	0.319	0.280
100	0	0	0.646	0.646	0.072	1.567	1.558	0.589	0.185	0.185	0.394
50	50	0	0.757	0.757	0.062	1.836	1.825	0.599	0.255	0.256	0.415
50	100	0	0.708	0.706	0.243	1.657	1.642	0.949	0.218	0.219	0.422
100	50	0	0.621	0.611	1.751	1.469	1.426	3.076	0.158	0.163	3.048
100	100	0	0.581	0.584	0.499	1.322	1.324	0.146	0.148	0.147	0.855
0	0	10	0.757	0.761	0.569	1.854	1.855	0.050	0.258	0.257	0.342
50	0	10	0.594	0.598	0.630	1.397	1.398	0.101	0.155	0.154	0.400
100	0	10	0.484	0.487	0.575	1.084	1.084	0.048	0.099	0.099	0.440



0	0	20	0.554	0.559	0.800	1.278	1.279	0.030	0.131	0.131	0.123
50	0	20	0.459	0.460	0.309	1.017	1.008	0.849	0.086	0.087	0.488
100	0	20	0.388	0.389	0.275	0.822	0.814	0.999	0.060	0.060	0.180
50	50	10	0.571	0.571	0.031	1.315	1.302	0.954	0.138	0.139	0.605
50	50	20	0.447	0.450	0.652	0.973	0.970	0.303	0.082	0.082	0.066
50	100	10	0.551	0.550	0.235	1.242	1.225	1.339	0.126	0.127	0.674
50	100	20	0.438	0.440	0.541	0.941	0.937	0.517	0.078	0.078	0.026
100	50	10	0.484	0.474	2.146	1.080	1.035	4.392	0.090	0.093	2.744
100	50	20	0.381	0.384	0.568	0.796	0.792	0.530	0.058	0.058	0.177
100	100	10	0.461	0.462	0.183	0.999	0.992	0.731	0.088	0.088	0.070
100	100	20	0.380	0.378	0.429	0.787	0.773	1.933	0.056	0.056	0.195

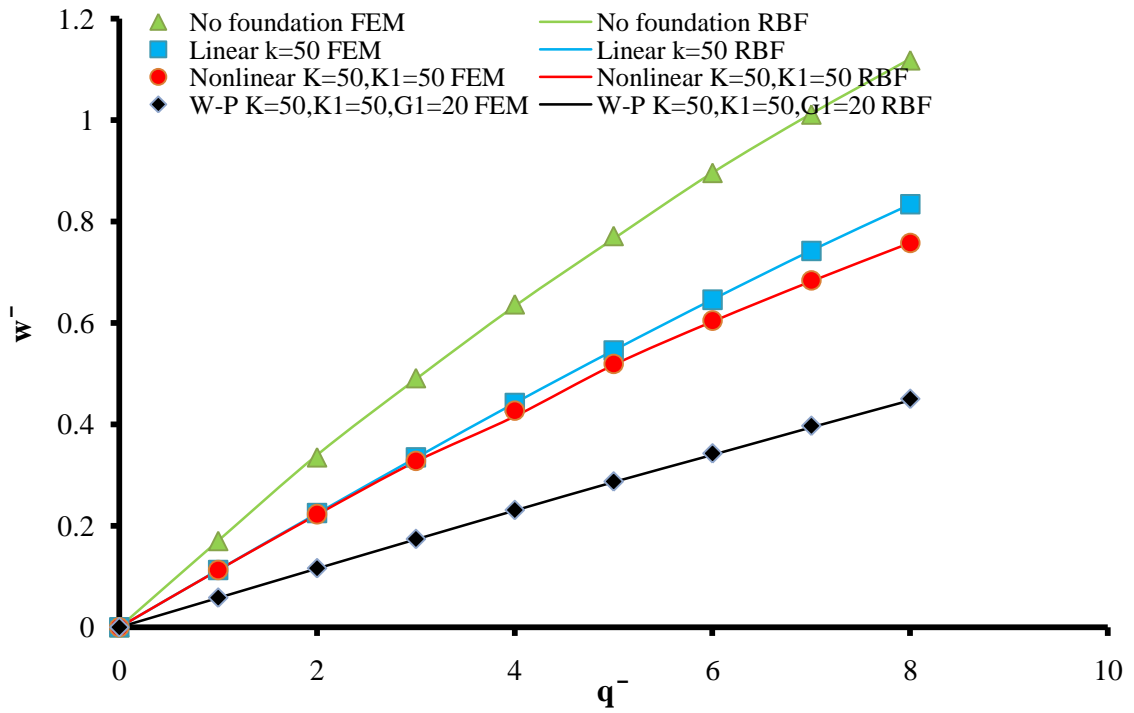


Figure 7.44  $\bar{w}$  vs  $\bar{q}$  on Different Foundations for CICC MO

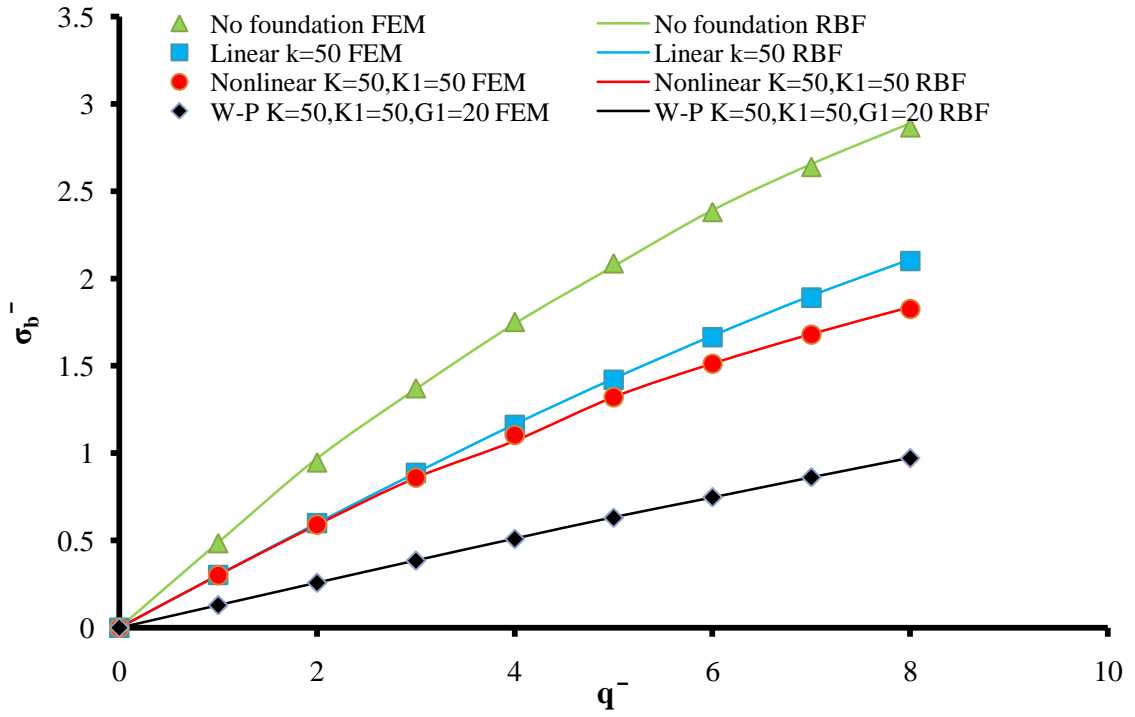


Figure 7.45  $\bar{\sigma}_b$  vs  $\bar{q}$  on Different Foundations for CICCMO

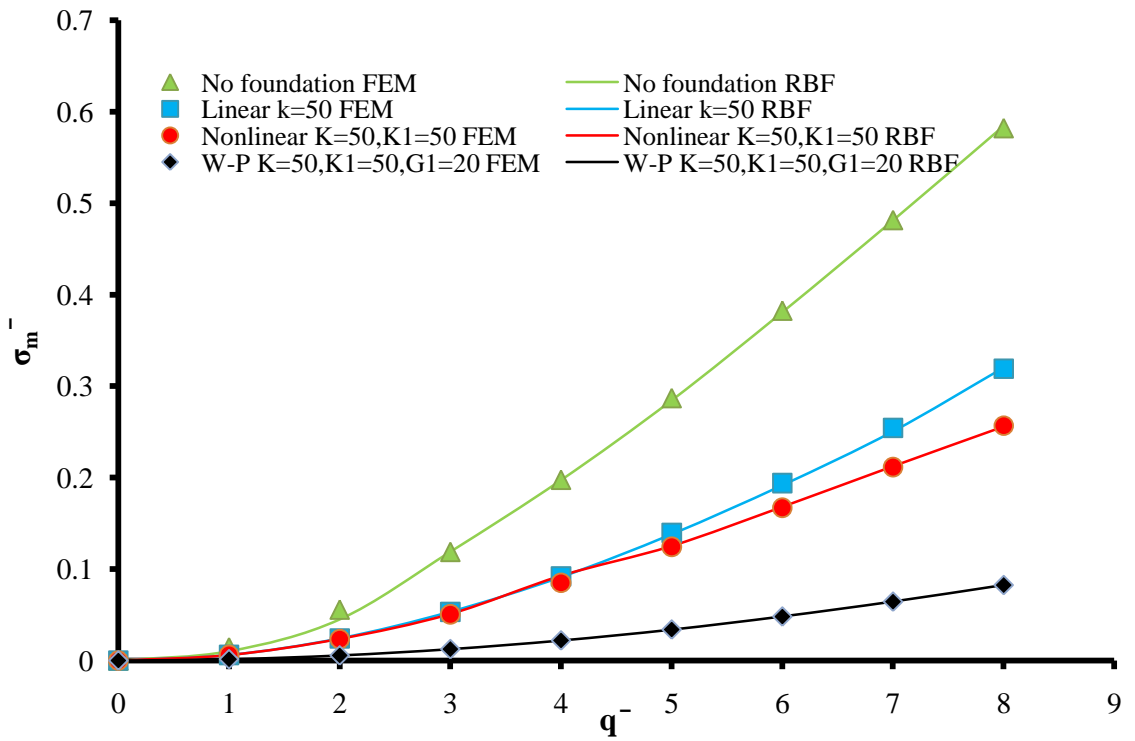


Figure 7.46  $\bar{\sigma}_m$  vs  $\bar{q}$  on Different Foundations for CICCMO

- CISSMO

In this example, the plate is a simply supported circular plate with movable edges, ( $w = M_n = F = \frac{\partial F}{\partial n} = 0$ ) resting on the Winkler-Pasternak foundation. It is subjected to uniformly distributed load  $\bar{q}$  ranging from 0.5 – 4. The selected results of some cases representing various foundation parameters are given in Table 7-17 and Figures 7.47, 7.48, and 7.49. In the shown Table 7-17 the RBF and FEM results with their percentage errors at the center of the plate for  $\bar{w}$ ,  $\bar{\sigma}_b$ , and  $\bar{\sigma}_m$  are presented only at load  $\bar{q} = 3$ . The results for  $\bar{q}$  versus  $\bar{w}$ ,  $\bar{\sigma}_b$ , and  $\bar{\sigma}_m$  at the center of the plate are provided in Figures 7.47, 7.48, and 7.49 respectively. All three figures show a good agreement between RBF and FEM solutions. The RBF results compare very well with the FEM results with maximum relative difference of 5.4%, for  $\bar{w}$ ,  $\bar{\sigma}_b$  and  $\bar{\sigma}_m$ .

Table 7.17 CISSMO Results of  $\bar{w}$ ,  $\bar{\sigma}_b$ ,  $\bar{\sigma}_m$  at Load  $\bar{q} = 3$

Foundation Parameters			$\bar{w}$			$\bar{\sigma}_b$			$\bar{\sigma}_m$		
K	K1	G1	FEM	RBF	Error %	FEM	RBF	Error %	FEM	RBF	Error %
0	0	0	1.365	1.374	0.659	2.122	2.157	1.649	0.512	0.494	3.516
0	0	5	0.857	0.845	1.400	1.397	1.389	0.573	0.207	0.198	4.348
0	0	10	0.588	0.563	4.252	0.956	0.911	4.707	0.097	0.093	4.124
0	25	0	1.033	1.038	0.484	1.518	1.545	1.779	0.287	0.277	3.484
0	25	5	0.754	0.747	0.928	1.179	1.184	0.424	0.157	0.149	5.096
0	25	10	0.556	0.562	1.079	0.884	0.858	2.941	0.086	0.083	3.488
0	50	0	0.897	0.902	0.557	1.263	1.289	2.059	0.213	0.206	3.286
0	50	5	0.693	0.688	0.722	1.05	1.06	0.952	0.131	0.127	3.053
0	50	10	0.532	0.512	3.759	0.829	0.795	4.101	0.078	0.074	5.128
25	0	0	0.905	0.911	0.663	1.416	1.436	1.412	0.226	0.216	4.425
25	0	5	0.612	0.607	0.817	0.962	0.962	0.000	0.103	0.099	3.884
25	0	10	0.453	0.431	4.857	0.705	0.678	3.830	0.056	0.053	5.357
25	25	0	0.783	0.788	0.639	1.163	1.183	1.720	0.165	0.159	3.636
25	25	5	0.575	0.572	0.522	0.879	0.884	0.569	0.09	0.088	2.222
25	25	10	0.44	0.419	4.773	0.674	0.641	4.896	0.053	0.051	3.774

25	50	0	0.714	0.719	0.700	1.019	1.04	2.061	0.135	0.13	3.704
25	50	5	0.547	0.546	0.183	0.817	0.826	1.102	0.081	0.079	2.469
25	50	10	0.429	0.408	4.895	0.648	0.615	5.093	0.05	0.048	4.000
50	0	0	0.637	0.643	0.942	0.956	0.973	1.778	0.109	0.105	3.670
50	0	5	0.466	0.485	4.077	0.697	0.712	2.152	0.058	0.055	5.172
50	0	10	0.366	0.346	5.464	0.542	0.513	5.351	0.036	0.034	5.556

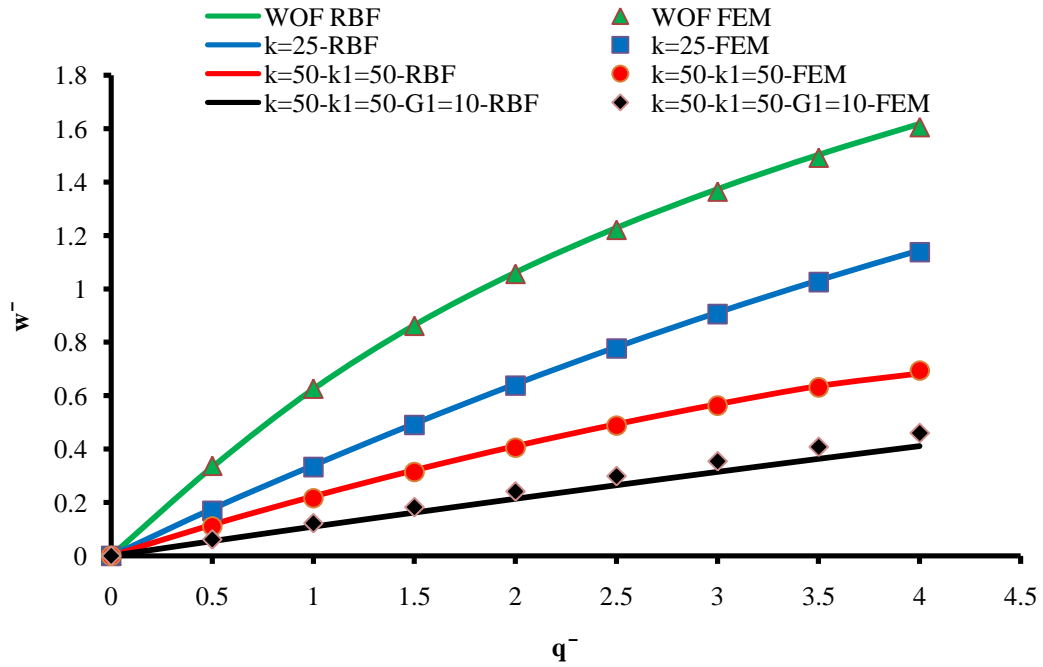


Figure 7.47  $\bar{w}$  vs  $\bar{q}$  on Different Foundations for CISSMO

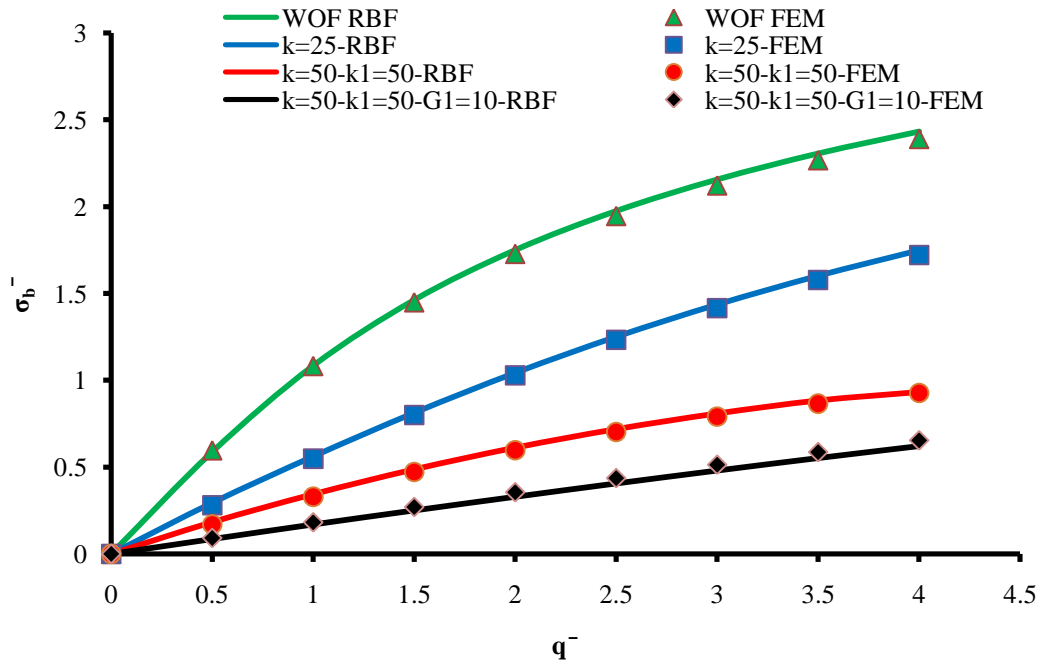


Figure 7.48  $\bar{\sigma}_b$  vs  $\bar{q}$  on Different Foundations for CISSMO

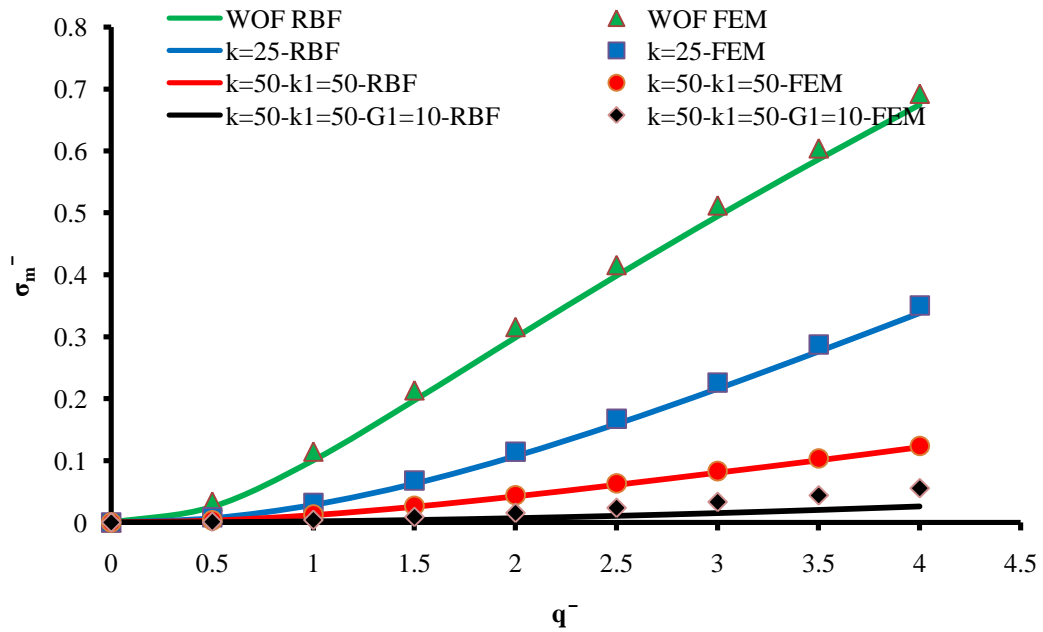


Figure 7.49  $\bar{\sigma}_m$  vs  $\bar{q}$  on Different Foundations for CISSMO

- CICFMO

The plate in this example is a clamped with two free edges supported circular plate with movable edges,  $w = \frac{\partial w}{\partial n} = (V_n \text{ and } M_n \text{ at the free edges}) = F = \frac{\partial F}{\partial n} = 0$  resting on the Winkler-Pasternak foundation. It is subjected to uniformly distributed load  $\bar{q}$  ranging from 0.8 – 6.4. The selected results of some cases representing various foundation parameters are given in Table 7-18 and Figures 7.50, 7.51, and 7.52. In the shown Table 7- 18 the RBF and FEM results with their percentage errors at the center of the plate for  $\bar{w}$ , and  $\bar{\sigma}_b$ , are presented only at load  $\bar{q} = 4.8$ . The results for  $\bar{q}$  versus  $\bar{w}$ ,  $\bar{\sigma}_b$ , and  $\bar{\sigma}_m$  at the center of the plate are provided in Figures 7.50, 7.51, and 7.52 respectively. All three figures show a good agreement between RBF and FEM solutions. The RBF results compare very well with the FEM results with maximum relative difference of 6%, for  $\bar{w}$ , and  $\bar{\sigma}_b$ .

Table 7.18 CICFMO Results of  $\bar{w}$ ,  $\bar{\sigma}_b$ , at Load  $\bar{q} = 4.8$

Foundation Parameters			$\bar{w}$			$\bar{\sigma}_b$		
K	K1	G1	FEM	RBF	Error %	FEM	RBF	Error %
0	0	0	1.150	1.168	1.567	2.367	2.456	3.756
0	0	5	0.878	0.920	4.784	1.711	1.820	6.351
0	0	10	0.704	0.745	5.921	1.301	1.368	5.131
0	25	0	0.946	0.998	5.534	1.859	1.916	3.088
0	25	5	0.782	0.822	5.083	1.474	1.525	3.478
0	25	10	0.656	0.684	4.296	1.185	1.226	3.466
0	50	0	0.846	0.875	3.365	1.613	1.631	1.112
0	50	5	0.723	0.751	3.904	1.330	1.363	2.449
0	50	10	0.621	0.643	3.553	1.103	1.133	2.754
25	0	0	0.844	0.896	6.132	1.693	1.765	4.235
25	0	5	0.677	0.717	5.829	1.279	1.342	4.860
25	0	10	0.565	0.586	3.841	1.012	1.046	3.329
25	25	0	0.759	0.791	4.203	1.472	1.506	2.368
25	25	5	0.635	0.663	4.456	1.173	1.213	3.486
25	25	10	0.542	0.558	2.954	0.957	0.979	2.293
25	50	0	0.705	0.724	2.734	1.333	1.345	0.896

25	50	5	0.604	0.622	3.059	1.094	1.115	1.899
25	50	10	0.523	0.537	2.591	0.912	0.929	1.908
50	0	0	0.656	0.686	4.660	1.272	1.314	3.320
50	0	5	0.547	0.569	4.133	1.000	1.034	3.416
50	0	10	0.469	0.487	3.688	0.816	0.845	3.495

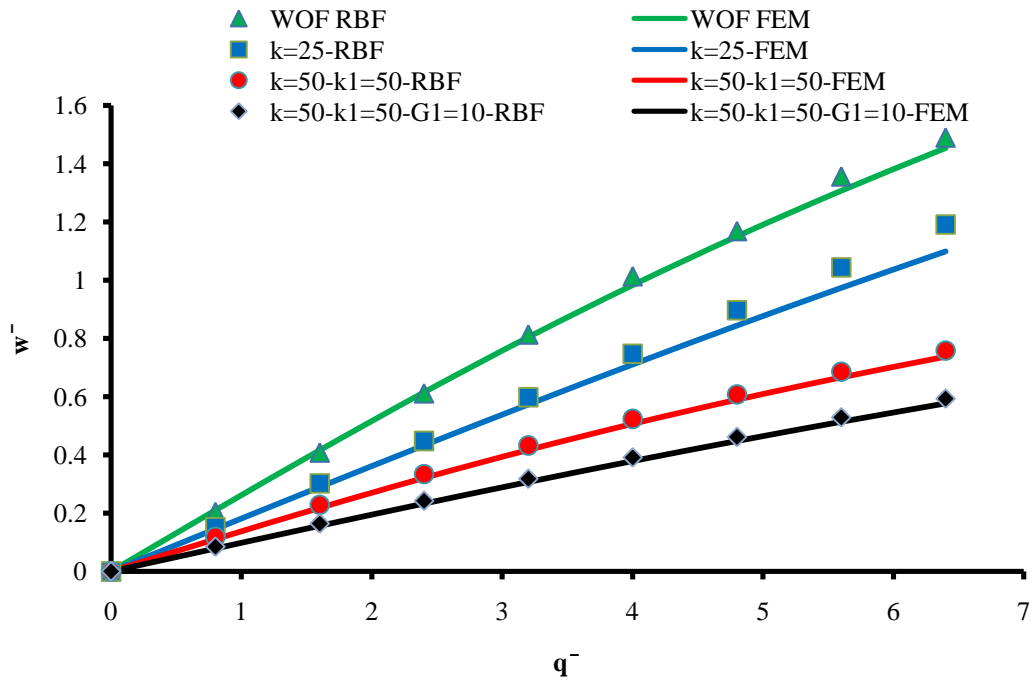


Figure 7.50  $\bar{w}$  vs  $\bar{q}$  on Different Foundations for CICFMO

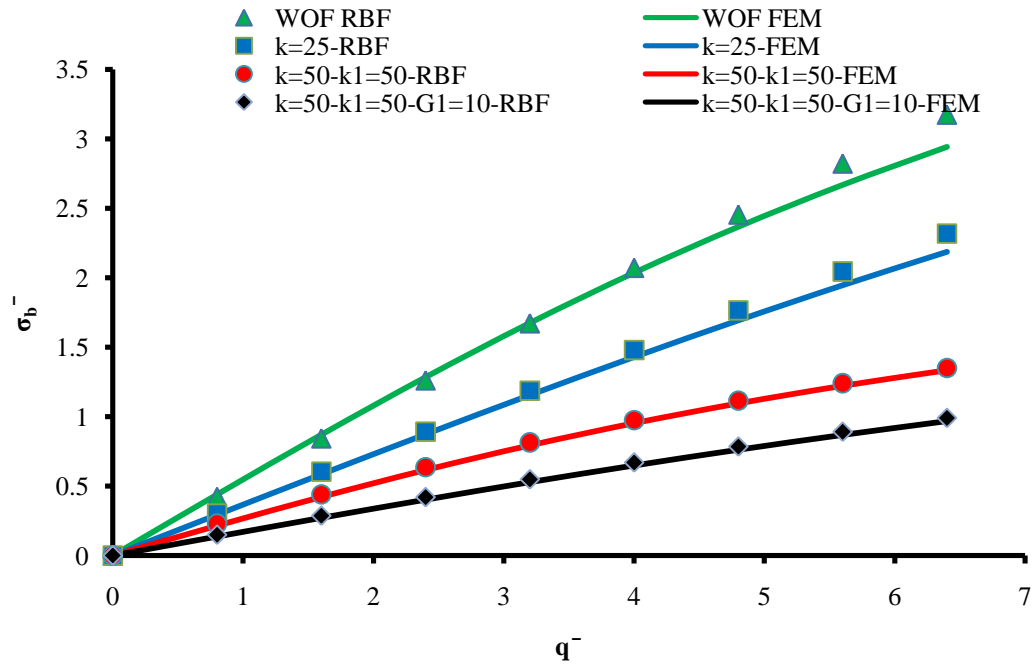


Figure 7.51  $\bar{\sigma}_b$  vs  $\bar{q}$  on Different Foundations for CICFMO

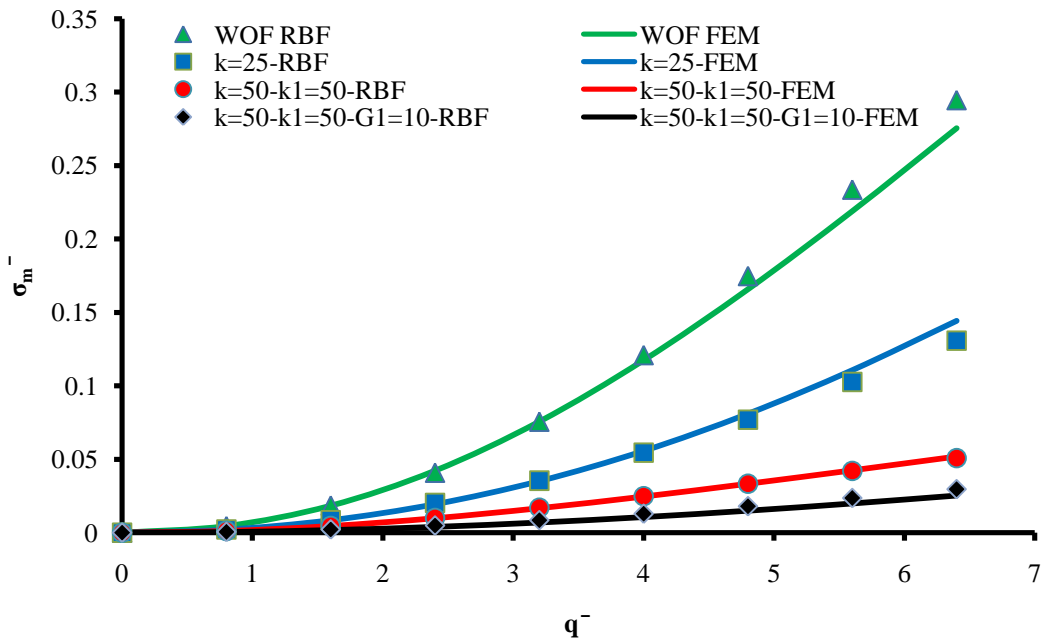


Figure 7.52  $\bar{\sigma}_m$  vs  $\bar{q}$  on Different Foundations for CICFMO



- CISFMO

In this example, the plate is a simply with two free edges supported circular plate with movable edges,  $w = M_n = (V_n \text{ and } M_n \text{ at the free edges}) = F = \frac{\partial F}{\partial n} = 0$ ) resting on the Winkler-Pasternak foundation. It is subjected to uniformly distributed load  $\bar{q}$  ranging from 0.25 – 2. The selected results of some cases representing various foundation parameters are given in Table 7-19 and Figures 7.53, and 7.54. In the shown Table 7-19 the RBF and FEM results with their percentage errors at the center of the plate for  $\bar{w}$ ,  $\bar{\sigma}_b$ , and  $\bar{\sigma}_m$  are presented only at load  $\bar{q} = 1.5$ . The results for  $\bar{q}$  versus  $\bar{w}$ , and  $\bar{\sigma}_b$  at the center of the plate are provided in Figures 7.53, and 7.54, respectively. Both two figures show a good agreement between RBF and FEM solutions. The RBF results compare very well with the FEM results with maximum relative differences of 5.1%, 5.4% and 5.6% for  $\bar{w}$ ,  $\bar{\sigma}_b$  and  $\bar{\sigma}_m$  respectively.

Table 7.19 CISFMO Results of  $\bar{w}$ ,  $\bar{\sigma}_b$ ,  $\bar{\sigma}_m$  at Load  $\bar{q} = 1.5$

Foundation Parameters			$\bar{w}$			$\bar{\sigma}_b$			$\bar{\sigma}_m$		
K	K1	G1	FEM	RBF	Error %	FEM	RBF	Error %	FEM	RBF	Error %
0	0	0	0.663	0.631	4.731	0.897	0.942	4.966	0.0132	0.0139	5.1756
0	0	1.5	0.535	0.561	4.806	0.717	0.684	4.586	0.0076	0.0073	4.3949
0	0	3	0.447	0.445	0.466	0.592	0.594	0.468	0.0037	0.0037	0.6687
0	10	0	0.570	0.573	0.538	0.759	0.755	0.535	0.0051	0.0051	0.3364
0	10	1.5	0.488	0.483	1.040	0.645	0.652	1.051	0.0032	0.0032	1.2527
0	10	3	0.422	0.423	0.240	0.553	0.552	0.239	0.0014	0.0014	0.0396
0	20	0	0.523	0.543	3.831	0.688	0.663	3.690	0.0015	0.0015	3.4969
0	20	1.5	0.458	0.472	3.002	0.601	0.583	2.915	0.0009	0.0008	2.7208
0	20	3	0.404	0.414	2.376	0.526	0.514	2.321	0.0000	0.0000	2.1257
10	0	0	0.479	0.475	0.681	0.639	0.643	0.685	0.0065	0.0065	0.8867
10	0	1.5	0.405	0.390	3.916	0.535	0.557	4.076	0.0030	0.0032	4.2837
10	0	3	0.352	0.348	1.324	0.459	0.466	1.342	0.0010	0.0010	1.5449
10	10	0	0.445	0.440	1.219	0.588	0.595	1.234	0.0032	0.0032	1.4360

10	10	1.5	0.388	0.382	1.562	0.507	0.515	1.587	0.0014	0.0014	1.7904
10	10	3	0.342	0.342	0.053	0.444	0.444	0.053	0.0001	0.0001	0.2536
10	20	0	0.423	0.430	1.541	0.554	0.546	1.518	0.0013	0.0013	1.3211
10	20	1.5	0.374	0.371	0.825	0.486	0.491	0.832	0.0003	0.0003	1.0338
10	20	3	0.334	0.328	1.957	0.431	0.439	1.996	-0.0005	-0.0005	2.1996
20	0	0	0.371	0.360	2.961	0.487	0.502	3.051	0.0025	0.0026	3.2571
20	0	1.5	0.326	0.330	1.302	0.423	0.417	1.286	0.0007	0.0007	1.0881
20	0	3	0.291	0.284	2.416	0.374	0.383	2.476	-0.0003	-0.0003	2.6811
20	10	0	0.358	0.361	0.980	0.467	0.462	0.971	0.0013	0.0013	0.7725
20	10	1.5	0.318	0.312	2.054	0.411	0.420	2.097	0.0001	0.0001	2.3015
20	10	3	0.287	0.272	5.161	0.366	0.386	5.442	-0.0006	-0.0007	5.6526
20	20	0	0.348	0.338	2.863	0.451	0.464	2.948	0.0004	0.0004	3.1535
20	20	1.5	0.312	0.298	4.558	0.401	0.420	4.775	-0.0004	-0.0004	4.9848
20	20	3	0.283	0.275	2.744	0.360	0.370	2.821	-0.0009	-0.0009	3.0270

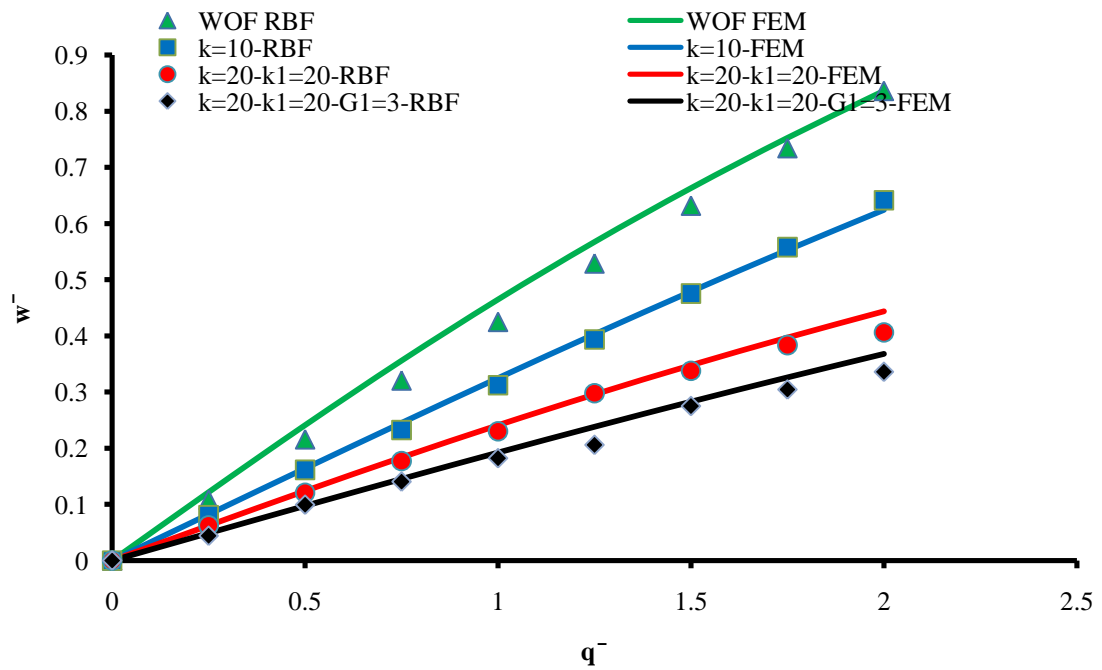


Figure 7.53  $\bar{w}$  vs  $\bar{q}$  on Different Foundations for CISFMO

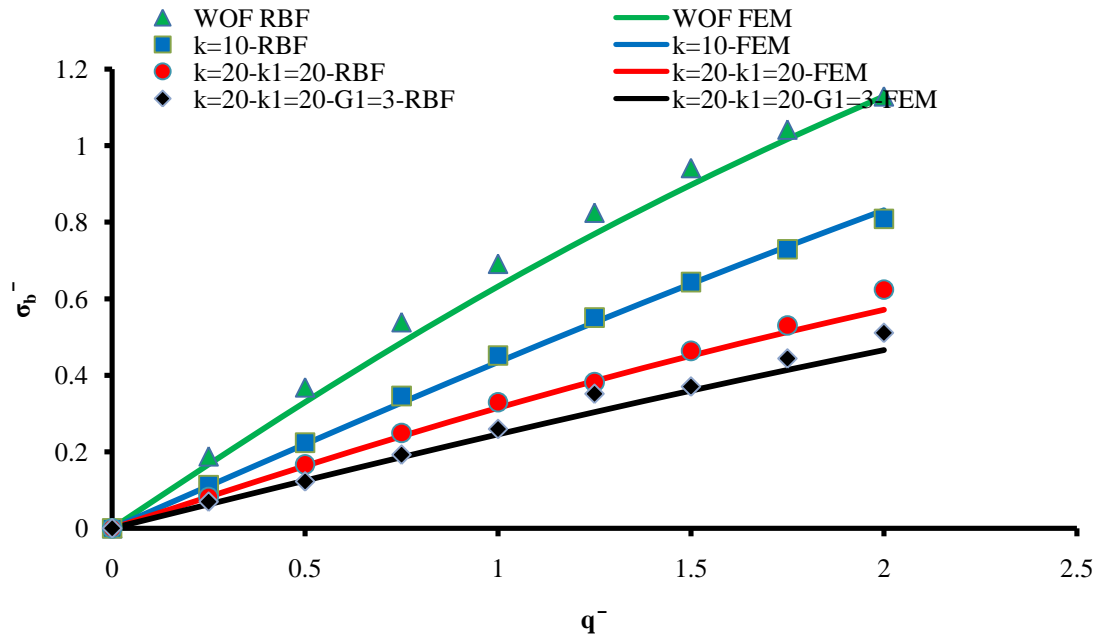


Figure 7.54  $\bar{\sigma}_b$  vs  $\bar{q}$  on Different Foundations for CISFMO

- CISF1MO

In this example, the plate is a simply with one free edge supported circular plate with movable edges,  $w = M_n = (V_n \text{ and } M_n \text{ at the free edge}) = F = \frac{\partial F}{\partial n} = 0$ ) resting on the Winkler-Pasternak foundation. It is subjected to uniformly distributed load  $\bar{q}$  ranging from 0.25 – 2. The selected results of some cases representing various foundation parameters are given in Table 7-20 and Figures 7.55, 7.56, and 7.57. In the shown Table 7-20 the RBF and FEM results with their percentage errors at the center of the plate for  $\bar{w}$ ,  $\bar{\sigma}_b$ , and  $\bar{\sigma}_m$  are presented only at load  $\bar{q} = 2$ . The results for  $\bar{q}$  versus  $\bar{w}$ ,  $\bar{\sigma}_b$ , and  $\bar{\sigma}_m$  at the center of the plate are provided in Figures 7.55, 7.56 and 7.57, respectively. All three figures show a good agreement between RBF and FEM

solutions. The RBF results compare very well with the FEM results with maximum relative differences of 4.4%, 5.8% and 5.7% for  $\bar{w}$ ,  $\bar{\sigma}_b$  and  $\bar{\sigma}_m$  respectively.

Table 7.20 CISF1MO Results of  $\bar{w}$ ,  $\bar{\sigma}_b$ ,  $\bar{\sigma}_m$  at Load  $\bar{q} = 2$

Foundation Parameters			$\bar{w}$			$\bar{\sigma}_b$			$\bar{\sigma}_m$		
K	K1	G1	FEM	RBF	Error %	FEM	RBF	Error %	FEM	RBF	Error %
0	0	0	1.255	1.269	1.133	1.799	1.867	3.804	0.286	0.2950	3.1469
0	0	1.5	1.016	0.999	1.642	1.491	1.479	0.808	0.198	0.2030	2.5253
0	0	3	0.843	0.817	3.069	1.249	1.215	2.737	0.140	0.1460	4.2857
0	10	0	1.022	0.988	3.274	1.451	1.410	2.847	0.199	0.2053	3.1658
0	10	1.5	0.886	0.861	2.757	1.280	1.249	2.361	0.153	0.1590	3.9216
0	10	3	0.769	0.774	0.627	1.121	1.142	1.810	0.116	0.1170	0.8621
0	20	0	0.915	0.934	2.058	1.281	1.336	4.273	0.161	0.1570	2.4845
0	20	1.5	0.812	0.831	2.290	1.157	1.206	4.211	0.129	0.1260	2.3256
0	20	3	0.720	0.737	2.271	1.036	1.077	3.963	0.102	0.1000	1.9608
10	0	0	0.938	0.914	2.526	1.373	1.348	1.887	0.173	0.1950	12.7168
10	0	1.5	0.786	0.757	3.755	1.158	1.118	3.514	0.124	0.1270	2.4194
10	0	3	0.672	0.674	0.227	0.990	1.002	1.222	0.091	0.0911	0.1099
10	10	0	0.837	0.833	0.404	1.203	1.213	0.823	0.138	0.1400	1.4493
10	10	1.5	0.728	0.760	4.400	1.054	1.115	5.787	0.105	0.0990	5.7143
10	10	3	0.638	0.659	3.406	0.925	0.973	5.099	0.081	0.0780	3.7037
10	20	0	0.775	0.791	2.062	1.096	1.140	4.004	0.118	0.1150	2.5424
10	20	1.5	0.687	0.702	2.264	0.981	1.020	4.047	0.094	0.0910	3.1915
10	20	3	0.611	0.621	1.612	0.876	0.903	3.166	0.074	0.0730	1.3514
20	0	0	0.738	0.709	3.904	1.078	1.039	3.636	0.110	0.1210	10.0000
20	0	1.5	0.636	0.662	4.215	0.926	0.980	5.852	0.082	0.0790	3.6585
20	0	3	0.556	0.573	3.041	0.806	0.843	4.634	0.062	0.0600	3.2258
20	10	0	0.691	0.711	2.890	0.991	1.038	4.671	0.096	0.0920	4.1667
20	10	1.5	0.607	0.624	2.823	0.872	0.911	4.553	0.074	0.0720	2.7027
20	10	3	0.538	0.545	1.247	0.771	0.792	2.717	0.058	0.0581	0.1724
20	20	0	0.656	0.668	1.765	0.928	0.961	3.559	0.086	0.0840	2.3256
20	20	1.5	0.584	0.590	1.011	0.829	0.850	2.575	0.068	0.0681	0.1471
20	20	3	0.523	0.546	4.256	0.742	0.770	3.774	0.054	0.0530	1.8519

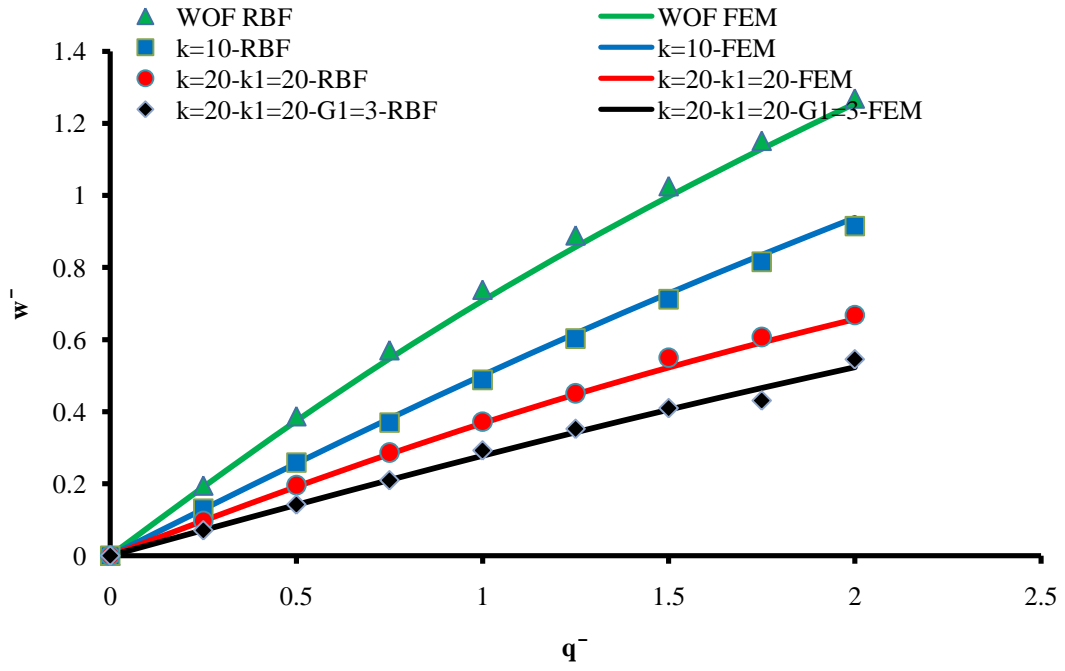


Figure 7.55  $\bar{w}$  vs  $\bar{q}$  on Different Foundations for CISF1MO

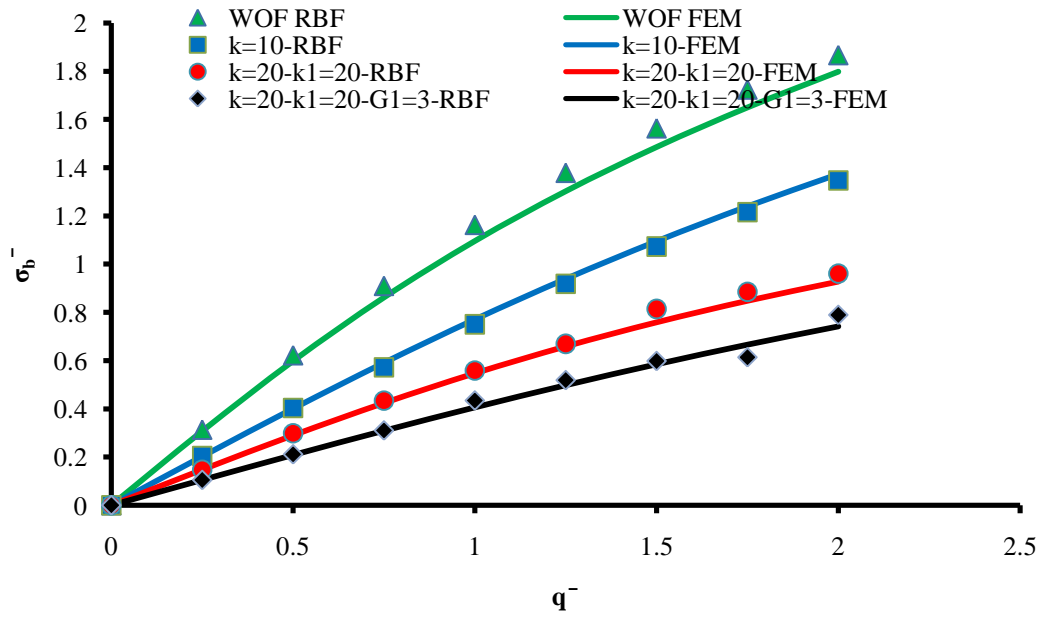


Figure 7.56  $\bar{\sigma}_b$  vs  $\bar{q}$  on Different Foundations for CISF1MO

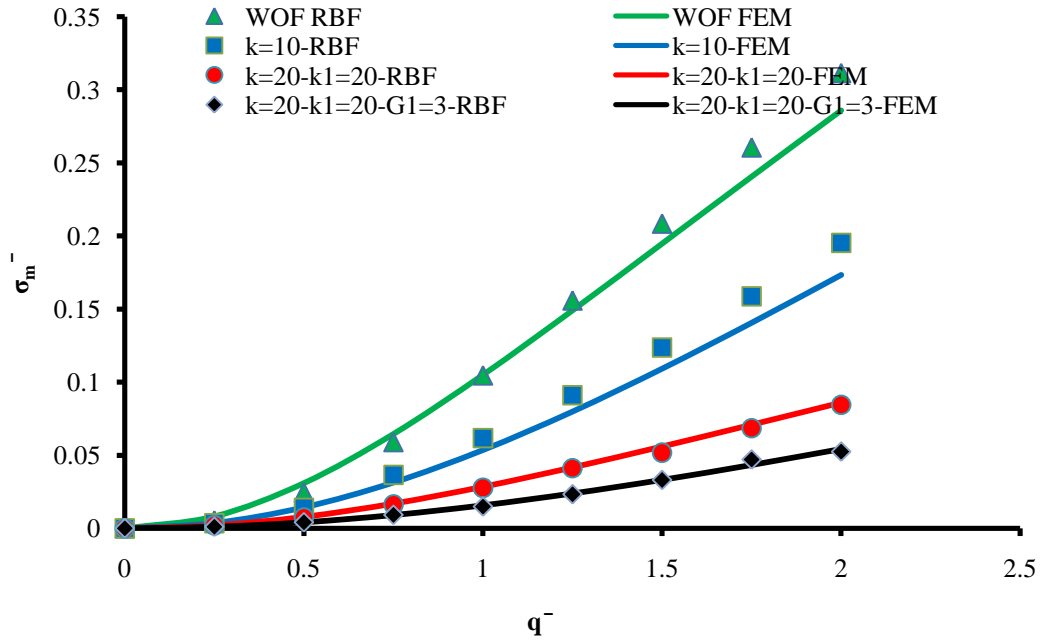


Figure 7.57  $\bar{\sigma}_m$  vs  $\bar{q}$  on Different Foundations for CISFIMO

### 7.2.5 WPF Small Deflection and Large Deflection Analyses

In this section, the comparison of the results obtained from the large deflection and small deflection analyses theories is presented. The small deflection theory is mainly the classical plate bending theory which does not take the effect of the in-plane deformation into account which means that the nonlinear terms were removed from the previous formulations and corresponding codes. Two different examples have been done, square (SQCCIM) and circular (CICCMO). The two examples are similar to the previous ones done before in terms of the nodes distributions, loads, foundation parameters, etc.

The comparison results are given in Figures 7.58 to 7.61 for  $\bar{w}$ , and  $\bar{\sigma}_b$  versus  $\bar{q}$  for both SQCCIM and CICCMO. Figures 7.58 and 7.59 are for SQCCIM for both

$\bar{w}$ , and  $\bar{\sigma}_b$  respectively whereas Figures 7.60 and 7.61 are for CICCIMO for  $\bar{w}$ , and  $\bar{\sigma}_b$  respectively as well. In the shown figures, different foundation models have been selected depending on the foundation parameters values adopted in those examples. The letters S and L are provided for the designation of small and large deflection theory analysis.

From the shown figures, it is clear that the difference between the large deflection analysis theory and the small deflection theory are high in SQCCIM compared to CICCIMO because of the in-plane boundary condition, immovable and movable respectively. In addition, the presence of the foundations makes the difference between the two theories smaller in both examples.

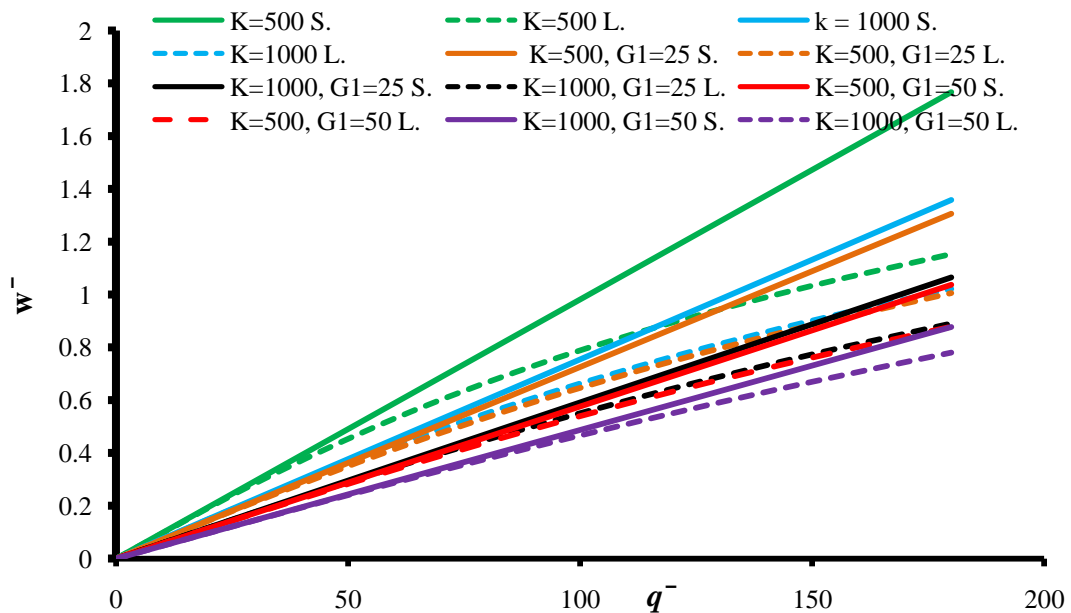


Figure 7.58 Comparison between Small Deflection (S) and Large Deflection (L) Formulations for the Central Deflection of SQCCIM Plate on Different Foundations

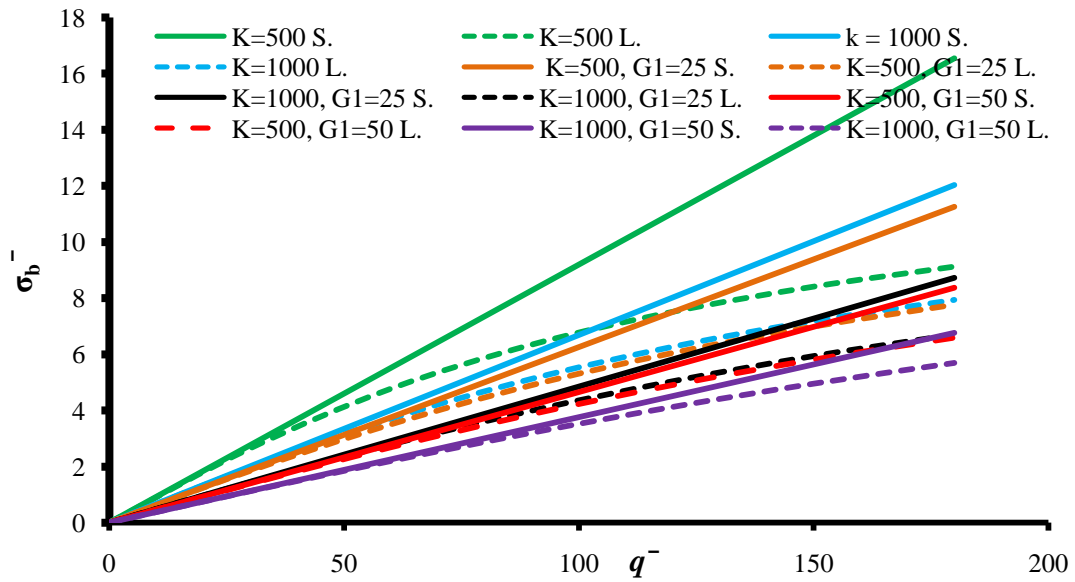


Figure 7.59 Comparison between Small Deflection (S) and Large Deflection (L) Formulations for the Maximum Bending Stress in SQCCIM Plate on Different Foundations

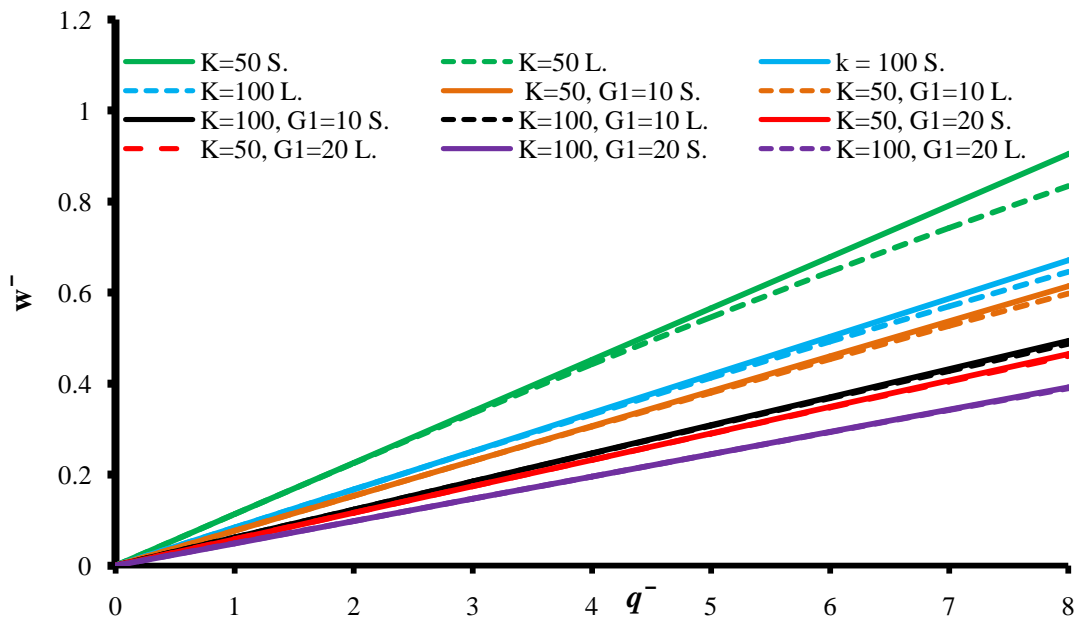


Figure 7.60 Comparison between Small Deflection (S) and Large Deflection (L) Formulations for the Central Deflection of CICCIMO Plate on Different Foundations



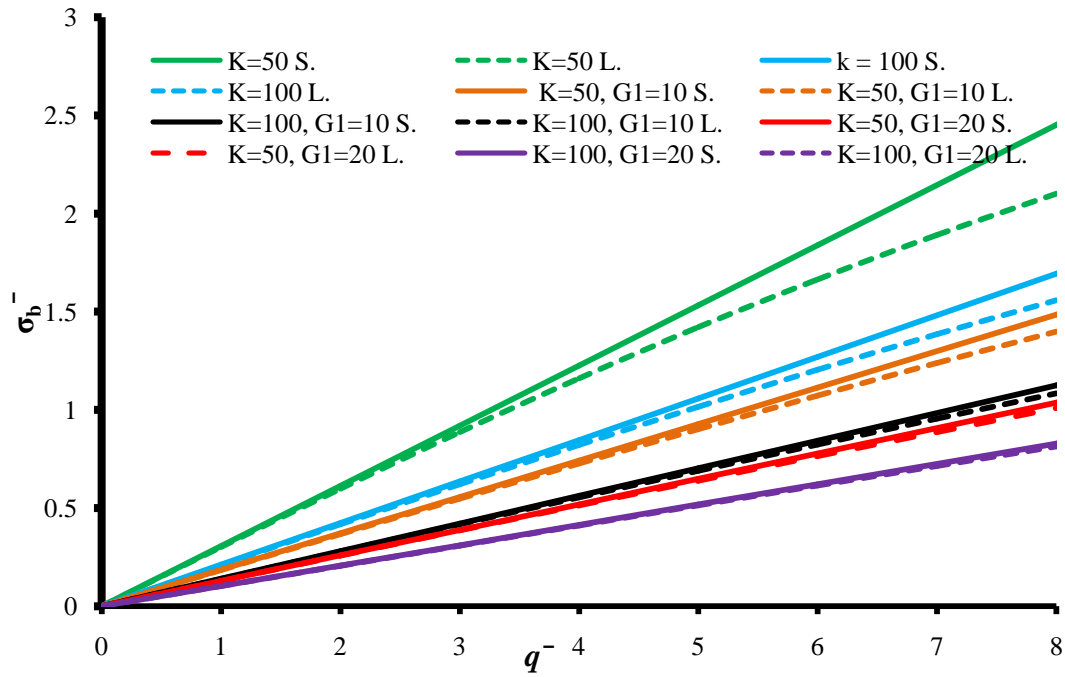


Figure 7.61 Comparison between Small Deflection (S) and Large Deflection (L) Formulations for the Maximum Bending Stress in CICCMO Plate on Different Foundations

### 7.2.6 WPF Comparing Results with Available Case

For more verification for the proposed method and codes in this work, the obtained results using MQ-RBF for one example (CICCMO) has been compared to the obtained results by Katsikadelis (1991) using the boundary element method (BEM). The results of the comparisons are given in Table 7.21. In Table 7.21, the variations of the deflection  $\bar{w}$ , the radial membrane stress  $\bar{\sigma}_m$ , and the radial bending stress  $\bar{\sigma}_b$  due to the maximum load of  $\bar{q} = 15$  and the foundation parameters  $G_1=K_1=0$ ;  $K=100$  at various radial locations are presented. The table shows a reasonable agreement between RBF and BEM by Katsikadelis (1991) solutions for the deflection with a maximum difference of

(1.18%), (1.64%) and (7.50%)  $\bar{w}$ ,  $\bar{\sigma}_b$  and,  $\bar{\sigma}_m$  respectively.

Table 7.21 Comparison Between RBF and BEM for CICC MO ( $\bar{q} = 15$ ,  $G_1=K_1=0$ ;

$K=100$ )

r/a	$\bar{w}$		Diff. %	$\bar{\sigma}_b$		Diff. %	$\bar{\sigma}_m$		Diff. %
	KAT.	RBF		KAT.	RBF		KAT.	RBF	
0.098	1.108	1.104	0.361	2.547	2.567	0.785	0.536	0.518	3.358
0.304	0.961	0.956	0.520	2.366	2.381	0.634	0.470	0.453	3.617
0.562	0.592	0.585	1.182	1.277	1.256	1.644	0.303	0.292	3.630
0.800	0.179	0.178	0.559	-1.820	-1.793	1.484	0.127	0.120	5.512
0.960	0.009	0.009	0.000	-5.490	-5.446	0.801	0.040	0.037	7.500

## CHAPTER EIGHT

# VERIFICATION OF THE COMPUTER CODE FOR LARGE DEFLECTION OF THIN PLATE ON ELASTIC CONTINUOUS FOUNDATION

### 8.1 General

In this Chapter, the verification of the proposed RBF method as applied to large deflection of thin plates on elastic continuous foundations is presented. In all examples, the load is assumed to be uniformly distributed =  $q$ , Poisson ratio  $\nu$  is assumed 0.3 and the analysis is performed for several combinations of the foundation parameters and boundary conditions. For generality of the solutions, all results are made dimensionless, so that the coordinates, the load, the deflection, and the stress are represented by  $\bar{x} = \frac{x}{a}, \bar{y} = \frac{y}{a}, \bar{q} = \frac{qa^4}{Et^4}, \bar{w} = \frac{w}{t}, \bar{\sigma} = \frac{\sigma a^2}{Et^2}$ , respectively. The shape factor,  $c$ , of the RBF is changed according to the boundary conditions, the geometry, and the type of foundation models. Its optimum value ranges between 0.1 and 0.8.

As explained in the Chapter 3 and 4, plate-foundation interaction is based on Boussinesq's solution of the elastic half-space. Both RBF and Boussinesq's solutions are dependent on the radial distances between nodes which makes coupling of the two methods advantageous for modeling the interaction. The FEM model used for verification of the results is according to the approach due to [Kukreti and Ko1992].

[Kukreti and Ko1992] have reported that the soil boundary can be truncated at  $10 \cdot a$  in the vertical direction and  $3 \cdot a$  in the horizontal direction where  $a$  is the plate dimension. The 3D configuration is shown in Figure 8.1. The boundary conditions of the soil domain are represented by zero normal displacement at the bottom and sides and by zero traction at the top free surface.

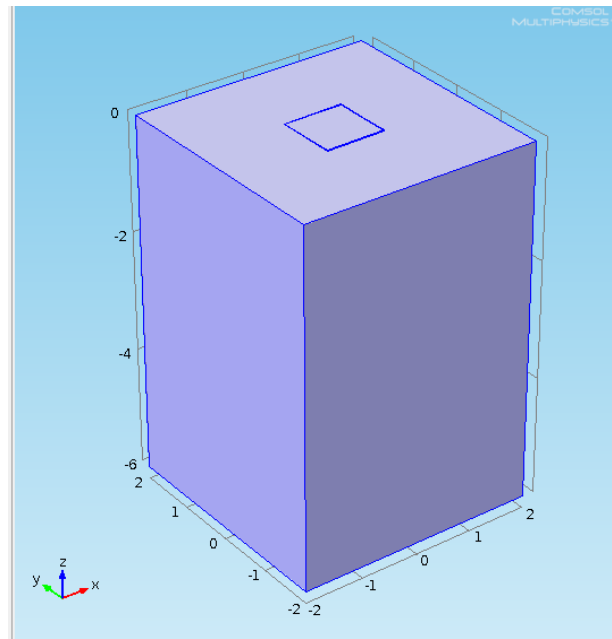


Figure 8.1 3D FEM Square Plate on Elastic Half Space Soil Model

The Mathematica codes developed earlier for the discrete foundation models have been modified to implement the procedure explained in Chapter 4 for modeling the plate-continuous foundation interaction.

The following section presents RBF results of several examples for plates on continuous foundations with different boundary conditions along with their comparisons with FEM results

## 8.2 Numerical Examples for Plates on Continuous Foundations

- SQCCIM

In this example, a clamped immovable square plate ( $w = \frac{\partial w}{\partial n} = u = v = 0.0$ ), resting on an isotropic elastic half space soil with Boussinesq dimensions is considered. The analysis is performed for two different values of soil Young's modulus,  $E_s = 10000$  and  $40000 \frac{\text{kN}}{\text{m}^2}$  and Poisson ratio  $\nu_s = 0.35$  whereas the Young's modulus and the Poisson ratio of the plate are  $10^8 \text{kN/m}^2$  and  $0.3$  respectively and the thickness,  $t = 0.01$ . The plate is subjected to a uniform dimensionless loads,  $\bar{q}$ , ranging from 50 to 400 with an increment of 50. The results of both FEM and RBF for the non-dimensional deflection,  $\bar{w}$ , bending stresses,  $\bar{\sigma}_b$ , and membrane stresses,  $\bar{\sigma}_m$ , at the center of the plate are given in Table 8.1. The RBF results compare very well against FEM results with maximum differences of 3.2%, 4.8% and 4.4% for  $\bar{w}$ ,  $\bar{\sigma}_b$ , and  $\bar{\sigma}_m$  respectively.

Table 8.1  $\bar{w}$ ,  $\bar{\sigma}_b$ , and  $\bar{\sigma}_m$  at the Center of SQCCIM Plate on Continuous Foundation

$E_s$ * $10^4$	$\bar{q}$	$\bar{w}$		Error %	$\bar{\sigma}_b$		Error %	$\bar{\sigma}_m$		Error %
		FEM	RBF		FEM	RBF		FEM	RBF	
1	50	0.2071	0.2028	2.0628	1.4936	1.4746	1.2739	0.1373	0.1368	0.3409
	100	0.4049	0.3965	2.0828	2.8809	2.8556	0.8760	0.5248	0.5255	0.1298
	150	0.5878	0.5777	1.7241	4.1010	4.1106	0.2344	1.1054	1.1152	0.8884
	200	0.7539	0.7434	1.3979	5.1440	5.2128	1.3379	1.8173	1.8470	1.6315
	250	0.9039	0.8937	1.1262	6.0291	6.1687	2.3152	2.6113	2.6707	2.2732
	300	1.0396	1.0300	0.9177	6.7845	6.9955	3.1109	3.4532	3.5496	2.7916
	350	1.1629	1.1539	0.7782	7.4369	7.7121	3.7000	4.3209	4.4593	3.2023
	400	1.2758	1.2685	0.5722	8.0086	8.3571	4.3516	5.2006	5.3979	3.7934
4	50	0.0622	0.0638	2.6404	0.1480	0.1530	3.3504	0.0137	0.0131	4.3163
	100	0.1243	0.1282	3.1485	0.2966	0.3050	2.8390	0.0547	0.0523	4.3666
	150	0.1862	0.1898	1.9302	0.4461	0.4563	2.2888	0.1227	0.1175	4.2642

	200	0.2479	0.2511	1.3213	0.5970	0.6140	2.8424	0.2174	0.2082	4.2136
	250	0.3092	0.3122	0.9693	0.7498	0.7770	3.6263	0.3381	0.3240	4.1807
	300	0.3701	0.3729	0.7438	0.9048	0.9356	3.4098	0.4842	0.4644	4.0879
	350	0.4306	0.4331	0.5911	1.0622	1.1130	4.7875	0.6548	0.6287	3.9797
	400	0.4905	0.4928	0.4849	1.2222	1.2604	3.1247	0.8490	0.8162	3.8626

- SQCFIIM

In this example, the plate is a clamped one free-edge immovable square plate ( $w = \frac{\partial w}{\partial n} = (V_n \text{ and } M_n \text{ at the free edge}) = u = v = 0.0$ ) resting on isotropic elastic half space soil model with Boussinesq dimensions. The same soil and plate properties of the SQCCIM and the loads are utilized in this example. The results of both FEM and RBF for  $\bar{w}$ ,  $\bar{\sigma}_b$ , and  $\bar{\sigma}_m$  at the free edge of the plate are shown in Table 8.2 and at the center of the plate are shown in Figures 8.2, 8.3 and 8.4 respectively. All three figures show a good agreement between RBF and FEM solutions. The RBF results compare very well against FEM results with maximum differences of 6.5%, 6% and 8.4% for  $\bar{w}$ ,  $\bar{\sigma}_b$ , and  $\bar{\sigma}_m$  respectively.

Table 8.2  $\bar{w}$ ,  $\bar{\sigma}_b$ , and  $\bar{\sigma}_m$  at the Free Edge of SQCFIIM Plate on Continuous Foundation

$E_s$ * 10 <sup>4</sup>	$\bar{q}$	$\bar{w}$		Error %	$\bar{\sigma}_b$		Error %	$\bar{\sigma}_m$		Error %
		FEM	RBF		FEM	RBF		FEM	RBF	
1	50	0.2539	0.2403	5.3521	1.4635	1.5131	3.3842	0.0260	0.0277	6.2195
	100	0.4929	0.4657	5.5164	2.8746	3.0182	4.9954	0.0982	0.1031	5.0216
	150	0.7097	0.6674	5.9542	4.2069	4.3629	3.7078	0.2035	0.2154	5.8411
	200	0.9037	0.8564	5.2302	5.4577	5.7814	5.9323	0.3297	0.3542	7.4404
	250	1.0775	1.0142	5.8733	6.6344	6.9177	4.2709	0.4677	0.5069	8.3956
	300	1.2343	1.1694	5.2588	7.7463	8.1153	4.7636	0.6117	0.6547	7.0333
	350	1.3769	1.3026	5.3984	8.8015	9.1540	4.0051	0.7581	0.7976	5.2089
	400	1.5078	1.4143	6.2026	9.8066	10.2540	4.5620	0.9048	0.9456	4.5112

4	50	0.0698	0.0664	5.0045	0.0820	0.0867	5.6397	0.0033	0.0016	53.0005
	100	0.1396	0.1319	5.4938	0.1671	0.1750	4.7739	0.0133	0.0064	52.1566
	150	0.2091	0.1972	5.7257	0.2580	0.2730	5.8080	0.0298	0.0140	52.9237
	200	0.2784	0.2622	5.7956	0.3576	0.3765	5.2972	0.0527	0.0248	52.8871
	250	0.3472	0.3281	5.5153	0.4681	0.4951	5.7743	0.0818	0.0393	51.9559
	300	0.4156	0.3898	6.2157	0.5916	0.6234	5.3814	0.1169	0.0564	51.7948
	350	0.4835	0.4522	6.4735	0.7297	0.7654	4.8989	0.1578	0.0762	51.7235
	400	0.5508	0.5205	5.5005	0.8836	0.9210	4.2383	0.2040	0.0987	51.6279

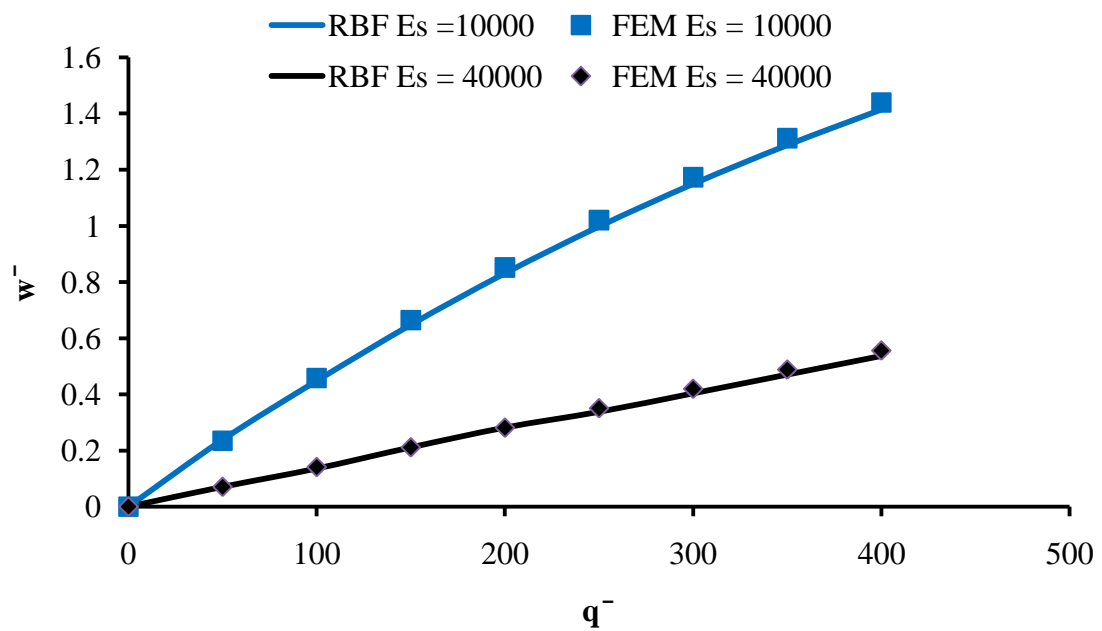


Figure 8.2 Load-Central Deflections for SQCF1IM Plate on Continuous Foundation

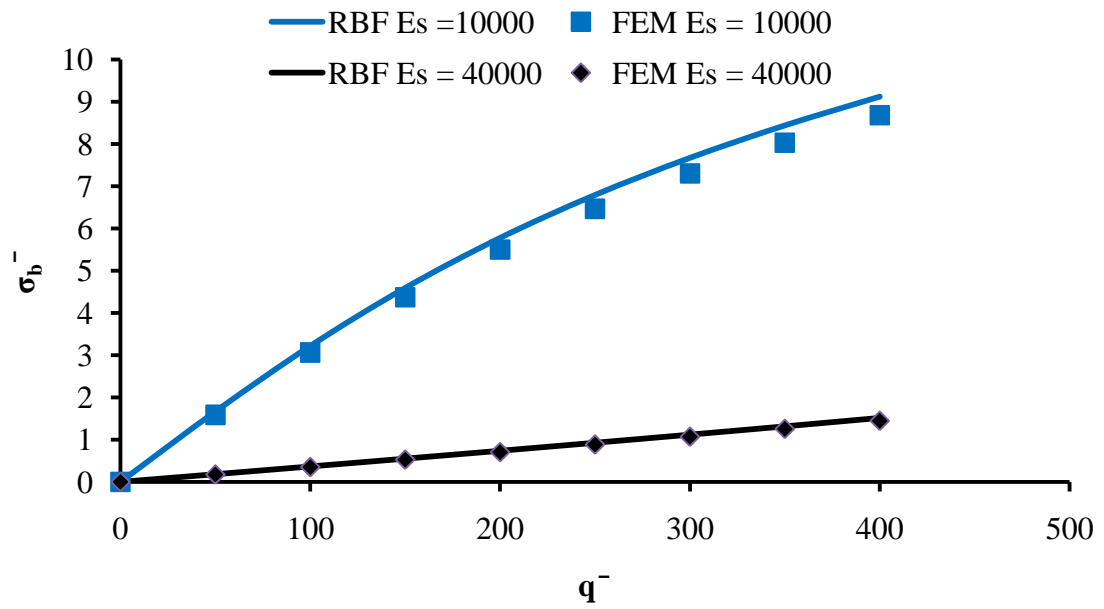


Figure 8.3 Loads-Central Bending Stresses for SQCF1IM Plate on Continuous Foundation

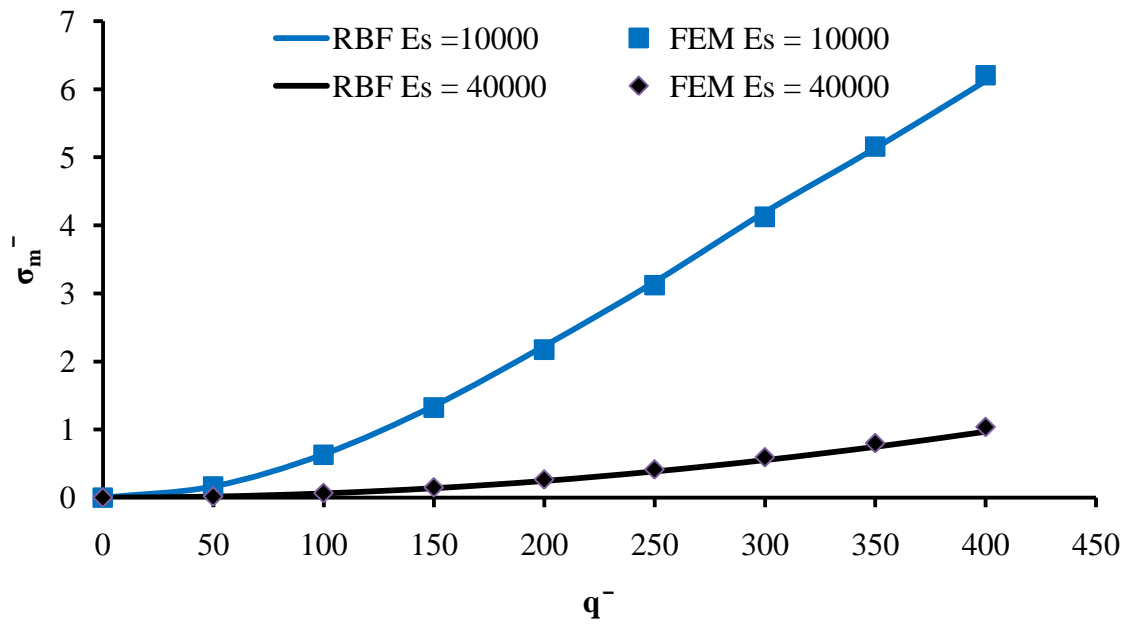


Figure 8.4 Loads-Central Membrane Stresses for SQCF1IM Plate on Continuous Foundation



- SQCFIM

This example presents a plate with a clamped two free-edges immovable square plate ( $w = \frac{\partial w}{\partial n} = (V_n \text{ and } M_n \text{ at the free edges}) = u = v = 0.0$ ), resting on isotropic elastic half space soil model with Boussinesq dimensions. The same soil and plate properties of the SQCCIM whereas the loads ranging from 40 to 320. The results of both FEM and RBF for  $\bar{w}$ , and  $\bar{\sigma}_b$ , at the free edge of the plate are shown in Table 8.3 and at the center of the plate are shown in Figures 8.5, 8.6, and 8.7 respectively. All three figures show a good agreement between RBF and FEM solutions. The RBF results compare well against FEM results with maximum differences of 8.3%, 6.7% and more for  $\bar{w}$ , and  $\bar{\sigma}_b$  respectively.

Table 8.3  $\bar{w}$ ,  $\bar{\sigma}_b$ , and  $\bar{\sigma}_m$  at the Free Edge of SQCFIM Plate on Continuous Foundation

$E_s$ * $10^4$	$\bar{q}$	$\bar{w}$		Error %	$\bar{\sigma}_b$		Error %
		FEM	RBF		FEM	RBF	
1	40	0.2290	0.2333	1.8772	1.3848	1.4530	4.9239
	80	0.4459	0.4353	2.3789	2.7212	2.9030	6.6821
	120	0.6439	0.6130	4.7912	3.9823	4.2540	6.8225
	160	0.8221	0.7642	7.0414	5.1633	5.4897	6.3206
	200	0.9823	0.9342	4.8999	6.2705	6.6055	5.3419
	240	1.1271	1.0632	5.6702	7.3131	7.7630	6.1514
	280	1.2590	1.1822	6.0981	8.3002	8.8655	6.8117
	320	1.3801	1.2670	8.1922	9.2391	9.7650	5.6925
4	40	0.0646	0.0624	3.5359	0.1132	0.1170	3.3598
	80	0.1292	0.1198	7.2582	0.2285	0.2437	6.6295
	120	0.1935	0.1824	5.7505	0.3481	0.3665	5.2744
	160	0.2576	0.2345	8.9695	0.4739	0.5012	5.7581
	200	0.3213	0.2976	7.3836	0.6076	0.6437	5.9369
	240	0.3846	0.3528	8.2714	0.7508	0.7965	6.0864
	280	0.4474	0.4165	6.9070	0.9047	0.9543	5.4814
	320	0.5096	0.4797	5.8740	1.0703	1.1340	5.9476

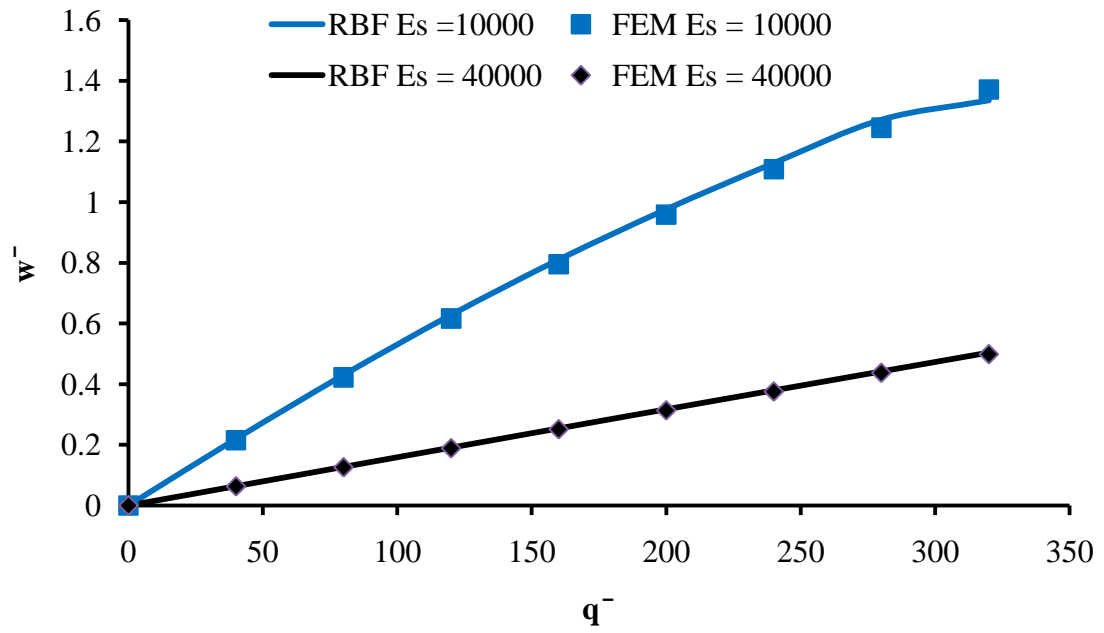


Figure 8.5 Loads-Central Deflections for SQCFIM Plate on Continuous Foundation

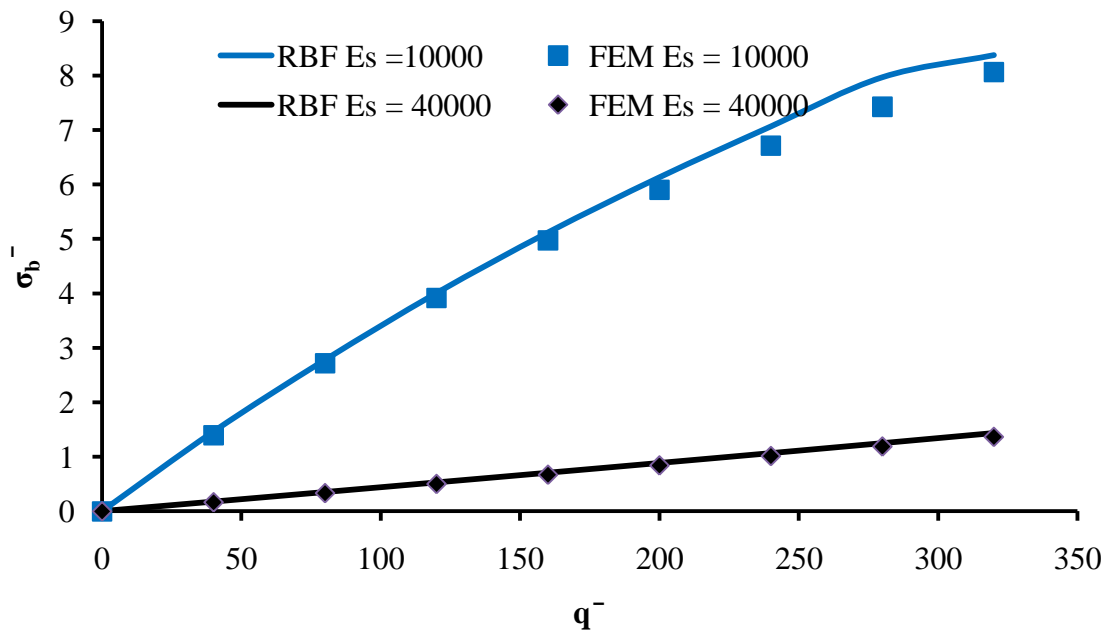


Figure 8.6 Loads-Central Bending Stresses for SQCFIM Plate on Continuous Foundation

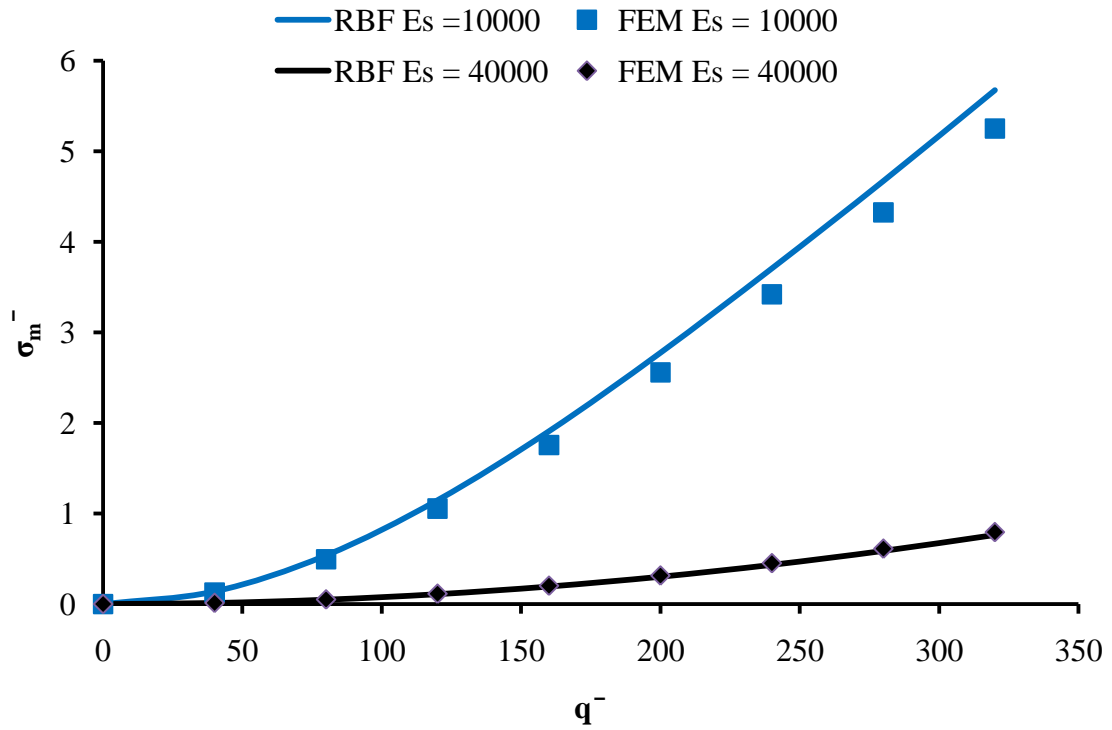


Figure 8.7 Loads-Central Membrane Stresses for SQCFIM Plate on Continuous Foundation

- CICCIM

This example is similar to SQCCIM with a circular shape. It has been exposed to uniform loads,  $\bar{q}$ , ranging from 25 to 200 with incremental loads of 25 increment. The results of both FEM and RBF for  $\bar{w}$ ,  $\bar{\sigma}_b$ , and  $\bar{\sigma}_m$  at the center of the plate are shown in Table 8.4. The RBF results compare very well against FEM results with maximum differences of 5.7%, 5.02% and 5.5% for  $\bar{w}$ ,  $\bar{\sigma}_b$ , and  $\bar{\sigma}_m$  respectively.

Table 8.4  $\bar{w}$ ,  $\bar{\sigma}_b$ , and  $\bar{\sigma}_m$  at the Center of CICCIM Plate on Continuous Foundation

$E_s$ * $10^4$	$\bar{q}$	$\bar{w}$		Error %	$\bar{\sigma}_b$		Error %	$\bar{\sigma}_m$		Error %
		FEM	RBF		FEM	RBF		FEM	RBF	
1	25	0.2429	0.2506	3.1799	0.0336	0.0346	2.9149	0.0705	0.0712	1.0216
	50	0.4829	0.5048	4.5421	0.0892	0.0903	1.2332	0.2766	0.2876	3.9618

	75	0.7175	0.6981	2.7081	0.1808	0.1860	2.8647	0.6044	0.6123	1.3054
	100	0.9446	0.8702	7.8744	0.3120	0.3254	4.3082	1.0350	1.0470	1.1633
	125	1.1627	1.1163	3.9890	0.4780	0.4902	2.5609	1.5487	1.6340	5.5085
	150	1.3709	1.2922	5.7442	0.6703	0.6897	2.8988	2.1277	2.2130	4.0090
	175	1.5690	1.5044	4.1204	0.8799	0.8991	2.1867	2.7568	2.8980	5.1215
	200	1.7571	1.6670	5.1283	1.0990	1.1542	5.0275	3.4237	3.5520	3.7465
4	25	0.0622	0.0643	3.3430	-0.0367	-0.0375	2.2913	0.0077	0.0080	3.7468
	50	0.1245	0.1304	4.7642	-0.0730	-0.0756	3.6326	0.0309	0.0321	3.8163
	75	0.1868	0.1954	4.6319	-0.1085	-0.1108	2.1481	0.0695	0.0720	3.6717
	100	0.2491	0.2601	4.4201	-0.1429	-0.1481	3.6534	0.1231	0.1281	4.0364
	125	0.3115	0.3273	5.0722	-0.1758	-0.1812	3.0541	0.1917	0.2013	4.9969
	150	0.3740	0.3954	5.7248	-0.2070	-0.2161	4.3961	0.2749	0.2864	4.1682
	175	0.4366	0.4595	5.2409	-0.2361	-0.2460	4.1976	0.3724	0.3901	4.7445
	200	0.4993	0.5264	5.4360	-0.2628	-0.2728	3.7933	0.4838	0.5102	5.4590

- CICF11M

In this example the plate is a clamped one free-edge immovable circular plate ( $w = \frac{\partial w}{\partial n} = (V_n \text{ and } M_n \text{ at the free edge}) = u = v = 0.0$ ), resting on isotropic elastic half space soil model with Boussinesq dimensions. It has been analyzed under loads ranging from 30 to 240. The results of both FEM and RBF for  $\bar{w}$ , and  $\bar{\sigma}_b$ , at the free edge of the plate are shown in Table 8.5 and at the center of the plate including  $\bar{\sigma}_m$ , are shown in Figures 8.8, 8.9, and 8.10 respectively. All three figures show a good agreement between RBF and FEM solutions. The RBF results compare well against FEM results with maximum differences of 9%, and 8.7% for  $\bar{w}$ , and  $\bar{\sigma}_b$ , respectively.

Table 8.5  $\bar{w}$ , and  $\bar{\sigma}_b$  at the Free Edge of CICF1IM Plate on Continuous Foundation

$E_s$ $\times 10^4$	$\bar{q}$	$\bar{w}$		Error %	$\bar{\sigma}_b$		Error %
		FEM	RBF		FEM	RBF	
1	30	0.3103	0.3240	4.4062	0.2051	0.2103	2.5226
	60	0.6131	0.6371	3.9122	0.4230	0.4378	3.4994
	90	0.9031	0.9432	4.4352	0.6596	0.6856	3.9393
	120	1.1779	1.2520	6.2910	0.9135	0.9345	2.3002
	150	1.4367	1.5320	6.6321	1.1791	1.2530	6.2694
	180	1.6800	1.7853	6.2706	1.4502	1.5020	3.5723
	210	1.9085	2.0340	6.5765	1.7217	1.8317	6.3889
	240	2.1234	2.3210	9.3055	1.9900	2.1630	8.6956
4	30	0.0822	0.0834	1.4535	0.0018	0.0019	5.3356
	60	0.1644	0.1734	5.4666	0.0042	0.0044	4.1354
	90	0.2466	0.2655	7.6544	0.0078	0.0082	4.5342
	120	0.3288	0.3510	6.7405	0.0132	0.0140	6.3544
	150	0.4110	0.4331	5.3653	0.0207	0.0221	6.8105
	180	0.4933	0.5213	5.6867	0.0309	0.0326	5.6656
	210	0.5754	0.6012	4.4770	0.0440	0.0477	8.3989
	240	0.6576	0.6873	4.5173	0.0604	0.0643	6.3973

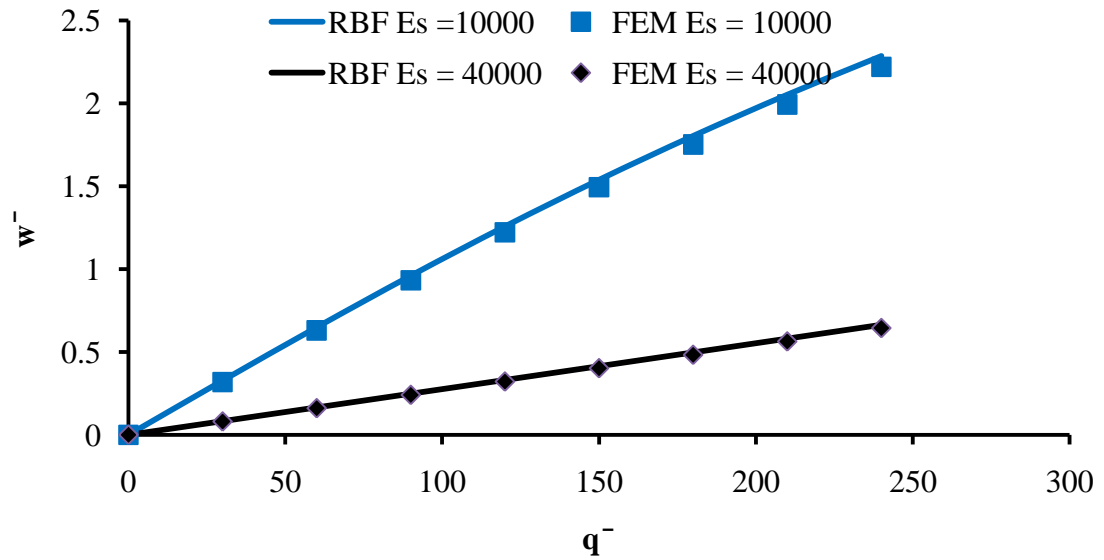


Figure 8.8 Loads-Central Deflections for CICF1IM Plate on Continuous Foundation

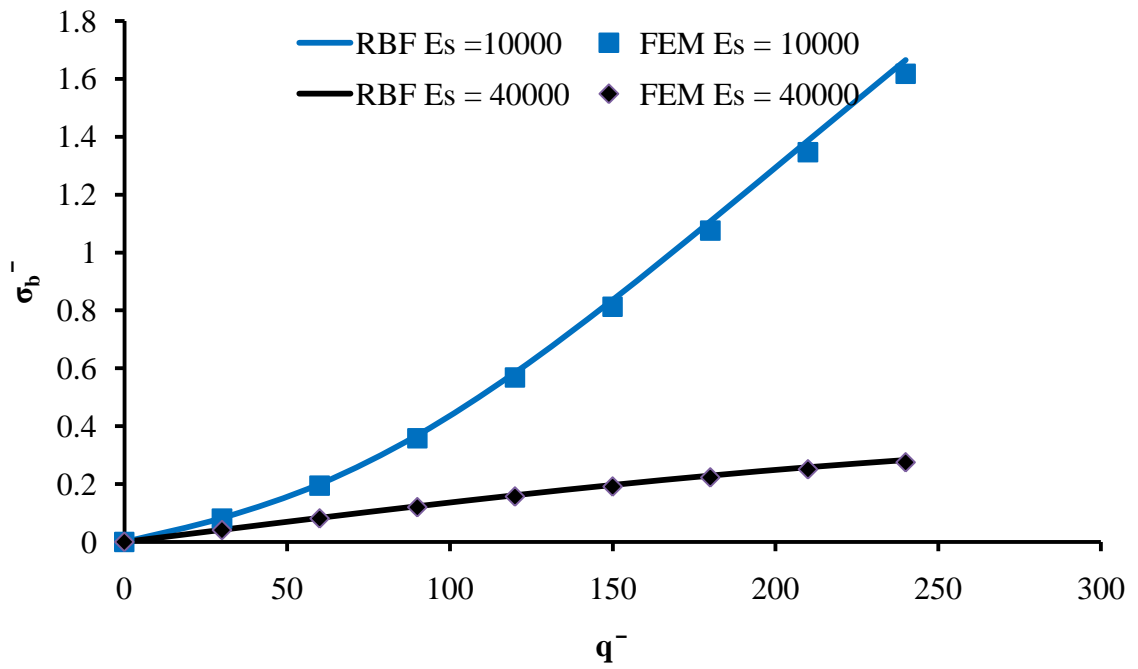


Figure 8.9 Loads-Central Bending Stresses for CICF1IM Plate on Continuous Foundation

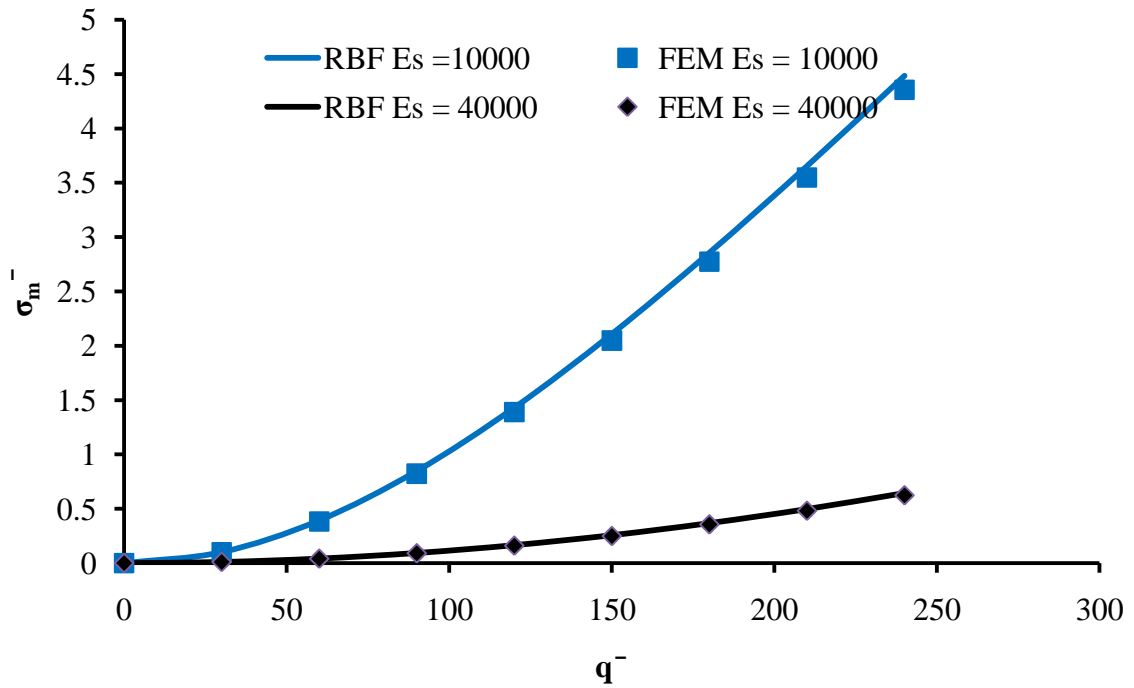


Figure 8.10 Loads-Central Membrane Stresses for CICF1IM Plate on Continuous Foundation

- CICFIM

The plate in this example is a clamped two free-edges immovable circular plate ( $w = \frac{\partial w}{\partial n} = (V_n \text{ and } M_n \text{ at the free edges}) = u = v = 0.0$ ), resting on isotropic elastic half space soil model with Boussinesq dimensions. The same soil and plate properties of the SQCCIM whereas the loads ranging from 20 to 160. The results of both FEM and RBF for  $\bar{w}$ , and  $\bar{\sigma}_b$  at the free edge of the plate are shown in Table 8.6 and at the center of the plate including  $\bar{\sigma}_m$  are shown in Figures 8.11, 8.12 and 8.13 respectively. All three figures show a good agreement between RBF and FEM solutions. The RBF results compare well against FEM results with maximum differences of 7.8%, and 8.7% for  $\bar{w}$ , and  $\bar{\sigma}_b$  respectively.

Table 8.6  $\bar{w}$ , and  $\bar{\sigma}_b$  at the Free Edge of CICFIM Plate on Continuous Foundation

$E_s$ * $10^4$	$\bar{q}$	$\bar{w}$		Error %	$\bar{\sigma}_b$		Error %
		FEM	RBF		FEM	RBF	
1	20	0.2236	0.2315	3.5276	0.1552	0.1604	3.3609
	40	0.4440	0.4589	3.3474	0.3157	0.3271	3.6138
	60	0.6587	0.6871	4.3143	0.4851	0.5017	3.4256
	80	0.8658	0.8978	3.6920	0.6645	0.6865	3.3123
	100	1.0646	1.1290	6.0509	0.8529	0.8860	3.8797
	120	1.2546	1.3260	5.6891	1.0482	1.1240	7.2327
	140	1.4360	1.5250	6.1959	1.2478	1.3270	6.3484
	160	1.6091	1.7350	7.8255	1.4493	1.5432	6.4784
4	20	0.0593	0.0615	3.6677	0.0028	0.0030	5.4850
	40	0.1186	0.1248	5.1853	0.0059	0.0062	3.8355
	60	0.1780	0.1906	7.0967	0.0095	0.0102	7.3048
	80	0.2373	0.2501	5.3986	0.0138	0.0148	7.2801
	100	0.2966	0.3149	6.1680	0.0190	0.0205	7.8695
	120	0.3559	0.3751	5.3904	0.0254	0.0274	7.7062
	140	0.4152	0.4423	6.5231	0.0331	0.0360	8.7792

	160	0.4745	0.5078	7.018	0.0423	0.0456	7.8814
--	-----	--------	--------	-------	--------	--------	--------

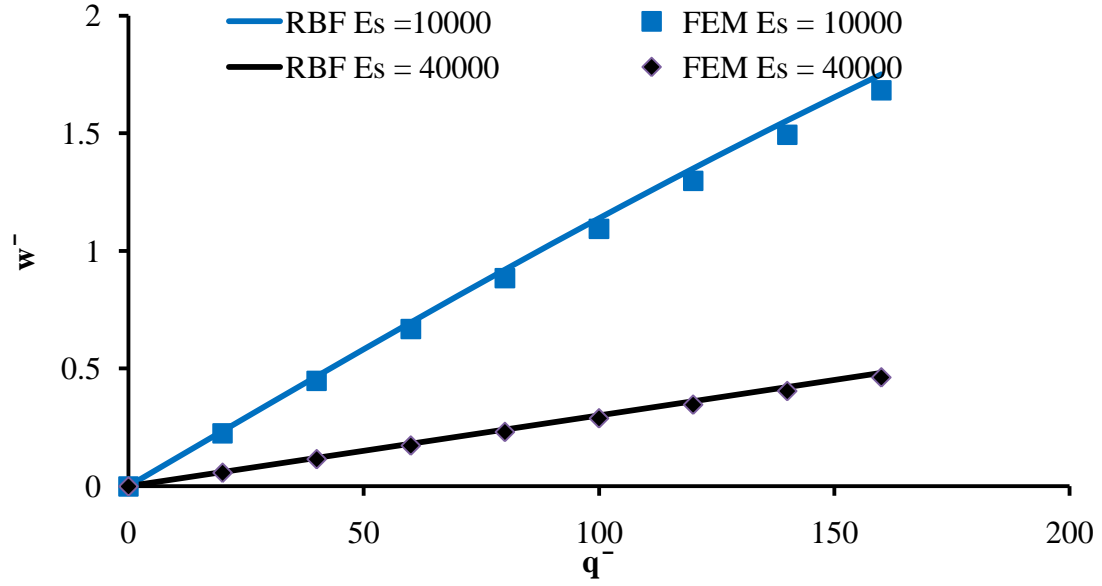


Figure 8.11 Loads-Central Deflections for CICFIM Plate on Continuous Foundation

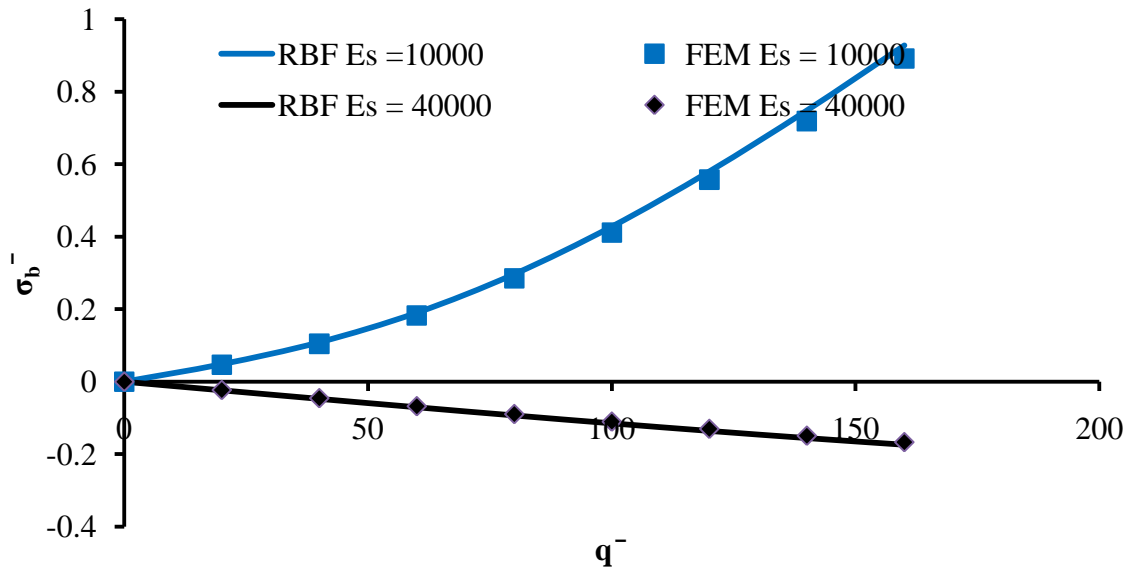


Figure 8.12 Loads-Central Bending Stresses for CICFIM Plate on Continuous Foundation



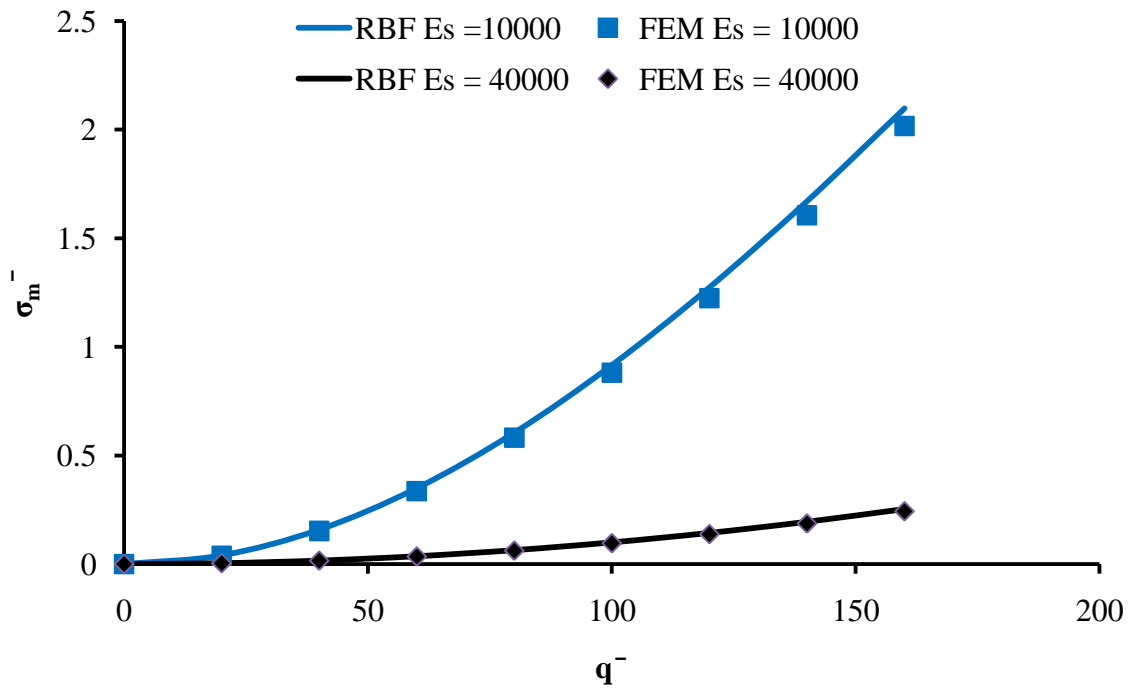


Figure 8.13 Loads-Central Membrane Stresses for CICFIM Plate on Continuous Foundation

## CHAPTER NINE

# CORRELATIONS BETWEEN DISCRETE AND CONTINUOUS FOUNDATION MODELS

### 9.1 General

The analyses performed in the previous two chapters clearly show that the task of modeling the soil-plate interaction using discrete models is much easier than by using the continuous model. Furthermore, the discrete models constants  $k$ ,  $k_1$  and  $g_p$  are difficult to characterize.

On the other hand, the soil parameters of elastic continuous models, Young's modulus  $E_s$  and Poisson's Ratio  $\nu_s$  are easy to find. So, it is a matter of importance to try to get some relationships that can relate the Winkler-Pasternak model parameters ( $k$ ,  $k_1$  and  $g_p$ ) to the elastic continuous model parameters ( $E_s$  and  $\nu_s$ ). From the literature survey, there was no such attempt for the large deflection of thin plate resting on foundation. This chapter contains a detailed study to obtain the required relationships.

The young's moduli of the different type of soils have been collected from the literature, geotechnical information.

([http://www.geotechnicalinfo.com/youngs\\_modulus.html](http://www.geotechnicalinfo.com/youngs_modulus.html)).

as they are as shown in Table 9-1.

Table 9.1 Young's Modulus of Different Types of Soils

Soil Type	$E_s$ (ton/sf)		$E_s$ (N/m <sup>2</sup> )	
	Min.	Max.	Min.	Max.
very soft clay	5	50	536255	5362550
soft clay	50	200	5362550	21450200
medium clay	200	500	21450200	53625500
stiff clay, silty clay	500	1000	53625500	107251000
sandy clay	250	2000	26812750	214502000
clay shale	1000	2000	107251000	214502000
loose sand	100	250	10725100	26812750
dense sand	250	1000	26812750	107251000
dense sand and gravel	1000	2000	107251000	214502000
silty sand	250	2000	26812750	214502000

The data in Table 9-1 ranges from a minimum Young's modulus of 536255 N/m<sup>2</sup> for very soft clay to a maximum Young's modulus of 214502000 N/m<sup>2</sup> for clay shale, dense sand, gravel, and silty sand. The Poisson's ratios range from 0.1 to 0.45 for most of the soil types according to the literature.

## 9.2 Study Details

In this parametric study, the values of soil Young's modulus,  $E_s$ , and Poisson's ratios,  $\nu_s$ , have been varied when conducting the analysis of large deflection of thin plate on elastic continuous soil based on Boussinesq model formula. The plate shape is square with a thickness of 0.01 m and Young's Modulus of  $10^8$  N/m<sup>2</sup> resting on the elastic

continuous soil and subjected to a uniform load. A total load of  $12 \text{ (N/m}^2\text{)}$  has been applied incrementally with step load of  $1 \text{ (N/m}^2\text{)}$ .

The analysis has been done under different values of  $E_s$  ranged from 100 to 3000  $\text{N/m}^2$  and  $\nu_s$  ranging from 0.15 to 0.45. At each value of Poisson's ratio and Young's modulus  $E_s$ , the reactions of the soil,  $P$ 's, at different locations in the plate from both the transverse and the in-plane directions and their corresponding deflections as well as  $\nabla^2 w$  values (according to Boussinesq formulas) have been collected.

The Winkler-Pasternak model parameters ( $k$ ,  $k_1$  and  $g_p$ ) have been calculated at different locations in the plate. Since the calculated parameters are almost the same at different locations of the plate with a maximum deviation of less than 5% near the boundary, only the values at the center of the plate is presented here. One sample of the collected results for the loads, deflection,  $w$ , the corresponding supporting soil reactions,  $P$ , and the corresponding Young's modulus ( $\text{N/m}^2$ ) is given in Table C-1 in Appendix C for  $\nu_s = 0.35$ .

From the collected results, the foundation parameters can be easily determined by solving the resulting linear algebra equations as they are described below for each foundation model.

### 9.2.1 Linear Winkler (L-W)

The linear Winkler foundation model is defined by  $kw$ . The soil reaction based on Boussinesq formulas is equated to the reaction based on L-W model to obtain  $k$ , i.e.

$$P - kw = 0 \Rightarrow k = \frac{P}{w} \quad (9 - 1)$$

Applying the Equation 9-1 for all cases of Table C-1 in the appendix C at  $\nu_s = 0.35$  and the other similar results for the other Poisson's ratios, the corresponding values of the Winkler parameter  $k$  are obtained and then converted to their dimensionless values,  $K = \frac{a^4 k}{D}$ , where;  $a$  is the plate dimension and  $D$  is the plate stiffness. The results are given in Table 9-2.

Table 9.2 Results of  $K$ 's at Different Values of  $\nu_s$  and  $E_s$  for L-W

$E_s$	LW, $K$ at different values of $\nu_s$						
	0.15	0.2	0.25	0.3	0.35	0.40	0.45
100	15.6953	15.6953	15.7318	15.7685	15.8795	16.03	16.3004
200	30.9458	30.9458	31.0275	31.2751	31.6114	32.1296	33.1251
400	60.5743	60.7735	60.9741	61.5839	62.6277	64.5985	67.6746
600	89.3994	89.3994	89.7541	91.2018	93.0783	96.6583	102.344
800	117.32	117.32	117.865	119.533	123.015	127.985	136.979
1000	145.189	145.189	145.965	148.345	152.489	159.623	171.67
1200	171.762	171.762	173.844	175.978	181.546	189.962	206.362
1400	197.614	198.94	200.285	203.028	210.228	221.21	239.049
1600	226.199	226.199	227.887	231.34	238.569	252.371	272.65
1800	249.401	249.401	251.429	257.715	266.601	278.611	306.196
2000	276.278	276.278	278.723	283.745	294.352	311.839	338.634
2200	303.419	303.419	306.336	312.343	321.846	339.903	371.235
2400	327.215	327.573	330.653	337.314	349.104	369.001	403.505
2600	352.224	352.619	355.986	363.265	376.144	397.874	435.535
2800	377.037	377.47	381.124	389.02	402.985	426.538	467.34
3000	401.67	402.142	406.084	414.595	429.642	455.011	498.94

The nature of the relationship between  $K$  and  $E_s$  is linear as it is shown in Figure 9-1 for each value of  $\nu_s$ . However, the linear equation constants are functions of the Poisson's ratio,  $\nu_s$  as they are shown in Table 9-3. These functions are determined by fitting the constants values and their corresponding Poisson's ratios. The final model of L-W parameter  $K$  is given by Equation 9-2.

$$K = C_1(\nu_s)E_s + C_2(\nu_s) \quad (9 - 2)$$

Where;

$$C_1(\nu_s) = 0.547 \nu_s^2 - 0.221 \nu_s + 0.135$$

$$C_2(\nu_s) = -97.8 \nu_s^2 + 39.8 \nu_s + 5.04$$

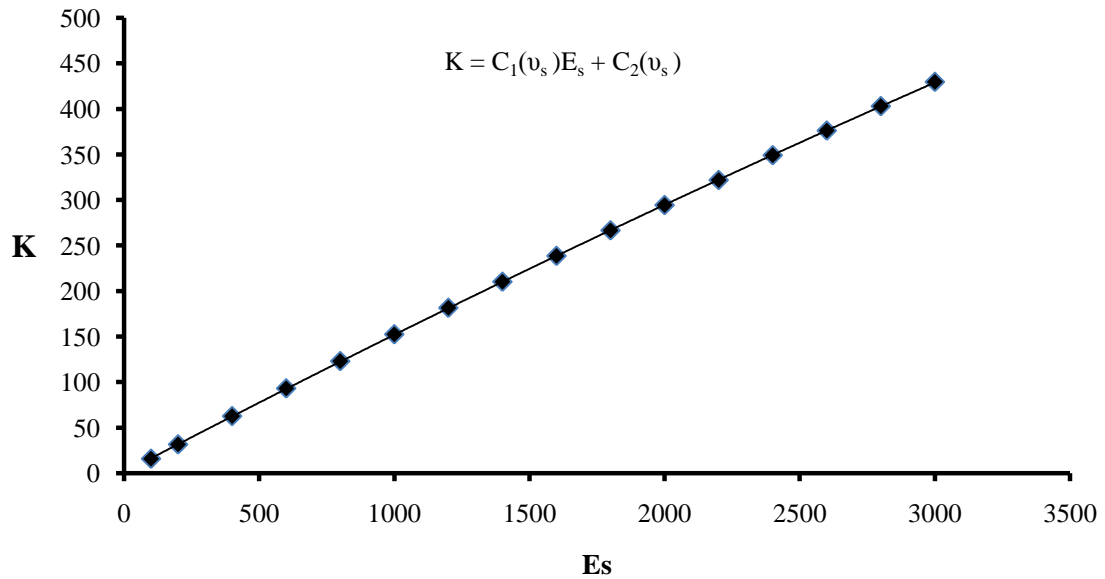


Figure 9.1  $K$  vs  $E_s$  (L-W)

Table 9.3 Poisson's Ratios and Corresponding Values of Equation Constants for L-W

$\nu_s$	$C_1$	$C_2$
0.15	0.132	8.97
0.2	0.1328	8.98
0.25	0.1343	8.64
0.3	0.1373	8.013
0.35	0.1425	7.22
0.4	0.1514	5.632
0.45	0.1669	2.85

### 9.2.2 Non-Linear Winkler (NL-W)

The foundation reaction based on the non-linear Winkler foundation model is represented by  $kw + k_1w^3$ . Equating the soil reactions as obtained from the continuous foundation model to the one corresponding to non-linear Winkler model, we get

$$P - kw - k_1w^3 = 0 \quad (9 - 3)$$

Where;  $k$  and  $k_1$  are determined by trial and error using Excel solver. Following the same procedure carried out for L-W and omitting the details, we can obtain similar relationships between NL-W model parameters and the soil elastic modulus and Poisson's ratio (the results are summarized in the Appendix C, Tables (C-2, C-3, and C-4). The obtained relationships are given by Equations 9-4 and 9-5 and plotted in Figures 9-2 and 9-3.

$$K = C_1(\nu_s)E_s + C_2(\nu_s) \quad (9 - 4)$$

$$K_1 = C_3(\nu_s)E_s^4 + C_4(\nu_s)E_s^3 + C_5(\nu_s)E_s^2 + C_6(\nu_s)E_s + C_7(\nu_s) \quad (9 - 5)$$

Where:

$$C_1(v_s) = 0.562 v_s^2 - 0.231 v_s + 0.1558$$

$$C_2(v_s) = -98.33 v_s^2 + 39.8 v_s + 4.6$$

$$C_3(v_s) = (-18.24 v_s^2 + 7.585 v_s - 8.61) * 10^{-14}$$

$$C_4(v_s) = (14.697 v_s^2 - 6.12 v_s + 6.28) * 10^{-10}$$

$$C_5(v_s) = (-4.23 v_s^2 + 1.77 v_s - 1.56) * 10^{-6}$$

$$C_6(v_s) = (4.79 v_s^2 - 2 v_s + 1.36) * 10^{-3}$$

$$C_7(v_s) = -0.222 v_s^2 + 0.1 v_s + 0.27$$

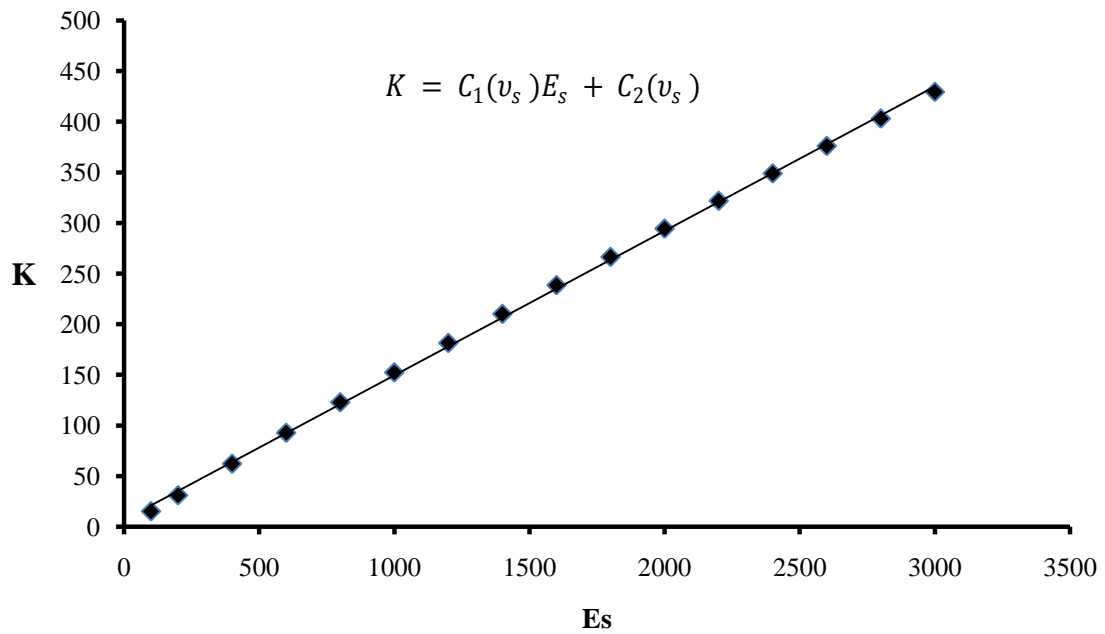


Figure 9.2 K vs Es (NL-W)



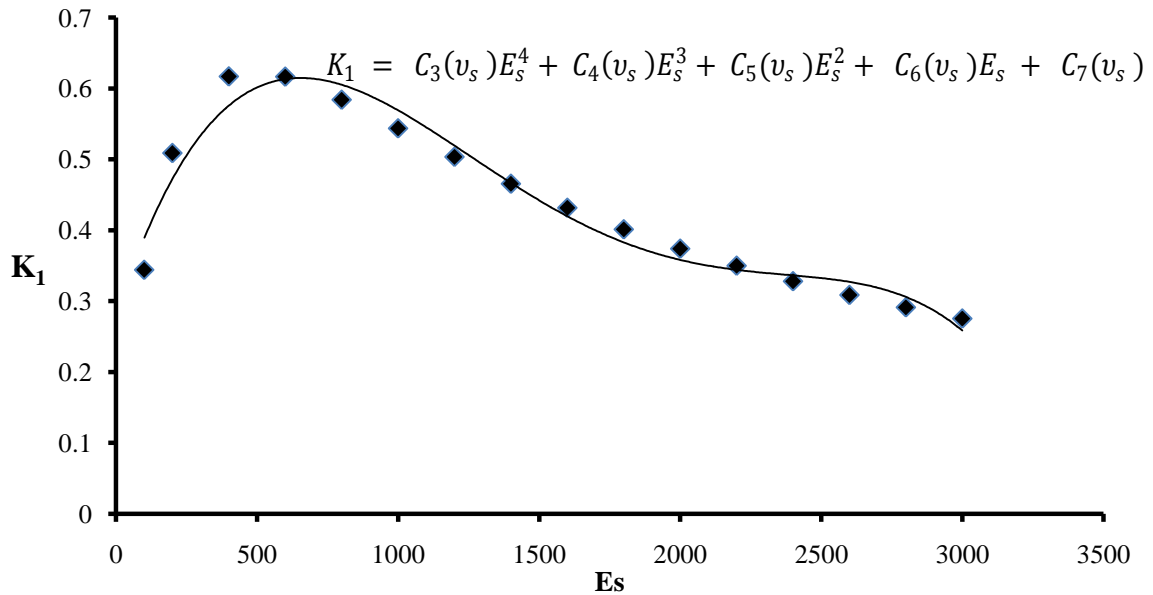


Figure 9.3  $K_1$  vs  $E_s$  (NL-W)

### 9.2.3 Pasternak Model (P)

The foundation reaction based on Pasternak foundation model is represented by  $kw - g_p \nabla^2 w$ . Equating the soil reaction as obtained by the continuous foundation model to the one corresponding to Pasternak model, we get.

$$P - kw + g_p \left( \frac{\partial^2 w}{\partial x^2} + \frac{\partial^2 w}{\partial y^2} \right) = 0 \quad (9 - 6)$$

Where;  $k$  and  $g_p$  are determined by trial and error using Excel solver. Following the same procedure carried out for NL-W and omitting the details, one can draw charts illustrating the relationships that relate  $E_s$  to  $K$  and  $G_1$  (the results are summarized in the Appendix C, Tables (C-5, C-6, and C-7). The nature of the relationship between  $K$  and

$G_1$  and  $E_s$  are almost linear as they are shown in Figures 9-4 and 9-5 respectively for each value of  $v_s$ .

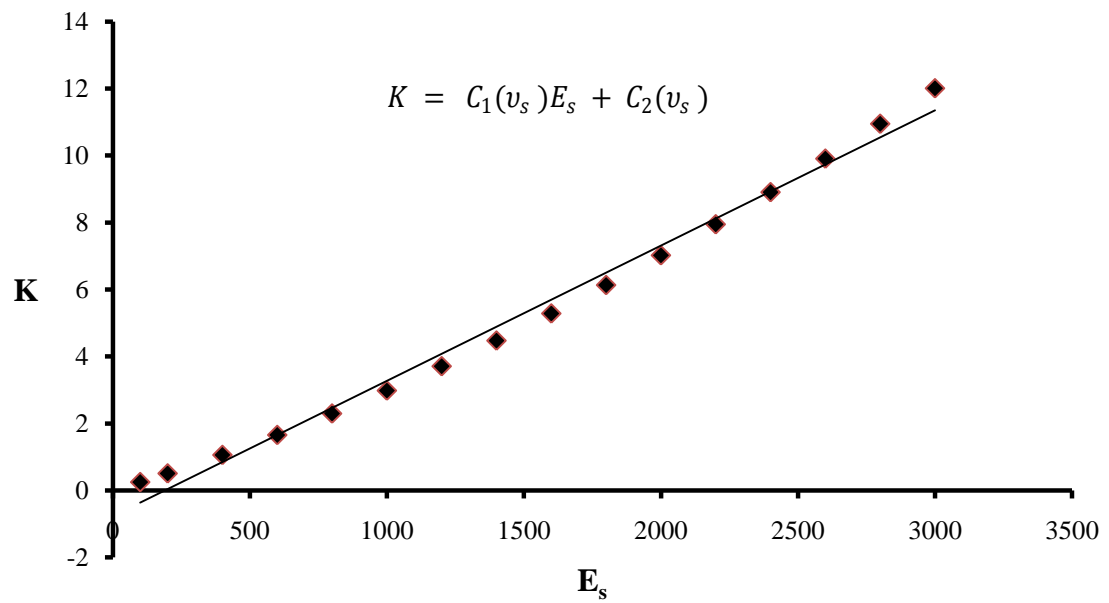


Figure 9.4  $K$  vs  $E_s$  (P)

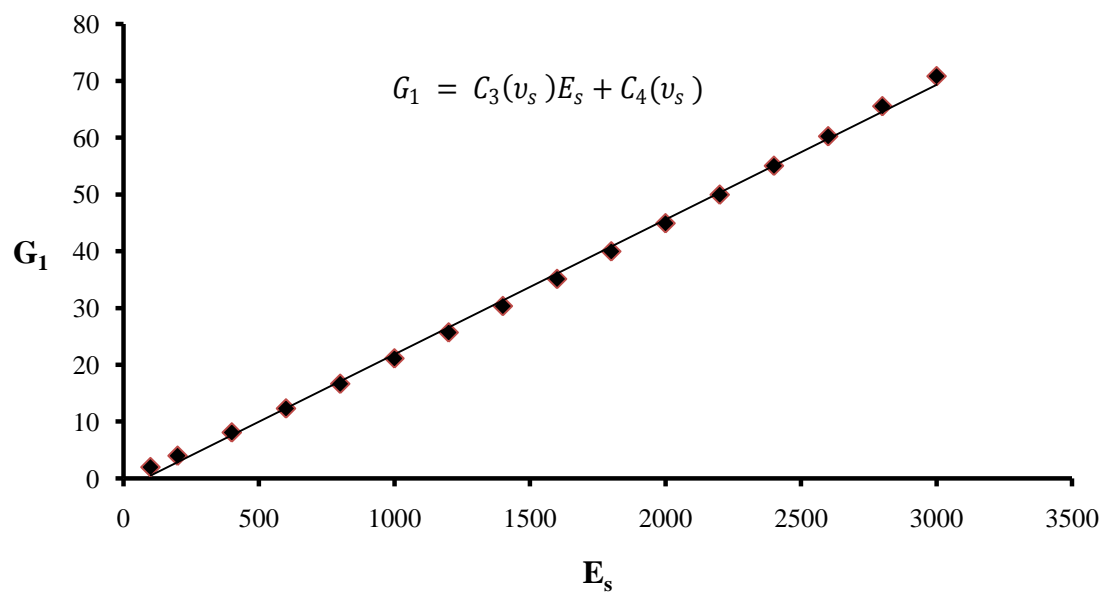


Figure 9.5  $G_1$  vs  $E_s$  (P)

The obtained equations relating K and  $G_1$  to soil Young's modulus  $E_s$  are given by

$$K = C_1(v_s)E_s + C_2(v_s) \quad (9 - 7)$$

$$G_1 = C_3(v_s)E_s + C_4(v_s) \quad (9 - 8)$$

Where:

$$C_1(v_s) = (15.56 v_s^2 - 6.429 v_s + 4.411) * 10^{-3}$$

$$C_2(v_s) = (-5.1 v_s^2 + 2.1 v_s - 0.884)$$

$$C_3(v_s) = (9.26 v_s^2 - 3.83 v_s + 2.6) * 10^{-2}$$

$$C_4(v_s) = (-23.62 v_s^2 + 9.67 v_s - 2.44)$$

## 9.2.4 Winkler-Pasternak Model (W-P)

Finally, The Winkler-Pasternak foundation model is defined by  $P(x, y) = kw + kw^3 - g_p \nabla^2 w$ . Equating the soil as obtained from the continuous foundation model to the one corresponding to Pasternak model, we get

$$P - kw - k_1 w^3 + g_p \left( \frac{\partial^2 w}{\partial x^2} + \frac{\partial^2 w}{\partial y^2} \right) = 0 \quad (9 - 9)$$

After repeating the same procedure followed previously, it was found that the correlations between K and  $G_1$  and  $E_s$  are almost identical to the ones obtained for them in the Pasternak model. Similarly, the correlations between  $K_1$  and  $E_s$  obtained earlier for the NL-W model holds for W-P model.

### 9.3 Verification of the Selected Best Statistical Models

To verify the above developed correlations, the models have been used to carry out the analysis of large deflection of plate on an elastic foundation due to two types of loading: a uniformly distributed load and a central point load. The elastic modulus of the soil,  $E_s$ , has been varied (500, 1000, 2000, 3000) where the developed  $K$ ,  $K_1$ , and  $G_1$  have been used to represent the discrete models and  $E_s$  and Poisson ratio,  $\nu_s$  was assumed 0.35. Then the discrete foundation parameters  $K$ ,  $K_1$ , and  $G_1$  have been computed from the correlations developed in the previous section. The results for the deflection at the center of the plate as computed by the continuous foundation model and the corresponding discrete models are compared in Figures 9.6 to 9.12.

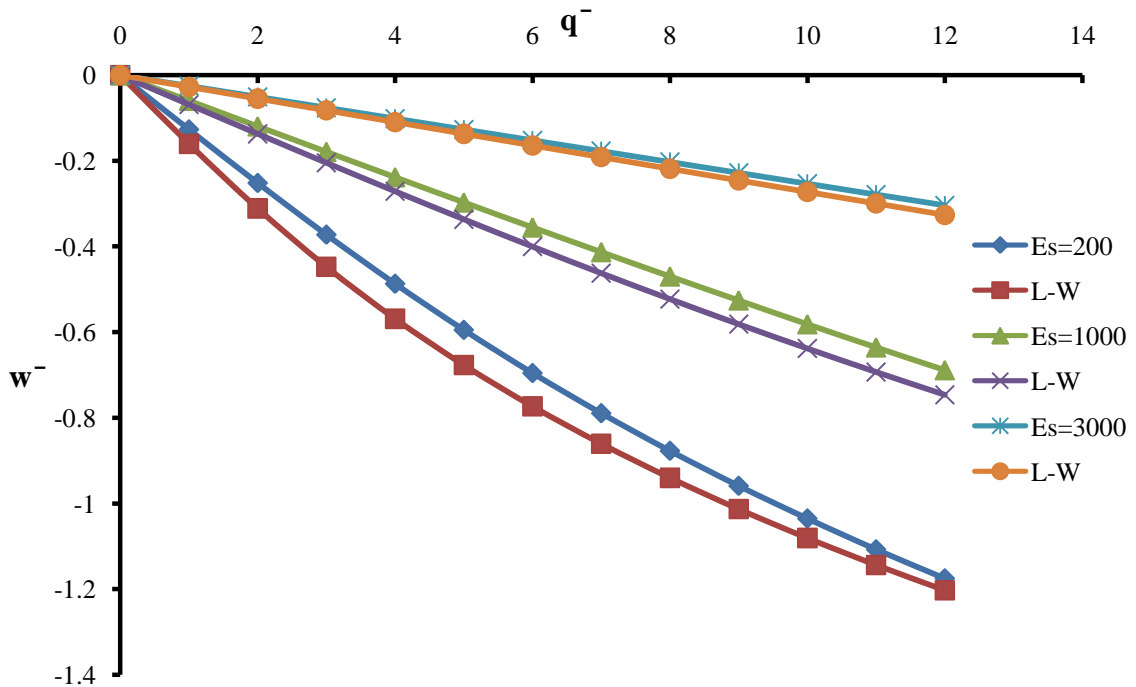


Figure 9.6  $\bar{w}$  vs  $\bar{q}$  for Continuous and L-W Models

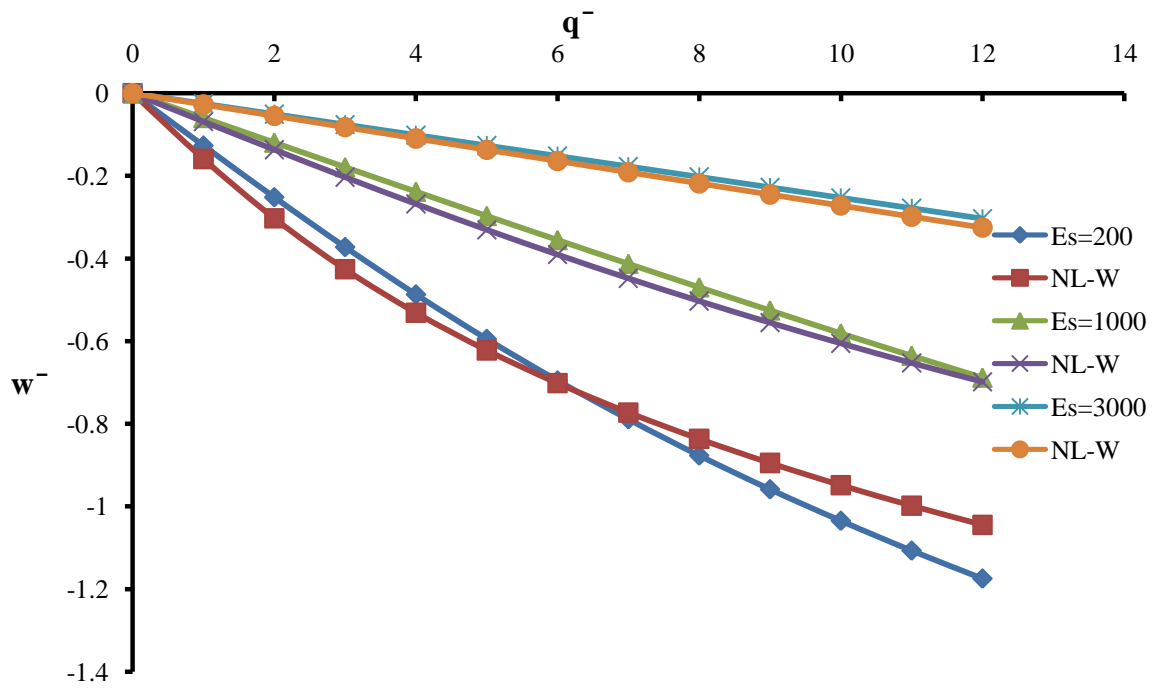


Figure 9.7  $\bar{w}$  vs  $\bar{q}$  for Continuous and NL-W Models

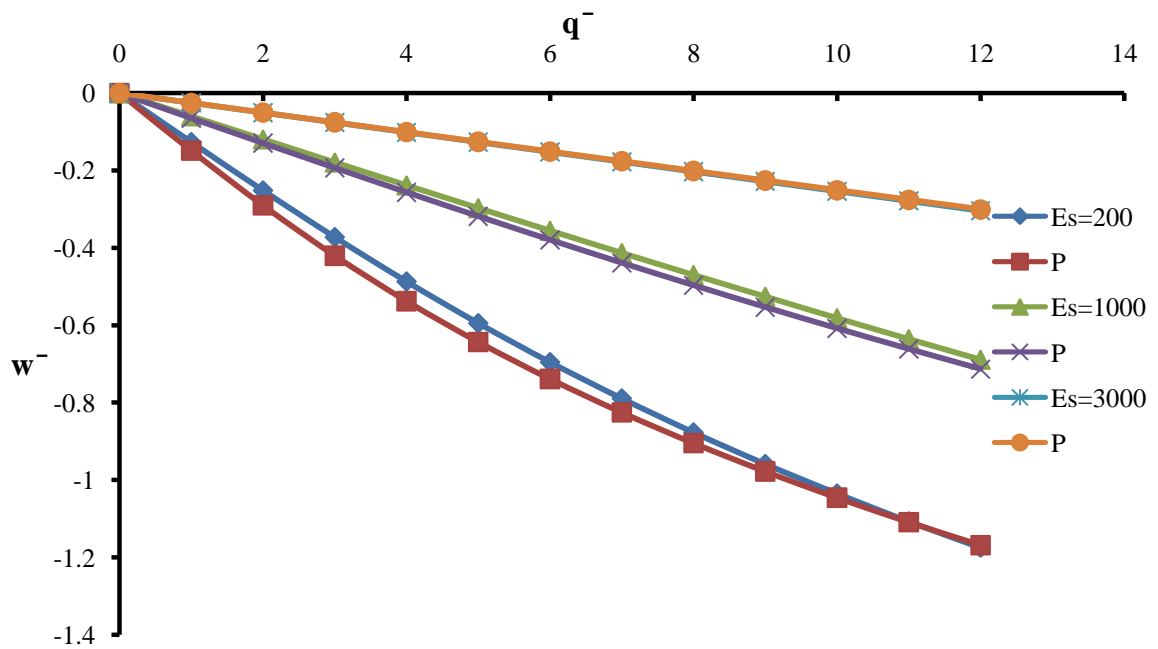


Figure 9.8  $\bar{w}$  vs  $\bar{q}$  for Continuous and Pasternak (P) Models.

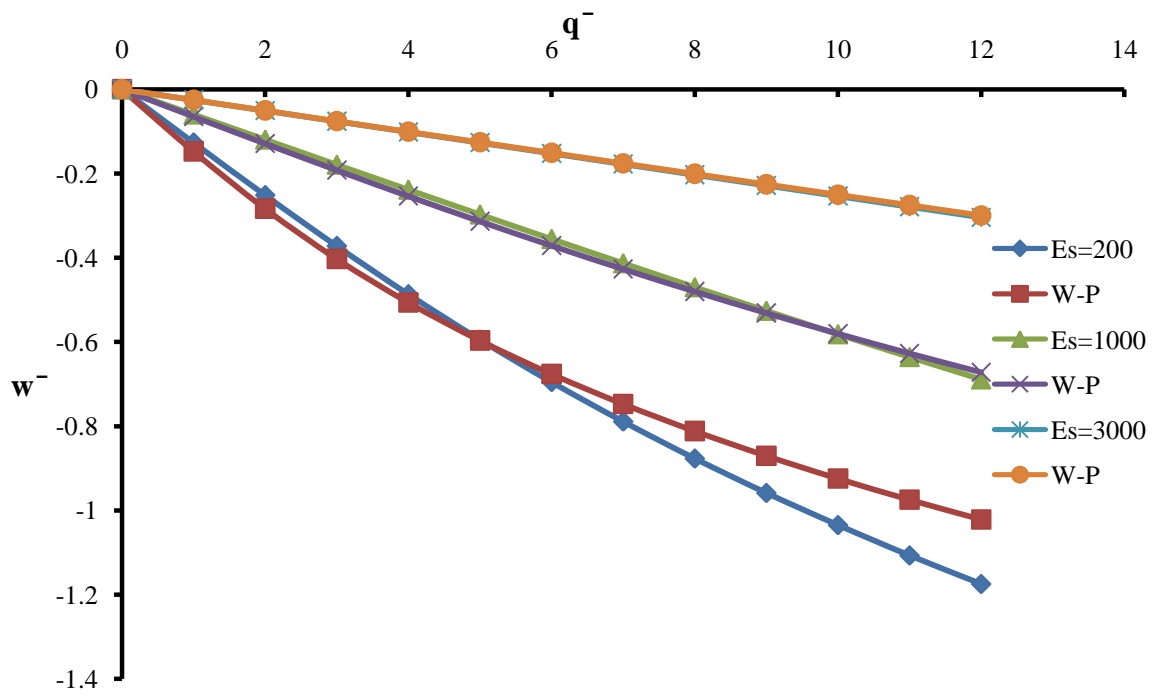


Figure 9.9  $\bar{w}$  vs  $\bar{q}$  for Continuous and W- P Models

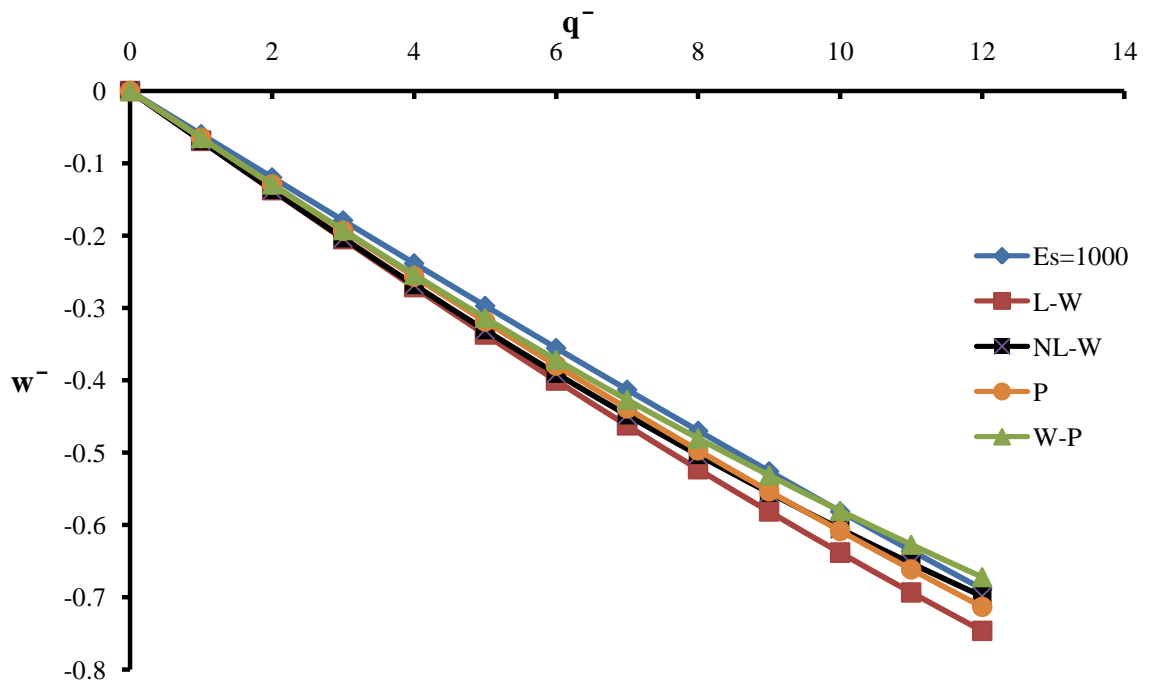


Figure 9.10  $\bar{w}$  vs  $\bar{q}$  for all Models (Es = 1000)

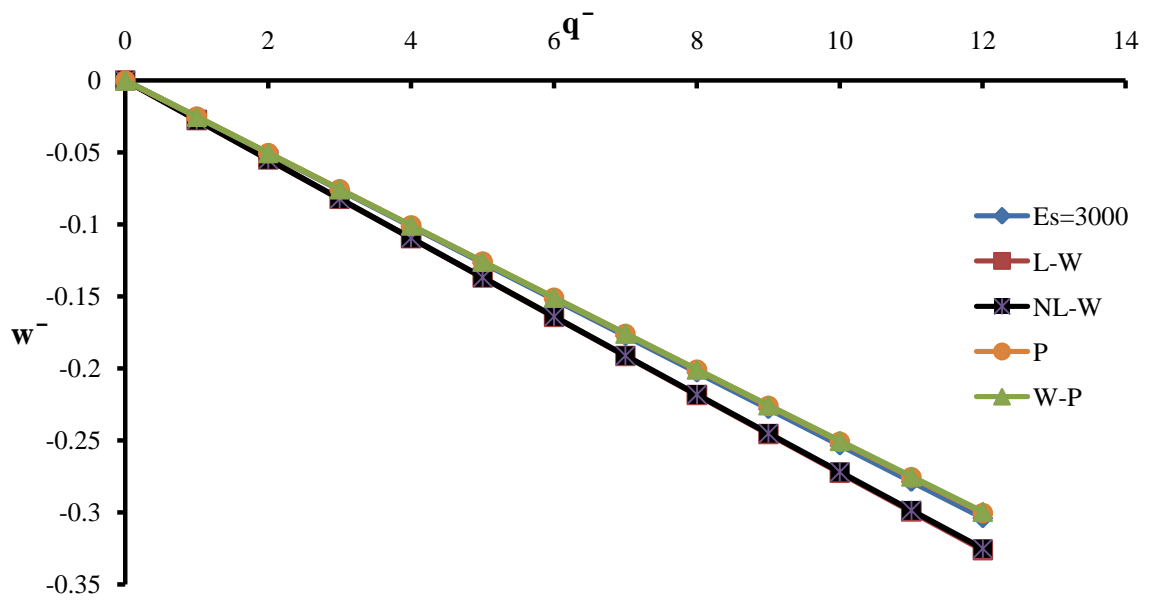


Figure 9.11  $\bar{w}$  vs  $\bar{q}$  for all Models ( $E_s = 3000$ )

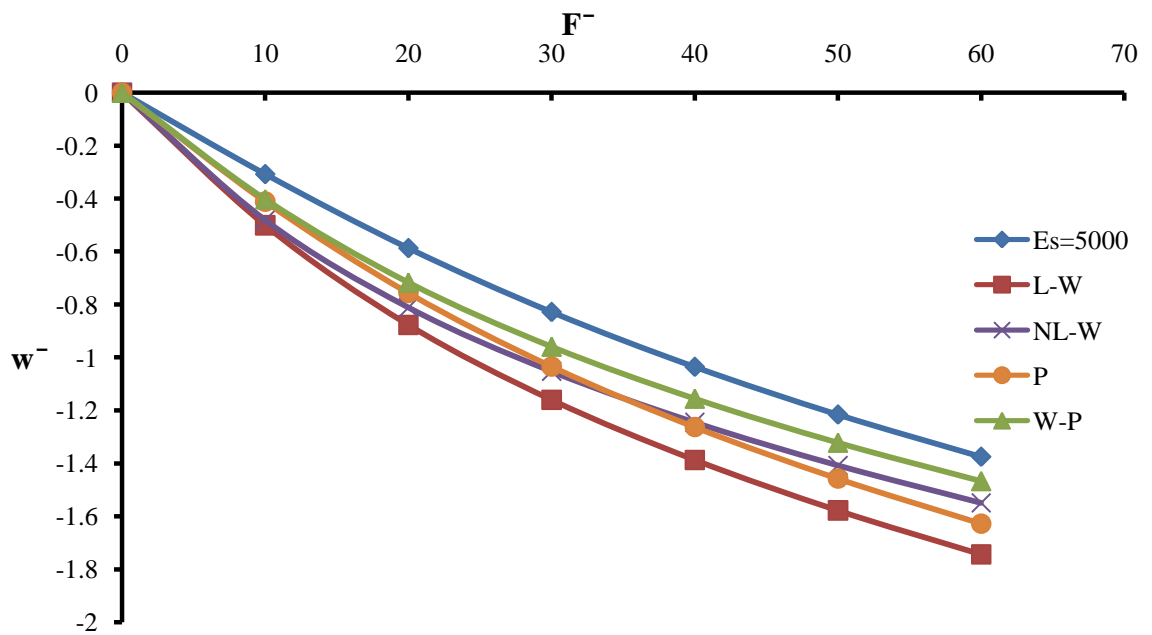


Figure 9.12  $\bar{w}$  vs  $\bar{F}$  for all Models ( $E_s = 5000$ ) due to a Point Load

The results in the above figures indicate that P and W-P model are the most in agreement with the continuous foundation model. The agreement is valid for both small and large deflection. On the other hand, L-W and NL-W models yield reasonable agreements for small deflection (up to  $\bar{w} = 0.35$ ), then the results of both deviate from those based on the continuous foundation model.

For more verification, the L-W model is compared with the available formulas in the literature. The most common formulas from the literature are due to Biot (1937) and Vesic (1961) which are given by Equations 9-10 and 9-11 respectively. The computed differences between the developed L-W model and those suggested by Biot and Vesic are given in Table 9-4.

$$\text{Biot (1937); } k = \frac{0.95E_s}{a(1 - \nu_s^2)} \left[ \frac{a^4 E_s}{(1 - \nu_s^2)EI} \right]^{0.108} \quad (9 - 10)$$

$$\text{Vesic (1961); } k = \frac{0.65E_s}{a(1 - \nu_s^2)} \sqrt[12]{\frac{a^4 E_s}{EI}} \quad (9 - 11)$$

Where; EI is the foundation plate stiffenes.



Table 9.4 Comparison of L-W Model and Biot (1937) and Vesic (1961)

v <sub>s</sub>	E <sub>s</sub>	L-W				Biot		Vesic	
		c <sub>1</sub>	c <sub>2</sub>	K	k	k	Diff.%	k	Diff.%
0.15	10000000	0.13	8.81	1332433.8	520340.4	467384.3	10.18	234635.3	54.91
0.2	10000000	0.13	9.09	1317609.1	514551.1	476833.8	7.33	238912.5	53.57
0.25	10000000	0.13	8.88	1330133.9	519442.3	489530.1	5.76	244646.4	52.90
0.3	10000000	0.14	8.18	1370008.2	535013.9	505947.8	5.43	252039.5	52.89
0.35	10000000	0.14	6.99	1437232.0	561266.1	526751.4	6.15	261374.3	53.43
0.4	10000000	0.15	5.31	1531805.3	598198.7	552868.8	7.58	273042.8	54.36
0.45	10000000	0.17	3.15	1653728.1	645811.9	585606.6	9.32	287593.7	55.47
0.15	30000000	0.13	8.81	3997283.81	1561014.4	1578790.51	1.14	771391.10	50.58
0.2	30000000	0.13	9.09	3952809.09	1543646.2	1610710.01	4.34	785452.92	49.12
0.25	30000000	0.13	8.88	3990383.88	1558319.8	1653597.13	6.11	804303.79	48.39
0.3	30000000	0.14	8.18	4110008.18	1605035.4	1709054.93	6.48	828609.68	48.37
0.35	30000000	0.14	6.99	4311681.99	1683792.8	1779328.23	5.67	859298.92	48.97
0.4	30000000	0.15	5.31	4595405.31	1794592.1	1867550.85	4.07	897660.48	49.98
0.45	30000000	0.17	3.15	4961178.15	1937433.2	1978136.60	2.10	945498.19	51.20

The comparison clearly shows that the developed L-W model is reasonably close to Biot's model with a maximum difference of 11%. It should be noted that Biot's model is widely used in the technical literature for mat foundations which gives more reliability to the developed L-W model.

## CHAPTER TEN

### PRACTICAL APPLICATION: LARGE DEFLECTION OF THE BASE PLATE OF LARGE STORAGE TANK

#### 10.1 General

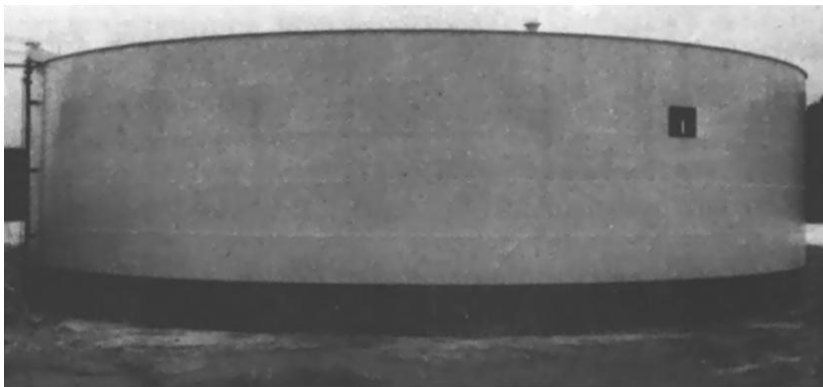
The large deflection of the thin plates rested on nonlinear foundation has wide range of real applications in different engineering fields. Thin films of metals, synthetic materials on the surface of electronic devices are considered as thin plate (the thin film and synthetic material) on an elastic foundation (electronic devices) Mofid and Noroozi (2009). In the evaluation of the structural safety of ships and ship-shaped offshore structures comprise of metal plates, the non linear behavior of the plates is a fundamental requirement Paik et. al (2012).

In Structural engineering, the structure footings are one of the important applications. Depending on the footing types (raft, isolated, etc.) and construction materials such as steel, plain and reinforced concrete, the thickness of the footing is determined. For the plain and reinforced concrete, the raft footings are considered as thin whereas the isolated footings are considered as thick plate resting on foundation.

Large storage tanks are classified as thin-walled structures in which the large deflection analysis is fundamental. These tanks are used to store several kinds of fluids such as water, oil, etc. The most common shapes of such tanks are cylindrical (Figure 10.1).



(a)



(b)



(c)

Figure 10.1 Steel Tanks. a) Bolted, b) Welded, and c) Construction

The large storage tanks are classified as thin-walled structures in which the large deflection analysis is a fundamental. These tanks are used to store several kinds of fluids such as water, oil, etc. The most common shapes of the tanks are the cylindrical and square which consists of plate on in the bottom and shells in the sides.

The bottom plates of the tanks are commonly flat plates. The boundary supports of the bottom plates can be considered as fixed or simply supported according to the rigidity of the side shells and existence of the gasket at the connection. The cross section of a typical tank with its loading and supporting conditions are shown in Figure 10.2 (Ventsel and Krauthammer (2001)).

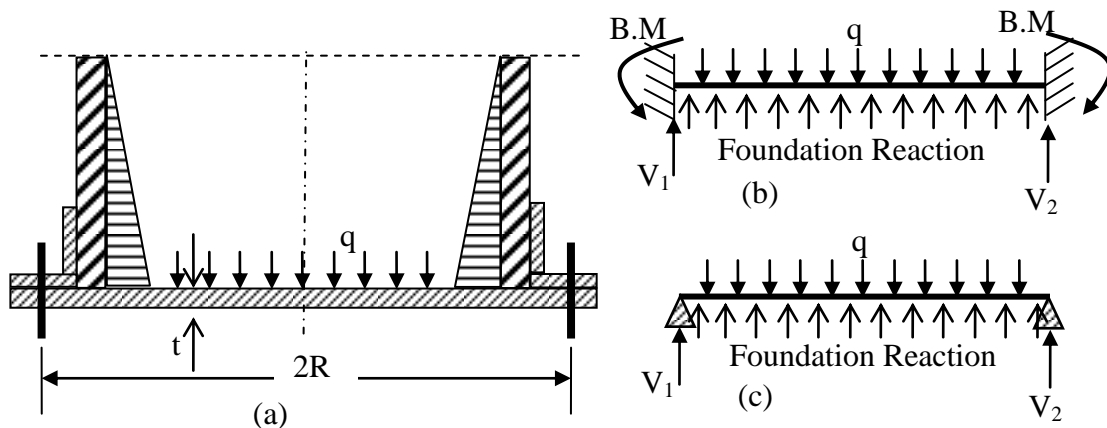


Figure 10.2 Typical Tank Section and Static Systems. a) Typical Tank Cross Section, b) Fixed Connection, and c) Simple Connection

In this chapter, a cylindrical tank with a circular bottom plate is considered. The two boundary conditions of fixed and simple edges are considered. The foundation reactions are represented by the models developed in Chapter 9.

## 10.2 Details of the Large Storage Tank

Consider a circular tank with total capacity of 100000 m<sup>3</sup> of water, unit weight of water is 10 kN/m<sup>3</sup>. The radius of the tank, R, is 40 m and the total height is 22 m. the tank is steel tank with E = 1\*10<sup>9</sup> N/m<sup>2</sup> and ν = 0.3, thickness t = 0.2 m. The supported soil properties: E<sub>s</sub> = 3\*10<sup>7</sup> N/m<sup>2</sup> and ν<sub>s</sub> = 0.4.

The uniform load distribution on the bottom of the tank is as follows:

$$q = 10 * 22 = 220000 \frac{N}{m^2}$$

To calculate the foundation parameters of the discrete models, the developed relationships in Chapter 9 can be used to get their dimensionless values. Then the dimensional values can be calculated from:

$$k = \frac{DK}{R^4}, k_1 = \frac{DK_1}{R^4 t^2}, g_p = \frac{D G_1}{R^2}, \text{Where : } D = \frac{E_{plate} t_{plate}^3}{12(1 - \nu_{plate}^2)}$$

The calculated foundations parameters are as shown in Table 10.1.

Table 10.1 Discrete Foundation Parameters

Foundation Model	K	k	K <sub>l</sub>	k <sub>l</sub>	G <sub>1</sub>	g <sub>p</sub>
L-W	4550000	1302083	0	0	0	0
NL-W	4548000	1301511	2918	20876	0	0
Pasternak	127000	36434	0	0	750000	3.43*10 <sup>8</sup>
NLW-P	127000	36434	2918	20876	750000	3.43*10 <sup>8</sup>

The boundary connection is assumed fixed, and the analysis is carried out using all the foundation models: discrete models (Linear Winkler (L-W), Non-Linear Winkler (NL-W), Pasternak (P), and Non-Linear Winkler Pasternak (NLW-P)) and the continuous model (Boussinesq-based approach). The results of all cases are summarized in Table 10.2 which gives the non-dimensional values of  $\bar{w}$ ,  $\bar{\sigma}_b$ , and  $\bar{\sigma}_m$  at the center of the plate due to the highest dimensionless load  $\bar{q} = 220000$ . The variations of the same quantities versus load are given in Figures 10.3 to 10.5.

The variation of the dimensionless deflection,  $\bar{w}$ , along the radial direction is given in Figure 10.6 for the all foundation models due to the maximum dimensionless load of  $\bar{q} = 220000$ .

Table 10.2  $\bar{w}$ ,  $\bar{\sigma}_b$ , and  $\bar{\sigma}_m$  at the Plate Center For fixed Connection Case ( $\bar{q} = 220000$ )

Foundation model	$\bar{w}$	$\bar{\sigma}_b$	$\bar{\sigma}_m$
Continuous	-1.5754	-2.62752	2.10867
L-W	-0.8441	-0.67522	8.11716
NL-W	-0.8176	-0.6954	7.65526
Pas.	-1.4605	-2.87077	2.14626
NLW-P	-1.3542	-2.57468	1.88274

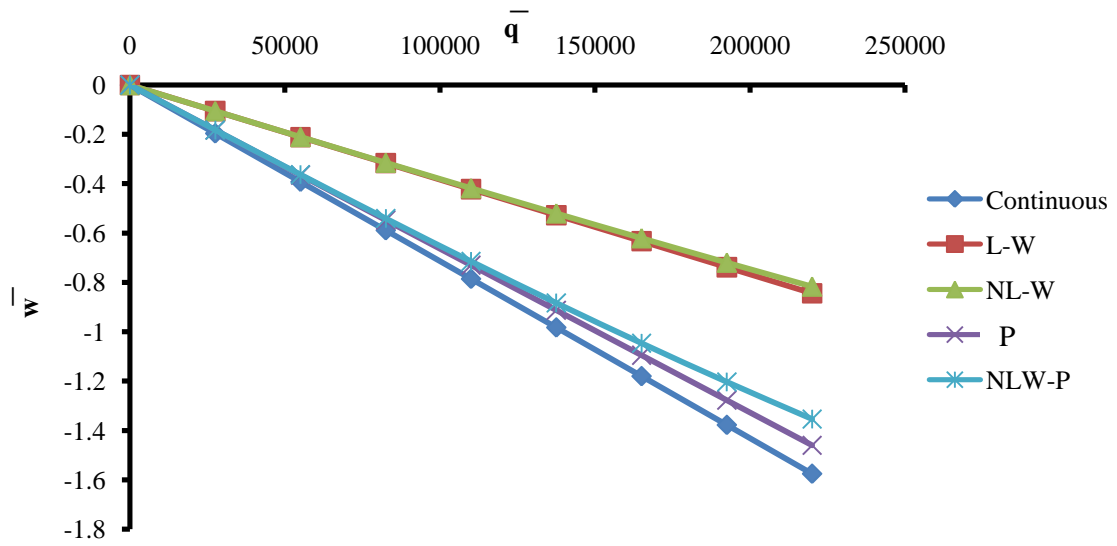


Figure 10.3  $\bar{w}$  vs.  $\bar{q}$  for the Fixed Connection Case

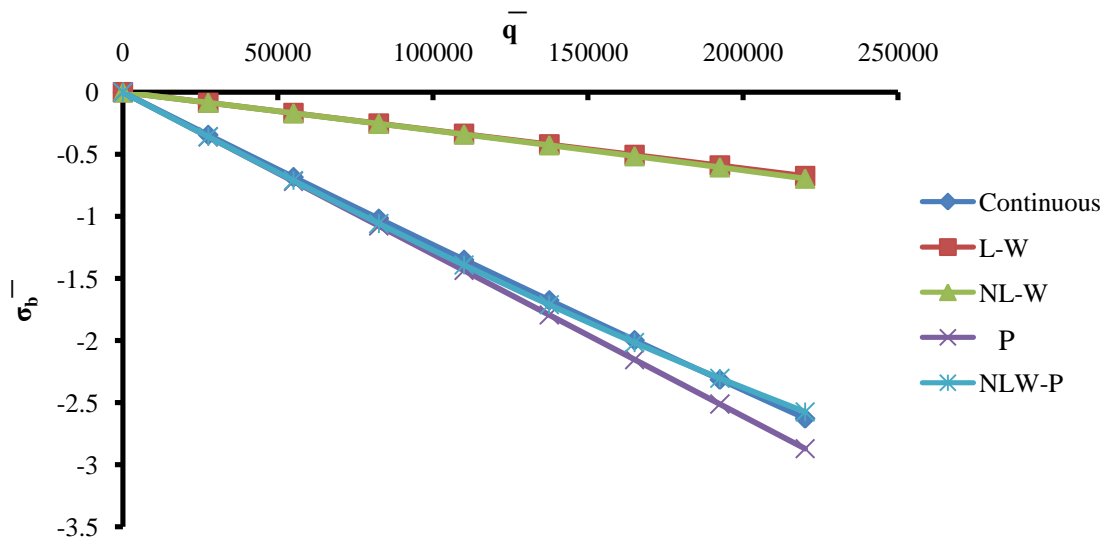


Figure 10.4  $\bar{\sigma}_b$  vs  $\bar{q}$  for the Fixed Connection Case

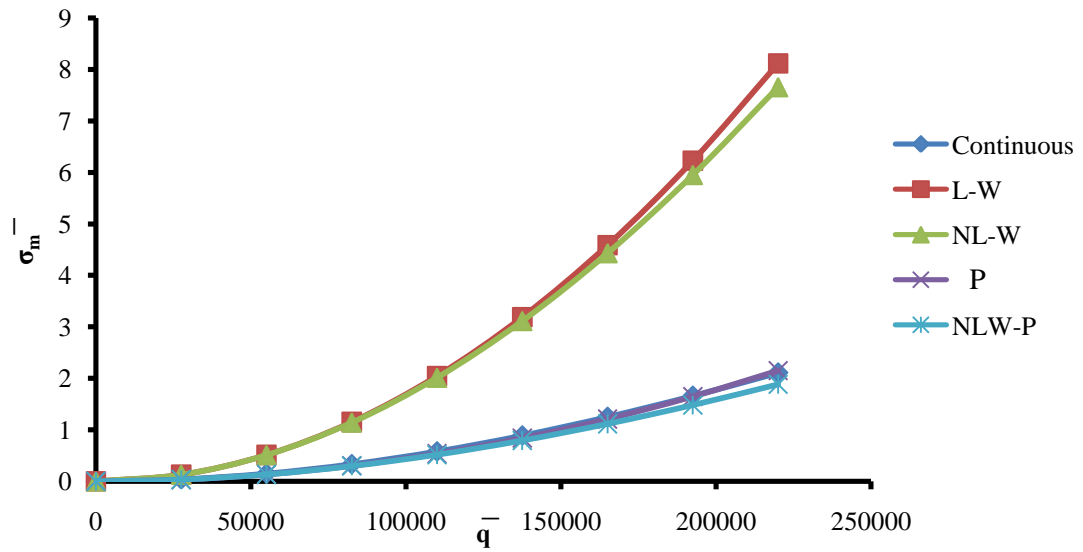


Figure 10.5  $\bar{\sigma}_m$  vs  $\bar{q}$  for the Fixed Connection Case

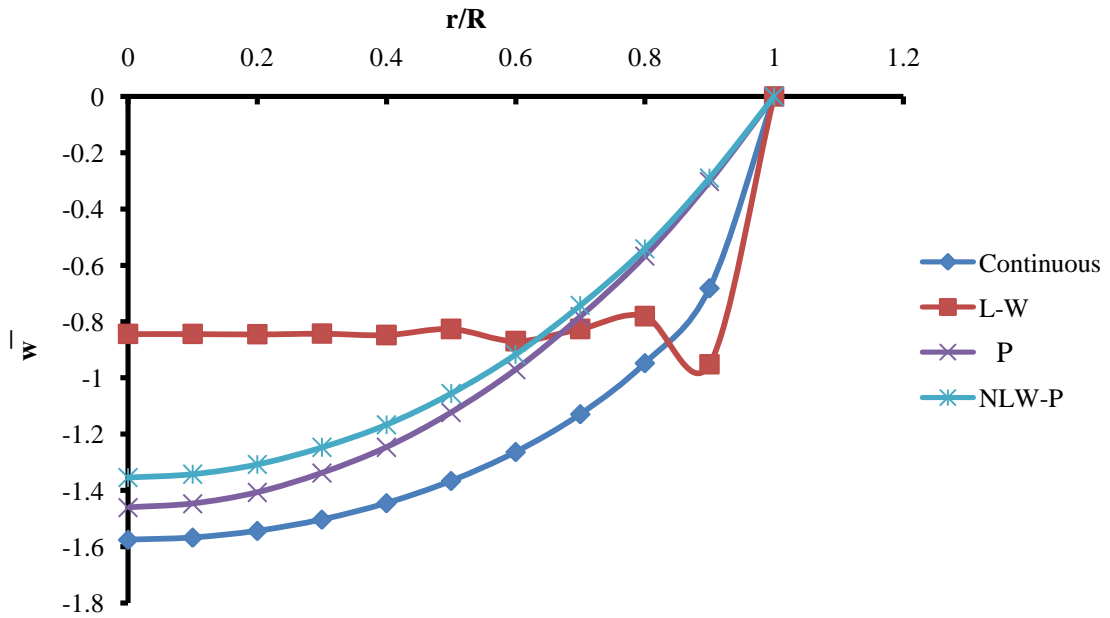


Figure 10.6  $\bar{w}$  along the Radial Directions of Different Foundation Models for the Fixed Connection Case



All results clearly indicate that Pasternak and non-linear Winkler-Pasternak produce results that are more in agreement with the continuous foundation as compared to Winkler and Nonlinear Winkler models. This is attributed to the similarity between these two models and continuous foundation model in accounting for the vertical and horizontal contact between the plate and the foundation. The linear Winkler model, on the other hand, results in a strange behavior (almost a constant value of deflection with a peak value near the boundary) which indicates that such model is not suitable for modeling the plate-foundation interaction for plates undergoing large deflection.

Repeating the above analysis for the pinned connection, similar results are obtained as given in Table 10.3 and Figures 10.7 to 10.10. The results reveal the same conclusions stated above for the fixed connection case.

Table 10.3  $\bar{w}$ ,  $\bar{\sigma}_b$ , and  $\bar{\sigma}_m$  at the Plate Center for Pinned Connection Case ( $\bar{q} = 220000$ )

Foundation model	$\bar{w}$	$\bar{\sigma}_b$	$\bar{\sigma}_m$
Continuous	-1.3723	-1.9406	1.64995
L-W	-0.8446	-0.1363	10.4719
NL-W	-0.8181	-0.1363	9.86631
Pas.	-1.2419	-1.75616	1.49315
NLW-P	-1.1796	-1.58862	1.36384

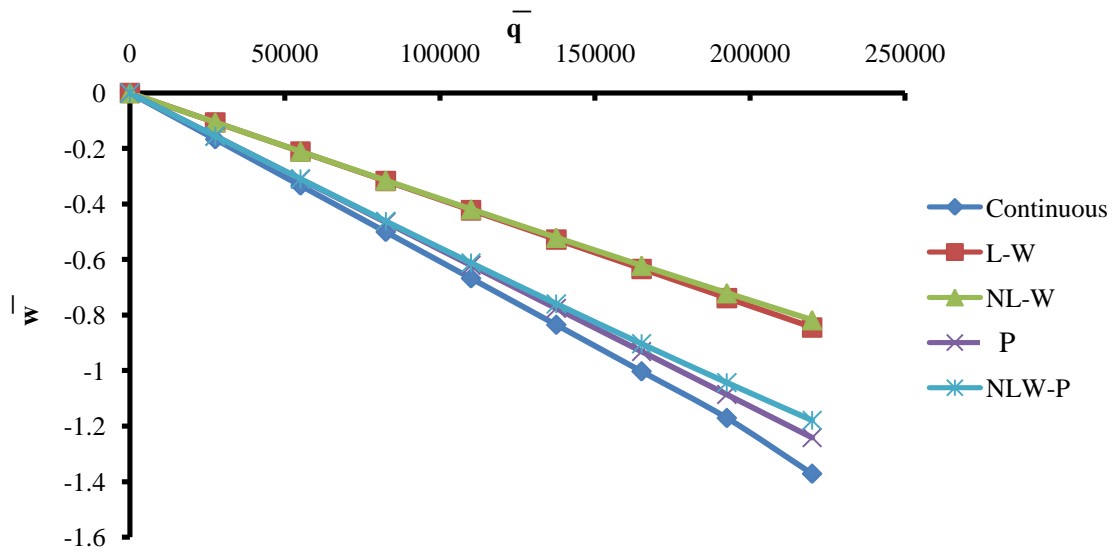


Figure 10.7  $\bar{w}$  vs.  $\bar{q}$  for the Pinned Connection Case

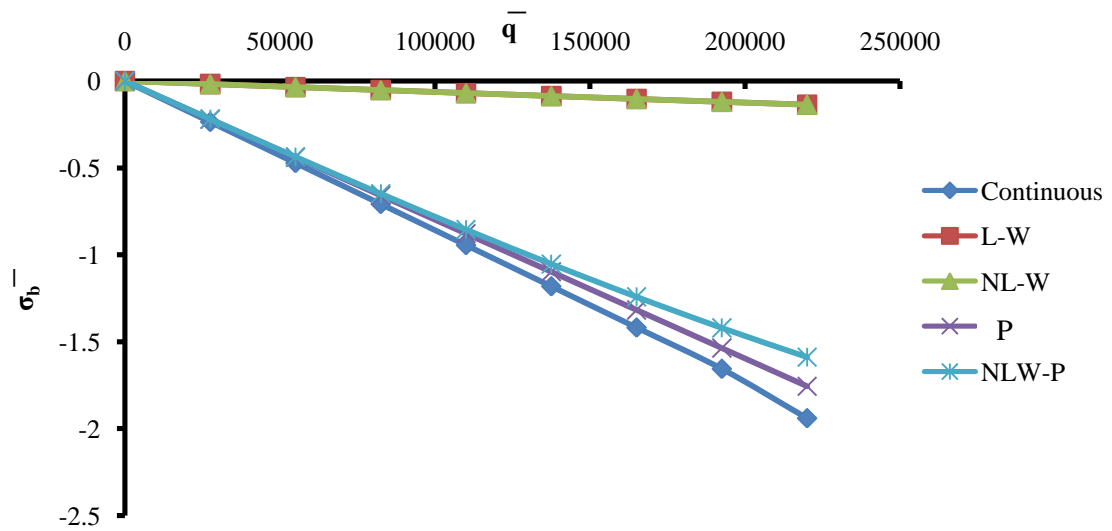


Figure 10.8  $\bar{\sigma}_b$  vs  $\bar{q}$  for the Pinned Connection Case

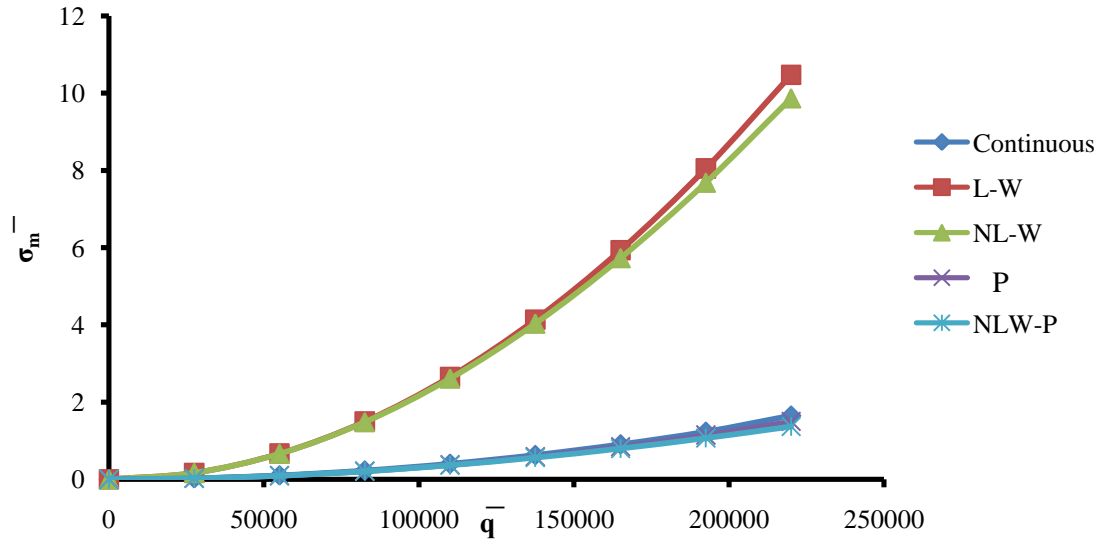


Figure 10.9  $\bar{\sigma}_m$  vs  $\bar{q}$  for the Pinned Connection Case

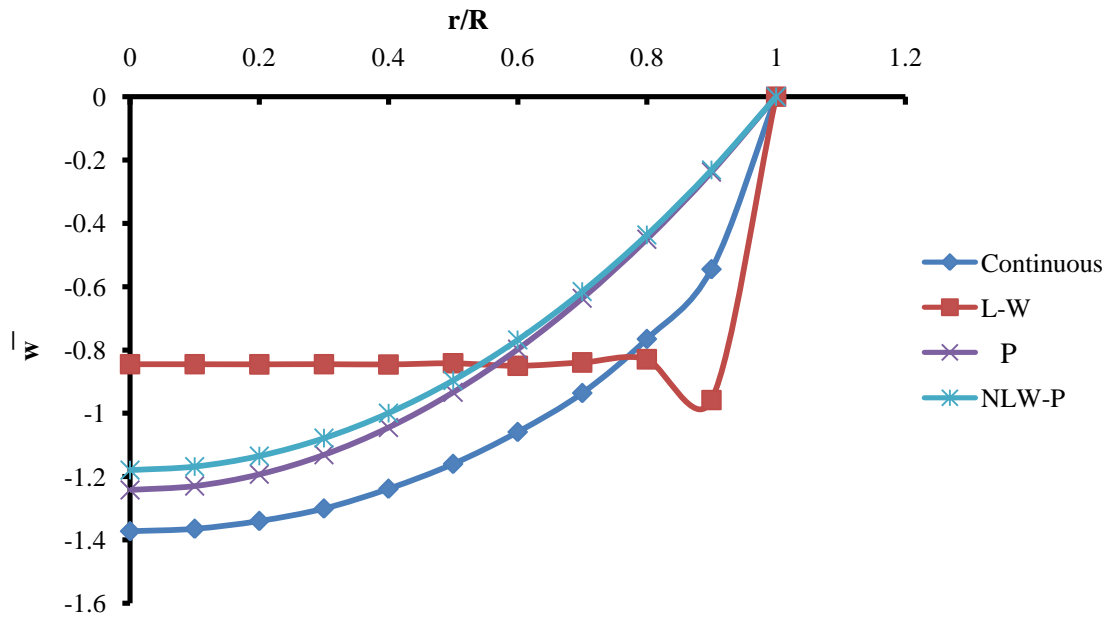


Figure 10.10  $\bar{w}$  along the Radial Directions of Different Foundation Models for the Pinned Connection Case

# CHAPTER ELEVEN

## CONCLUSIONS AND RECOMMENDATIONS

The main objective of this dissertation is the development of an RBF-based meshless method capable of modeling the problem of large deflection of thin plates resting on nonlinear foundations. This chapter summarizes the main accomplishments of the research work undertaken in this dissertation, then it outlines the conclusions drawn from the results obtained and finally it recommends some directions for future research.

### 11.1 Summary

RBF-based meshless model for the analysis of thin elastic plates resting on linear/non-linear different foundations and undergoing large deflection has been developed. The meshless model is based on collocation with multi-quadric functions. This is achieved by firstly developing a model for the problem of large deflection without foundation, to basically establish its reliability in preparation to the more complicated case of large deflection of plate on nonlinear foundation. The model was implemented into a computer code using the MATHEMATICA software and then utilized in carrying out a comprehensive parametric study to obtain the optimum RBF shape factor. The parametric study included the two basic shapes of circular and square, several boundary conditions (simply supported, clamped, free and mixed) and two supporting conditions (with and without foundation).

In solving the coupled and highly nonlinear governing differential equations, two incremental-iterative algorithms have been utilized to address the two cases of in-plane boundary conditions, namely, movable and immovable. For the case of movable edge condition, the w-F formulation has been employed while for the immovable in-plane edge condition, the three dimensional u-v-w formulation has been employed, due to the extreme difficulty in representing the immovable in-plane edge condition in terms of the stress function. The soil-plate interaction has been modeled by four discrete foundation models: Winkler, non-linear Winkler, Pasternak and non-linear Winkler-Pasternak, in addition to the continuous elastic model.

The accuracy of the developed algorithms and computer codes have been verified by solving numerous practical cases involving different boundary conditions and foundations models and comparing the results with FEM solutions obtained by COMSOL. The verified computer codes have been utilized to perform a parametric study for the purpose of generating correlations between the discrete and continuous foundation parameters. The obtained correlations have been verified through several practical cases. As a final demonstration of the efficiency of the developed foundation parameters correlations, the RBF model has been applied to the industrial problem of deflection of large tank bottom plate where the Winkler parameter  $k$  has been expressed through the elastic constants of the supporting soil and proved to yield results that are very close to the ones obtained by FEM employing the more involved continuous foundation model.

## 11.2 Conclusions

Based on the developed RBF-based meshless models and the results presented in the last six chapters, the following conclusions can be drawn:

- 1- Mesh-free collocation model using MQ-RBF offers an attractive alternative to the conventional numerical methods in solving the problem of large deflection of thin elastic plates on linear and nonlinear foundations. This is basically, due to its flexibility with respect to the geometric modeling, computational efficiency, and application simplicity. Another important advantage of the RBF-based model is its capability, if programmed using Mathematica, of obtaining the primary solution, the deflection, in a functional symbolic form. The secondary solutions (forces, moments and stresses) can then be obtained by direct differentiation of the deflection function. This provides more accurate solutions when compared to other numerical methods like FEM and FDM, where interpolation would be required considering their built in discrete nature.
- 2- The proper selection of the shape factor “c” of MQ-RBF plays is very important to get accurate results and stable solutions. The optimum value of c ranges between 0.6 and 0.65 for plates without foundations. For plates on foundations, there exist several ranges of the optimum c depending on the plate geometry and boundary conditions.
- 3- In general, MQ-RBF solutions for all the studied cases of different plate geometries and boundary conditions and foundations models are very close to

those obtained by FEM. The percentage error in RBF solution as compared to FEM ranges from as low as 1-3% for simply supported and clamped square plates with immovable edges to as high as 8% for circular plates with free and movable edges. The less accuracy in RBF solutions has been observed generally for secondary variables at the boundary.

- 4- The comparisons performed between the solutions based on small deflection and those based on large deflection formulations show the expected reduction in plate deflection and stress due to the plate stiffening caused by large deflection.
- 5- The difference between the solutions of the small and large deflection theories is smaller for Pasternak and nonlinear Winkler foundations as compared to the linear Winkler model.
- 6- The task of implementing the continuous foundation model in the RBF method is easier than with other numerical methods. This fact is due to meshless nature of RBF. Furthermore, the codes developed for the discrete foundation models can be easily modified to account for the continuous model.
- 7- The generated symbolic solutions for both plates on discrete foundations and plates on continuous models enabled conducting a parametric study which produced symbolic correlations between the discrete foundation parameters and the elastic constants ( $E$  and  $\nu$ ) of the continuous foundation model.

- 8- The obtained foundation parameters correlations have been tested through several numerical examples and found to be accurate and efficient in modeling the plate soil interaction.
  
- 9- Among discrete models, Pasternak model's and non-linear Winkler-Pasternak solutions are most in agreement with the continuous foundation. This is attributed to the similarity between the two models in accounting for the vertical and horizontal contact between the plate and the foundation.



### 11.3 Recommendations

Finally, as is the case with other numerical methods, there is a scope for further application and enhancement of the method. Below are some of the recommendations that can be made:

- 1- The employed RBF models were based on uniform node spacing. Non-uniform spacing should be tried for possible improvement in the solution accuracy.
- 2- The plate is considered to be thin and elastic. This assumption is valid to some applications such as the bottom plates of large storage tanks. For other applications such as the reinforced concrete foundations, the model should be modified to include the elasto-plastic behavior.
- 3- This research considers a single layer of homogeneous elastic soil. The model would be further enhanced if provisions were made for the inclusion of different soil layers for the soil supporting the plate.
- 4- The soil is considered to isotropic, but soils are inherently anisotropic. The model would be strengthened through the provision of anisotropic soil behavior.
- 5- The foundation parameters are assumed to be constant and equal in both compression and tension. In the general case, the foundation cannot take any tension. An iterative technique can be adapted to this solution for plates on tensionless foundations.

## REFERENCES

1. ([http://www.geotechnicalinfo.com/youngs\\_modulus.html](http://www.geotechnicalinfo.com/youngs_modulus.html))).
2. A. Andakhshideh, S. Maleki, M.M. Aghdam. “Non-linear bending analysis of laminated sector plates using Generalized Differential Quadrature”. *Composite Structures* 92 (2010) 2258–2264.
3. A. C. J. Luo; C. D. Mote; Asymmetric responses of rotating, thin disk experiencing large deflections, *Computers and \mathematics with Applications*, v 45, n 1-3, January/February, 2003, pp 217-228.
4. A. I. Fedoseyev, M. J. Friedman, and E. J. Kansa, Improved multi-quadric method for elliptic partial differential equations via PDE collocation on the boundary. *Comput. Math. Appl.* (2002).
5. A. J./ M. Ferreira; C. M. C. Roque; P. A. L. S. Martins; Radial basis functions and higher-order shear deformation theories in the analysis of laminated composite beams and plates, *Composite Structures*, v 66, 2004, p 287-293.
6. A. Saygun; M. Celik; Analysis of circular plates on two-parameter elastic foundation, *Structural Engineering and Mechanics*, v 15, n 2, February 2003, pp 249-267.
7. A. Soh; C. Soh; K. Hoon; Development of a simplified plate element for large deflection elasto-plastic finite element analysis, *Computers and Structures*, v 61, n 1, August 14, 1996, pp 183-188.
8. A.R. Shahidi, M. Mahzoon, M.M. Saadatpour, M. Azhari. “Nonlinear static analysis of arbitrary quadrilateral plates in very large deflections”. *Communications in Nonlinear Science and Numerical Simulation* 12 (2007) 832–848.

9. Ames, W. F., (1977). Numerical Methods for Partial Differential Equations, Section 1.6. Academic Press, New York. ISBN 0-12-056760-1.
10. Anant R. Kukreti and Man-Gi Ko . Analysis of rectangular plate resting on an elastic half space using an energy approach. Appt. Math. Modelling, 1992, Vol. 16, July.
11. Atluri S, Zhu T. A new meshless local Petrov–Galerkin (MLPG) approach to nonlinear problems in computer modeling and simulation. Comput Model EngSci 1998;3:187–96.
12. Atluri S, Zhu T. A new meshless local Petrov–Galerkin (MLPG) approach in computational mechanics. ComputMech 1998;22:117–27.
13. Avram, C., et al., Numerical Analysis of Reinforced Concrete Structures, Elsevier, Amsterdam, 1993.
14. Babuška I, Melenk JM. The partition of unity finite element method: basic theory and applications. Comput Methods ApplMech Eng 1996;139:289–314.
15. Banerjee, P. K., and Butterfield, R., Boundary Element Methods in Engineering Science, McGraw-Hill Book Co., London, 1981.
16. Batoz, J. L., “An Explicit Formulation for an Efficient Triangular Plate Bending Element,” Int. J. Num. Meth. Eng., 18 (1982), 1077–1089.
17. Batoz, J. L., and TAHAR, M. B., “Evaluation of a New Quadrilateral Thin Plate Bending Element,” Int. J. Num. Meth. Eng., 18 (1982), 1655–1677.
18. Batoz, J. L., BATHE, J.-K., and HO, L., “A Study of Three-Node Triangular Plate Bending Elements,” Int. J. Num. Meth. Eng., 15 (1980), 1771–1812.
19. BEER, G., and WATSON, J. O., Introduction to Finite and Boundary Element Methods for Engineers, John Wiley & Sons, New York, 1992.

20. Belytschko T, Krongauz Y, Organ D, Fleming M, Krysl P. Meshless methods: an overview and recent developments. *Comput Methods ApplMech Eng* 1996;139:3–47.
21. Belytschko T, Lu YY, Gu L. Element-free Galerkin methods. *Int J Numer Methods Eng* 1994;37:229–56.
22. Benard, E. F., “A Study of the Relationship between Lattice and Continuous Structures,” Ph.D. Thesis, University of Illinois, Urbana, Illinois, 1965.
23. Biot, M. A. (1937) “Bending of Infinite Beams on an Elastic Foundation,” *J. Appl. Mech.Trans. Am. Soc. Mech. Eng.*, 59: A1-7.
24. Booker JR, Balaam NP & Davis EH. The behaviour of an elastic nonhomogeneous half-space, Part I: Line and point loads. *International Journal for Numerical and Analytical Methods in Geomechanics* 1985: 9: 353–367.
25. Booker JR, Balaam NP & Davis EH. The behaviour of an elastic nonhomogeneous half-space, Part II: Circular and strip footings. *International Journal for Numerical and Analytical Methods in Geomechanics* 1985: 9: 369–381.
26. Boussinesq J. *Application des Potentiels à l’Etude de l’Equilibre et du Mouvement des Solides Elastique*. Paris: Gauthier-Villars, 1885.
27. Brebbia, C. A. (Ed.), *Recent Advances in Boundary Element Method, Proceedings of the First Conference on Boundary Element Methods*, Pentech Press, London, 1978.
28. Brownlee RA. Error estimates for interpolation of rough data using the scattered shifts of a radial basis function. *Numer Algorithms* 2005;39: 57–68.

29. Chen JS, Pan C, Wu T, Liu WK. Reproducing kernel particle methods for large deformation analysis of non-linear structures. *Comput Methods ApplMech Eng* 1996;139:195–227.
30. Chen, C., and ZHOU, J., *Boundary Element Methods*, Academic Press, London, 1992.
31. Cheng, A.H.; Young, D.L.; Tsai, C.C.; Solution of Poisson's equation by iterative DRBEM using compactly supported, positive definite radial basis function', *Engineering Analysis with Boundary Elements* v 24 n 7-8, Jul 2000, pp 549-557.
32. Cheung, M. S., et al., *Finite Strip Analysis of Bridges*, E&F Spon, London, 1996.
33. Cheung, Y. K., "The Finite Strip Method in the Analysis of Elastic Plates with Two Opposite Simply Supported Ends," *Proc. Inst. Civ. Eng.*, 40 (1968), 1–7.
34. Cheung, Y. K., and THAM, L. G., *Finite Strip Method*, CRC Press, Boca Raton, Florida, 1998.
35. CHEUNG, Y. K., O.C. ZIENKIEWICZ, "Plates And Tanks On Elastic Foundations-An Application Of Finite Element Method". *ht. J. Solids Structures*, 1965, Vol. 1, pp. 451 +I 461. Pergamon F'mss Ltd. Printed in Great Britain
36. Civalek, O. "Nonlinear analysis of thin rectangular plates on Winkler-Pasternak elastic foundations by DSC-HDQ methods". *Applied Mathematical Modelling*, 31 (3), pp. 606-624., 2007.
37. Cook, R. D., D. S. Malkus, and M. E. Plesha "Concepts and applications of finite element analysis". New York: John Wiley. 1989
38. Dhatt, G., et al., "New Triangular Discrete Kirchhoff Plate/Shell Element," *Int. J. Num. Meth. Eng.*, 23 (1986), 453–470.
39. Dhatt, G., et al., "Numerical Analysis of Thin Shells by Curved Triangular Elements Based on Discrete Kirchhoff Hypothesis," in *Proceedings of the ASCE*

Symposium on Application of FEM in Civil Engineering, Vanderbilt University, Nashville, Tennessee, 1969, pp. 255–278.

40. Driscoll TA. Interpolation in the limit of increasingly flat radial basis functions. *Comput Math Appl* 2002;43(3):413–22.
41. Du, Q., YAO, Z., and SONG, G., “Solution of Some Plate Bending Problems Using the Boundary Element Method,” *Appl. Math. Modeling*, 8 (1984), 15–22.
42. Duarte CA, Oden JT. An hp adaptive method using clouds. *Comput Methods ApplMech Eng* 1996;139:237–62.
43. Duarte CA, Oden JT. Hp cloud-an hp meshless method. *Numer Methods Part Differ Equat* 1996;12:673–705.
44. Dumir, P. C. “Large Deflection axis-symmetric Analysis Of Orthotropic Annular Plates On Elastic Foundations”. *J. Solut. Structures* Vol. 24.No.8.Pp.777-787, 1988.
45. Dumir, P. C. And A. Bhaskar. “Nonlinear Static Analysis Of Rectangular Plates On Elastic Foundations By The Orthogonal Point Collocation Method”. *Computer Methods In Applied Mechanics And Engineering* 67 (1988) 111-124.
46. E. Larson, B. Fornberg; A Numerical Study of some Radial Basis Function based Solution Methods for Elliptic PDEs. *Computers & Mathematics with Applications*. Volume 46, Issues 5–6, September 2003, Pages 891–902
47. Eduard Ventsel, and Theodor Krauthammer. “Thin Plates and Shells Theory, Analysis, and Applications”. Marcel Dekker, Inc.2001.
48. El-Zafrany, A., Fadhil, S.” A modified Kirchhoff theory for boundary element analysis of thin plates resting on two-parameter foundation”. *Engineering Structures*, 18 (2), pp. 102-114., 1996.

49. EL-Zarany, A., FADHIL, S., and DEBBIH, M., “An Efficient Approach for Boundary Element Bending Analysis of Thin and Thick Plates,” *Comp. Struct.*, 56 (1995), 565–576.
50. Fenglin Zhou, Jianming Zhang ,Xiaomin Sheng, Guangyao Li. “Shape variable radial basis function and its application in dual reciprocity boundary face method”. *Engineering Analysis with Boundary Elements* 35 (2011) 244–252
51. Ferreira AJM. A formulation of the multiquadric radial basis function method for the analysis of laminated composite plates. *Compos Struct* 2003;59:385–92.
52. Ferreira AJM. Free vibration analysis of Timoshenko beams and Mindlin plates by radial basis functions. *Int J Comput Methods* 2005;2(1):15–31.
53. Florez, W., Power, H. and Chejne, F., Multi-domain dual reciprocity BEM approach for the Navier-Stokes systems of equations, *Communications in Numerical methods in Engineering*, v 16, n 10, Oct. 2000, pp 671-681.
54. Forsyth, G. E., and WASOW, W. R., *Finite Difference Methods for Partial Differential Equations*, John Wiley & Sons, New York, 1960.
55. G. J. Turvey and M. Salehi. “Dr Large Deflection Analysis Of Sector Plates”. *Computers & Structures* Vol. 34. No. I, pp. 101-I 12, 1990.
56. G. J. Turvey; M. Salehi; Circular plates with one diametral stiffener- an elastic large deflection analysis; *Computers and structures*, v 63, n 4, may 1997, pp 775-783.
57. G. J. Turvey; M. Salehi; Elastic large deflection analysis of stiffened annular sector plates, *Int. Journal of mechanical sciences*, v 40, n 1, January, 1998, pp 51-70.
58. George Z. Voyiadjis, ShahramSarkan. “Engineering Large Deflection Theory For Thick Plates”. *Journal of Engineering Mechanics*, Vol. 115, No.5, May, 1989.

59. Gingold RA, Monaghan JJ. Smoothed particle hydrodynamics: theory and allocation to non-spherical stars. *Mon Not Roy Astron Soc* 1977;181:375–89.
60. Golberg, M.A., Chen, C.S., Bowman, H.; Some recent results and proposals for the use of radial basis functions in the BEM, *Engng. Anal. Bound. Elem* 1999; 23:285-96.
61. Hardy RL. Multiquadric equations of topography and other irregular surfaces. *Geophys Res* 1971;176:1905–15.
62. He Xiao-Qiao and Qin Qing-Hua, “Nonlinear Analysis of Resisner Plates by the Variational Boundary Elements Method”, *Appl. Math. Modeling*, 1993.
63. Hemsely, J. A. *Elastic Analysis of Raft Foundations*. 1998.
64. Hildebrand, F. B., (1968). *Finite-Difference Equations and Simulations*, Section 2.2, Prentice-Hall, Englewood Cliffs, New Jersey.
65. Horibe, T., Asano, N.” Large deflection analysis of rectangular plates on two-parameter elastic”. *JSME International Journal, Series A: Solid Mechanics and Material Engineering*, 44 (4), pp. 483-489, 2001.
66. HRENNIKOFF, A., “Solution of Problems of Elasticity by the Framework Method,” *J. Appl. Mech., ASME*, 8 (Dec. 1941), A169–A175.
67. Hu, W.-J., Long, S.-Y., Xia, P. , Cui, H.-X. “Bending analysis of thick plate on the elastic foundation by the meshless radial point interpolation method”. *Gong chengLixue/Engineering Mechanics*, 26 (5), pp. 58-61+79, 2009
68. Huang, M.-H., Thambiratnam, D.P.” Analysis of plate resting on elastic supports and elastic foundation by finite strip method”. *Computers and Structures*, 79 (29-30), pp. 2547-2557., 2001.



69. Husain J. Al-Gahtani, Mahmoud Naffa'a. "RBF meshless method for large deflection of thin plates with immovable edges". *Engineering Analysis with Boundary Elements* 33 (2009) 176– 183.
70. Ibearugbulem O. M., L. O.Ettu, And J. C. Ezeh. "Direct Integration and Work Principle as New Approach in Bending Analyses of Isotropic Rectangular Plates". *The International Journal of Engineering And Science (IJES)*, Volume2 , Issue3, Pages 28-36, 2013, ISSN: 2319 – 1813 ISBN: 2319 – 1805.
71. Igor Shufrin, OdedRabinovitch, MosheEisenberger. "A semi-analytical approach for the geometrically nonlinear analysis of trapezoidal plates". *International Journal of Mechanical Sciences* 52 (2010) 1588–1596.
72. J. Alamatian, M.E. Golmakani. "Large deflection analysis of the moderately thick general theta ply laminated plates on nonlinear elastic foundation with various boundary conditions". *Mechanics Research Communications* 51 (2013) 78– 85.
73. J. Amdahl, E. Byklum; A simplified method for elastic large deflection analysis of plates and stiffened planes due to local buckling, *Thin-Walled structures*, v 40, n 11, November, 2002, pp 925-953.
74. J. Sladek; V. Sladek; A meshless method for large deflection of plates, *Computational Mechanics*, v 30, 2003, p 155-163.
75. J. T. Katsikadelis. "Large Deflection Analysis Of Plates On Elastic Foundation By The Boundary Element Method". *Int. J. Solut. Structures* Vol. 27.No.15.Pp.1867-1878, 1991.
76. J. Yang, L. Zhang. "Nonlinear analysis of imperfect laminated thin plates under transverse and in-plane loads and resting on an elastic foundation by a semi analytical approach". *Thin-Walled Structures* 38 (2000) 195–227.

77. JánBalaš, JánSládeck and Vladimir Sládeck, Boundary Integral Equation(BIE) Solution for Circular Plate on Elastic Foundations, Studies in Applied Mechanics 23, Stress Analysis by Boundary Element Methods, Elsevier, pp 615-620, 1989.
78. JánBalaš, JánSládeck and Vladimir Sládeck, Large Deflections-Berger Equation, Studies in Applied Mechanics 23, Stress Analysis by Boundary Element Methods, Elsevier, pp 578-599, 1989.
79. Jeom Kee Paik, JuHye Park, and Bong Ju Kim. “Analysis of the Elastic Large Deflection Behavior for Metal Plates under Nonuniformly Distributed Lateral Pressure with In-Plane Loads”. Hindawi Publishing Corporation Journal of Applied Mathematics Volume 2012, Article ID 734521.
80. Jianqiao, Ye, “Large deflection of imperfect plates by iterative BE-FE method”, J. Eng. Mech., v 120 n 3, Mar 1994, pp 431-444.
81. Ji-Huan He. “A Lagrangian for von Karman equations of large deflection problem of thin circular plate” Applied Mathematics and Computation 143 (2003) 543–549.
82. Jumarchon, B.; Amini, S.; Chen, K.; Hermite collocation method using radial basis functions, Engineering Analysis with Boundary Elements, v 24 n 7-8, Jul 2000, pp 607-611.
83. K. J. Dai; G. R. Liu; K. M. Lim; X. Han; S. Y. Du; A meshfree radial point interpolation method for analysis of functionally graded material (FGM) plates, Computational Mechanics, v 34, 2004, p 213-223.
84. K.G. Muthurajan, K. Sankaranarayananasamy, S.B. Tiwari, B. NageswaraRao. “Nonlinear vibration analysis of initially stressed thin laminated rectangular plates on elastic foundations”. Journal of Sound and Vibration 282 (2005) 949–969.
85. K.M. Liew ,Xin Zhao, Antonio J.M. Ferreira. “A review of meshless methods for laminated and functionally graded plates and shells”. Composite structures, 2011.

86. Kane, J. H., "Boundary Element Analysis in Engineering Continuum Mechanics", Prentice- Hall, Englewood Cliffs, New Jersey, 1994.
87. Kansa EJ, Carlson RE. "Improved accuracy of multiquadric interpolation using variable shape parameters". *Comput Math Appl* 1992;24:99–120
88. Kansa EJ, Hon YC. "Circumventing the ill-conditioning problem with multiquadric radial basis functions: applications to elliptic partial differential equations". *Comput Math Appl* 2000;39:123–37.
89. Kansa EJ. "Multi-quadrics—a scattered data approximation scheme with applications to computational fluid-dynamics. I. Surface approximations and partial derivative estimates". *Comput Math Appl* 1990;19(8/9):127–45.
90. Kansa EJ. "Multiquadrics—a scattered data approximation scheme with applications to computational fluid-dynamics. II. Solutions to hyperbolic, parabolic and elliptic partial differential equations". *Comput Math Appl* 1990;19:147–61.
91. Katsilkadelis, J. T. and Nerantzaki, M. S., "Nonlinear analysis of plates by the analog method equation method", *Computational mechanics*, v 14, n 2, may 1994, pp 154-164.
92. Kikuchi, F., "On the Finite Element Scheme Based on the Discrete Kirchhoff Assumption," *Num. Math.*, 24 (1975), 2005–2029.
93. Krysl P, Belytschko T. "Analysis of thin plates by the element-free Galerkin method". *ComputMech* 1996;17:26–35
94. Levy, H.; Lessman, F. (1992). "Finite Difference Equations". Dover. ISBN 0-486-67260-3.
95. Li S, Liu WK. "Meshfree and particle methods and their application". *ApplMech Rev* 2002;55:1–34.

96. Li, Q.S., Jie Liu, H.B. Xiao. "A new approach for bending analysis of thin circular plates with large deflection". *International Journal of Mechanical Sciences* 46 (2004) 173–180.
97. Little, G. H., "Efficient large deflections of rectangular plates with transverse edges remaining straight", *J. Computers and Structures*, v 71, n 3, May 1999, pp 353-357.
98. Little, G. H., "Large deflections of rectangular plates with general transverse form of displacement", *J. Computers and Structures*, v 71 n 3, May 1999, pp 333-352.
99. Liu WK, Chen Y, Jun S, Chen JS, Belytschko T, Pan C, et al. "Overview and applications of reproducing kernel particle methods". *Arch Comput Methods Eng* 1996;3:3–80.
100. Liu WK, Jun S, Zhang YF. "Reproducing kernel particle methods". *Int J Numer Methods Fluids* 1995;20:1081–106.
101. Liu WK, Li S, Belytschko T. "Moving least-square reproducing kernel methods (I) methodology and convergence". *Comput Methods ApplMech Eng* 1997;143:113–54.
102. Lucy LB. "A numerical approach to the testing of the fission hypothesis". *J Astron* 1977;82:1013–24.
103. M. Duan; M. Mahendran; "Large deflection analyses of skew plates using hybrid/mixed finite element method", *Computers and Structures*, v 81, n 13, may, 2004, pp 1415-1424.
104. M. Gorji. "Nonlinear Deformation of Axisymmetrically Loaded Polar Orthotropic Annular Plates". *Composites Science and Technology* 34 (1989) 187-203.

105. M. Mofid, and M. Noroozi. "A Plate on Winkler Foundation with Variable Coefficient". *Scientia Iranica, Transaction A: Civil Engineering*, Vol. 16, No. 3, pp. 249-255, (2009).
106. M.C.M. Bakker, M. Rosmanit, H. Hofmeyer. "Approximate large-deflection analysis of simply supported rectangular plates under transverse loading using plate post-buckling solutions". *Thin-Walled Structures* 46 (2008) 1224– 1235.
107. Mahmoud Naffa, Husain J. Al-Gahtani. "RBF-based meshless method for large deflection of thin plates". *Engineering Analysis with Boundary Elements* 31 (2007) 311–317.
108. Malekzadeh, P., Setoodeh, A.R. "Large deformation analysis of moderately thick laminated plates on nonlinear elastic foundations by DQM". *Composite Structures*, 80 (4), pp. 569-579, 2007.
109. Masa. Tanaka, T. Matsumoto & Z.-D. Zheng. "Incremental analysis of finite deflection of elastic plates via boundary-domain-element method". *Engineering Analysis with Boundary Elements* 17 (1996) 123-131.
110. Mikhailov, M.D.; "Integrals of radial functions for boundary element method, *Communications in Numerical methods in Eng*", v 16 n 10, Oct 2000, pp 683-685.
111. Narcowich FJ, Ward JD, Wendland H. "Refined error estimates for radial basis function interpolation". *ConstrApprox* 2003;19:541–64.
112. Nardini D, Brebbia CA. "A new approach to free vibration analysis using boundary elements". *Appl Math Model* 1982;7(3):157–62.
113. Nayak M. Elastic settlement of a cross-anisotropic medium under axisymmetric loading. *Soil and Foundations* 1973: 13(2): 83–90.

114. Nayroles B, Touzot G, Villon P. "Generalizing the finite element method: diffuse approximation and diffuse elements". *ComputMech* 1992;10:307–18.
115. Nguyen VP, Rabczuk T, Bordas S, Duflot M. "Meshless methods: a review and computer implementation aspects". *Math.Comput.Simul.* 2008;79:763–813.
116. Papakaliatakis, G., and Simos, T. E., "A Finite Difference Method for the Numerical Solution of Fourth-Order Differential Equations with Engineering Applications," *Comp. Struct.*, 65 (1997), 491–495.
117. Pasternak PL. On a new method of analysis of an elastic foundation by means of two foundation constants. *Gosudarstvennoe Izdatelstro Liberaturipo Stroitelstvui Arkhitekture, Moscow (in Russian), 1954.*
118. Pollandt, R, "Solving nonlinear differential equations of mechanics with the boundary element method and radial functions", *Int. J. Num. Methods in Engineering*, v 40 n 1, Jan 1997, pp 61-73.
119. Qin, Q. H.; "Nonlinear Analysis of resisner Plates on Elastic Foundation by the Boundary Element Method", *Int. J. Solids Struct.*, 1993, 30(22), pp 3101- 3111.
120. Ramachandra, L. S. and Roy, D., "A novel technique in the solution of axis-symmetric large deflection analysis of a circular plate". *J. App. Mech.*, v 68 (5), Sep. 2001, pp 814-816.
121. Rao, S. S. (1989). "The finite element method in engineering". 2nd Ed. Oxford: Pergamon press.
122. Rashed, Y.F ,Aliabadi, M.H., Brebbia, C.A. "The boundary element method for thick plates on a winkler foundation". *International Journal for Numerical Methods in Engineering*, 41 (8), pp. 1435-1462, 1998.

123. Ritz, W. (1908). "Übereine neue method zur Lösung gewisser variations probleme der mathematischen Physik. Zeitschrift für Reine und Angewandte Mathematik". 135, 1-61.
124. Robert A., VanGorder. "Analytical method for the construction of solutions to the Föppl-vonKármán equations governing deflections of a thin flat plate". International Journal of Non-Linear Mechanics 47 (2012) 1–6.
125. S. N. Atluri; T. Zhu; "New concepts in meshless methods", Intl. J. for Numerical Methods in Engineering, v 47, n 1, January, 2000, pp 537-556.
126. Salonen, E.-M., "A Gridwork Method for Plates in Bending," Acta Polytec. Scand., Civil Engineering and Building Construction Series No. 8. (1969), 1–31.
127. Schaback R. "Error estimates and condition numbers for radial basis function interpolation". Adv Comput Math 1995;3:251–64.
128. Shen, H.-S." Large deflection of Reissner-Mindlin plates on elastic foundations". Journal of Engineering Mechanics, 124 (10), pp. 1080-1089, 1998.
129. Sneddon IN. Fourier Transforms. New York: McGraw-Hill, 1951.
130. Stark RF & Booker JR. Surface displacements of a non-homogeneous elastic half-space subjected to uniform surface tractions, International Journal for Numerical and Analytical Methods in Geomechanics 1997: 21: 361–378; 379–395.
131. Szilard R. "Theory and analysis of plates". (New Jersey: Prentice-Hall, Englewood Cliffs). 1974
132. Szilard, R. "Theories and Applications of Plate Analysis". New Jersey: John Wiley & Sons Inc. 2004
133. T. Kawai and N. Yoshima, Analysis of Large Deflection of plates by Finite Element Method, Int. J. Num. Methods in Eng., 1969, pp 1-(123 thru 133).

134. Timoshenko S P, Gere J M "Theory of elastic stability. (New York: McGraw-Hill), 1961.
135. Timoshenko, S. and Woinowsky-Krieger, S. "Theory of plates and shells". McGraw-Hill New York, 1959.
136. Tottenham, H., "The Boundary Element Method for Plates and Shells", in Banerjee, P. K., and Butterfield, R. (Eds.), *Developments in Boundary Element Method Applied Science*, London, 1979.
137. Vesic, A. B. (1961) "Beams on Elastic Subgrade and Winkler's Hypothesis," Proc. 5<sup>th</sup> Int. Conf. on Soil Mechanics and Foundation Engineering, Paris: 845-850.
138. Voyiadjis, G. Z., and Pecquet, R. W., "Isotropic Plate Element with Shear and Normal Strain Deformations," *Int. J. Num. Meth. Eng.*, 24 (1987), 1671-1695.
139. Wand, W., X. Ji, M. Tanaka; "A dual reciprocity boundary element approach for the problems of large deflection of thin elastic plates", *J. Computational Mechanics*, v 26 n 1, July 2000, pp 58-65.
140. Wang C M, Wang Y C, Reddy J N "Problems and remedy for the Ritz method in determining stress resultant of corner supported rectangular plates". *Comput. Struct.* 80: 145-154.2002.
141. Wang D, El-Sheikh A I "Large deflection mathematical analysis of rectangular plates". *J. Eng. Mech.* 131: 809-821, 2005.
142. Wang Y & Ishikawa I. "A method for linear elastic-static analysis of multi-layered axi-symmetrical bodies using Hankel's transform". *Computational Mechanics* 2001: 27: 474-483.



143. Wang YH, Tham LG, Tsui Y & Yue ZQ. "Plate on layered foundation analyzed by a semi-analytical and semi-numerical method". *Computers and Geotechnics* 2003; 30: 409–418.
144. Wang, Y H, L G Tham and Y K Cheung "Beams and plates on elastic foundations: a review". *Wiley InterScience* DOI: 10.1002/pse.202, May 2005.
145. Wen, P.H.; Aliabadi, M. H.; Young, A., "Application of dual reciprocity method to plates and shells, *Engineering Analysis with Boundary Elements*" v 24 n 7-8, Jul 2000, pp 583-590.
146. Wendland H. "Error estimates for interpolation by radial basis functions of minimal degree". *J Approx Theory* 1998;93:258–72.
147. Winkler E. *Die Lehre von der Elastizitat und Festigkeit*. Dominicus, Prague, 1867.
148. Xiao, Y.-G., Fu, Y.-M. , Zha, X.-D." Nonlinear static analysis of moderately thick rectangular plate considering the coupled effect of elastic foundation". *Gong cheng Lixue/Engineering Mechanics*, 21 (4), pp. 189-193+198, 2004.
149. Xiao-Ting He, Jun-Yi Sun, Zhi-Xiang Wang, Qiang Chen, Zhou-Lian Zheng. "General perturbation solution of large-deflection circular plate with different moduli in tension and compression under various edge conditions". *International Journal of Non-Linear Mechanics* 55 (2013) 110–119.
150. Xiao-Ting He, Qiang Chen, Jun-Yi Sun, Zhou-Lian Zheng. "Large-deflection axisymmetric deformation of circular clamped plates with different moduli in tension and compression". *International Journal of Mechanical Sciences* 62 (2012) 103–110.
151. Xue, Y., V. A. Jairazbhov, X. Niu, J. Qu; "Large deflection of thin plates under certain mixed boundary conditions-cylindrical bending", *J. Electronic Packaging*, ASME transactions, v 125, n 1, 2003, pp 53-58.

152. Yen-Liang Yeh, Cheng Chi Wang, Ming-Jyi Jang. "Using finite difference and differential transformation method to analyze of large deflections of orthotropic rectangular plate problem". *Applied Mathematics and Computation* 190 (2007) 1146–1156.
153. Yettram, A. I., and Hussain, H. M., "Gridwork Method for Plates in Flexure," *J. Struct. Div., ASCE*, 97 (1971), 149–153.
154. Yin YP, Wang YH & Zhu JQ. "Solutions of axisymmetric load applied to layered foundation". *Rock and Soil Mechanics* 2001: 22(2): 156–158 (in Chinese).
155. Yoo, W., J. Lee, S. Park, J. Sohn, D. Pogorelov, O. Dmitrochenko; "Large deflection analysis of a thin plate, Computer simulation and experiments", *Multibody system Dynamics*, v 11, n 2, March 2004, pp 185-208.
156. Yuanhan Wang, Jun Ni, Y.K. Cheung. "Plate on non-homogeneous elastic half-space analysed by FEM". *Structural Engineering and Mechanics*, Vol. 9, No. 2 (2000) 127-139.
157. Zhang, X.; Song, K.Z.; Lu, M.W; Liu, X.; "Meshless methods based on collocation with radial basis functions", *Computational mechanics* v 26 n 4, Oct 2000, pp 333-343.
158. Zienkiewicz O. C., "Geometrically Nonlinear Problems, Large Displacement and Structural Stability, The Finite Element Method", 3<sup>rd</sup> Edition, McGraw-Hill, New York, 1978, pp 506-514.
159. Zienkiewicz, O. C., "Finite Element Procedures in the Solution of Plate and Shell Problems," in Zienkiewicz, O. C., and Holister, G. S. (Eds.), *Stress Analysis*, John Wiley & Sons, London, 1965.

## APPENDICES

### Appendix A MATHEMATICA CODES (W-U-V)

Mathematica Code for Large Deflection of Immovable Thin Plates (u-v-w-formulation)

- **Definitions of Variables**

sf : shape factor = 1 for square and 2 for circle  
t : Thickness of the plate  
 $\nu$  = Poison' ratio of the plate material  
e = Elastic modulus of the plate material  
c = Shape factor of the eadial basis function  
a; b; lx; ly : plate diemnsions  
 $\alpha$  : Aspect ratio of the plate  
 $\beta$  : Plate length / depth ratio  
nb : Number of boundary nodes  
nf : Number of field nodes  
np : Total number of boundary nodes  
xb, yb : x and y Coordinates of boundary nodes  
xf, yf : x and y Coordinates of field (domain) nodes  
xs, ys : x and y Coordinates of fictitios off - boundary nodes  
dx = space between nodes in x - direction  
dy = space between nodes in y - direction  
nx, ny : x and y components of the unit vector normal to the boundary  
tbcw1 : First boundary condition (tbcw1 = 1 for deflection and 2 for shear)  
tbcw2 : Second boundary condition (tbcw2 = 1 for slope and 2 for moment)  
bcw1 : Value of first boundary condition  
bcw2 : Value of fsecond boundary condition

**LUV11**; LUV12; LUV21; LUV22 : Differential operators for the Linear part of the differential equation governing the inplane deflection  
Aw : Coeficient matrix for the transverse deflection w  
AUV : Coeficient matrix for the inplane deflections u and v  
NLUVW1 : First part of the differential operators for the non - linear part of the differential equation governing the transverse deflection  
NLUVW2 : Second part of the differential operators for the non - linear part of the differential equation governing the transverse deflection  
NLW11 : First part of the differential operators for the non - linear part of the differential equation governing the inplane deflection  
NLW22 : Second part of the differential operators for the non - linear part of the differential equation governing the inplane deflection  
NLSHEAR : Non - linear part of the shear force  
MX : Bending moment per unit length at the edge whose normal vector is directed along x  
MY : Bending moment per unit length at the edge whose normal vector is directed along xy  
MXY : Twisting moment per unit length at the edge whose normal vector is directed along x  
SXXB : Bending stress in x - direction  
SYYB : Bending stress in y - direction  
SXXM : Membrane stress in x - direction  
SYYM : Membrane stress in y - direction  
K : Winkler model parameter  
K1 : Non - linear Winkler model parameter  
G : Pasternak model parameter  
relf : Relaxation facor

## ■ Geometry Modeling

---

```
Clear["Global"]
sf = 2;
If[sf == 1, a = 1.;
b = 1.;
lx = 1.;
ly = 1.;
α = a/b;
β = a/t;
nn = 9;
nb = 4*nn;
nf = nn*nn;
np = nb + nf;
dx = 4. lx/(nb + 4) ;
dy = dx; xbl = Table[dx i, {i, 1, nb/4}];
xb2 = Table[1, {i, 1, nb/4}];
xb3 = Table[1. - dx i, {i, 1, nb/4}];
xb4 = Table[0., {i, 1, nb/4}];
yb1 = Table[0., {i, 1, nb/4}];
yb2 = Table[dy i, {i, 1, nb/4}];
yb3 = Table[1, {i, 1, nb/4}];
yb4 = Table[1. - dy i, {i, 1, nb/4}];
nx1 = Table[0., {i, 1, nb/4}];
nx2 = Table[1., {i, 1, nb/4}];
nx3 = Table[0., {i, 1, nb/4}];
nx4 = Table[-1., {i, 1, nb/4}];
ny1 = Table[-1., {i, 1, nb/4}];
ny2 = Table[0., {i, 1, nb/4}];
ny3 = Table[1., {i, 1, nb/4}];
ny4 = Table[0., {i, 1, nb/4}];
xb = Join[xb1, xb2, xb3, xb4];
yb = Join[yb1, yb2, yb3, yb4];
nx = Join[nx1, nx2, nx3, nx4];
ny = Join[ny1, ny2, ny3, ny4];
d1 = 0.1;
xs1 = xb + d1*nx;
ys1 = yb + d1*ny;
xs2 = xb + 2*d1*nx;
ys2 = yb + 2*d1*ny;
xf = Flatten[Table[dx i, {j, 1, nb/4}, {i, 1, nb/4}]];
yf = Flatten[Table[dy j, {j, 1, nb/4}, {i, 1, nb/4}]];
xf2 = {0.05, 0.35, 0.65, 0.95, 0.05, 0.35, 0.65, 0.95, 0.05, 0.35, 0.65, 0.95};
yf2 = {0.083, 0.083, 0.083, 0.083, 0.5, 0.5, 0.5, 0.5, 0.917, 0.917, 0.917, 0.917};
xf3 = Join[xf2, xf2];
yf3 = Join[yf2, yf2];
xp = Join[xb, xf];
yp = Join[yb, yf];
xps1 = Join[xb, xf, xs1];
yps1 = Join[yb, yf, ys1];
xps2 = Join[xb, xf, xs1, xs2];
yps2 = Join[yb, yf, ys1, ys2];
dat1 = Table[{xb[[i]], yb[[i]]}, {i, 1, nb}];
dat2 = Table[{xs1[[i]], ys2[[i]]}, {i, 1, nb}];
dat3 = Table[{xf[[i]], yf[[i]]}, {i, 1, nf}];
p1 = ListPlot[dat1, PlotStyle -> PointSize[0.02], PlotMarkers -> "/"];
p2 = ListPlot[dat2, PlotStyle -> PointSize[0.02], PlotMarkers -> "\\\\"*
StyleBox["°", \nFontSize->24]\\\"]; p3 = ListPlot[dat3, PlotStyle -> PointSize[0.02],
PlotMarkers -> "●"];
Show[p1, p2, p3, PlotRange -> All];
```

```

a = 1.;
b = 1.;
α = a/b;
β = a/t;
RR = a;
XL = -RR;
XR = RR;
YB = -RR;
YT = RR;
dx = 0.2;
dy = 0.2;
ds = 0.05; n = 0;
Do[xx = XL + dx j;
yy = YB + dy i;
If[ xx^2 + yy^2 < (RR - ds)^2, n = n + 1;
x[n] = xx; y[n] = yy], {i, 1, Ceiling[(YT - YB)/dy]}, {j, 1, Ceiling[(XR - XL)/dx]}; dat =
Table[{x[i], y[i]}, {i, 1, n}]; p5 = ListPlot[dat, AspectRatio -> 1, PlotStyle ->
PointSize[0.02]];
p6 = Show[Graphics[Circle[{0, 0}, RR]]];
nb = 32;
nf = n;
np = nb + nf;
Do[xb[i] = -XR*Cos[360. Degree/nb *i];
yb[i] = -YT*Sin[360. Degree/nb *i], {i, 0, nb}];
datb = Table[{xb[i], yb[i]}, {i, 0, nb}];
p7 = ListPlot[datb, AspectRatio -> 1, PlotStyle -> PointSize[0.02]];
Show[p5, p6, p7, PlotRange -> All];
xf = Flatten[Table[x[i], {i, 1, n}]];
yf = Flatten[Table[y[i], {i, 1, n}]];
xb = Flatten[Table[xb[i], {i, 1, nb}]];
yb = Flatten[Table[yb[i], {i, 1, nb}]];
xp = Join[xb, xf];
yp = Join[yb, yf];
nx = Table[-Cos[360./nb Degree*i], {i, 1, nb}];
ny = Table[-Sin[360./nb Degree*i], {i, 1, nb}];
d1 = 0.1;
xs1 = xb + d1*nx;
ys1 = yb + d1*ny;
xs2 = xb + 2*d1*nx;
ys2 = yb + 2*d1*ny;
xps1 = Join[xb, xf, xs1];
yps1 = Join[yb, yf, ys1];
xps2 = Join[xb, xf, xs1, xs2];
yps2 = Join[yb, yf, ys1, ys2];
dat1 = Table[{xb[[i]], yb[[i]]}, {i, 1, nb}];
dat2 = Table[{xs1[[i]], ys1[[i]]}, {i, 1, nb}];
dat3 = Table[{xf[[i]], yf[[i]]}, {i, 1, nf}];
p1 = ListPlot[dat1, PlotStyle -> PointSize[0.02], PlotMarkers -> "*"];
p2 = ListPlot[dat2, PlotStyle -> PointSize[0.02], PlotMarkers -> "#"];
p3 = ListPlot[dat3, PlotStyle -> PointSize[0.02], PlotMarkers -> "●"];
Show[p1, p2, p3, PlotRange -> All]]

```

## • Generation of Matrices Elements

```

t = 0.1; v = 0.3; e = 10000;
c = 0.08; c1 = c^2;
B11 = 2; B12 = 1; B13 = 1; B14 = 1;
B21 = 2; B22 = 1; B23 = 1; B24 = 1;
ndomain = np;
If[ndomain == nf, xdomain = xf, ydomain = yf, xdomain = xp, ydomain = yp];
tbcw1 = Table[If[i ≤ nb/4, B11, If[nb/4 < i ≤ nb/2, B12, If[nb/2 < i ≤ 3*nb/4, B13, B14]]], {i, 1, nb}];
tbcw2 = Table[If[i ≤ nb/4, B21, If[nb/4 < i ≤ nb/2, B22, If[nb/2 < i ≤ 3*nb/4, B23, B24]]], {i, 1, nb}];
vbcw1 = Table[0, {i, 1, nb}];
vbcw2 = Table[0, {i, 1, nb}];
vbcu = Table[If[i ≤ nb/4, 0, If[nb/4 < i ≤ nb/2, 0, If[nb/2 < i ≤ 3*nb/4, 0, 0]]], {i, 1, nb}];
vbcv = Table[If[i ≤ nb/4, 0, If[nb/4 < i ≤ nb/2, 0, If[nb/2 < i ≤ 3*nb/4, 0, 0]]], {i, 1, nb}];
r2 = (x - xi)^2 + (y - yi)^2; r = Sqrt[r2]; phi = Sqrt[r2 + c1];

```

$$\text{LUV11}[f\_] := D[f, \{x, 2\}] + \frac{\alpha^2}{2} D[f, \{y, 2\}] (1 - v);$$

$$\text{LUV12}[f\_] := \frac{\alpha^2}{2} D[f, \{x, 1\}, \{y, 1\}] (1 + v);$$

$$\text{LUV21}[f\_] := \frac{\alpha}{2} D[f, \{x, 1\}, \{y, 1\}] (1 + v);$$

$$\text{LUV22}[f\_] := \alpha \left( \alpha^2 D[f, \{y, 2\}] + \frac{1}{2} D[f, \{x, 2\}] (1 - v) \right);$$

Do[bcw1[f\_, i\_] :=

$$\begin{aligned} & \text{If}[tbcw1[[i]] = 1, f, \frac{1}{12(-1+v^2)} ((ny[[i]] * \alpha^3 - nx[[i]]^2 * ny[[i]] * \alpha^3 * (v-1)) * D[f, \{y, 3\}] \\ & + (nx[[i]] - ny[[i]]^2 * nx[[i]] * v + ny[[i]]^2 * nx[[i]]) * D[f, \{x, 3\}] \\ & + (2 * nx[[i]]^2 * ny[[i]] * \alpha * (v-1) + ny[[i]] * \alpha + ny[[i]]^3 * \alpha - ny[[i]]^3 * \alpha * v) D[D[f, \{x, 2\}], y] \\ & + (-nx[[i]]^3 * \alpha^2 * (v-1) + nx[[i]] * \alpha^2 - 2 * nx[[i]] * ny[[i]]^2 * \alpha^2 + \\ & 2 * nx[[i]] * ny[[i]]^2 * \alpha^2 * v) D[D[f, x], \{y, 2\}]), \{i, 1, nb\}]; \end{aligned}$$

Do[bcw2[f\_, i\_] := If[tbcw2[[i]] = 1, D[f, x] nx[[i]] + D[f, y] ny[[i]],  
(-2 nx[[i]] ny[[i]] D[D[f, x], y] α (-1+v) + ny[[i]]<sup>2</sup> (D[f, {y, 2}] α<sup>2</sup> + D[f, {x, 2}] v) +  
nx[[i]]<sup>2</sup> (D[f, {x, 2}] + D[f, {y, 2}] v α<sup>2</sup>)), {i, 1, nb}];

Lw[f\_] := D[f, {x, 4}] + 2 D[f, {x, 2}, {y, 2}] α<sup>2</sup> + D[f, {y, 4}] α<sup>4</sup>;

```

Aw = Table[0., {i, 1, 2 nb + ndomain}, {j, 1, 2 nb + ndomain}];
Auv = Table[0., {i, 1, 2 nb + 2 ndomain}, {j, 1, 2 nb + 2 ndomain}];

Do[Aw[[i, j]] = bcw1[phi, i] /. {x -> xb[[i]], y -> yb[[i]], xi -> xps2[[j]], yi -> yps2[[j]]},
  {i, 1, nb}, {j, 1, ndomain + 2 nb}];
Do[Aw[[i + nb, j]] = bcw2[phi, i] /. {x -> xb[[i]], y -> yb[[i]], xi -> xps2[[j]], yi -> yps2[[j]]},
  {i, 1, nb}, {j, 1, ndomain + 2 nb}];
Do[Aw[[i + 2 nb, j]] = Lw[phi] /. {x -> xdomain[[i]], y -> ydomain[[i]], xi -> xps2[[j]], yi -> yps2[[j]]},
  {i, 1, ndomain}, {j, 1, 2 nb + ndomain}];

Do[Auv[[i, j]] = phi /. {x -> xb[[i]], y -> yb[[i]], xi -> xps1[[j]], yi -> yps1[[j]]},
  {i, 1, nb}, {j, 1, ndomain + nb}];
Do[Auv[[i + nb, j]] = LUV11[phi] /. {x -> xdomain[[i]], y -> ydomain[[i]], xi -> xps1[[j]], yi -> yps1[[j]]},
  {i, 1, ndomain}, {j, 1, ndomain + nb}];
Do[Auv[[i + nb, j + nb + ndomain]] =
  LUV12[phi] /. {x -> xdomain[[i]], y -> ydomain[[i]], xi -> xps1[[j]], yi -> yps1[[j]]},
  {i, 1, ndomain}, {j, 1, ndomain + nb}];

Do[Auv[[i + nb + ndomain, j + nb + ndomain]] =
  phi /. {x -> xb[[i]], y -> yb[[i]], xi -> xps1[[j]], yi -> yps1[[j]]}, {i, 1, nb}, {j, 1, ndomain + nb}];
Do[Auv[[i + 2 * nb + ndomain, j]] = LUV21[phi] /. {x -> xdomain[[i]], y -> ydomain[[i]],
  xi -> xps1[[j]], yi -> yps1[[j]]}, {i, 1, ndomain}, {j, 1, ndomain + nb}];
Do[Auv[[i + 2 * nb + ndomain, j + nb + ndomain]] = LUV22[phi] /. {x -> xdomain[[i]],
  y -> ydomain[[i]], xi -> xps1[[j]], yi -> yps1[[j]]}, {i, 1, ndomain}, {j, 1, ndomain + nb}];
Awinv = Inverse[Aw]; Auvinv = Inverse[Auv];

```

## • Incremental – Iterative Procedure

```

Do[If[nk == 1, K = 2300, If[nk == 2, K = 25, K = 50]];
Do[If[nk1 == 1, K1 = 0, If[nk1 == 2, K1 = 25, K1 = 50]]; Do[If[ng1 == 1, G1 = 0, If[ng1 == 2, G1 = 10, G1 = 20]];
Ruv = Table[0, {i, 1, 2 nb + 2 ndomain}]; Rw = Table[0, {i, 1, 2 nb + ndomain}];
RP = Table[0, {i, 1, ndomain}]; AP = Table[0, {i, 1, ndomain}, {j, 1, ndomain}];
ps = Table[0, {i, 1, ndomain}]; pp = Table[0, {i, 1, ndomain}]; con = Table[0, {i, 1, ndomain}];
Rwuv = Table[0, {i, 1, 4 nb + 3 ndomain}]; auv = Table[0, {i, 1, 2 nb + 2 ndomain}];
aw = Table[0, {i, 1, 2 nb + ndomain}]; awuv = Table[0, {i, 1, 4 nb + 3 ndomain}];
NLW11 = Table[0, {i, 1, ndomain}]; NLW22 = Table[0, {i, 1, ndomain}]; sp = Table[0, {i, 1, ndomain}];
NLUVW1 = Table[0, {i, 1, ndomain}]; reaction = Table[0, {i, 1, ndomain}];
NLSHEAR = Table[0, {i, 1, nb}]; NLUVW1b = NLUVW1; NLW22b = NLW22; NLW11b = NLW11; NLSHEARb = NLSHEAR;

nout = 8; nincr = 1 * nout; m = nincr / nout;
elaso = 2; vs = 0.35; Es = 10 000;
relf = 0.65; px = 0; py = 0;

pz = 400;

```



```

Do[qz = (incr / nincr) * pz; qzb =  $\frac{qz \beta^4}{e}$ ; qx = (incr / nincr) px; qy = (incr / nincr) py;
iter = 0; wci[0] = 0; error = 1; While[iter = iter + 1; Nor[error < 0.01, iter ≥ 100],
Do[Rw[[i]] = If[tbcw1[[i]] > 1, vbcw1[[i]] + relf * NLSHEAR[[i]] + (1 - relf) * NLSHEARb[[i]],
vbcw1[[i]]], {i, 1, nb}];
Do[Rw[[i + 2 nb]] =  $\frac{1}{e} 12 * qz * \beta^4 * (1 - \nu^2) - \frac{12 * \beta^4 * (1 - \nu^2)}{e} * ps[[i]] +$ 
relf * NLUVW1[[i]] + (1 - relf) * NLUVW1b[[i]], {i, 1, ndomain}];
Do[Ruv[[i + nb]] =  $\frac{\beta^3 qx (-1 + \nu^2)}{e} + relf * NLW11[[i]] + (1 - relf) * NLW11b[[i]]$ , {i, 1, ndomain}];
Do[Ruv[[i + 2 * nb + ndomain]] =
 $\frac{\beta^3 qy (-1 + \nu^2)}{e} + relf * NLW22[[i]] + (1 - relf) * NLW22b[[i]]$ , {i, 1, ndomain}];

aw = Awinv.Rw; auv = Auvinv.Ruv;

w = Sum[aw[[j]] * bcw1[phi, j] /. {xi → xb[[j]], yi → yb[[j]]}, {j, 1, nb}] +
Sum[aw[[j + nb]] * bcw2[phi, j] /. {xi → xb[[j]], yi → yb[[j]]}, {j, 1, nb}] +
Sum[aw[[j]] * phi /. {xi → xdomain[[j]], yi → ydomain[[j]]}, {j, 1, ndomain}];
u = Sum[auv[[j]] phi /. {xi → xps1[[j]], yi → yps1[[j]]}, {j, 1, nb + ndomain}];
v = Sum[auv[[j + ndomain + nb]] phi /. {xi → xps1[[j]], yi → yps1[[j]]}, {j, 1, nb + ndomain}];

wx = D[w, x]; wwx = Table[wxx /. {x → xdomain[[i]], y → ydomain[[i]]}, {i, 1, ndomain}];
wxx = D[w, {x, 2}]; wwxx = Table[wxxx /. {x → xdomain[[i]], y → ydomain[[i]]}, {i, 1, ndomain}];
wxy = D[w, {x, 1}, {y, 1}]; wwxy = Table[wxy /. {x → xdomain[[i]], y → ydomain[[i]]}, {i, 1, ndomain}];
wy = D[w, y]; wwy = Table[wyy /. {x → xdomain[[i]], y → ydomain[[i]]}, {i, 1, ndomain}];
wyy = D[w, {y, 2}]; wwyy = Table[wyyy /. {x → xdomain[[i]], y → ydomain[[i]]}, {i, 1, ndomain}];

NLUVW1b = NLUVW1; NLW11b = NLW11; NLW22b = NLW22; NLSHEARb = NLSHEAR;

NLW11 = Table[
(-wwx[[i]] wwxx[[i]] +  $\frac{1}{2}$  wwx[[i]] wwyy[[i]]  $\alpha^2 (-1 + \nu) - \frac{1}{2}$  wwxy[[i]] wwy[[i]]  $\alpha^2 (1 + \nu)$ ),
{i, 1, ndomain}];
NLW22 = Table[
(-wwy[[i]] wwyy[[i]]  $\alpha^3 + \frac{1}{2}$  wwxx[[i]] wwy[[i]]  $\alpha (-1 + \nu) - \frac{1}{2}$  wwx[[i]] wwxy[[i]]  $\alpha (1 + \nu)$ ),
{i, 1, ndomain}];

```

```

ww = Table[w /. {x -> xdomain[[i]], y -> ydomain[[i]]}, {i, 1, ndomain}];
wxx = Table[wxx /. {x -> xdomain[[i]], y -> ydomain[[i]]}, {i, 1, ndomain}];
wxxx = Table[wxxx /. {x -> xdomain[[i]], y -> ydomain[[i]]}, {i, 1, ndomain}];
wxy = Table[wxy /. {x -> xdomain[[i]], y -> ydomain[[i]]}, {i, 1, ndomain}];
wyy = Table[wyy /. {x -> xdomain[[i]], y -> ydomain[[i]]}, {i, 1, ndomain}];
wyyy = Table[wyyy /. {x -> xdomain[[i]], y -> ydomain[[i]]}, {i, 1, ndomain}];
uu = Table[u /. {x -> xdomain[[i]], y -> ydomain[[i]]}, {i, 1, ndomain}]; ux = D[u, x];
uux = Table[uux /. {x -> xdomain[[i]], y -> ydomain[[i]]}, {i, 1, ndomain}];
uy = D[u, y]; uuy = Table[uuy /. {x -> xdomain[[i]], y -> ydomain[[i]]}, {i, 1, ndomain}];
vv = Table[v /. {x -> xdomain[[i]], y -> ydomain[[i]]}, {i, 1, ndomain}]; vx = D[v, x];
vxx = Table[vxx /. {x -> xdomain[[i]], y -> ydomain[[i]]}, {i, 1, ndomain}]; vy = D[v, y];
vyy = Table[vyy /. {x -> xdomain[[i]], y -> ydomain[[i]]}, {i, 1, ndomain}];

reaction = Table[K*ww[[i]], {i, 1, ndomain}];
NLUVW1 =
Table[(-K*ww[[i]] K1*ww[[i]]^3 + G1*wxxx[[i]] + 12*uux[[i]]*wxxx[[i]] + 6*wxx[[i]]^2*wxxx[[i]] +
12*uuy[[i]]*wxy[[i]]*alpha^2 + 12*vvx[[i]]*wxy[[i]]*alpha^2 + 12*wxx[[i]]*wxy[[i]]*wyy[[i]]*alpha^2 +
G1*wyyy[[i]]*alpha^2 + 12*vvy[[i]]*wyyy[[i]]*alpha^4 + 6*wyy[[i]]^2*wyyy[[i]]*alpha^4 +
12*vvy[[i]]*wxxx[[i]]*alpha^2*U - 12*uuy[[i]]*wxy[[i]]*alpha^2*U - 12*vvx[[i]]*wxy[[i]]*alpha^2*U -
12*wxx[[i]]*wxy[[i]]*wyy[[i]]*alpha^2*U + 6*wxxx[[i]]*wyy[[i]]^2*alpha^2*U +
12*uux[[i]]*wyyy[[i]]*alpha^2*U + 6*wxx[[i]]^2*wyyy[[i]]*alpha^2*U), {i, 1, ndomain}];

wxx = Table[wxx /. {x -> xb[[i]], y -> yb[[i]]}, {i, 1, nb}];
wyy = Table[wyy /. {x -> xb[[i]], y -> yb[[i]]}, {i, 1, nb}];
uux = Table[uux /. {x -> xb[[i]], y -> yb[[i]]}, {i, 1, nb}];
uuy = Table[uuy /. {x -> xb[[i]], y -> yb[[i]]}, {i, 1, nb}];
vxx = Table[vxx /. {x -> xb[[i]], y -> yb[[i]]}, {i, 1, nb}];
vyy = Table[vyy /. {x -> xb[[i]], y -> yb[[i]]}, {i, 1, nb}];

NLSHEAR =
Table[1/(12*(-1+U^2))* (12 ny[[i]] alpha^3 vvy[[i]] wyy[[i]] + 6 ny[[i]] alpha wxx[[i]]^2 wyy[[i]] + 6 ny[[i]] alpha^3
wyy[[i]]^3 - 6 ny[[i]] alpha uuy[[i]] wxx[[i]] (-1 + U) - 6 ny[[i]] alpha vvx[[i]] wxx[[i]] (-1 + U) +
12 ny[[i]] alpha uux[[i]] wyy[[i]] U + 12 nx[[i]] uux[[i]] wxx[[i]] + 6 nx[[i]] wxx[[i]]^3 +
6 nx[[i]] alpha^2 uuy[[i]] wyy[[i]] + 6 nx[[i]] alpha^2 vvx[[i]] wyy[[i]] -
6 nx[[i]] alpha^2 uuy[[i]] wyy[[i]] U - 6 nx[[i]] alpha^2 vvx[[i]] wyy[[i]] U +
6 nx[[i]] alpha^2 wxx[[i]] (wyy[[i]]^2 + 2 vvy[[i]] U)), {i, 1, nb}];

If[elaso == 1, rp = Table[Sqrt[(x-xj)^2 + (y-yj)^2] /. {x -> xdomain[[i]], y -> ydomain[[i]],
xj -> xdomain[[j]], yj -> ydomain[[j]]}, {i, 1, ndomain}, {j, 1, ndomain}];
RP = Table[t*w /. {x -> xdomain[[i]], y -> ydomain[[i]]}, {i, 1, ndomain}];
AP = Table[If[rp[[i, j]] == 0, 3.525*(1-vs^2)/(d1*Pi*Es),
(1-vs^2)/(Pi*Es*rp[[i, j]])], {i, 1, ndomain}, {j, 1, ndomain}];
ps = Inverse[AP].RP;,]

```

```

If[sf == 1, wci[iter] = w /. {x -> 0.5, y -> 0.5}; uc[incr] = u /. {x -> 0.5, y -> 0.5}; vc[incr] =
v /. {x -> 0.5, y -> 0.5}, wci[iter] = w /. {x -> 0.0, y -> 0.0}; uc[incr] = u /. {x -> 0.0, y -> 0.0};
vc[incr] = v /. {x -> 0.0, y -> 0.0}]; error = Abs[(wci[iter] - wci[iter - 1]) / wci[iter]];
qzbi[incr] = qzb; iteri[incr] = iter;]; If[sf == 1, wc[incr] = (w) /. {x -> 0.5, y -> 0.5};
wf[incr] = (w) /. {x -> 0.5, y -> 0.0}, wc[incr] = (w) /. {x -> 0.0, y -> 0.0};
wf[incr] = (w) /. {x -> -0.7071, y -> -0.7071}];
Def[nk, nk1, ng1, incre, incr] = w;
MX[nk, nk1, ng1, incre, incr] = (D[w, {x, 2}] + D[w, {y, 2}]  $\alpha^2 \nu$ ) / (12 (-1 +  $\nu^2$ ));
MY[nk, nk1, ng1, incre, incr] = (D[w, {x, 2}]  $\nu$  + D[w, {y, 2}]  $\alpha^2$ ) / (12 (-1 +  $\nu^2$ ));
MXY[nk, nk1, ng1, incre, incr] = D[w, {x, 1}, {y, 1}]  $\alpha$  / (12 (1 +  $\nu$ ));
SXXB[nk, nk1, ng1, incre, incr] = (D[w, {x, 2}] + D[w, {y, 2}]  $\alpha^2 \nu$ ) / (2 (-1 +  $\nu^2$ ));
SYYB[nk, nk1, ng1, incre, incr] = (D[w, {x, 2}]  $\nu$  + D[w, {y, 2}]  $\alpha^2$ ) / (2 (-1 +  $\nu^2$ ));
SXXM[nk, nk1, ng1, incre, incr] =
- (2 D[u, x] + (D[w, x])^2 + (2 D[v, y] + (D[w, y])^2)  $\alpha^2 \nu$ ) / (2 * (-1 +  $\nu^2$ ));
SYYM[nk, nk1, ng1, incre, incr] = - (2 D[v, y]  $\alpha^2$  +  $\alpha^2$  (D[w, y])^2 + 2 D[u, x]  $\nu$  + (D[w, x])^2  $\nu$ ) /
(2 (-1 +  $\nu^2$ ));
Print[qzbi[incr], " ", iteri[incr], " ", wc[incr], " ", wf[incr]],
{incr, 1, nincre}]; Print["K ", "= ", K, " ", "K1 ", "= ", K1, " ", "G1",
" = ", G1, " ", "relf", " = ", relf, " ", "c", " = ", c, " ", "Es", " = ", Es];,
{ng1, 1, 1}], {nk1, 1, 1}], {nk, 1, 1}]]

```

## • Post-processing

```

If[sf == 1, deflections = Do[Do[Do[Do[Print[Def[nk, nk1, ng1, incre, incr] /. {x -> 0.5, y -> 0.5}, {x -> 0.5, y -> 0.5}, {x -> 0.5, y -> 0.0}, {x -> 0.5, y -> 0.0}], {incr, m, nincre, m}], {ng1, 1, 1}], {nk1, 1, 1}], {nk, 1, 1}], deflections = Do[Do[Do[Do[Print[Def[nk, nk1, ng1, incre, incr] /. {x -> Table[i, {i, -1.2, 1.2, 0.2}], y -> 0}], {incre, 1, nincre}], {incr, m, nincre, m}], {ng1, 1, 3}], {nk1, 1, 3}], {nk, 1, 3}]]];

```

```

If[sf == 1, bendingstress = Do[Do[Do[Do[Print[SXXB[nk, nk1, ng1, incre, incr] /. {x -> 0.5, y -> 0.5}, {x -> 0.5, y -> 0.5}, {x -> 0.5, y -> 0.0}, {x -> 0.5, y -> 0.0}, {x -> 1.0, y -> 0.5}, {x -> 1.0, y -> 0.5}], {incr, m, nincre, m}], {ng1, 1, 1}], {nk1, 1, 1}], {nk, 1, 1}], bendingstress =
Do[Do[Do[Do[Print[SYYB[nk, nk1, ng1, incre, incr] /. {x -> Table[i, {i, -1.2, 1.2, 0.2}], y -> 0}], {incre, 1, nincre}], {incr, m, nincre, m}], {ng1, 1, 3}], {nk1, 1, 3}], {nk, 1, 3}]]];

```

```

If[sf == 1, membranestress = Do[Do[Do[Do[Print[SXXM[nk, nk1, ng1, incre, incr] /. {x -> 0.5, y -> 0.5}, {x -> 0.5, y -> 0.5}, {x -> 0.5, y -> 0.0}, {x -> 0.5, y -> 0.0}, {x -> 1.0, y -> 0.5}, {x -> 1.0, y -> 0.5}], {incr, m, nincre, m}], {ng1, 1, 1}], {nk1, 1, 1}], {nk, 1, 1}], membranestress =
Do[Do[Do[Do[Print[SXXM[nk, nk1, ng1, incre, incr] /. {x -> Table[i, {i, -1.2, 1.2, 0.2}], y -> 0}], {incre, 1, nincre}], {incr, m, nincre, m}], {ng1, 1, 3}], {nk1, 1, 3}], {nk, 1, 3}]]];

```

## Appendix B Optimization of Shape Variable C

Table B.1 Shape Variables And Average Errors % for SQ-CC-IM and SQ-SS-IM

SQ-CC-IM				SQ-SS-IM			
C	WOF	WF	Notes	C	WOF	WF	Notes
	Average Error %	Average Error %			Average Error %	Average Error %	
<b>0.1</b>	26.78	13.87		<b>0.10</b>	23.40	13.90	
<b>0.12</b>	10.10	3.69		<b>0.12</b>	4.38	3.10	
<b>0.14</b>	2.65	2.41		<b>0.14</b>	2.69	5.14	
<b>0.16</b>	0.69	4.05		<b>0.16</b>	4.63	8.11	
<b>0.18</b>	1.51	4.76		<b>0.18</b>	4.83	9.31	
<b>0.2</b>	1.96	5.01		<b>0.20</b>	4.55	6.86	
<b>0.22</b>	2.13	5.09		<b>0.22</b>	4.18	6.75	
<b>0.24</b>	2.19	5.11		<b>0.24</b>	3.84	6.49	
<b>0.26</b>	2.20	5.10		<b>0.26</b>	3.55	6.09	
<b>0.28</b>	2.20	5.08		<b>0.28</b>	3.30	5.76	
<b>0.3</b>	2.19	5.07		<b>0.30</b>	3.10	5.52	
<b>0.32</b>	2.19	5.06		<b>0.32</b>	2.94	5.46	
<b>0.34</b>	2.19	5.05		<b>0.34</b>	2.81	5.46	
<b>0.36</b>	2.20	5.05		<b>0.36</b>	2.70	5.45	
<b>0.38</b>	2.21	5.05		<b>0.38</b>	2.61	5.44	
<b>0.4</b>	2.22	5.05		<b>0.40</b>	2.54	5.43	
<b>0.42</b>	2.24	5.06		<b>0.42</b>	2.49	5.42	
<b>0.44</b>	2.26	5.07		<b>0.44</b>	2.44	5.42	
<b>0.46</b>	2.28	5.08		<b>0.46</b>	2.41	5.43	
<b>0.48</b>	2.31	5.09		<b>0.48</b>	2.39	5.43	
<b>0.5</b>	2.33	5.10		<b>0.50</b>	2.37	5.45	
<b>0.52</b>	2.36	5.11		<b>0.52</b>	2.36	5.46	
<b>0.54</b>	2.39	5.14		<b>0.54</b>	2.36	5.48	
<b>0.56</b>	2.41	5.16		<b>0.56</b>	2.36	5.50	
<b>0.58</b>	2.44	5.11		<b>0.58</b>	2.37	5.52	
<b>0.6</b>	2.49	5.27		<b>0.60</b>	2.35	5.54	
<b>0.62</b>	2.29	4.92		<b>0.62</b>	2.41	5.59	
<b>0.64</b>	2.30	5.04		<b>0.64</b>	2.39	5.61	
<b>0.66</b>	2.45	4.92		<b>0.66</b>	2.49	5.66	
<b>0.68</b>	2.64	5.19		<b>0.68</b>	2.25	5.58	
<b>0.7</b>	3.23	3.54		<b>0.70</b>	1.56	5.30	
<b>0.72</b>	5.74	5.04		<b>0.72</b>	1.50	5.39	
				<b>0.74</b>	3.35	6.26	
				<b>0.76</b>	6.22	5.19	
				<b>0.78</b>	2.05	4.84	
				<b>0.80</b>	18.49	10.42	

Table B.2 Shape Variables and Average Errors % for SQ-CC-MO and SQ-SS-MO

SQ-CC-MO				SQ-SS-MO			
C	WOF	WF	Notes	C	WOF	WF	Notes
	Average Error %	Average Error %			Average Error %	Average Error %	
<b>0.10</b>	32.41	14.51		<b>0.10</b>	36.76	16.02	
<b>0.12</b>	13.15	3.96		<b>0.12</b>	9.41	3.76	
<b>0.14</b>	4.38	2.42		<b>0.14</b>	2.37	5.10	
<b>0.16</b>	0.89	3.94		<b>0.16</b>	5.52	6.66	
<b>0.18</b>	0.68	4.66		<b>0.18</b>	5.67	6.84	
<b>0.20</b>	1.00	4.91		<b>0.20</b>	5.02	6.64	
<b>0.22</b>	1.15	4.99		<b>0.22</b>	4.25	6.38	
<b>0.24</b>	1.20	5.01		<b>0.24</b>	3.57	6.13	
<b>0.26</b>	1.20	5.00		<b>0.26</b>	3.00	5.92	
<b>0.28</b>	1.18	4.98		<b>0.28</b>	2.53	5.75	
<b>0.30</b>	1.17	4.96		<b>0.30</b>	2.15	5.61	
<b>0.32</b>	1.15	4.95		<b>0.32</b>	1.84	5.51	
<b>0.34</b>	1.14	4.94		<b>0.34</b>	1.58	5.42	
<b>0.36</b>	1.13	4.93		<b>0.36</b>	1.37	5.36	
<b>0.38</b>	1.12	4.93		<b>0.38</b>	1.20	5.31	
<b>0.40</b>	1.12	4.93		<b>0.40</b>	1.07	5.27	
<b>0.42</b>	1.13	4.94		<b>0.42</b>	0.96	5.25	
<b>0.44</b>	1.14	4.94		<b>0.44</b>	0.89	5.24	
<b>0.46</b>	1.15	4.95		<b>0.46</b>	0.85	5.24	
<b>0.48</b>	1.16	4.96		<b>0.48</b>	0.82	5.24	
<b>0.50</b>	1.17	4.97		<b>0.50</b>	0.80	5.25	
<b>0.52</b>	1.19	4.98		<b>0.52</b>	0.79	5.27	
<b>0.54</b>	1.20	5.00		<b>0.54</b>	0.78	5.28	
<b>0.56</b>	1.21	5.01		<b>0.56</b>	0.78	5.31	
<b>0.58</b>	1.27	4.97		<b>0.58</b>	0.79	5.33	
<b>0.60</b>	1.21	5.11		<b>0.60</b>	0.80	5.36	
<b>0.62</b>	1.18	4.80		<b>0.62</b>	0.81	5.39	
<b>0.64</b>	1.07	4.90		<b>0.64</b>	0.82	5.42	
<b>0.66</b>	1.45	4.81		<b>0.66</b>	0.83	5.45	
<b>0.68</b>	1.43	5.06		<b>0.68</b>	0.87	5.46	
<b>0.70</b>	1.77	3.52		<b>0.70</b>	0.88	5.56	
<b>0.72</b>	0.87	4.03		<b>0.72</b>	0.96	5.68	
<b>0.74</b>	1.30	3.47		<b>0.74</b>	1.04	5.67	
<b>0.76</b>	2.80	12.36		<b>0.76</b>	1.21	5.56	
<b>0.78</b>	13.23	27.24		<b>0.78</b>	1.12	5.59	
<b>0.80</b>	9.28	17.37		<b>0.80</b>	0.40	5.71	

Table B.3 Shape Variables And Average Errors % for SQ-CF-IM and SQ-SF-IM

SQ-CF-IM				SQ-SF-IM			
C	WOF	WF	Notes	C	WOF	WF	Notes
	Average Error %	Average Error %			Average Error %	Average Error %	
<b>0.10</b>	33.00	22.78		<b>0.10</b>	42.18	39.83	
<b>0.12</b>	16.27	9.79		<b>0.12</b>	25.04	27.09	
<b>0.14</b>	8.55	4.16		<b>0.14</b>	17.66	21.51	
<b>0.16</b>	5.29	2.26		<b>0.16</b>	14.73	18.99	
<b>0.18</b>	3.88	1.60		<b>0.18</b>	13.33	17.52	
<b>0.20</b>	3.20	1.29		<b>0.20</b>	12.39	16.32	
<b>0.22</b>	2.81	1.11		<b>0.22</b>	11.55	15.16	
<b>0.24</b>	2.55	1.05		<b>0.24</b>	10.71	14.00	
<b>0.26</b>	2.33	1.01		<b>0.26</b>	9.87	12.82	
<b>0.28</b>	2.13	0.98		<b>0.28</b>	9.02	11.65	
<b>0.30</b>	1.95	0.94		<b>0.30</b>	8.18	10.49	
<b>0.32</b>	1.78	0.92		<b>0.32</b>	7.37	9.35	
<b>0.34</b>	1.61	0.92		<b>0.34</b>	6.57	8.26	
<b>0.36</b>	1.47	0.99		<b>0.36</b>	5.81	7.20	
<b>0.38</b>	1.35	1.15		<b>0.38</b>	5.07	6.19	
<b>0.40</b>	1.24	1.34		<b>0.40</b>	4.38	5.22	
<b>0.42</b>	1.17	1.53		<b>0.42</b>	3.72	4.35	
<b>0.44</b>	1.11	1.74		<b>0.44</b>	3.10	3.88	
<b>0.46</b>	1.11	1.95		<b>0.46</b>	2.53	3.67	
<b>0.48</b>	1.12	2.16		<b>0.48</b>	1.99	4.85	
<b>0.50</b>	1.13	2.37		<b>0.50</b>	1.49	7.16	
<b>0.52</b>	1.23	2.59		<b>0.52</b>	1.03	10.06	
<b>0.54</b>	1.34	2.80		<b>0.54</b>	0.61	2147.04	
<b>0.56</b>	1.43	3.01		<b>0.56</b>	0.22		
<b>0.58</b>	1.53	3.21		<b>0.58</b>	0.15		
<b>0.60</b>	1.70	3.45		<b>0.60</b>	0.50		
<b>0.62</b>	1.68	3.54		<b>0.62</b>	0.70		
<b>0.64</b>	1.91	3.73		<b>0.64</b>	0.99		
<b>0.66</b>	1.89	3.87		<b>0.66</b>	1.03		
<b>0.68</b>	3.19	4.47		<b>0.68</b>	1.80		
<b>0.70</b>	14.47	7.83		<b>0.70</b>	5.75		
<b>0.72</b>	27.81	10.14		<b>0.72</b>	13.02		
<b>0.74</b>		14.02		<b>0.74</b>			
<b>0.76</b>				<b>0.76</b>			
<b>0.78</b>				<b>0.78</b>			
<b>0.80</b>				<b>0.80</b>			

Table B.4 Shape Variables and Average Errors % for SQ-CF-MO and SQ-SF-MO

SQ-CF-MO				SQ-SF-MO			
C	WOF	WF	Notes	C	WOF	WF	Notes
	Average Error %	Average Error %			Average Error %	Average Error %	
<b>0.10</b>	50.70	28.17		<b>0.10</b>	75.17	51.36	
<b>0.12</b>	32.71	14.01		<b>0.12</b>	62.88	39.27	
<b>0.14</b>	22.71	7.49		<b>0.14</b>	55.79	33.57	
<b>0.16</b>	18.09	5.04		<b>0.16</b>	52.54	30.91	
<b>0.18</b>	15.99	4.16		<b>0.18</b>	50.85	29.29	
<b>0.20</b>	14.92	3.73		<b>0.20</b>	49.58	27.93	
<b>0.22</b>	14.29	3.48		<b>0.22</b>	48.34	26.57	
<b>0.24</b>	13.83	3.32		<b>0.24</b>	47.02	25.17	
<b>0.26</b>	13.44	3.19		<b>0.26</b>	45.58	23.71	
<b>0.28</b>	13.07	3.08		<b>0.28</b>	44.04	22.21	
<b>0.30</b>	12.69	2.97		<b>0.30</b>	42.41	20.70	
<b>0.32</b>	12.28	2.85		<b>0.32</b>	40.71	19.19	
<b>0.34</b>	11.84	2.72		<b>0.34</b>	38.95	17.69	
<b>0.36</b>	11.36	2.63		<b>0.36</b>	37.14	16.21	
<b>0.38</b>	10.84	2.53		<b>0.38</b>	35.29	14.76	
<b>0.40</b>	10.30	2.42		<b>0.40</b>	33.42	13.34	
<b>0.42</b>	9.72	2.30		<b>0.42</b>	31.53	11.97	
<b>0.44</b>	9.13	2.17		<b>0.44</b>	29.64	10.64	
<b>0.46</b>	8.51	2.04		<b>0.46</b>	27.76	9.55	
<b>0.48</b>	7.89	1.98		<b>0.48</b>	25.89	8.77	
<b>0.50</b>	7.26	1.92		<b>0.50</b>	24.07	8.04	
<b>0.52</b>	6.62	1.89		<b>0.52</b>	22.28	7.36	
<b>0.54</b>	5.98	1.92		<b>0.54</b>	20.56	6.73	
<b>0.56</b>	5.35	2.00		<b>0.56</b>	18.90	6.15	
<b>0.58</b>	4.72	2.17		<b>0.58</b>	17.31	5.61	
<b>0.60</b>	4.10	2.45		<b>0.60</b>	15.80	5.12	
<b>0.62</b>	3.48	2.75		<b>0.62</b>	14.38	4.67	
<b>0.64</b>	2.87	3.04		<b>0.64</b>	13.05	4.26	
<b>0.66</b>	2.23	3.37		<b>0.66</b>	11.81	4.02	
<b>0.68</b>	1.56	3.72		<b>0.68</b>	10.64	3.78	
<b>0.70</b>	0.51	5.02		<b>0.70</b>	9.57	3.58	
<b>0.72</b>	0.41	4.46		<b>0.72</b>	8.60	3.50	
<b>0.74</b>	0.75	5.29		<b>0.74</b>	7.72	3.45	
<b>0.76</b>	0.10	4.64		<b>0.76</b>	6.86	3.46	
<b>0.78</b>	1.08	2.15		<b>0.78</b>	6.03	3.50	
<b>0.80</b>	0.88	2.17		<b>0.80</b>	5.42	3.58	

Table B.5 Shape Variables And Average Errors % for CI-CC-IM and CI-SS-IM

CI-CC-IM				CI-SS-IM			
C	WOF	WF	Notes	C	WOF	WF	Notes
	Average Error %	Average Error %			Average Error %	Average Error %	
<b>0.10</b>	91.72	83.95		<b>0.10</b>	88.68	77.46	
<b>0.12</b>	84.30	72.17		<b>0.12</b>	79.05	65.36	
<b>0.14</b>	73.03	57.24		<b>0.14</b>	64.76	53.19	
<b>0.16</b>	58.21	41.21		<b>0.16</b>	47.19	42.54	
<b>0.18</b>	42.13	26.68		<b>0.18</b>	30.27	34.67	
<b>0.20</b>	27.82	15.33		<b>0.20</b>	16.96	8.21	
<b>0.22</b>	16.96	7.39		<b>0.22</b>	7.74		
<b>0.24</b>	9.56	3.73		<b>0.24</b>	1.84		
<b>0.26</b>	4.86	2.54		<b>0.26</b>	1.76		
<b>0.28</b>	2.01	2.87		<b>0.28</b>	3.89		
<b>0.30</b>	0.47	3.84		<b>0.30</b>	5.13		
<b>0.32</b>	0.86	4.43		<b>0.32</b>	5.84		
<b>0.34</b>	1.20	4.77		<b>0.34</b>	6.24		
<b>0.36</b>	1.54	5.02		<b>0.36</b>	6.47		
<b>0.38</b>	1.77	5.32		<b>0.38</b>	6.60		
<b>0.40</b>	2.02	High		<b>0.40</b>	6.67		
<b>0.42</b>	5.96	High		<b>0.42</b>	6.71		
<b>0.44</b>	1.54	High		<b>0.44</b>	6.73		
<b>0.46</b>	1.75	High		<b>0.46</b>	6.74		
<b>0.48</b>	1.85	5.01		<b>0.48</b>	6.75		
<b>0.50</b>	1.91	5.09		<b>0.50</b>	6.76		
<b>0.52</b>	1.96	5.15		<b>0.52</b>	6.77		
<b>0.54</b>	2.00	5.21		<b>0.54</b>	6.77		
<b>0.56</b>	2.03	5.26		<b>0.56</b>	6.78		
<b>0.58</b>	2.07	5.30		<b>0.58</b>	6.79		
<b>0.60</b>	2.09	5.35		<b>0.60</b>	6.80		
<b>0.62</b>	2.12	5.38		<b>0.62</b>	6.81		
<b>0.64</b>	2.14	5.42		<b>0.64</b>	6.82		
<b>0.66</b>	2.16	5.45		<b>0.66</b>	6.83		
<b>0.68</b>	2.18	5.48		<b>0.68</b>	6.84		
<b>0.70</b>	2.20	5.50		<b>0.70</b>	6.85		
<b>0.72</b>	2.21	5.53		<b>0.72</b>	6.87		
<b>0.74</b>	2.23	5.55		<b>0.74</b>	6.88		
<b>0.76</b>	2.24	5.57		<b>0.76</b>	6.90		
<b>0.78</b>	2.25	5.59		<b>0.78</b>	6.91		
<b>0.80</b>	2.26	5.60		<b>0.80</b>	6.92		



Table B.6 Shape Variables and Average Errors % for CI-CC-MO and CI-SS-MO

CI-CC-MO				CI-SS-MO			
C	WOF	WF	Notes	C	WOF	WF	Notes
	Average Error %	Average Error %			Average Error %	Average Error %	
<b>0.10</b>	93.46	84.57		<b>0.10</b>	93.64	77.79	
<b>0.12</b>	87.59	73.23		<b>0.12</b>	87.84	63.11	
<b>0.14</b>	78.54	58.76		<b>0.14</b>	78.73	46.40	
<b>0.16</b>	66.15	43.03		<b>0.16</b>	65.70	30.44	
<b>0.18</b>	51.44	28.49		<b>0.18</b>	49.50	17.12	
<b>0.20</b>	36.66	16.87		<b>0.20</b>	33.07	9.75	
<b>0.22</b>	24.13	8.59		<b>0.22</b>	19.75	20.25	
<b>0.24</b>	14.94	4.53		<b>0.24</b>	10.61		
<b>0.26</b>	8.84	2.96		<b>0.26</b>	4.91		
<b>0.28</b>	5.06	2.83		<b>0.28</b>	1.77		
<b>0.30</b>	2.79	3.37		<b>0.30</b>	1.22		
<b>0.32</b>	1.47	3.99		<b>0.32</b>	1.66		
<b>0.34</b>	0.69	4.37		<b>0.34</b>	2.09		
<b>0.36</b>	0.45	4.63		<b>0.36</b>	2.41		
<b>0.38</b>	0.45	4.95		<b>0.38</b>	2.57		
<b>0.40</b>	0.57	High		<b>0.40</b>	2.64		
<b>0.42</b>	2.10	High		<b>0.42</b>	2.58		
<b>0.44</b>	0.35	High		<b>0.44</b>	2.74		
<b>0.46</b>	0.41	High		<b>0.46</b>	2.72		
<b>0.48</b>	0.46	4.63		<b>0.48</b>	2.71		
<b>0.50</b>	0.50	4.71		<b>0.50</b>	2.70		
<b>0.52</b>	0.52	4.78		<b>0.52</b>	2.69		
<b>0.54</b>	0.55	4.84		<b>0.54</b>	2.68		
<b>0.56</b>	0.58	4.89		<b>0.56</b>	2.67		
<b>0.58</b>	0.61	4.94		<b>0.58</b>	2.66		
<b>0.60</b>	0.63	4.98		<b>0.60</b>	2.66		
<b>0.62</b>	0.65	5.02		<b>0.62</b>	2.66		
<b>0.64</b>	0.67	5.06		<b>0.64</b>	2.65		
<b>0.66</b>	0.69	5.09		<b>0.66</b>	2.65		
<b>0.68</b>	0.71	5.12		<b>0.68</b>	2.65		
<b>0.70</b>	0.72	5.15		<b>0.70</b>	2.65		
<b>0.72</b>	0.73	5.17		<b>0.72</b>	2.65		
<b>0.74</b>	0.75	5.20		<b>0.74</b>	2.65		
<b>0.76</b>	0.76	5.21		<b>0.76</b>	2.64		
<b>0.78</b>	0.77	5.23		<b>0.78</b>	2.64		
<b>0.80</b>	0.77	5.25		<b>0.80</b>	2.64		

Table B.7 Shape Variables And Average Errors % for CI-CF-IM and CI-SF-IM

CI-CF-IM				CI-SF-IM			
C	WOF	WF	Notes	C	WOF	WF	Notes
	Average Error %	Average Error %			Average Error %	Average Error %	
<b>0.10</b>	90.69	84.36		<b>0.10</b>	89.48	81.82	
<b>0.12</b>	82.40	72.38		<b>0.12</b>	80.62	69.33	
<b>0.14</b>	70.14	56.98		<b>0.14</b>	67.30	53.95	
<b>0.16</b>	54.61	40.37		<b>0.16</b>	50.32	38.05	
<b>0.18</b>	38.29	25.33		<b>0.18</b>	33.31	24.34	
<b>0.20</b>	24.02	13.62		<b>0.20</b>	19.50	14.14	
<b>0.22</b>	13.25	5.49		<b>0.22</b>	9.70	7.17	
<b>0.24</b>	5.91	2.24		<b>0.24</b>	3.34	3.05	
<b>0.26</b>	1.26	2.80		<b>0.26</b>	1.79		
<b>0.28</b>	1.54	4.56		<b>0.28</b>	3.45		
<b>0.30</b>	3.18	5.50		<b>0.30</b>	5.10		
<b>0.32</b>	4.13	5.99		<b>0.32</b>	6.18		
<b>0.34</b>	4.74	6.28		<b>0.34</b>	6.93		
<b>0.36</b>	5.25	6.56		<b>0.36</b>	7.47		
<b>0.38</b>	5.95	7.12		<b>0.38</b>	7.89		
<b>0.40</b>	7.44	9.46		<b>0.40</b>	8.23		
<b>0.42</b>	High	High		<b>0.42</b>	8.51		
<b>0.44</b>	High	High		<b>0.44</b>	8.76		
<b>0.46</b>	High	High		<b>0.46</b>	8.98		
<b>0.48</b>	5.03	1.56		<b>0.48</b>	9.17		
<b>0.50</b>	3.17	2.18		<b>0.50</b>	9.35		
<b>0.52</b>	2.51	2.50		<b>0.52</b>	9.51		
<b>0.54</b>	2.38	2.70		<b>0.54</b>	9.65		
<b>0.56</b>	2.35	2.82		<b>0.56</b>	9.78		
<b>0.58</b>	2.36	2.91		<b>0.58</b>	9.90		
<b>0.60</b>	2.39	2.96		<b>0.60</b>	10.01		
<b>0.62</b>	2.46	3.00		<b>0.62</b>	10.11		
<b>0.64</b>	2.54	3.01		<b>0.64</b>	10.20		
<b>0.66</b>	2.60	3.01		<b>0.66</b>	10.28		
<b>0.68</b>	2.66	2.98		<b>0.68</b>	10.35		
<b>0.70</b>	2.70	2.95		<b>0.70</b>	10.42		
<b>0.72</b>	2.72	2.89		<b>0.72</b>	10.50		
<b>0.74</b>	2.73	2.81		<b>0.74</b>	10.59		
<b>0.76</b>	2.74	2.72		<b>0.76</b>	10.70		
<b>0.78</b>	2.76	2.60		<b>0.78</b>	10.83		
<b>0.80</b>	2.76	2.46		<b>0.80</b>	10.96		

Table B.8 Shape Variables and Average Errors % for CI-CF-MO and CI-SF-MO

CI-CF-MO				CI-SF-MO			
C	WOF	WF	Notes	C	WOF	WF	Notes
	Average Error %	Average Error %			Average Error %	Average Error %	
<b>0.10</b>	92.83	83.48		<b>0.10</b>	92.39	82.44	
<b>0.12</b>	86.38	71.17		<b>0.12</b>	85.82	69.94	
<b>0.14</b>	76.54	55.63		<b>0.14</b>	75.78	54.31	
<b>0.16</b>	63.26	39.09		<b>0.16</b>	61.66	37.44	
<b>0.18</b>	47.57	24.20		<b>0.18</b>	43.71	21.77	
<b>0.20</b>	31.45	12.60		<b>0.20</b>	23.53	9.09	
<b>0.22</b>	17.04	5.06		<b>0.22</b>	7.11	2.63	
<b>0.24</b>	6.48	2.32		<b>0.24</b>	13.16	6.73	
<b>0.26</b>	4.70	3.85		<b>0.26</b>	26.02	10.95	
<b>0.28</b>	6.82	5.62		<b>0.28</b>	34.91	13.57	
<b>0.30</b>	9.51	6.55		<b>0.30</b>	40.65	14.85	
<b>0.32</b>	10.93	7.00		<b>0.32</b>	44.12	15.31	
<b>0.34</b>	11.70	7.26		<b>0.34</b>	46.07	16.13	
<b>0.36</b>	12.34	7.53		<b>0.36</b>	47.03	16.95	
<b>0.38</b>	13.56	8.19		<b>0.38</b>	47.30	17.30	
<b>0.40</b>	19.70	12.28		<b>0.40</b>	45.79	17.20	
<b>0.42</b>	High	High		<b>0.42</b>	48.08	16.96	
<b>0.44</b>	6.00	High		<b>0.44</b>	48.50	16.63	
<b>0.46</b>	High	High		<b>0.46</b>	66.22	16.25	
<b>0.48</b>	8.44	1.48		<b>0.48</b>	45.39	16.04	
<b>0.50</b>	4.29	2.08		<b>0.50</b>	45.25	15.87	
<b>0.52</b>	3.02	2.44		<b>0.52</b>	44.99	15.74	
<b>0.54</b>	2.47	2.70		<b>0.54</b>	44.71	15.66	
<b>0.56</b>	2.15	2.85		<b>0.56</b>	44.45	15.60	
<b>0.58</b>	1.97	2.94		<b>0.58</b>	44.23	15.55	
<b>0.60</b>	1.82	2.99		<b>0.60</b>	44.04	15.52	
<b>0.62</b>	1.69	3.01		<b>0.62</b>	43.89	15.49	
<b>0.64</b>	1.55	3.01		<b>0.64</b>	43.77	15.47	
<b>0.66</b>	1.44	2.98		<b>0.66</b>	43.68	15.45	
<b>0.68</b>	1.36	2.93		<b>0.68</b>	43.62	15.43	
<b>0.70</b>	1.29	2.86		<b>0.70</b>	43.59	15.42	
<b>0.72</b>	1.28	2.77		<b>0.72</b>	43.56	15.41	
<b>0.74</b>	1.34	2.65		<b>0.74</b>	43.56	15.40	
<b>0.76</b>	1.49	2.51		<b>0.76</b>	43.55	15.39	
<b>0.78</b>	1.72	2.36		<b>0.78</b>	43.55	15.38	
<b>0.80</b>	2.08	2.29		<b>0.80</b>	43.53	15.38	

## Appendix C Correlations of Foundation Parameters

Table C.1 Results of loads, soil reactions, Young's Modulus and  $w$  at  $\nu_s=0.35$

Es	q	$P * 100$	w	Es	q	$P * 100$	w	Es	q	$P * 100$	w
100	1	-0.002144	-0.001470	100	4	-0.008026	-0.005528	100	7	-0.012602	-0.008730
200	1	-0.003678	-0.001268	200	4	-0.014081	-0.004869	200	7	-0.022712	-0.007892
400	1	-0.005697	-0.000992	400	4	-0.022324	-0.003894	400	7	-0.037311	-0.006529
600	1	-0.006941	-0.000814	600	4	-0.027479	-0.003224	600	7	-0.046812	-0.005503
800	1	-0.007766	-0.000689	800	4	-0.030898	-0.002743	800	7	-0.053196	-0.004728
1000	1	-0.008340	-0.000597	1000	4	-0.033272	-0.002382	1000	7	-0.057635	-0.004130
1200	1	-0.008755	-0.000526	1200	4	-0.034984	-0.002104	1200	7	-0.060836	-0.003660
1400	1	-0.009063	-0.000471	1400	4	-0.036242	-0.001882	1400	7	-0.063164	-0.003281
1600	1	-0.009295	-0.000425	1600	4	-0.037190	-0.001702	1600	7	-0.064911	-0.002971
1800	1	-0.009474	-0.000388	1800	4	-0.037916	-0.001553	1800	7	-0.066242	-0.002713
2000	1	-0.009612	-0.000357	2000	4	-0.038477	-0.001427	2000	7	-0.067269	-0.002495
2200	1	-0.009721	-0.000330	2200	4	-0.038916	-0.001320	2200	7	-0.068067	-0.002309
2400	1	-0.009806	-0.000307	2400	4	-0.039260	-0.001228	2400	7	-0.068692	-0.002148
2600	1	-0.009873	-0.000287	2600	4	-0.039531	-0.001147	2600	7	-0.069183	-0.002008
2800	1	-0.009926	-0.000269	2800	4	-0.039744	-0.001077	2800	7	-0.069569	-0.001884
3000	1	-0.009968	-0.000253	3000	4	-0.039912	-0.001014	3000	7	-0.069872	-0.001775
100	2	-0.004232	-0.002905	100	5	-0.009694	-0.006689	100	8	-0.013873	-0.009629
200	2	-0.007297	-0.002517	200	5	-0.017172	-0.005947	200	8	-0.025198	-0.008769
400	2	-0.011356	-0.001978	400	5	-0.027541	-0.004809	400	8	-0.041850	-0.007331
600	2	-0.013863	-0.001625	600	5	-0.034097	-0.004003	600	8	-0.052875	-0.006221
800	2	-0.015524	-0.001377	800	5	-0.038456	-0.003415	800	8	-0.060341	-0.005365
1000	2	-0.016681	-0.001194	1000	5	-0.041482	-0.002971	1000	8	-0.065546	-0.004698
1200	2	-0.017515	-0.001053	1200	5	-0.043662	-0.002626	1200	8	-0.069305	-0.004170
1400	2	-0.018132	-0.000942	1400	5	-0.045259	-0.002351	1400	8	-0.072030	-0.003742
1600	2	-0.018598	-0.000851	1600	5	-0.046461	-0.002126	1600	8	-0.074073	-0.003390
1800	2	-0.018956	-0.000776	1800	5	-0.047380	-0.001940	1800	8	-0.075627	-0.003097
2000	2	-0.019233	-0.000713	2000	5	-0.048090	-0.001783	2000	8	-0.076825	-0.002849
2200	2	-0.019450	-0.000660	2200	5	-0.048644	-0.001650	2200	8	-0.077755	-0.002637
2400	2	-0.019620	-0.000614	2400	5	-0.049078	-0.001535	2400	8	-0.078482	-0.002454
2600	2	-0.019755	-0.000573	2600	5	-0.049419	-0.001434	2600	8	-0.079053	-0.002294
2800	2	-0.019861	-0.000538	2800	5	-0.049688	-0.001346	2800	8	-0.079501	-0.002153
3000	2	-0.019944	-0.000507	3000	5	-0.049900	-0.001268	3000	8	-0.079852	-0.002028
100	3	-0.006203	-0.004264	100	6	-0.011215	-0.007754	100	9	-0.015042	-0.010459
200	3	-0.010780	-0.003723	200	6	-0.020048	-0.006954	200	9	-0.027504	-0.009587
400	3	-0.016916	-0.002949	400	6	-0.032541	-0.005688	400	9	-0.046160	-0.008095
600	3	-0.020723	-0.002431	600	6	-0.040548	-0.004764	600	9	-0.058728	-0.006915
800	3	-0.023245	-0.002063	800	6	-0.045896	-0.004077	800	9	-0.067318	-0.005989
1000	3	-0.024998	-0.001790	1000	6	-0.049609	-0.003554	1000	9	-0.073329	-0.005258
1200	3	-0.026263	-0.001579	1200	6	-0.052284	-0.003145	1200	9	-0.077679	-0.004675
1400	3	-0.027196	-0.001412	1400	6	-0.054237	-0.002817	1400	9	-0.080826	-0.004199
1600	3	-0.027899	-0.001277	1600	6	-0.055704	-0.002549	1600	9	-0.083182	-0.003807
1800	3	-0.028439	-0.001165	1800	6	-0.056824	-0.002327	1800	9	-0.084973	-0.003480
2000	3	-0.028856	-0.001070	2000	6	-0.057689	-0.002139	2000	9	-0.086351	-0.003202
2200	3	-0.029183	-0.000990	2200	6	-0.058362	-0.001979	2200	9	-0.087420	-0.002965
2400	3	-0.029439	-0.000921	2400	6	-0.058890	-0.001841	2400	9	-0.088255	-0.002759
2600	3	-0.029642	-0.000860	2600	6	-0.059304	-0.001721	2600	9	-0.088910	-0.002580
2800	3	-0.029801	-0.000807	2800	6	-0.059631	-0.001615	2800	9	-0.089424	-0.002422
3000	3	-0.029926	-0.000760	3000	6	-0.059887	-0.001521	3000	9	-0.089827	-0.002282

Table C.2 Results of  $K$ 's at different values of  $v_s$  and  $E_s$  for NL-W

$E_s$	NL-W, $K$ at different values of $v_s$						
	0.15	0.2	0.25	0.3	0.35	0.40	0.45
100	15.0431	15.0431	15.0781	15.1132	15.2196	15.3639	15.623
200	30.3361	30.3361	30.4161	30.6588	30.9884	31.4965	32.4724
400	60.1419	60.3397	60.5389	61.1443	62.1806	64.1374	67.1915
600	89.0987	89.0987	89.4523	90.8951	92.7654	96.3333	102
800	117.146	117.146	117.691	119.356	122.832	127.795	136.776
1000	145.068	145.068	145.844	148.222	152.362	159.49	171.528
1200	171.66	171.66	173.741	175.872	181.438	189.849	206.239
1400	197.535	198.86	200.204	202.946	210.143	221.121	238.953
1600	226.168	226.168	227.856	231.308	238.537	252.337	272.614
1800	249.242	249.242	251.268	257.55	266.431	278.432	306
2000	276.326	276.326	278.771	283.794	294.403	311.893	338.693
2200	303.406	303.406	306.323	312.33	321.832	339.889	371.22
2400	327.032	327.39	330.468	337.125	348.908	368.794	403.279
2600	352.128	352.523	355.888	363.166	376.042	397.765	435.416
2800	377.172	377.605	381.261	389.16	403.13	426.691	467.508
3000	401.519	401.991	405.932	414.439	429.48	454.841	498.753

Table C.3 Results of  $K_1$ 's at different values of  $v_s$  and  $E_s$  for NL-W

$E_s$	NL-W, $K_1$ at different values of $v_s$						
	0.15	0.2	0.25	0.3	0.35	0.40	0.45
100	0.34018	0.34018	0.34097	0.34176	0.34417	0.34743	0.35329
200	0.49809	0.49809	0.4994	0.50339	0.5088	0.51714	0.53316
400	0.59652	0.59848	0.60046	0.60646	0.61674	0.63615	0.66644
600	0.59204	0.59204	0.59438	0.60397	0.6164	0.64011	0.67776
800	0.55686	0.55686	0.55945	0.56736	0.58389	0.60748	0.65017
1000	0.51755	0.51755	0.52032	0.5288	0.54358	0.56901	0.61195
1200	0.47629	0.47629	0.48206	0.48798	0.50342	0.52676	0.57223
1400	0.43754	0.44048	0.44346	0.44953	0.46547	0.48979	0.52929
1600	0.40923	0.40923	0.41228	0.41853	0.43161	0.45658	0.49327
1800	0.37539	0.37539	0.37844	0.3879	0.40128	0.41935	0.46087
2000	0.35102	0.35102	0.35413	0.36051	0.37399	0.3962	0.43025
2200	0.32994	0.32994	0.33312	0.33965	0.34998	0.36962	0.40369
2400	0.30754	0.30787	0.31077	0.31703	0.32811	0.34681	0.37924
2600	0.28915	0.28947	0.29224	0.29821	0.30878	0.32662	0.35754
2800	0.27258	0.27289	0.27554	0.28124	0.29134	0.30837	0.33787
3000	0.25759	0.25789	0.26042	0.26588	0.27553	0.2918	0.31997

Table C.4 Poisson's Ratios and Corresponding Values of Equation Constants for NL-W

NL-W, K			NL-W, K <sub>1</sub>				
$\nu_s$	C <sub>1</sub>	C <sub>2</sub>	C <sub>3</sub>	C <sub>4</sub>	C <sub>5</sub>	C <sub>6</sub>	C <sub>7</sub>
0.15	0.1327	8.52	-7.86E-14	5.67E-10	-1.38E-06	1.15E-03	0.2825
0.2	0.133	8.53	-7.86E-14	5.67E-10	-1.38E-06	1.16E-03	0.2826
0.25	0.1344	8.2	-7.85E-14	5.67E-10	-1.39E-06	1.16E-03	0.2829
0.3	0.13743	7.56	-8.03E-14	5.80E-10	-1.42E-06	1.19E-03	0.2816
0.35	0.1427	6.75	-8.14E-14	5.90E-10	-1.45E-06	1.23E-03	0.2802
0.4	0.1516	5.164	-8.47E-14	6.16E-10	-1.52E-06	1.31E-03	0.2764
0.45	0.1671	2.368	-8.92E-14	6.53E-10	-1.63E-06	1.43E-03	0.2713

Table C.5 Results of K's at different values of  $\nu_s$  and  $E_s$  for Pasternak

$E_s$	Pasternak (P), K at different values of $\nu_s$						
	0.15	0.2	0.25	0.3	0.35	0.4	0.45
100	0.24473	0.24473	0.2453	0.24587	0.2476	0.24995	0.25417
200	0.49596	0.49596	0.49727	0.50124	0.50663	0.51494	0.53089
400	1.02324	1.02661	1.02999	1.04029	1.05793	1.09122	1.14318
600	1.58877	1.58877	1.59508	1.62081	1.65416	1.71778	1.81882
800	2.18817	2.18817	2.19834	2.22945	2.29439	2.38709	2.55483
1000	2.83721	2.83721	2.85238	2.89888	2.97986	3.11927	3.35468
1200	3.50688	3.50688	3.54939	3.59294	3.70664	3.87847	4.2133
1400	4.20358	4.23179	4.26038	4.31875	4.47189	4.7055	5.08497
1600	5.00746	5.00746	5.04483	5.12127	5.28131	5.58684	6.03578
1800	5.73429	5.73429	5.78091	5.92543	6.12976	6.40588	7.04012
2000	6.5872	6.5872	6.64549	6.76523	7.01814	7.43506	8.07393
2200	7.489	7.489	7.56101	7.70926	7.94382	8.38952	9.16285
2400	8.34439	8.35352	8.43205	8.60192	8.90257	9.40998	10.2899
2600	9.27339	9.28379	9.37242	9.56408	9.90317	10.4753	11.4668
2800	10.2394	10.2512	10.3504	10.5649	10.9441	11.5838	12.6918
3000	11.2229	11.2361	11.3462	11.584	12.0045	12.7133	13.9407

Table C.6 Results of  $G_1$ 's at different values of  $\nu_s$  and  $E_s$  for Pasternak

$E_s$	Pasternak (P), $G_1$ at different values of $\nu_s$						
	0.15	0.2	0.25	0.3	0.35	0.40	0.45
100	1.9478	1.9478	1.95233	1.95688	1.97066	1.98934	2.0229
200	3.89163	3.89163	3.9019	3.93303	3.97532	4.04049	4.16569
400	7.81118	7.83687	7.86273	7.94136	8.07596	8.3301	8.72677
600	11.8154	11.8154	11.8623	12.0536	12.3017	12.7748	13.5263
800	15.8743	15.8743	15.9481	16.1738	16.6448	17.3174	18.5343
1000	20.1035	20.1035	20.211	20.5406	21.1143	22.1021	23.7702
1200	24.2982	24.2982	24.5927	24.8945	25.6823	26.8728	29.1928
1400	28.511	28.7024	28.8963	29.2921	30.3309	31.9153	34.4891
1600	33.2801	33.2801	33.5285	34.0365	35.1001	37.1307	40.1144
1800	37.3786	37.3786	37.6825	38.6246	39.9565	41.7563	45.8906
2000	42.15	42.15	42.523	43.2892	44.9075	47.5752	51.6632
2200	47.0786	47.0786	47.5312	48.4632	49.9378	52.7396	57.601
2400	51.5733	51.6297	52.1151	53.165	55.0232	58.1592	63.5976
2600	56.3905	56.4537	56.9927	58.1582	60.2201	63.6989	69.7284
2800	61.3012	61.3715	61.9658	63.2495	65.5201	69.3495	75.9833
3000	66.1906	66.2683	66.918	68.3204	70.8	74.9807	82.2196

Table C.7  $\nu_s$  and Corresponding Values of Equation Constants for Pasternak

$\nu_s$	Pasternak, K		Pasternak, $G_1$	
	$C_1$	$C_2$	$C_3$	$C_4$
0.15	3.77E-03	-6.76E-01	2.21E-02	-1.48E+00
0.2	3.77E-03	-6.77E-01	2.21E-02	-1.48E+00
0.25	3.81E-03	-6.91E-01	2.24E-02	-1.55E+00
0.3	3.89E-03	-7.21E-01	2.29E-02	-1.69E+00
0.35	4.04E-03	-7.66E-01	2.37E-02	-1.90E+00
0.4	4.28E-03	-8.47E-01	2.52E-02	-2.27E+00
0.45	4.71E-03	-9.88E-01	2.77E-02	-2.94E+00

## VITA

**Name** : Mohammed Mohammed Hussein Al-Tholaia

**Nationality** : Yemeni.

**Date of Birth** : 4<sup>th</sup> March 1979

**Education** :

- Graduated from high school in 1996 with grade of 92.63%, scientific section, Thamar, Yemen.
- Received a scholarship from the Ministry of Higher Education to study B.Sc. at Ain Shams University, Egypt, in 1997.
- Graduated from Ain Shams University with **B.Sc.** degree in the civil engineering, structural section in 2002 with accumulative grade of very good.
- Received a scholarship from the Ministry of Higher Education and Thamar University to study MS degree at KFUPM in 2007.
- Received a ward as one of the top ten graduate students in MS program at KFUPM on June 1, 2010, for achieving high GPA (3.94/4).
- Got MS degree from KFUPM in June, 2010 in CE, Structure.
- Worked as lecturer B at KFUPM from Sep.2010 to January, 2105.

## PUBLICATIONS

### A. Journals

- **Mohammed M. Hussein Al-Tholaia**, Abul K. Azad, Shamsad Ahmad, Muhammed H. Baluch. “ *A comparative study of corrosion resistance of different coatings for mortar-embedded steel plates*”. Construction and Building Materials, Volume 56, Pages 74-80.



- Shamsad Ahmad, **Mohammed M. Hussein Al-Tholaia**. “*Evaluation of corrosion resistance of coated steel strips embedded in mortar under chloride exposure*”. Anti-Corrosion Methods and Materials, (accepted January 9<sup>th</sup>, 2014).
- **Mohammed M. Hussein Al-Tholaia**, Husain Jubran Al-Gahtani. “*RBF-Based Meshless Method for Large Deflection of Elastic Thin Plates On Nonlinear Foundation*”. Engineering Analysis with Boundary Elements, Volume 51, February 2015, Pages 146–155.

## **B. Conferences**

- S. Alghamdi, **M. Al-Tholaia**, J. Leiva. “*Towards Unified Sizing-Shape Optimal Design Of Cable-Stayed Stiffened Box-Type Steel Bridges – A Comparative Design Experimentation With Strength And Stiffness Constraints*”. Experimental Vibration Analysis for Civil Engineering Structures, EVACES’13, 28-30 October 2013, Ouro Preto, Brazil, pages 232-240.
- **M. M. Al-Tholaia**, B. Al-Gohi, M.K.Rahman, A.H.Al-Gadhib, M.H.Baluch. “*Review of State-of-Art in the Behavior of Masonry Walls Subject to Lateral Axial Loading*”. Concrete for Sustainable Construction, 9<sup>th</sup> International Concrete Conference (9CONCRETE-2013), 11<sup>th</sup> -13<sup>th</sup> February, 2013, Kingdom of Bahrain.

## **Work and Experience:**

In 2003, appointed as a graduate assistant at Tamar University, college of engineering and I am still working there as a faculty member. During the period from 2002 right 2007, I worked as a supervisor and engineer designer for a lot of reinforced concrete projects in both the national and private sectors in Yemen.

**Emails:** [altholaia@gmail.com](mailto:altholaia@gmail.com); [al\\_tholaia1978@yahoo.com](mailto:al_tholaia1978@yahoo.com)

